UNIVERSITAT DE BARCELONA

New insights into the crosstalk between the TGF-β and the EGF Receptor pathways during liver regeneration and hepatocarcinogenesis

Judit López Luque

New insights into the crosstalk between the TGF-β and the EGF Receptor pathways during liver regeneration and hepatocarcinogenesis

Report presented by

Judit López Luque

to obtain the title of

Doctor of Philosophy (Ph.D.)

Supervised by:

Isabel Fabregat, PhD. **Emilio Ramos, PhD, MD.**

TGF-β and cancer
Bellvitge Biomedical Research Institute (IDIBELL)
and
Section Head of General and Digestive Surgery Service
Bellvitge University Hospital (HUB)

PhD program in Biomedicine (Universitat de Barcelona)

This work has been developed at the Laboratory d'Oncologia Molecular (LOM) at IDIBELL (L'Hospitalet de Llobregat, Barcelona).

The author enjoyed the following financial support:

- "IDIBELL pre-doctoral fellowship" from IDIBELL (January 2013 - December 2016).

The author enjoyed the following short-term stages:

- Short-term stay in Complutense University of Madrid (UCM) - Allowing the author to learn specific procedures for animal experimentation (June 2015) in Aránzazu Sánchez and Margarita Fernández's laboratory in the Biochemistry and Molecular Biology Department II (Madrid, Spain).

This work has been possible thanks to the financial support of the following institutions:

- Generalitat de Catalunya - Agència de Gestió d'Ajuts Universitaris i de Recerca (AGAUR) (2009-2013). 2009SGR-312. *Title of the project*: Mecanismos moleculares y celulares asociados al fenotipo tumoral y metastásico.

- Gobierno de España - Ministerio de Economía y Competitividad (MINECO) through Instituto de Salud Carlos III (ISCIII) - Red Temática de Investigación Cooperativa en Cáncer (RTICC). RD12-0036-0029 (2013-2015).

- Gobierno de España - Ministerio de Economía y Competitividad (MINECO) - cofounded by FEDER funds/European Regional Development Fund (2013-2015). BFU2012-35538. *Title of the project*: Papel del tráfico intracelular, el citoesqueleto y las integrinas en la señalización inducida por TGF-beta en células hepáticas. Relevancia en fibrosis y hepatocarcinogénesis.

- People Programme (Marie Curie Actions) of the European Union's Seventh Framework Programme (FP7/2007-2013) under REA grant agreement nº PITN-GA-2012-316549 (IT LIVER) (2012-2016). *Title of the project*: Inhibiting TGF-β in liver disease.

- Generalitat de Catalunya - Agència de Gestió d'Ajuts Universitaris i de Recerca (AGAUR) (2014-2016). 2014SGR-334. *Title of the project*: Papel del factor de crecimiento transformante-beta (TGF-β) en patologías humanas.

- Gobierno de España - Ministerio de Economía y Competitividad (MINECO) - cofounded by FEDER funds/European Regional Development Fund (2016-2019). SAF2015-64149-R. *Title of the project*: Nuevos conocimientos sobre el papel de la NADPH oxidasa NOX4 en hepatocarcinogénesis. Relevancia en la vías de señalización del TGF-beta y del receptor del EGF.

Aquí no caben ni fantasías ni ocurrencias

Copa de cerámica lacónica en Esparta en la primera mitad del siglo VI A.C. y atribuida a Archesillas II. Se muestra el castigo del titán Prometeo, según la mitología griega. Éste sería atormentado por un águila enviada por Zeus para comerse su hígado a diario, el cual regeneraba durante las noches, como castigo por robar el fuego de los dioses y entregarlo a los hombres (Museo del Vaticano). No obstante, Prometeo también es un satélite de Saturno. Esta luna presenta una forma muy alargada, con numerosas crestas y valles, de cuerpo helado y poroso, y debe su nombre al titán. (Fotografía de la portada por Andrea Malfettone).

AKNOWLEDGEMENTS

Gracias.

“Gracias” es la palabra que me permite romper la hoja en blanco de este apartado de la tesis. No sé si se podría decir que es el más importante, pero sí el imprescindible para llevar a cabo todo mi doctorado y uno de los más difíciles de escribir. Por este motivo, y por mi afición a enrollarme sin necesidad, me he limitado el espacio a 5-6 páginas, sabiendo de antemano que no seré capaz de agradecer a todas y cada una de las personas que debería. Por ello, tenéis total libertad de sentiros agradecidos si no os encontráis en estas líneas. Y si lo estáis, tened por seguro que no se aproxima ni a una ínfima parte de lo que realmente querría decir. Por el contrario, espero que sí que lo veáis día a día, porque definitivamente esto es un trabajo en equipo. AVISO: abstenerse de leer este apartado los que no estén dispuestos a leer un tostón ni estén acostumbrados a las ñoñerías.

En primer lugar, mis primeras palabras y pensamientos son para mis padres. Sin ellos a mi lado siempre, yo no hubiera llegado hasta aquí, y ya no solo durante el doctorado, si no des de que tengo uso de razón. Y esto lo tengo muy claro, solo espero que ellos también. Sé que no ha sido fácil, pero aún así han estado siempre apoyándome, en los mejores y sobre todo en los peores momentos o los más críticos. Ambas partes hemos aprendido la una de la otra y nos hemos comprendido. Por todo esto, por el apoyo incondicional, por creer en mí, por siempre intentar hacerme ver que podía más y que me superase aunque yo no quisiera o no lo creyera, y por infinidad de cosas más, estaré siempre agradecida. Os quiero. No puedo dejar de lado a mi hermano, que aunque ahora esté lejos, a su manera, siempre está ahí para dejarme continuamente sin palabras con su forma de ser y sus placajes humorísticos. Estoy muy orgullosa de que persigas tus objetivos y siempre consigas lo que te propones. Para acabar, agradecer todo el apoyo al resto de la familia: abuelos, tíos y primos. Cada uno habéis estado presentes de una forma u otra. Eli, gracias por haber compartido todo conmigo, des de la trona hasta el día de hoy.

Y ya centrándome en la época del doctorado, como no podría ser de otra manera, agradecer a Isabel. Aún recuerdo el mail que envié des de Granada solicitando realizar solamente 3 meses de prácticas de verano en el IDIBELL en tu grupo. Ahora hace ya 5 años de eso, pero me parece que fue ayer. Nunca imaginé todo lo que me depararía el clickar el botón ENVIAR a ese mail. Casi con toda seguridad, ha sido una de las mejores etapas de mi vida y, sin lugar a duda, la más estimulante de todas ellas hasta el momento. En primer lugar, gracias por la oportunidad. La oportunidad de poder entrar en tu grupo y conocer gente maravillosa e inolvidable, así como la oportunidad de entrar en este mundo, abrirme puertas y guiarme en él. Valoro mucho tu gran capacidad científica, pero aún más tu enorme capacidad docente. Siempre dispuesta a transmitir tus conocimientos, tanto a tus “niños” como a nosotros. Gracias por enseñarme a aprender, por tu esfuerzo y por tu dedicación. Sin embargo, valoro y admiro aún más tu gran capacidad de trabajo y la predisposición a nuevos retos, nuevos conceptos en ciencia, y nuevos métodos o tecnologías. Aunque arriesgado, sin duda, es una de las cosas que te hace grande. Gracias siempre por tu apoyo, y por animarme a seguir en todo momento. Al escribir esta tesis y estos agradecimientos, me doy cuenta de todo lo que he aprendido y vivido estos años, tanto a nivel científico como humano. Y me hace muy feliz. Porque sí, se podría decir que el doctorado hace madurar a muchos niveles, y aunque no siempre de la mejor

manera, siempre merece la pena. Y todo eso debo agradecértelo de corazón. Gracias Isabel por creer en mí.

Seguidamente, agradecer a Emilio. Des de pequeña siempre me ilusionaba la idea de poder formar parte de un hospital trabajando en la clínica o en un laboratorio. El realizar esta tesis me ha permitido poder juntar ambas partes, y esto te lo debo agradecer. Gracias por haber podido contar contigo todos estos años. Siempre dispuesto a discutir des de un punto de vista totalmente distinto pero completamente imprescindible para este trabajo. Por tus ánimos, por las preguntas que hacen reflexionar, por tu humor y por transmitir seguridad. Y también gracias por la atención tan personal a mi abuela. Gracias Emilio.

Sin más, ahora toca agradecer y pedir disculpas, a todos aquellos que habéis tenido que lidiar conmigo todos estos años de manera más o menos intensa, des de una posición muy cercana. Mi familia en el laboratorio. Sin vosotros, yo no estaría escribiendo esta tesis, y eso lo tengo muy claro. Fuisteis, soys y seréis más importantes de lo que imagináis. Mi primer pensamiento en el laboratorio (COM4) de los IFs es para Esther. "A ver un tema…", poco puedo decir o escribir, porque no será justo de todas maneras. No me imagino un doctorado sin tenerte siempre a mi lado: fuiste la primera persona que me dio la mano el primer día que llegué al lab, y aún me la sigues dando hoy en día. Porque has sido multitud de cosas para mí estos años: mi mentora en el laboratorio (des de todo lo referente a cultivos celulares hasta en nueva terminología, véase "mindundi" ;)), co-directora de tesina de máster, mi compañera de poyata, de largas discusiones (científicas), de desayunos, de escaleras, de confocal y de infinidad de momentos más. Pero también una de las personas que más me conoce y me comprende. Eres una pieza clave. Gracias por estar siempre dispuesta a escuchar y a ayudar, tanto a mí como a todos, en cualquier momento, por siempre decirme la verdad, aunque duela, por animarme a seguir en todo momento, por hacerme ver la parte positiva de las cosas, por rescatarme de los momentos de dudas e inseguridades, por motivarme científicamente cada día, y por tantos y tantos consejos. Como compañera y amiga, gracias de corazón. No olvido el tiempo compartido con Laia y Patty, aunque breve, importante en mis primeros pasos en este mundillo. Gràcies Laia, per ensenyar-me a fer WBs, per la teva increible motivació i il·limitada capacitat de treball, i per transmetre transparència, bones vibracions i gran fortalesa. A Patty, por enseñarme a hacer immunohistoquímicas y cuestionar siempre las cosas. Eres ejemplo de lo importante que es perseguir lo que te propones. Y ahora sí, empezando por los mayores (que no viejos…), a Joan le debo rescatarme cuando andaba más perdida a mi llegada. Gràcies per transmetre seguretat i tranquil·litat sense dir ni una sola paraula, per la teva paciència ensenyant-me citometria, pels Lacasitos, per inculcar-me el valor de l'humor absurd (sigui divendres o no), per tenir sempre les paraules justes, per ser un referent (tot i que no responable) i un dels pilars fonamentals per a mi al lab. Ets un crack! I gràcies Raquel. Formeu una parella ideal, genials per separat, únics junts. Molt feliç d'haver compartit tants moments amb vosaltres. Mi otro pilar en el lab, y fuera de él: Eva. Doncs no sé què dir, … o tot o res. Ho intentaré. Et trobo molt a faltar, molt. Gràcies per ser la meva profe, companya de lab i sobretot amiga. Ets una ment brillant i treballadora incansable (superwoman!) i has arribat molt lluny, i he pogut aprendre moltíssim i de

la millor: a part de tots els protocols de cultius en 2D ½ i 3D i moltíssims més, ara ja sé formular preguntes més concretes (o ho intento…), posar a punt protocols ("Un chorrito?!"), redimensionar figures d'un powerpoint a mida de la gent normal, i mil coses més. Per tots els moments compartits que ara no podria nomenar: poiata, riures, projectes, discussions científiques (amb cafès o sense), congressos, riures fins plorar, canyes, riures, desesperacions, curses, mosquits, riures, etc. Et dec moltíssim, i no em cansaré de dir-ho. Sé que puc comptar amb tu sempre, només espero que tu també ho sàpigues. Y a continuación llegan los Thunders! La vidilla del laboratorio! Joaquim, t'estimo amb bogeria, ja ho saps. Inclús quan ets una explosió saturant d'energia, plans, conceptes, i mil històries. Gràcies per ensenyar-me a fer servir l'Illustrator i demés programes que et fan tornar boja. Perquè ets increiblemnet decidit i eficaç. Però lo que et caracteritza, i poca gent té, és un gran cor i l'habilitat de trobar la part positiva sempre de tot i de tothom. Tots hauriem de tenir un mini-JQ a dins. No et perdis mai. Simplement gràcies per haver-me permès coneixe't, i espero que quan siguis famòs no oblidis (com a la tornada de la India) una de les teves primeres fans. P.D. Et dec un APOLO. El capitán, Edgar. Siempre con una respuesta para todo, y transmitiendo una seguridad abrumadora, de la que intento aprender. Pero incluso las dudas que no muestras o no quieres mostrar, te hacen grande. Gracias por siempre cuidar de mí, por animarme, por tus habilidades docentes y las discusiones científicas, por enseñarme a hacer powerpoints *cool*, y por tener siempre un plan para todo, tanto fuera como dentro del lab. Y sí, ahora entiendo y respeto el humor absurdo. He sucumbido a él, y esto también te lo tengo que agradecer. Y gracias Laura, por aguantar y entender nuestras frikadas en tantos y tantos momentos. Soys perfectos juntos! EHHHHH Quindi Andrea!! Uff…qué difíciles somos separados y juntos jaja! Sin darme cuenta y poco a poco te has convertido en imprescindible para mí. Siendo compañero de escritura de tesis, poco más puedo decir. Gracias por enseñarme a ver la parte clínica de todo esto, por entenderme y comprenderme en cosas que nadie hace, por tu espíritu "empalagoso" y soñador, ya sea de verdad o de mentira (nunca lo sabremos), por el niño que llevas dentro, por confiar en mí y mimarme, por las increíbles fotos sacadas a la luna de la tapa, por las charlas filosóficas que no tienen sentido, por lo brillante que eres y todo lo que puedes enseñar y demostrar (aunque no lo quieras ver), y por tu risa que se propaga por el COM. Pero sobretodo por tener un corazón enorme y haberme permitido conocerlo. Dani, qué decirte…si por telepatía ya lo sabes. Mi alma gemela, tan iguales en algunas cosas que asusta (véase que envíes tú un mail y me contesten a mí XD): porque llegamos a ser uno solo. Estoy muy contenta de haber compartido contigo todo este tiempo y proyecto, y fácil, casi innato. Porque aunque siempre hay momentos difíciles, hemos sabido salir aprendiendo el uno del otro, siendo un equipo, y eso es lo que más valoro, porque hace que merezca la pena. Gracias por enseñarme a perfeccionar los WBs, por compartir las largas horas de estabulario y mil momentos más, por siempre estar pendiente de mí, cuidarme, y animarme en todo momento. Eres energía y alegría pura, si las canalizas junto con todo lo que sabes (y que no te crees) y lo que ansías saber, llegarás donde quieras. Y por último a Jitka. Gracias por acabar de quitarme el miedo al citómetro, por ser tan clara y directa, y por decir cosas que otros no se atreven. Por ser divertida de una manera única. Escondes una gran persona que hace que se te coja cariño. Y también a Estanis, por siempre aportar ideas y planteamientos originales. No obstante, por el grupo han pasado muchísimas personas que

han dejado su granito o playa de arena. Empezando por Miguel, Filip (a genious! I hope you still remember "La llegenda de Sant Jordi), Ewa, Sergei, Michal and Gosia, Annalisa (eres todo amor, hasta cuando me "persigues todo el rato" ;)), Ann and Daria, Alba, Roser, Giulia (única e inigualable en terremoto), Laia, Maria, Patricia, Iván, Bhavna (with Love), Uxue, Sandra (adorable con tus spoilers), Nemani, Joana (de risa contagiosa, gràcies per ser única, somiadora i inspiradora de la tapa ;)), Gerard, Irene i Paula (senzillament feta per tenir fans). Para acabar los IFs, la última incorporación, Irene, trayendo de nuevo aire fresco, muy necesario. Gracias por recordar la ilusión en cualquier experimento y permitir que te acojamos con los brazos abiertos.

Sin dejar el COM4, dar las gracias a los CCVs: Magdiel, por sus sosegados consejos, a Pep y Javi, y hace algún tiempo ya (no pensaba que tanto!) a Dani (coloso). Gracias por estar siempre dispuesto a ayudar y echar una mano en todo, por los piques y las risas, y por ser de la "familia". Y a Maribel, por transmitir tranquilidad y siempre buen humor. También a Sara y Aitor, porque tenemos que aprender mucho de vuestra increíble madurez y motivación. Saliendo a mano izquierda encontramos el COM5, el laboratorio AFF, compañeros de lab meetings y tantas otras muchas cosas. Antònia, gràcies per ser omnipresent. Sempre amb la resposta per a tot (més que el google), i si no, buscant-la. Ets clau, i això és indiscutible. Gràcies per les discussions i plantejaments contundents, i per tot el suport que he rebut, sempre disposada a donar-me un cop de mà, tant a nivell científic com personal. M'encanta la tranquil·litat i seguretat que transmets. Edu, el nuevo (ya viejo) doctorando. Nunca dejaré ni tú dejarás de chinchar, y espero que así siga! ;)

Y después de ponernos tapones, llegamos al COM3: las risas se oyen des de todo el departamento, y aunque nos neguemos a reconocerlo, nos alegra y da vida. De los CMPs, con Javi empecé, incluso ya en Granada, y sin embargo se me adelantó bastante. Gracias por compartir conmigo los comienzos de esta etapa. Raffaela (vecina!) eres pura motivación y persistencia, brillante y enormemente eficiente. Gracias por hacer todo con una sonrisa. Clara, te he visto en etapa de máxima locura y máxima serenidad. Gracias por tus consejos y masajes! Y llegamos a las ONAs: Helena y Adriana, las veteranas. Por acogerme en su día y mostrarme su gran capacidad de trabajo. Anguloo! Eres todo torbellino en la cabeza. Me encanta haber compartido todo el doctorado contigo, de principio a fin. Gracias por siempre transmitir alegría y ayudarme a relativizar las cosas cuando yo no soy capaz. Fonseca! Bon diaaaa! Compañera (fugaz) de piso, sencillamente te adoro. Eres una persona desmesuradamente fuerte, y con una empatía y saber actuar incalculables. Gracias por haberme levantado cuando me he caído, y por mostrarme a aprovechar y disfrutar la vida al "limit", como tú dices. Me siento muy afortunada de haberte conocido. Erika, conozco pocas personas tan motivadas y que disfruten tanto de la ciencia como tú. Gracias por mostrarlo y recordarlo cuando es necesario. Y también a Iñigo, gracias por estar constantemente activo y cercano, porque sigues formando parte del COM; a Estefanía, por regalar ánimos en cualquier momento del día, y a Gabi, por cuidarnos a todos. Para acabar el COM3, pero no nueva, agradecer a Laia: aunque te hayas movido por casi todos los labos del COM, siempre has estado presente. Gracias por hacer reír simplemente con tu manera de ser, tu gracia y tu salero, y por compartir aquellas tardes en el curso de animales (hay que repetir las pastitas de Farmacia!).

Y finalmente, el COM2, con el que siempre hemos estado muy unidos los IFs, como en las mejores familias. Gracias Miguel (alias el mejicano) por tu saber estar, tus historias y tus truquillos para polimerizar geles de acrilamida a las 9 de la noche. Lagares!!! Ha pasado mucho tiempo ya. Des de aquella noche de confesiones, hasta las charlas filosóficas el otro día intentando entender el mundo. Gracias por haber estado siempre a mi lado, por tus verdades como puños, por la Zumba, por tus desconcertantes ideas que hacen ver las cosas de manera totalmente distinta, por tus fortalezas, pero también por tus debilidades, por ser una amiga gallega, vasca, y lo que tú quieras, y por rebautizarme como Juuu! Juan, ya está. Lo hemos hecho, hemos acabado más locos que cuando empezamos, que ya es decir. Gracias por ser único en tu especie, porque eres la persona más *random* que conozco, y sin embargo no me desconciertas: para mí eres estar "en casa". Por tu ánimo siempre, y por ser el alma de muchas situaciones. Porque te adoro hasta cuando me sacas de quicio. Me alegra haber podido compartir contigo de principio a fin, y ver cómo has madurado sin perder tu esencia. Nos queda pendiente el tatuaje. Silviiiii! Eres todo corazón. Gracias por ser compi de cultivos (tienes que poner en práctica EL "truco") con los grandes hits: la cinta de OT! Porque a parte de cantar genial, tienes mucha luz. Nunca dejes que la apaguen. Por escuchar y por tan buenos y sinceros consejos. Olga! Perquè sí que t'entenc, no t'amoïnis jaja! Gràcies per ser tan divertida, ho has d'explotar més. Per entendre el que és viure en un poble, i estar-ne molt orgullosa. Y para acabar el lab, los bizarros post-docs: David, gracias por ser tan escandalosamente peculiar, por tener un corazón que no te cabe en el pecho (porque sí, aunque lo intentes esconder, sabemos que está ahí) y por tu gran sabiduría. Santi, gracias por saber absolutamente de todo y por transmitirlo de manera paciente. Por tu saber estar en toda situación y momento, aportando siempre un giro inesperado cual chiquillo, y por transmitir tu pasión por el cine. No podría acabar el COM2 sin agradecer a sus antiguos inquilinos: Naiara, ara tan lluny però gràcies per sempre estar tan a prop, amb els ànims i les paraules justes, facin mal o no, sent una amiga. Per ser genial i una crack. Per inculcar la motivació per la ciència sempre, per gaudir-ne i per lluitar-hi com una "jabata". Anna Roig, gràcies pel teu esperit de superació en tot moment i per fer-ho sempre amb un gran somriure. Ana García, gracias por ser tan fuerte y transmitir tan buenas vibraciones, por superar todo y por ayudarme a mí a hacerlo de manera inesperada. Tenemos pendiente un Okinawa por el barrio. No olvido, aunque breve, el tiempo compartido con Rubén, Miriam y Lavinia.

No puedo acabar sin agradecer a todos y cada uno de los habitantes del pasillo de los IPs: gràcies Àngels, per formar part del nostre grup sempre, pel teu esperit científic i per la teva gran capacitat de treball, per tants i tan bons consells, i per sempre haver-me ajudat i sempre haver estat disponible, inclús tenint el temps just. Cristina Costa, gracias por tus siempre interesantes puntos de vista. Cristina Muñoz, gracias por ser tan cercana e inspiradora, siempre teniendo los pies en el suelo. Roser, gracias por las charlas que siempre acaban en risas. Mariona, gracias por mostrar el trabajo en equipo y la motivación por la ciencia. Y finalmente, gracias Òscar por formar parte de este gran equipo aportando muchos y diferentes puntos de vista. Para finalizar con el COM y el IDIBELL, dar las gracias a Javier Márquez y Rosa, por siempre estar presentes, ayudando sin reservas. De fuera, agradecer profundamente a Arancha y Margarita, por todo el esfuerzo y trabajo

realizado. Sin él, yo no podría haber escrito esta tesis. Gracias por mantener y transmitir un gran espíritu y por todo lo que me habéis enseñado. Más cerquita, agradecer a Joan Gil. Gràcies per sempre haver format part del nostre grup, per l'ajuda i les oportunitats que m'has donat, i per sempre fer-ho amb un gran somriure. Por último, también agradecer a Gustavo, por todas las oportunidades brindadas y los proyectos compartidos.

Para acabar, a aquellos que habéis estado a mi lado fuera de estas paredes, y que también lo habéis vivido de manera intensa. A mis compis de piso (El piso de nuestros sueños!): gracias Marta, todo este tiempo juntas, de principio a fin, des del máster, al laboratorio, al piso y durante todo el doctorado. Porque ha sido simplemente genial conocerte, tenerte como amiga, y saber que siempre tenía tu apoyo, por tu positividad y tu alegría que se contagia, hasta acabar llorando de risa. Eres brillante, trabajadora incansable, y conseguirás todo lo que te propongas. Y Héctor, gracias por haber formado parte de esta mini familia. Ideales el uno para el otro, inmejorables juntos. Meri… gràcies per absolutament tot. Per sempre fer-me costat, des de fa molts anys ja, pels ànims, per cuidar-me quan jo no podía, per la paciència, per escoltar-me, per les tardes de sofà, pels dissabte matins de zafarrancho, pels viatges, pels tuppers que m'han salvat i pels moments de: ¿por qué no? Bailemos! Finalmente, a Alba, aunque llevamos poco tiempo juntas compartiendo piso, llevamos toda la vida compartiendo amistad. Gracias por los ánimos esta última y larga etapa. Prometo hacerte una fiesta de bienvenida como dios manda :) Y a los de siempre, a los de toda la vida. A mis amigos de Abrera: gracias Mónica por conocerme como la palma de tu mano, por decir las cosas que tocan, sin rodeos, por apoyarme todo este tiempo y por ese sexto sentido tuyo que adoro a la vez que temo. A Sergi, Dani, Albert, Aida y Ángel. Y a mis chicas del Carril del picón, Cristina y Sara, gracias por confiar en mí, por ayudarme a relativizar las cosas y por tener tanta paciencia.

Y, para finalizar, gracias abuelo por todo el apoyo que me diste, y porque siempre recordaré cómo te fascinaba cuando te contaba las prácticas en la universidad con las "moscas" y las diferentes formas de sus alas. Siento mucho que no puedas estar en estos momentos, viendo acabar lo que empecé. Quizá algún día vuelva a trabajar con *Drosphila melanogaster*.

ABBREVIATIONS

ADAM	A disintegrin and metalloproteinase
AFP	alpha-fetoprotein
ALK5	Activin receptor-like kinase 5
ALP	Alkaline phosphatase
ALT	Alanine aminotransferase
AMH	Anti-Mullerian Hormone
AMT	Ameboid-to-Mesenchymal Transition
AR	Amphiregulin
AST	Aspartate aminotransferase
ATP	Adenosine triphosphate
α-SMA	α-Smooth muscle actin
BAX	BCL-2-associated X protein
BEC	Bile duct Epithelial Cell
bHLH	basic Helix-Loop-Helix
BIL T	Total Bilirubin
BMP	Bone Morphogenetic Proteins
BSA	Bovine Serum Albumin
BTC	Betacellulin
CAF	Cancer-associated fibroblast
CAT	Collective-to-Ameboid Transition
CCl_4	Carbon tetrachloride
CDD	Choline Deficient Diet
CDK	Cyclin Dependent Kinase
CI	Cell Index
CIP	CDK-Interacting Protein
CK-19	Cytokeratin 19
CKI	CDK-Inhibitor
CLD	Chronic Liver Disease
Co-SMAD	Cooperating SMAD
D.A.B	Diaminobenzidine

DAMPs	Damage-Associated Molecular Patterns
DAPI	40'6-diamidino-2-phenylindole
DEN	Diethylnitrosamine
DTT	Dithiothreitol
ECM	Extracellular matrix
EDTA	Ethylenediaminetetraacetic acid
EGF	Epidermal Growth Factor
EGFR	Epidermal Growth Factor Receptor
EMT	Epithelial-to-Mesenchymal Transition
EPG	Epigen
EPR	Epiregulin
Eps15	EGFR pathway substrate 15
ERK	Extracellular signal-regulated kinase
FAK	Focal Adhesion Kinase
FBS	Fetal Bovine Serum
FGF	Fibroblast Growth Factor
GDF	Growth and Differentiation Factor
GMM	Genetically Modified Mice
GPCR	G-protein coupled receptor
Grb2	Growth factor receptor protein 2
h	Hours
H&E	Hematoxylin and Eosine
HB-EGF	Heparin Binding EGF-like Growth Factor
HBV	Hepatitis B Virus
HCC	Hepatocellular Carcinoma
HCV	Hepatitis C Virus
HGF	Hepatocyte Growth Factor
HIF1α	Hypoxia inducible factor 1α
HSC	Hepatic Stellate Cell
I-SMAD	Inhibitory SMAD

IGF	Insulin-like Growth Factor
IGFR	Insulin-like Growth Factor Receptor
IHC	Immunohistochemistry
IL-1β	Interleukin-1beta
IL-6	Interleukin-6
IL-8	Interleukin-8
JNK	c-Jun terminal kinase
LAP	Latency-Associated Peptide
LPS	Lipopolysaccharides
LR	Liver regeneration
MAPK	Mitogen-Activated Protein Kinase
MAT	Mesenchymal-to-Ameboid Transition
MET	Mesenchymal-to-Epithelial Transition
MFB	Myofibroblast
min	Minutes
MLC2	Myosin Light Chain 2
MMP	Matrix Metalloproteinase
mTOR	Mammalian Target of Rapamycin
NADPH	Nicotinamide Adenine Dinucleotide Phosphate
NAFLD	Non-Alcoholic Fatty Liver Disease
NASH	Non-Alcoholic Steatohepatitis
NF-κB	Nuclear Factor-kappa B
NP-40	Nonidet P-40
NRG	Neuregulin
OCT	Optimal Cutting Temperature
PAMPs	Pathogen-Associated Molecular Patters
PBS	Phosphate-Buffered Saline
PBS-T	PBS-Tween
PCR	Polymerase Chain Reaction
PDGF	Platelet-Derived Growth Factor

PFA	Paraformaldehyde
PH	Partial Hepatectomy
PI	Propidium Iodide
PI3K	Phosphatidylinositol-3-kinase
PKC	Protein Kinase C
PMSF	Phenylmethylsulfonyl fluoride
PTEN	Phosphatase and tensin homolog
PTP1B	Protein Tyrosine Phosphatase-1B
PVDF	Polyvinylidene fluoride
qRT-PCR	Quantitative Real Time Polymerase Chain Reaction
R-SMAD	Receptor-associated SMAD
Rb	Retinoblastoma
ROS	Reactive Oxygen Species
RT	Room Temperature
RT-PCR	Reverse transcriptase PCR
SARA	Smad Anchor for Receptor Activation
SDS	Sodium Dodecyl Sulfate
SEC	Sinusoidal Endothelial Cell
SEM	Standard Error of the Mean
Shc	Src homology 2 domain containing transforming protein
shRNA	Short-Hairpin RNA
STAT3	Signal Transducer and Activator of Transcription 3
TAA	Thioacetamide
TACE	TNF-α converting enzyme
TβR	TGF-β Receptor
TERT	Telomerase reverse-transcriptase
TG	Triglyceride
TGF-α	Transforming Growth Factor-alpha
TGF-β	Transforming Growth Factor-beta
TIMP	Tissue inhibitors of metalloproteinases

TKI	Tyrosine Kinase Inhibitor
TKR	Tyrosine Kinase Receptor
TNF-α	Tumor Necrosis Factor-alpha
TRIS	Tris(hydroxymethyl)aminomethane
VEGF	Vascular Endothelial Growth Factor
WT	Wild type
ZEB	Zinc-finger E-box-binding

TABLE OF CONTENTS

I. INTRODUCTION

1. The liver

1.1. Liver anatomy and physiology

The **liver** is structurally and functionally heterogeneous and complex, being considered second only to brain in its complexity (Malarkey et al., 2005). It is the largest organ, accounting for approximately 2% to 3% of average body weight, and the majority of the cells within the liver are hepatocytes (Abdel-Misih and Bloomston, 2010; Si-Tayeb et al., 2010).

The liver is a gland that exhibits both endocrine and exocrine **properties** to carry out numerous functions that are involved in maintaining homeostasis within the organism (Si-Tayeb et al., 2010; Spear et al., 2006). The major exocrine secretion is in the form of bile, while endocrine functions include the secretion of several hormones, such as Insuline-like growth factors (IGFs), Angiotensinogen, and Thrombopoietin (Si-Tayeb et al., 2010). Moreover, the liver also holds other essential functions such as glycogen storage; drug detoxification or defense against foreign macromolecules and xenobiotic agents; removal and breakdown of serum proteins, red blood cells and microbes; secretion of an extensive array of plasma proteins including Albumin, Transferrin and Apolipoproteins; control of metabolism: production or removal of glucose during periods of fasting or eating, respectively, the processing of fatty acids and triglycerides, regulation of cholesterol homeostasis via synthesis and transport or catabolism, urea metabolism, synthesis and interconversion of non-essential amino acids, etc. (Malarkey et al., 2005; Si-Tayeb et al., 2010; Spear et al., 2006).

The **liver structure** is of important relevance to carry out all these functions. The liver in mice and rats is macro structurally divided in 4 lobes: median (or middle), left, right and caudate, and all, except the left, are further subdivided into 2 or more parts. In humans, the liver is macro structurally divided also in 4 lobes, but they have been traditionally designated as right, left, quadrate and caudate. However, recently it has been proposed that the human liver can be subdivided into 8 segments (**Figure I**). Mice and humans have a gall bladder, but not the rat. Moreover, the liver is well positioned: it receives blood from two sources, the portal vein (which supplies about 70-75% of the blood flow and 40% of the oxygen, coming from the large intestine, as well as spleen and pancreas) and the hepatic artery (which supplies 25-30% of the blood flow and 60% of the oxygen). Then, the highly organized hepatic architecture facilitates the exchange of materials between the blood and hepatocytes and, in addition, the hepatic biliary system enables the liver to transport bile into the intestines (Abdel-Misih and Bloomston, 2010; Malarkey et al., 2005; Spear et al., 2006).

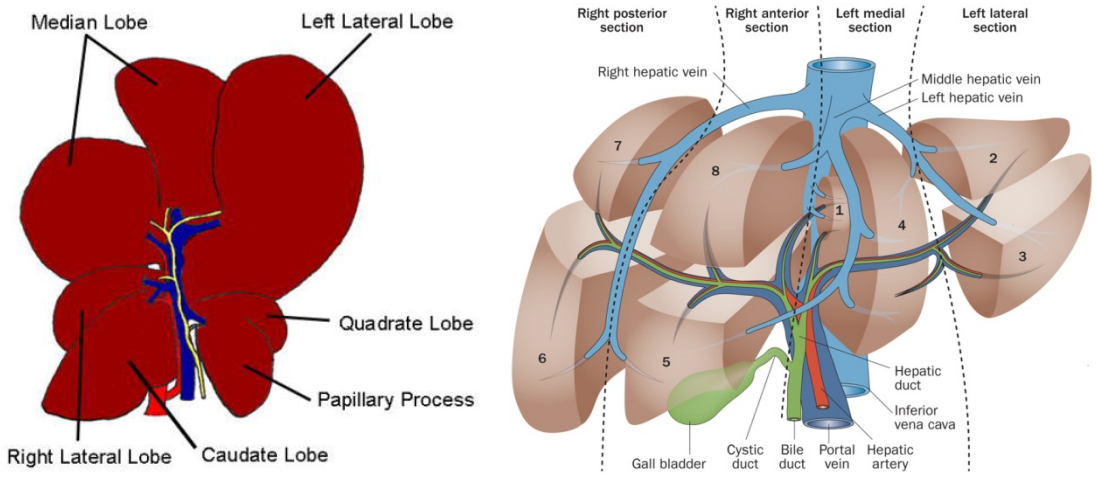

Figure I. **(Left)** Drawing depicting a ventral view of the normal mouse liver in which the left lateral and median lobes have been reflected back to exposure the portal vein (blue), hepatic artery (red), and common bile duct (green) (Abe et al., 2009). **(Right)** Segments of the human liver illustrating functional division into left and right hepatic lobes with Couinaud's segmental classification based on functional anatomy (Siriwardena et al., 2014).

The basic architectural unit of the liver is the **liver lobule** (**Figure II**). The lobule is a structure that consists of plates of hepatocytes lined by sinusoidal capillaries that radiate toward a central efferent vein. Liver lobules are roughly hexagonal with each of six corners demarcated by the presence of a portal triad of vessels, consisting of portal vein, bile duct, and hepatic artery, in a connective tissue matrix comprised mainly by type 1 collagen (Si-Tayeb et al., 2010). As mentioned before, both the portal vein and the hepatic artery supply blood to the lobule, which flows along plates of hepatocytes through small capillaries termed sinusoids. Sinusoidal blood flow is finally collected into terminal hepatic venules (also called central veins) prior to emptying into larger hepatic veins, which ultimately lead to the vena cava (Malarkey et al., 2005; Spear et al., 2006). Endothelial cells that line the sinusoids form the barrier between the blood and hepatocytes; the narrow region between these two cell types is termed the space of Disse. In the liver, the plates of hepatocytes are one to two cells thick. The sinusoidal side of these hepatocytes interfaces the space of Disse, whereas the opposite (apical) side forms the canalicular membrane. The bile canaliculi, small channels that are between adjacent hepatocytes, transport bile to the intrahepatic bile duct in a direction that is opposite to the sinusoidal blood flow. The transition region between the canaliculi and intrahepatic bile ducts is called the canal of Hering, narrow channels that are lined by hepatocytes and bile duct epithelial cells (BECs, also called cholangiocytes). These intrahepatic bile ducts converge into larger extrahepatic ducts, which ultimately join the common bile duct that transports bile either to the gall bladder (for storage) or directly to the small intestine. It is interesting to mention that the canals of Hering contain a small population of cells called Oval cells, that serve as resident stem cells in the adult liver. They can act as progenitor for both hepatocytes and BECs. They are also thought to play an important role in liver regeneration (Fausto and Campbell, 2003; Malarkey et al., 2005; Si-Tayeb et al., 2010; Spear et al., 2006).

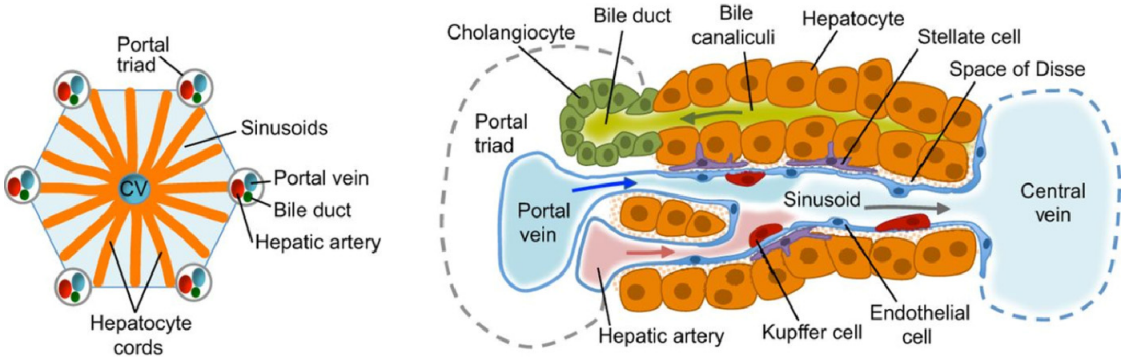

Figure II. Schematic hepatic lobule structure (Gordillo et al., 2015). Abbreviations: CV, central vein.

The adult liver is comprised of numerous **cell types**. Hepatocytes, which are polarized epithelial cells, carry out most of the functions. The basolateral surfaces of the hepatocyte face the fenestrated sinusoidal endothelial cells, which facilitates the transfer of endocrine secretions from the hepatocytes into the blood stream. Tight junctions formed between neighboring hepatocytes generate the canaliculus that surrounds each hepatocyte, which is responsible for collection of bile acids and bile salts that are transported across the hepatocytes' apical surface. (Si-Tayeb et al., 2010). Although hepatocytes are the major parenchymal cell type of the liver, and account for 78% of liver volume, other biologically important cell types are present, some of them mentioned above: a) Biliary Epithelial Cells (BEC) or cholangiocytes line the bile ducts. b) Sinusoidal Endothelial Cells (SECs) are the primary barrier between blood and hepatocytes and act as a filter of fluids, solutes and exchange particles between the blood and the space of Disse and, ultimately, hepatocytes. They have fenestrae, lack of basal lamina and can transfer molecules and particles by endocytosis. c) Kupffer cells (resident liver macrophages) are phagocytic cells. They can eliminate aged red blood cells and microbes, and they can present antigens, therefore influencing immune function. They are the major producers of cytokines as mediators of inflammation and provide crosstalk with other cells. d) Pit cells (resident natural killer cells in the liver) are important in immune function. e) And Hepatic Stellate Cells (HSCs) are the major player in regeneration and hepatic fibrogenesis and cirrhosis. HSC are located in the space of Disse and normally produce a variety of extracellular matrix (ECM) proteins. They can also synthesize numerous cytokines and chemokines, control microvascular tone, store and metabolize vitamin A and lipids, and when activated, due to chronic liver damage, transform to myofibroblasts (MFB) leading to fibrosis (Malarkey et al., 2005; Si-Tayeb et al., 2010; Spear et al., 2006).

In addition, it is important to highlight that **ECM** is important in the regulation and modulation of hepatic function. Between 5 and 10% of the ECM of the liver is collagen, which is important in the regulation and modulation of hepatic function. The ECM has numerous components including matrix metalloproteinases; glycoproteins like laminin, fibronectin, vitronectin, undulin and nidogen (entactin); and proteoglycans such as heparan sulfate (Malarkey et al., 2005).

The lobular organization of the liver has functional significance. While some liver functions can be carried out by all hepatocytes, other functions are limited to a subset of hepatocytes. This compartmentalization of function is determined by the position of hepatocytes within the liver lobule, a phenomenon called **positional (or zonal) heterogeneity** or **metabolic zonation**. This zonation allows opposing metabolic pathways to be carried out within distinct, non-overlapping regions of the liver. For example, periportal hepatocytes specialize in glycogenolysis and gluconeogenesis, while centrolobular hepatocytes are active in glycolysis and glycogen synthesis. In addition, not only the hepatocytes have gradients of gene and protein activity, but gradients also exist for SECs, Kupffer cells, HSCs, and the matrix in the space of Disse (Fausto and Campbell, 2003; Malarkey et al., 2005; Spear et al., 2006). This zonal heterogeneity is established during the perinatal period, a time when other dramatic changes occur in the liver (Spear et al., 2006).

1.2. Liver development

Liver development can be separated into several overlapping stages: in the first stage, when specification is established, cells become **"competent"** and are capable of taking a certain fate. Competent cells subsequently become **"committed"** to a particular lineage and exhibit morphological changes and express genes associated with commitment. Cells then **"differentiate"** along that lineage and are ultimately capable of carrying out the functions of a terminally differentiated cell. The recent understanding of competency, commitment, and differentiation in liver development has come from mouse studies (Spear et al., 2006).

Pluripotent embryonic stem cells from the blastocyst inner cell mass give rise to the three principal germ layers: ectoderm, mesoderm and endoderm. The anterior region of the endoderm will form the foregut. Coordinated signaling of fibroblast growth factors (FGF) from the cardiac mesoderm and bone morphogenetic proteins (BMP) from the septum transversum mesenchyme facilitate the commitment of competent foregut endoderm cells to become hepatoblasts. At the same time, early liver genes such as albumin and α-fetoprotein (AFP) are activated and also indicate commitment to the hepatic fate. Following hepatic specification of foregut endoderm, hepatoblasts proliferate and migrate into the septum transversum and continue to proliferate and differentiate, to form the liver bud. Hepatoblasts in the liver bud express serum proteins genes specific to hepatocytes, such as albumin, transthyretin, and AFP. These cells are bipotential and, soon after mesenchyme invasion, differentiate into hepatocytes (α-fetoprotein$^+$/albumin$^+$) and cholangiocytes (cytokeratin (CK)-19$^+$). Maturation into hepatocytes and bile epithelial cells continue until several weeks after birth (Kung et al., 2010; Spear et al., 2006).

1.3. Liver regeneration and proliferative capacity of adult hepatocytes

More relevant to this work is the development of new hepatocytes during adulthood where there is **liver regeneration (LR) or repair.** Interestingly, the liver has a unique ability to fully regenerate and, thus, differs significantly from other organs, which heal with a scar. Despite the low replicative rate of hepatocytes in the normal adult liver, these highly differentiated cells are not terminally differentiated and replicate in a highly regulated manner after loss of cell or tissue mass (Böhm et al., 2010; Fausto and Campbell, 2003). Adult hepatocytes, under basal conditions, remain in quiescent state (phase G_0 of the cell cycle), but maintain the ability to reinitiate the cell cycle, proliferate and regenerate the liver in response to surgical ablation, toxic injury, infections, exogenous stimulus, massive hepatocyte necrosis or apoptosis (Cienfuegos et al., 2014; Vacca et al., 2013).

A number of **experimental models** have been proposed for the study of liver regeneration. Loss of liver mass can be induced by administering hepatotoxic chemicals (such as carbon tetrachloride (CCl_4), D-galactosamine treatment, or acetaminophen intoxication); bacterial particles as lipopolysaccharides (LPS); and virus. This is followed by an inflammatory response which removes tissue debris, followed by the regenerative response. Most commonly and best-studied model for regeneration of the liver, however, is the one performing a surgical procedure which removes two/thirds of the liver mass in rodents (rats and mice). This technique is known as **2/3 partial hepatectomy (PHx),** and it was first proposed by Higgins and Anderson in 1931 (Higgins and Anderson, 1931). Due to the multi-lobe structure of the rodent liver, three of the five liver lobes (the large and median lobes, representing 70% or 2/3 of the liver mass) can be removed by an easy surgical procedure, without causing any tissue damage to the residual two lobes (**Figure III**). The latter grow in size to restore an aggregate equivalent to the mass of the original lobes. Normal liver regeneration is not accompanied by massive inflammation or necrosis and, thus, not induce a fibrotic response. The process, in rats and mice, is complete within 5-7 days after surgery. This model has allowed to compare the regeneration between control (wild type) with the genetic modified on signalizing molecules, receptors and cell cycle regulators. In a clinical setting, this procedure is also done in humans, in order to resect solitary liver metastases or repair trauma, etc. (Böhm et al., 2010; Cienfuegos et al., 2014; Mao et al., 2014; Michalopoulos, 2007).

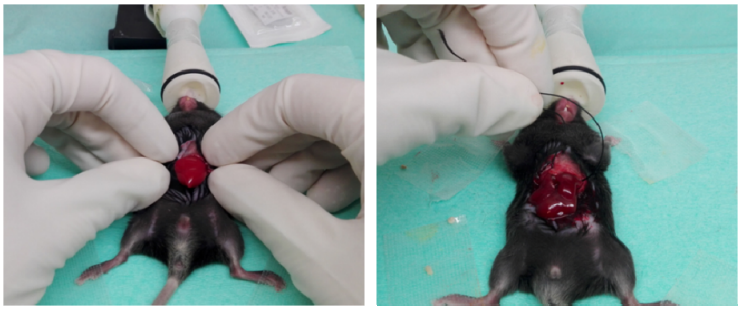

Figure III. Partial hepatectomy (PH) in an 8-weeks mouse.

Regeneration of the liver after resection is actually a "**compensatory hyperplasia and hypertrophy"** rather than a true restoration of the liver's original gross anatomy and architecture of the lost tissue, which takes place in the inferior vertebrate-Zebra fish, Salamander or amphibians. During liver "regeneration" after PH, the excised parts do not grow back, and the remaining liver expands in mass to compensate for the lost tissue. Thus, the cells in the remaining portion proliferate and/or increase in size to restore the original liver mass (Cienfuegos et al., 2014; Kang et al., 2012; Miyaoka et al., 2012; Riehle et al., 2011). The ability of the liver to carry out these normal duties is so essential that liver mass is maintained within a very narrow range in relation to the overall body mass. If there is loss or gain of liver mass, such as through liver injury or pregnancy, respectively, compensatory proliferation or apoptosis of cells allow restoration of original liver/body mass ratio once the stimulus is removed. This unique homeostatic relationship is termed as **"hepatostat"**. This strict regulation of the liver volume also occurs at the end of liver regeneration (Cienfuegos et al., 2014; Kang et al., 2012).

It is now well accepted that there are two **physiological forms of regeneration in the liver** in response to different types of liver injury. In the case of PH and some chemical liver injuries, such as CCl_4, the liver mass is replaced by replication of existing hepatocytes without activation of progenitor cells. This is considered the quickest and most efficient way to generate hepatocytes for liver regeneration and repair. In other cases of chemical liver injury, such as D-galactosamine, when injury is severe, or when mature hepatocytes are prevented from proliferating, due to senescent or arrest, then the activation, replication and differentiation of intrahepatic progenitor cells occurs (Fausto et al., 2006; Mao et al., 2014; Riehle et al., 2011).

There are two main proposals concerning the **physiological triggers for liver regeneration**. One is that the increased energy demand per unit liver volume after PH generates an early stress signal. Presumably, the increased metabolic demands placed on hepatocytes of the regenerating liver are linked to the machinery needed for hepatocyte replication, and may function as a sensor that calibrates the regenerative response according to body demands. The other is that liver regeneration is triggered by altered hemodynamic factors. After PHx in rats and mice, each residual lobe of the liver retains its supply of hepatic artery and portal vein branches. Whereas the amount of arterial blood going into every lobe remains essentially the same, the relative proportion and amount of portal vein blood going into each lobe increases threefold. This increases the availability of circulating growth factors and hormones (Fausto et al., 2006; Kang et al., 2012; Kwon et al., 2015; Michalopoulos, 2010).

Mainly **three clusters of networks mediate liver regeneration** after PH: cytokines, growth factor-mediated pathways and metabolic signals. Given the high redundancy existing among the intracellular components of each network, the loss of an individual gene rarely leads to complete inhibition but only a delay of liver regeneration (Mao et al., 2014; Riehle et al., 2011; Vacca et al., 2013). Hepatocyte regeneration proceeds along a sequence of distinctive phases: an initiation or "priming phase", rendering hepatocytes in a state of replicative competence; a

"proliferation or progression phase", where expansion of the entire hepatocyte population takes place; and a "termination phase", where cell proliferation is suppressed to terminate regeneration at a defined set point (**Figure IV**). However, the three phases are linked, and they share several mechanisms. In addition, proliferation in the expansion phase subsequently requires a complex re-design of the lobule, a remodeling process representing a "fourth phase" of regeneration (Zimmermann, 2004).

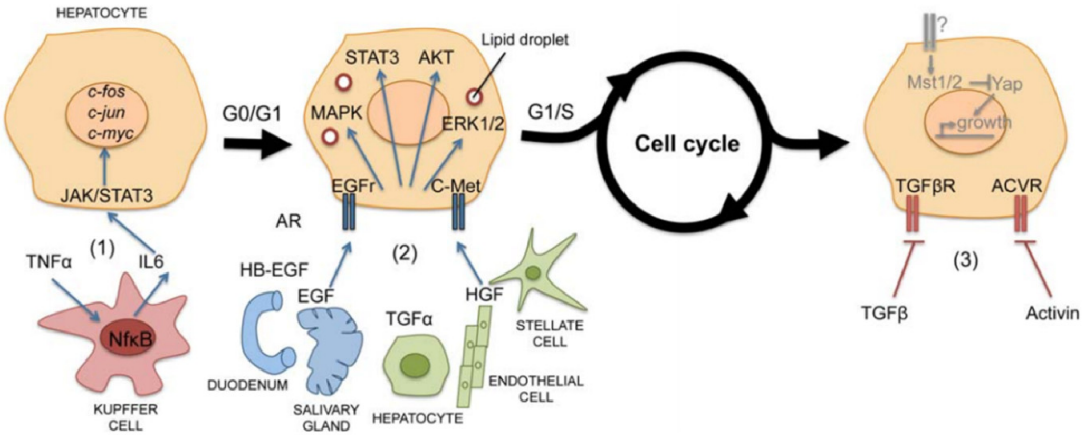

Figure IV. Main steps of liver regeneration after partial hepatectomy. 1) "Priming" phase. 2) "Progression/proliferation" phase. 3) "Termination" phase (Gilgenkrantz and Collin de l'Hortet, 2011).

The first phase is called, as mentioned before, the **"priming phase",** and occurs in the first 4 hours after PH (**Figure IV and V**). Hepatocytes resting in a proliferative quiescence (the G_0 phase) can rapidly and synchronously enter into the cell cycle upon stimulation, and undergo one to two rounds of replication before returning to quiescence. In their quiescent state, hepatocytes do not fully respond to growth factors and need to be "primed" to enter the cell cycle (G_1 phase) and respond to growth factors. The cytokine network acts as the priming phase of liver regeneration. Liver regeneration begins with the recognition of the pathogen-associated molecular patters (PAMPs) and the damage-associated molecular patterns (DAMPs) released from necrotic cells after tissue injury. They trigger the natural immune response-C3a and C5a complement fraction activation, tumor necrosis factor-alpha (TNF-α) secretion by Kupffer cells, and interleukins IL-6, IL-1β and IL-8 synthesis, which afterwards induce the hepatocytes to proliferate. In brief, there is an initial activation of nuclear factor-kappa B (NF-κB) in Kupffer cells via TNF, lymphotoxin (from T cells), and/or complement components, with downstream secretion of IL-6. In turn, IL-6 binds its receptor on hepatocytes and leads to activation of the transcription factor signal transducer and activator of transcription 3 (STAT3), among other pathways. Then, several immediate-early genes related to hepatocyte proliferation are induced within 2 hours, such as c-Fos, c-Jun and others. In fact, c-Jun terminal kinase (JNK)/c-Jun pathway is a critical component of the early proliferative response and induces the G_0 to G_1 transition via Cyclin D1 (Cienfuegos et al., 2014; Gilgenkrantz and Collin de l'Hortet, 2011; Michalopoulos, 2010; Riehle et al., 2011; Zimmermann, 2004).

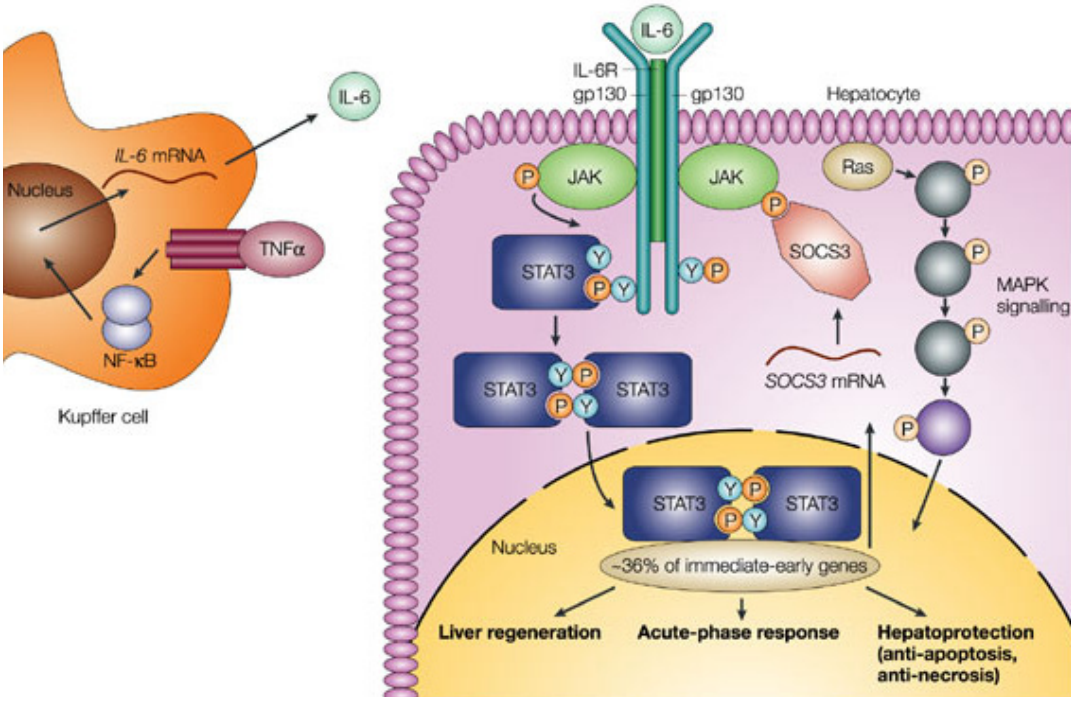

Figure V. The interleukin-6-STAT3 signaling pathway during the "priming phase" of liver regeneration (Taub, 2004).

Of special relevance for this work, related to the second "proliferation/progression" phase of LR, is the **control of cell cycle**. Cell cycle is divided into four phases: the gap 1 (G_1) phase, the DNA synthesis (S) phase, the gap 2 (G_2) phase and the mitosis (M) phase. Cellular division ends with the cytokinesis giving rise to two daughter cells, which can reinitiate the cell cycle or return to the previous G_0 state. G_1 and G_2 phases take place before DNA synthesis and mitosis, respectively, adding extra time for cellular growing and surveillance of the transition to the following phases according with extracellular and intracellular signals. The cell cycle has three **control checkpoints**: restriction or "R" checkpoint, which defines the entry into the cycle in late G_1 phase; and the two mitotic control checkpoints: the G_2/M, regulating the entrance in mitosis, and the control checkpoint of the progression through M phase. The progression of the cell cycle is tightly **regulated by cyclins and cyclin dependent kinases (CDKs)**, whose production and activity is affected by a wide variety of external factors, such as growth factors. During each of the phases, a specific cyclin forms a complex with a specific CDK. For instance, Cyclin D forms a complex with CDK4 or CDK6 at the beginning of G_1 phase, allowing the activation of CDK4/6. This complex then phosphorylates the retinoblastoma protein (Rb), leading to E2F transcription and subsequent transcription of genes required for cell cycle progression, such as Cyclin E and A. The cell cycle can be regulated by adjusting the expression of cyclins and CDKs but can also be influenced by modulating CDK activity by kinases and phosphatases such as cdc25. Nevertheless, CDK activity can also be modulated by CDK-inhibitors (CKIs) family, which consists of: inhibitor of CDKs (INK4) family and the CDK-interacting protein (CIP) family. The INK4 family consists of four proteins which inhibit Cyclin D

binding to CDK4 and CDK6: $p15^{INK4B}$, $p16^{INK4A}$, $p18^{INK4C}$ and $p19^{INK4D}$. The CIP family inhibits all cyclin-bound CDKs and consists of three proteins: $p21^{CIP1}$, $p27^{KIP}$ and $p57^{KIP2}$. The majority of mitogens and growth factors, such as epidermal growth factor (EGF), hepatocyte growth factor (HGF) and transforming growth factor-beta (TGF-β), regulate the rate of cell division in the "R" check point, when the cell is more sensitive to external factors (Cienfuegos et al., 2014).

Continuing with liver regeneration, the second phase or **"progression/proliferation phase"** corresponds to the transition from G_1 to the completion of mitosis (**Figure IV**). After cytokines have triggered the G_0 to G_1 transition, cell cycle progression is driven by growth factors, which override the G_1 restriction point denominated "R", which decides if the cells divide irreversible, allowing hepatocytes to pass into the S phase. This passage is associated with Rb phosphorylation, and an increased expression of the Rb family member p107 and of Cyclins D, E and A. DNA synthesis (S phase) has been reported during 24 and 36 hours post-hepatectomy in rat and in mouse, respectively. After, hepatocytes enter into mitosis at 48 hours post-PHx. Concomitantly, two main growth factors receptors, namely Epidermal growth factor receptor (EGFR) and c-Met will be activated, stimulating the progression of hepatocytes through the cell cycle during liver regeneration. It seems that both have unique and potentially overlapping functions. The receptor c-Met is activated by the mitogen HGF, which is released from the ECM following PH, but it is also produced by non-parenchymal cells, such as HSCs and SECs. On the contrary, EGFR on hepatocytes is activated through different sources: in an autocrine manner by amphiregulin (AR) and transforming growth factor-alpha (TGF-α); in a paracrine manner by heparin binding EGF-like growth factor (HB-EGF) derived from Kupffer cells and SECs; and in an endocrine manner by EGF, secreted from salivary glands and from Brunner's glands in the duodenum, from where it reaches the liver through the portal vein. Ligands of EGFR have different but often overlapping functions. Both c-Met and EGFR are receptor tyrosine kinases, which recruit enzymes and scaffolding proteins to phosphorylate intracellular domains of each receptor, thus activating multiple intracellular signaling pathways. Among them, Mitogen-activated protein kinase (MAPK), STAT3, Phosphatidylinositol-3-kinase (PI3K)/Akt and Extracellular signal-regulated kinase 1 and 2 (ERK1/2) are the most important for liver regeneration, which in turn regulate a multitude of transcription factors, initiate translation and regulate metabolic pathways. Indeed, the hepatocyte proliferative response during liver regeneration is coincident with a potent activation of immediate-early transcription factors including c-Jun, c-Fos, c-Myc, NF-κB, STAT3 and C/EBPβ proteins (which controls the G_1/S checkpoint). Together with the induction of intermediate and early-delayed genes, such as cyclins and CDKs, they facilitate the transition to DNA synthesis and mitosis. Proliferation of hepatocytes proceeds from the periportal to pericentral areas of the liver lobule. The cellular proliferation accounts in a chronological and sequential order: hepatocytes divide first, followed by Kupffer cells, endothelial cells, and finally vascular and biliary canaliculi neoformation (Böhm et al., 2010; Cienfuegos et al., 2014; Fausto et al., 2006; Gilgenkrantz and Collin de l'Hortet, 2011; Kang et al., 2012; Mao et al., 2014; Riehle et al., 2011; Zimmermann, 2004).

It is important to mention that, after PH, the **metabolic demands** of the liver during regeneration are immense. The liver must continue to regulate systemic energy levels while meeting its own demands for significant nucleotide and protein synthesis needed for cell division. Translation is the control point that integrates nutrient levels with mitogenic signals and most proteins involved are downstream of mammalian target of rapamycin (mTOR). Therefore, the mTOR complex may regulate regeneration by modulating cell size and proliferation based on energy demands (Fausto et al., 2006; Mao et al., 2014; Riehle et al., 2011).

ECM reorganization is another early feature after PH that has profound effects on initiation of liver regeneration by releasing locally available latent growth factors. In fact, there is a complete remodeling of the lobule architecture during liver regeneration, observing a reduction in the normal sinusoidal network, accompanied by at least a partial loss of the space of Disse and a degradation of ECM through metalloproteinases. By 48 hours post-PHx, insinuation of small vessels, associated with re-synthesis of ECM proteins, the reconstitution of a space of Disse, and the repopulation of this space with HSCs, is observed. The resulting parenchymal unit is oversized, and the final achievement of a normal lobule requires termination and remodeling mechanisms, such as the balance between apoptosis and hepatocyte survival (Kang et al., 2012; Zimmermann, 2004).

The last step is the **"termination"** of liver regeneration (**Figure IV**). The initial burst of hepatocyte proliferative activity is followed by secondary waves of mitosis until the original mass of the liver is restored. However, the growth response must finally be terminated, although the precise mechanisms leading to the proper termination remain poorly understood. It is known that it involves multiple factors, including the TGF-β family, such as TGF-β1 and activins. In fact, there is evidence that the number of hepatocytes produced during liver regeneration may exceed the original. Then, a small wave of hepatocyte apoptosis at the end of regeneration it seems to be observed, and TGF-β1 is a known suppressor of hepatocyte proliferation and inducer of apoptosis (Gilgenkrantz and Collin de l'Hortet, 2011; Mao et al., 2014; Michalopoulos, 2010; Zimmermann, 2004).

2. Liver disorders

The liver is unique in its response to injury, demonstrating an extraordinary capacity of compensatory growth in response to conditions that induce cell loss by physical, infectious, or toxic injury, simultaneously undergoing regeneration and fibrosis (Rozga, 2002; Zhang and Friedman, 2012).

Liver injuries can be divided into two different groups, accordingly to the duration or persistence of liver injury: **acute** and **chronic liver diseases**. The elimination of the damaging agent can rapidly revert acute liver injuries and usually there is a complete restoration of normal liver architecture and function, without evidence of the preceding insult. However, when liver injury persists for a long time, it drives to a chronic liver disease. Progressive fibrosis is the hallmark of chronic liver injury and it can eventually result in cirrhosis, liver failure or hepatocellular carcinoma (HCC) (**Figure VI**) (Malhi and Gores, 2008).

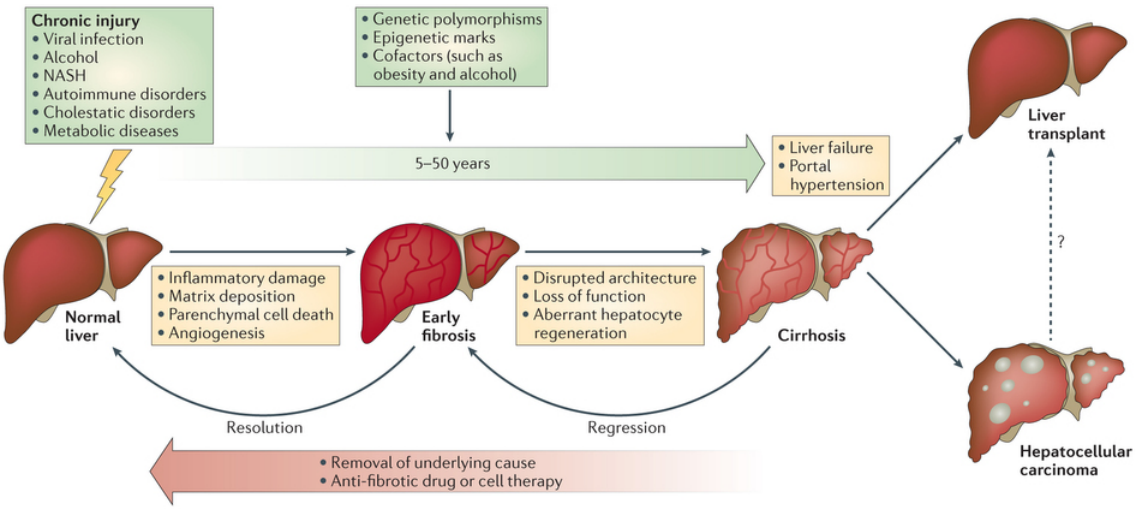

Figure VI. Natural history of liver disease (Pellicoro et al., 2014).

Briefly, the main liver disorders that affect population these days are acute liver injuries (mainly due to toxic insults), cholestatic liver injuries, chronic viral hepatitis, alcoholic and non-alcoholic steatohepatitis, fibrosis and liver cancer (Malhi and Gores, 2008).

2.1. Hepatocellular carcinoma

2.1.1. Epidemiology, risk factors and prevention

The liver displays an incredible wound healing and regenerative capacity, as it has been exposed above. However, when liver injury is chronic, these regenerative mechanisms become dysregulated, facilitating the accumulation of genetic alterations leading to uncontrolled cell proliferation and the development of **hepatocellular carcinoma (HCC).**

HCC is a major public health problem worldwide with over 700,000 new cases each year and its incidence is increasing in Europe and worldwide. HCC is the sixth most prevalent cancer and the third leading cause of cancer-related deaths, following lung and stomach cancers. HCC is the most common primary liver malignancy in adults. Intriguingly, there are important differences on the incidence when considering the gender, being the male to female ratio estimated to be 2.4. This difference is mainly attributed to the different exposition to risk factors, as well as the influence of androgens and estrogens on HCC progression. Exposition to risk factors also determines the incidence of liver cancer regarding age or ethnicity. In fact, the highest incidence of HCC is found in Asia and sub-Saharian Africa (Bruix et al., 2014; European Association For The Study Of The Liver and European Organisation For Research And Treatment Of Cancer, 2012; Tabrizian et al., 2014).

In most cases, HCC develops within an **established background** of chronic liver disease. The **main risk factors** for development of HCC include infection with hepatitis B virus (HBV), the dominant risk factor in eastern Asia and sub-Saharan Africa together with exposure to aflatoxin B1, or hepatitis C virus (HCV), which together with excessive alcohol consumption are the main risk factors in North America, Europe and Japan. Other risk factors include non-alcoholic fatty liver disease (NAFLD), non-alcoholic steatohepatitis (NASH), autoimmune hepatitis, and the presence of various metabolic diseases (such as insulin resistance, type II diabetes or obesity). Progressive hepatic fibrosis, which is a common pathway for all forms of chronic liver disease, evolves to cirrhosis, which is the largest risk factor for developing liver cancer. Up to 90% of cases of HCC arise in the setting of advanced fibrosis or cirrhosis regardless of etiology (**Figure VII**) (Bruix et al., 2014, 2016; Wallace and Friedman, 2014).

Since HCC develops within an established chronic liver disease, avoiding the exposure to risk factors for these chronic liver diseases is the best option to **prevent** HCC. HBV infection accounts for more than 50% of all HCC cases, and in HCV, 3-5% of the cases of established cirrhosis evolve to HCC. Thus, HCC can be prevented by avoiding the acquisition of risk factors for chronic liver disease, and vaccination and antiviral treatment will have a positive impact. However, if antiviral intervention is delayed until the establishment of cirrhosis, preventive efficacy will be diminished. Alcohol consumption constitutes also an important risk factor for HCC and it provokes a synergistic effect when there is an infection with HBV, HCV or both (Bruix et al., 2014; Forner et al., 2012).

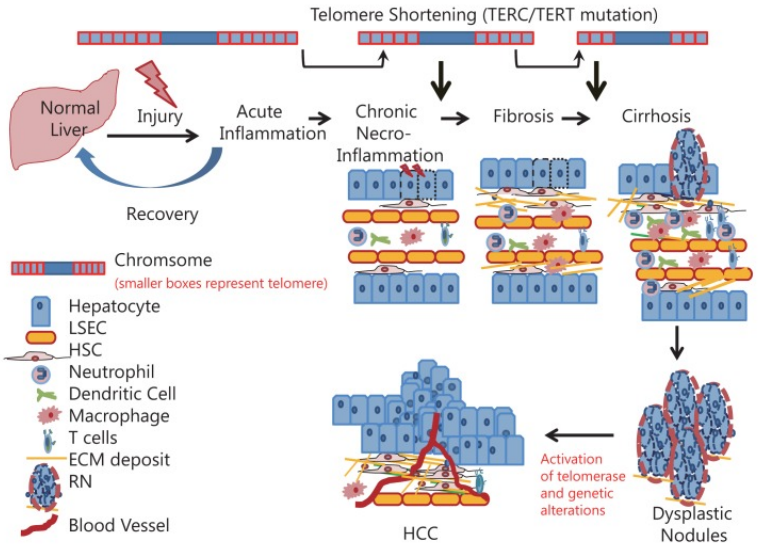

Figure VII. Diagrammatic representation of various pathological changes that lead to the appearance of HCC (Ramakrishna et al., 2013).

2.1.2. Animal models

Numerous experimental models have been developed to define the pathogenesis of HCC and to test novel drug candidates. Murine HCC models can be divided into four main categories: chemically induced HCC, oncogene driven HCC, xenograft models and genetically modified mice (GMM) (Hernandez-Gea et al., 2013).

Chemically induced models, especially Diethylnitrosamine (DEN) model, are among the most common used in HCC research, because of the similarity with the injury-fibrosis-malignancy cycle seen in humans. DEN belongs to the category of genotoxic chemical carcinogens, as its carcinogenic capacity is due to its capability of alkylating DNA structures and causing damage on it: DEN is hydroxylated to α-hydroxylnitrosamine; this bioactivation step is oxygen- and NADPH-dependent and is mediated by cytochrome P450. After cleavage of acetaldehyde, an electrophilic ethyldiazonium ion is formed. This ion causes DNA damage by reacting with nucleophiles such as DNA-bases. DEN works in a dose dependent manner and the time needed for HCC development also depends on sex, age and strain of mice. The liver lesions appear sequentially, starting with adenomas and the later development of hyperplasic nodules. Other chemicals used to induce HCC development are CCl_4, aflatoxin B1, thioacetamide (TAA) and a choline deficient diet (CDD) (Fausto and Campbell, 2010; Heindryckx et al., 2009; Hernandez-Gea et al., 2013).

Another model of HCC development is by means of conditional **overexpression** of the **oncogenic protein** Myc, in which the expression of human Myc is regulated in murine liver (Hernandez-Gea et al., 2013).

In **xenograft models**, tumors are generated by injecting human cancer cells from a lab

culture into immune deficient mice. The tumor xenograft can be established either by direct implantation of biopsy material or by inoculation of human tumor cell lines. Two main modalities can be distinguished: subcutaneous injection in the flank of the mice (ectopic model) or directly injected to the liver (orthotopic model). Subcutaneous model enables to follow the appearance and increase of the tumor mass easily, while implantation in the liver better replicates the tumor environment and it is more suitable for extrapolation to humans, giving information about the metastatic spread of the tumor (Heindryckx et al., 2009; Hernandez-Gea et al., 2013).

Finally, **GMM** are engineered to mimic pathophysiological and molecular features of HCC. The most common ones can be divided in two groups: transgenic mice, which carry the overexpression of a specific gene, and knock-out mice, in which a gene was deleted. There are many GMM models, such as overexpressing TGF-α, Myc, β-catenin and HRAS, or Phosphatase and tensin homolog (PTEN) knock-out mice, among others (Heindryckx et al., 2009; Hernandez-Gea et al., 2013; Sánchez and Fabregat, 2009).

2.1.3. Molecular mechanisms of HCC

Hepatocarcinogenesis is a **complex multistep process** in which many signaling cascades are altered, leading to a heterogeneous molecular profile. **Tumor heterogeneity** in HCC is impressive: it can be observed between patients, between nodules in the same patient (such as that found in second primary tumors after curative treatment or synchronous multifocal tumors of different clonality) and even within a single tumor nodule. However, some molecular pathways are known to be clearly involved in HCC (**Figure VIII**). HCC is a highly angiogenic solid tumor characterized molecularly by cell cycle dysregulation, aberrant angiogenesis, and evasion of apoptosis. The molecular pathogenesis of HCC is very complex, comprising of multiple genetic and epigenetic alterations, chromosomal aberrations, gene mutations, and altered molecular pathways. Angiogenesis plays a vital role in the growth, invasiveness and metastatic potential of HCC (Lu et al., 2016; Schlachterman et al., 2015).

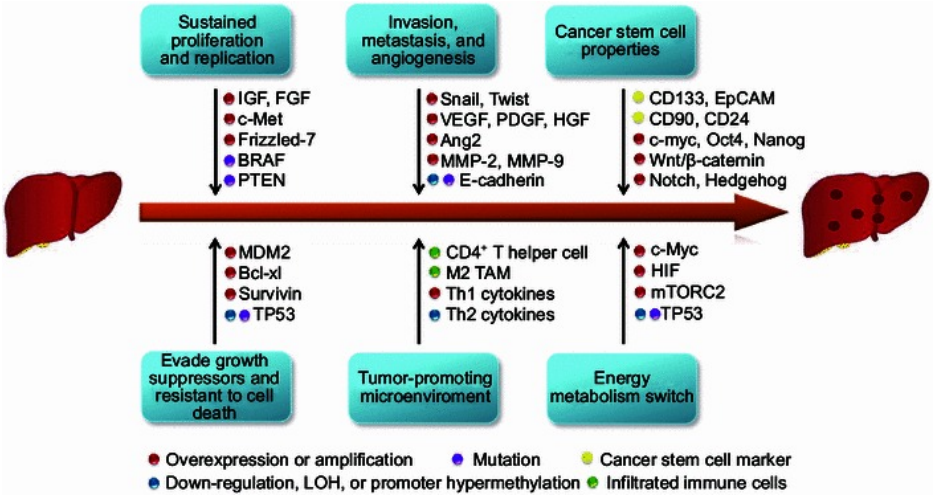

Figure VIII. Multiple cancer hallmarks and the underlying molecular alterations in the progression of HCC (Liu et al., 2014a).

Next-generation sequencing has helped deciphering the **mutational landscape** of HCC. The major pathways commonly altered by somatic mutations or homozygous deletions include Wnt/β-catenin, p53 and PI3K/Ras signaling pathways, oxidative and endoplasmic reticulum stress modulators, and processes responsible to chromatin remodeling (Bruix et al., 2014). The most common somatic mutation involves telomerase reverse-transcriptase (*TERT*) gene aberrant activation, observed in almost 70% of HCC cases. Following *TERT* mutations, the main ones include the tumor suppressor gene *TP53* (in about 30% of HCC cancers), and *CTNNB1*, the gene encoding for β-catenin (also in about 30% of HCCs, predominantly in HCV-related cases). In addition to *CTNNB1*, inactivating mutations of other members of the Wnt pathway, such as *AXIN1* (11%), are also recurrently described in HCC samples (Bruix et al., 2016; Lee, 2015; Schulze et al., 2016). Also chromosomal amplifications (such as 11q13, which contains the genes coding for Cyclin D1 and FGF19, and 7q31.2, which contains the gene encoding for MET), and deletions (such as 9p21.3, which contains tumor suppressor genes, like *CDKN2A*, *CDKN2B* or *PTEN*) are common (Wang et al., 2013). Silencing of tumor suppressors and reactivation of oncogenes by epigenetic alterations have been also described. Finally, transcription of key oncogenes can be also modulated by miRNAs (Toffanin et al., 2011). As a result of all these alterations, several signaling cascades related to cell survival and proliferation, angiogenesis, invasion and metastasis are dysregulated.

Altered **proliferation pathways** have been correlated with liver cancer, as it happens in most of the cancers. Among these alterations, the most frequently reported pathways involve growth factors such as EGF, HGF and IGF. **EGFR pathway** is overactivated in many patients with HCC. Different sources of evidence suggest activation of EGFR in a subset of HCCs, both at the transcriptomic and proteomic levels, reduced turnover of the receptor, DNA copy number gains in chromosome 7, where there is the locus of *EGFR*, and/or modifications in EGFR ligands levels (Sia and Villanueva, 2011). Considering the relevance of EGFR pathway in this work, it will be further discussed in a separate section (**Section 3**). **HGF/Met axis** is known to be involved in cell proliferation and tumor invasion or metastasis in several malignancies. In addition to tissue regeneration, mentioned in a previous section (**Section 1.3**), c-Met regulates cell proliferation, migration, survival, branching morphogenesis and angiogenesis. Met activation has been found in 20-40% of HCC, mainly through both the receptor and its ligand. c-Met-regulated expression signature defines a subset of HCC in humans, as these patients have a poor prognosis and an aggressive phenotype (Sia and Villanueva, 2011; Whittaker et al., 2010). **IGF signaling**, through IGF-1R, is important for the regulation of growth and development, but also in proliferation, motility and inhibition of apoptosis. It has been shown to be involved in the pathogenesis of several malignancies. Overexpression of IGF-1 and IGF-2 receptors and downregulation of IGF binding proteins contribute to proliferation of cancer cells, anti-apoptosis, and invasive behavior. Thus, *IGF-2* is overexpressed in 16-40% of human HCCs. It is upregulated by epigenetic mechanisms after an inflammatory response to liver damage or viral transactivation, or by an altered methylation of the gene (Schlachterman et al., 2015; Whittaker et al., 2010).

Upon EGFR, Met and IGFR activation, extracellular signals can be transduced through different cytoplasmatic intermediates, such as PI3K/Akt/mTOR or RAS/MAPK pathways. The RAS/Raf/MAPK pathway is typically activated in HCC as a result of increased signaling from upstream growth factors, and not due to RAS mutations, as it usually happens in other solid tumors. The PI3K/Akt/mTOR signaling, which controls proliferation, cell cycle and apoptosis, is overactivated in HCC. Akt can be activated through stimulation of tyrosine kinase receptor, particularly IGFR and EGFR, or through constitutive activation of PI3K or loss of function of the tumor suppressor gene PTEN by epigenetic silencing or somatic mutations (Llovet and Bruix, 2008; Whittaker et al., 2010).

Moreover, **cell cycle dysregulation** in HCC can be provoked not only as a consequence of the growth factor overactivated signaling pathways, but also of direct alteration of cyclins, CDKs and/or their regulators (Ao et al., 2014; Che et al., 2012).

Besides growth factor related pathways, some data indicate aberrant activation of pathways involved in **cell differentiation and development**, such as Wnt signaling. β-catenin, a key component of this pathway, is mutated in HCCs as mentioned before, and approximately 50-70% of HCC tumors have increased levels of it in the cytoplasm and nucleus (Whittaker et al., 2010). In addition, Wnt pathway overactivation might be as a consequence of overexpression of Frizzled receptors, or inactivation of E-cadherin or members of the degradation complex (GSK3β, AXIN and adenomatosis polyposis coli (APC)). Other pathways related to cell differentiation such as Hedgehog and Notch are also described to be overactivated in HCC (Sia and Villanueva, 2011).

The role of the **microenvironment** in tumor initiation and progression in HCC is critical. Together with other concurrent tissue responses such as angiogenesis, chronic inflammation and oxidative stress, defines the tumor biology. Important proliferative, angiogenic, and regenerative cytokines secreted by HSC contribute to the carcinogenic process. These include transforming growth factors (TGF-α and TGF-β), platelet-derived growth factors (PDGF-B and PDGF-C), HGF, vascular endothelial growth factor (VEGF) and IL-6 (Hernandez-Gea et al., 2013; Rani et al., 2014).

HCC is a highly vascularised cancer and **angiogenesis** plays an important role in hepatocarcinogenesis from its early stages. Indeed, experimental studies suggest that targeting angiogenesis is of major relevance in HCC. Normal angiogenesis is maintained by the balance between pro-angiogenic and anti-angiogenic factors and this balance is disturbed in HCC. The response due to chronic liver injury leading to fibrogenesis concurs with the secretion of several pro-angiogenic factors by the stromal cells, especially matrix metalloproteinases (MMPs), VEGF-A, angiopoietin-2, PDGF, FGF and TGF-β, and most of them have been shown to be upregulated in HCC (Forner et al., 2012; Hernandez-Gea et al., 2013; Whittaker et al., 2010).

HCC arises in a diseased liver with a **dynamic and chronic inflammatory environment**

that predisposes to the initiation of cancer. However, there still exist big gaps in the understanding of the molecular link between inflammation and HCC. It is suggested that chronic inflammation drives a maladaptive reparative reaction and stimulates liver cell death and regeneration, eventually associated with the development of dysplastic nodules and cancer. Some studies support the role of NF-κB, hypoxia inducible factor 1α (HIF1α) and STAT3 as the major molecular players linking inflammation and cancer. Also, altered cytokine profiles have been described in HCC not only in tumor cells but also in the surrounding tissue. Among all the inflammatory cytokines involved, IL-6, which in turn activates JAK-STAT and MAPK pathways, is thought to be the most abundant. Additionally, several growth factors such as HGF, EGF and TGF-β are known to regulate the immune and inflammatory response in HCC microenvironment (Capece et al., 2013; Hernandez-Gea et al., 2013; Ramakrishna et al., 2013).

Additionally, several alterations in the **ECM** occurring during progressive fibrosis/cirrhosis predispose to the development of HCC. Accumulation of collagenous and non-collagenous ECM is controlled in part by MMPs, which degrade substrates, and tissue inhibitors of metalloproteinases (TIMPs). HSC are the major source of MMP and TIMP, and their activity is controlled by cytokines. MMP and TIMP are important in progression of hepatocytes from dysplasia to the development of poorly differentiated HCC (Wallace and Friedman, 2014). Many cell-to-matrix interactions are transmitted via transmembrane adhesion molecules, in particular integrins, that bind growth factors and components of the ECM. Integrin expression patterns are altered in human HCC, linked to cell proliferation, adhesion, invasion, migration and apoptosis, favoring the progression of HCC and metastasis (Wu et al., 2011).

Finally, during last years it has become evident that **oxidative stress** is playing a relevant role in liver carcinogenesis. For example, overproduction of ROS provokes nitrosative and oxidative stress through interaction with DNA, RNA, lipid and proteins, leading to an increase in mutations, genomic instability, epigenetic changes and protein dysfunction (Hernandez-Gea et al., 2013). However, recently in our group, it has been described a relevant liver tumor suppressor role for the NADPH oxidase NOX4, negatively modulating hepatocyte proliferation an invasion (Crosas-Molist et al., 2014 and under revision manuscript).

2.1.4. HCC and metastasis

HCC is one of the most aggressive human malignancies, with high rate of recurrence that can be divided in intrahepatic and extrahepatic patterns. **Intrahepatic recurrences** can be as a result of multicentric occurrence or intrahepatic metastasis of HCC (Utsunomiya et al., 2010). On the other side, **extrahepatic metastasis** can occur by direct extension, hematogenous spread or lymphatic invasion. Reported HCC metastatic sides include lungs, lymph nodes, bone, peritoneum and/or omentum and brain. Other rare sides of metastasis have also been described (Becker et al., 2014). Being the metastasis an important process for this work, it will be further detailed in a separate section (**Section 4**).

2.1.5. Diagnosis and management of HCC

Very advanced HCC is untreatable, and most patients die within 3 to 6 months. In many patients, HCC is asymptomatic and when symptoms occur, they are usually related to those of chronic liver disease. Over the past decades, more asymptomatic patients are being diagnosed as a result of the active **surveillance** and the increased awareness of HCC in high risk patients, especially in those with cirrhosis. In fact, HCC is the main cause of death in patients with cirrhosis, and long-term disease-free survival will rely on its early detection and treatment. Patients with high risk of HCC development undergo surveillance through periodic hepatic ultrasonography (US) and AFP blood test (Flores and Marrero, 2014; Janevska et al., 2015; Bruix et al., 2016).

Patients can be **diagnosed** with HCC based on imaging or biposy analyses. **Imaging** has a central role in the diagnosis of HCC, based on a dynamic pattern of the arterial and venous blood in the HCC. In the absence of this typical appearance, a **biopsy** is required to detect HCC. Some biomarkers are currently used for tissue samples staining when diagnose of HCC is not clear. They include CD34, CK-7, glypican 3, HSP-70 and glutamine synthetase. CK-19 and EpCAM are recommended stainings for detection of progenitor cell features (Bruix et al., 2016; Flores and Marrero, 2014).

As in many cancers, assessment of **prognosis** is a crucial step in management of patients with HCC. Prognosis should be assessed accordingly to tumor stage, degree of liver dysfunction and presence of cancer-related symptoms. Among the many **HCC staging** systems that have been developed around the world, the **Barcelona Clinic Liver Cancer (BCLC) system** has been widely validated and is the most commonly used staging system for HCC (**Figure IX**). It determines cancer stage and patient prognosis, stratifying HCC patients according to outcome. It establishes treatment recommendations for all stages of HCC, depending on overall size of the tumor, number and size of the nodules, liver physical and functional status and cancer-related symptoms. Thus, BCLC identifies patients with very “early or early-stage” HCC (BCLC 0 or BCLC A), with solitary lesion or up to 3 nodules < 3 cm (without macrovascular invasion or extrahepatic spread) and preserved liver function, which are potentially curable (by resection, liver transplantation or ablation). Patients with “intermediate-stage” HCC (BCLC B) do not have symptoms, but they have large, multifocal tumors without vascular invasion or spread beyond the liver, and they can be candidates for transarterial chemoembolization (TACE). Those patients with “advanced stage” HCC (BCLC C) have tumors that have spread beyond the liver and/or vascular invasion and/or mild cancer-related symptoms. For patients with intermediate or advanced disease stage, there is no curative treatment, and palliative treatments offer the likelihood of extended survival. Finally, patients with “end-stage” disease (BCLC D), for whom treatment would provide more harm than benefit, require supportive care (Bruix et al., 2016; Forner et al., 2012).

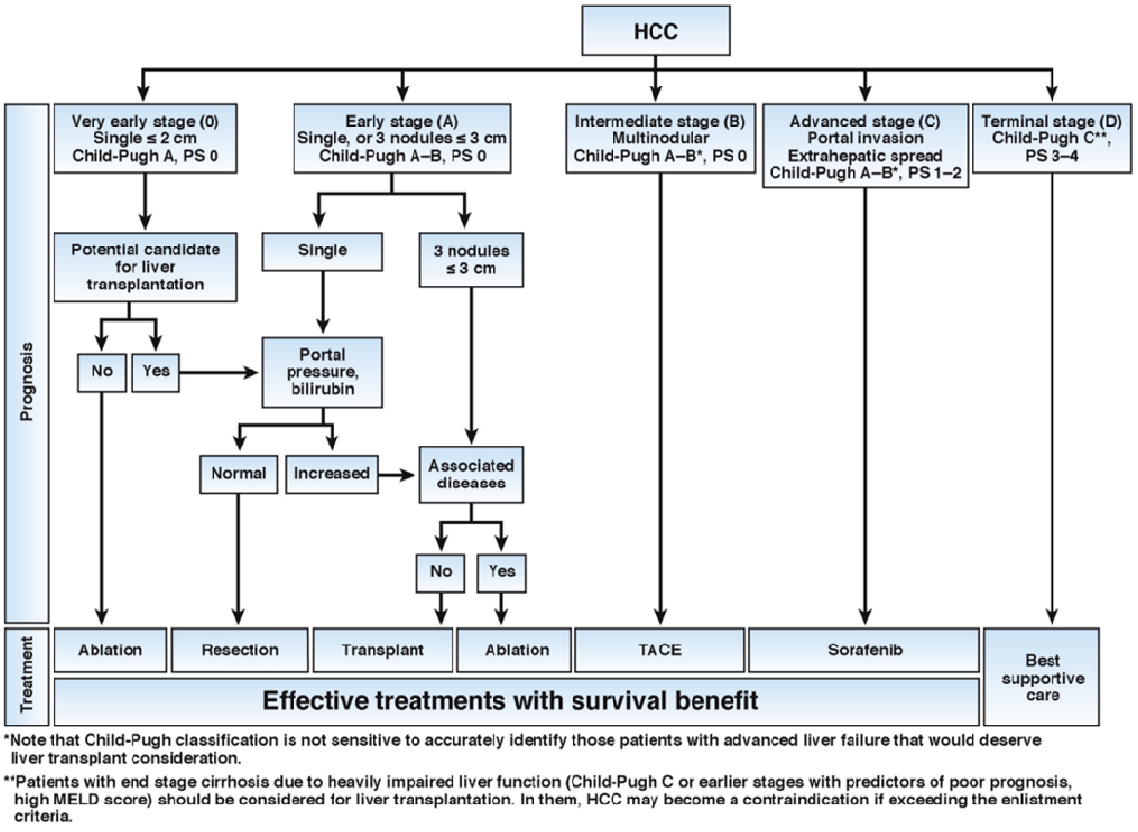

Figure IX. Staging and treatment for HCC according to the BCLC system.

Prior to 2007, there was no single systemic therapy with proven efficacy in advanced-stage HCC. This might be due to the high molecular heterogeneity and resistance to conventional chemotherapy. **Sorafenib** is the first oral multikinase inhibitor with broad inhibitory profile (for example BRAF, PDGFR, VEGFR-2 and c-Kit receptors) approved for the treatment of "unresectable" HCC by FDA in 2007, based on the results of two large multicenters randomized controlled trials: SHARP (Sorafenib Hepatocellular Carcinoma Assessment Randomized Protocol) Trial by Llovet et al., (Llovet et al., 2008) and Sorafenib Asia-Pacific Trial by Cheng et al. (Cheng et al., 2009). Both demonstrated an increase in the overall survival in the sorafenib group compared with the placebo group. Sorafenib was noted to have inhibitory effects on cell growth, induction of apoptosis, and down-regulation of anti-apoptotic protein Mcl-1 in preclinical models. The drug was also found to reduce tumor angiogenesis, tumor cell signaling, and tumor growth in a dose dependent manner in mouse xenograft models of HCC by blocking Raf/MEK/ERK pathway and other extracellular receptor tyrosine kinases (Flores and Marrero, 2014; Forner et al., 2012; Schlachterman et al., 2015; Tabrizian et al., 2014; Villanueva et al., 2013). Currently, sorafenib is the only treatment approved for patients at advanced stages of HCC, however there are no biomarkers for response. Thus, there is an urgent need to identify biomarkers to accurately predict patient's response to the drug. In this sense, a recent work from our group demonstrated that CD44 could play an important role in protecting HCC cells

from sorafenib-induced apoptosis in a TGF-β-induced mesenchymal background (Fernando et al., 2015).

There have been many trials of second-line agents after sorafenib; these include novel chemotherapy formulations that aim to increase entry of the drug into cells, agents that might replace cellular components, kinase inhibitors, and oncolytic viruses (Bruix et al., 2016). Similar to sorafenib, molecular targets offer potential new therapies. For example, phase 3 trials are ongoing with Sunitinib (another oral multikinase inhibitor for receptor tyrosine kinases), Linifanib and Brivanib (two-angiogenic therapies), Everolimus (a mTOR kinase inhibitor), or the combination of sorafenib with erlotinib (an EGFR inhibitor). However, most of them have been negative, as well as all agents tested in second line (Bruix et al., 2016; Flores and Marrero, 2014). The most feasible cause of these failures is the suboptimal understanding of oncogenic drivers and molecular subclasses in HCC, together with the common cirrhotic background of HCC patients, which might facilitate drug liver toxicity, impairing to meet the end points of the clinical trials. To try to improve the results from trials, it appears reasonable that the strategy design should be modified. A possible solution would be to incorporate molecular information of the mechanisms responsible for tumor progression in each patient, to design trials with enriched populations based on pathway activation, instead of including “all comers”, in order to maximize the chances of positive clinical outcome benefits (Llovet, 2014; Villanueva et al., 2013).

3. Epidermal Growth Factor Receptor (EGFR)

3.1. EGFR structure and activation

The **epidermal growth factor receptor (EGFR)**, also termed ErbB1 or HER-1, belongs to a family of **tyrosine kinases receptors (TKRs),** that includes other members: ErbB2/HER-2 (also called Neu), ErbB3/HER-3 and ErbB4/HER-4. These receptors are anchored in the cytoplasmic membrane and share similar structure, which is composed of an extracellular ligand-binding domain, a single short hydrophobic transmembrane domain, and an intracytoplasmic tyrosine kinase domain. These receptors play a major role in the activation and regulation of a variety of cellular responses, ranging from proliferation, differentiation or apoptosis, to migration and adhesion. Thus, EGFR family of ligands and receptors have been reported to have a role in embryonic development and physiology, as well as in pathology (Jorissen et al., 2003; Morandell et al., 2008; Scaltriti and Baselga, 2006).

The EGFR is synthesized from a 1210-residue polypeptide precursor; after cleavage of N-terminal sequence, a 1186-residue (170 kDa) glycoprotein is inserted into the cell membrane. Regarding its **structure**, the EGFR extracellular portion (or ectodomain) consists of four domains that are referred as L1 (domain I), CR1 (domain II), L2 (domain III) and CR2 (domain IV) (**Figure X**).

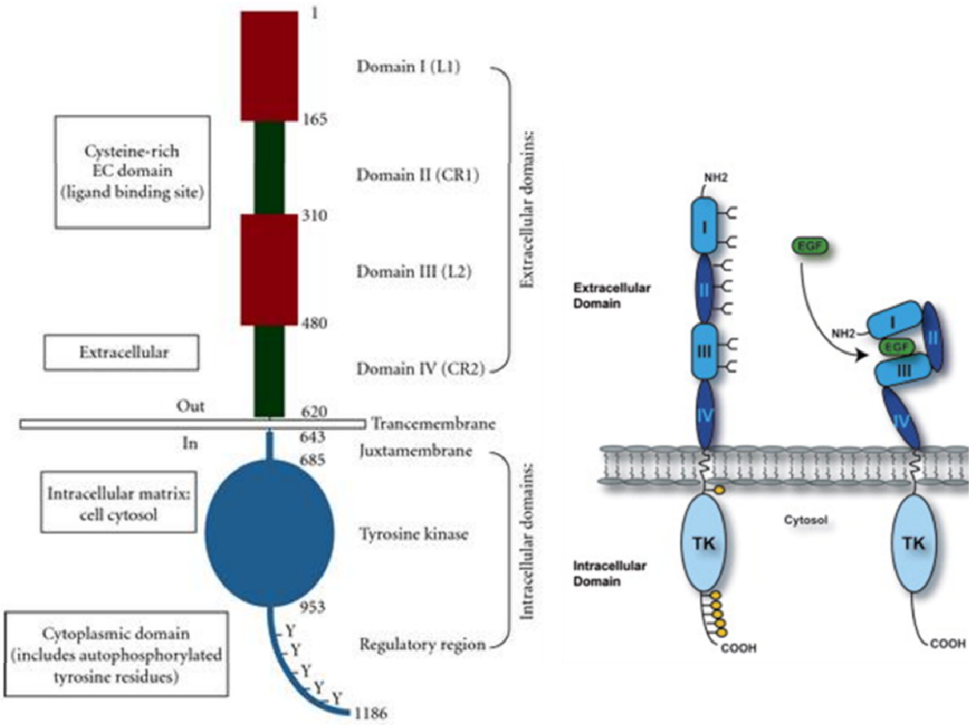

Figure X. (Left) Basic EGFR structure demonstrating relevant domains: an extracellular domain, a transmembrane domain and an intracellular domain containing the tyrosine kinase (TK) activity (Flynn et al., 2009). **(Right)** The EGFR extracellular domain is composed of four subdomains designated I, II, III and IV. The domains I, II and III form a ligand-binding pocket, where a ligand is docked between the domains I and III (Zandi et al., 2007).

Ligands bind between the domain I and domain III (leucine-rich domains) of the EGFR, domain II (cystein-rich domain as well as domain IV) participates in homo and heterodimer formation with ErbB family members, and the transmembrane domain (residues 622-644) is between the domain IV and the yuxtamembrane domain. Finally, the C-terminal domain of the EGFR contains tyrosine residues where their phosphorylation modulates EGFR-mediated signal transduction (Jorissen et al., 2003). Moreover, residues 984-996 in the C-terminus have been identified as a binding site for actin (den Hartigh et al., 1992).

There are six known **ligands** that bind to the EGFR, including EGF itself and TGF-α, but there are other EGF-family of peptides classified in three different groups on the basis of their receptor specificity: first, the already mentioned EGF and TGF-α, together with amphiregulin (AR), and epigen (EPG), which bind specifically to EGFR/ErbB1; the second group includes betacellulin (BTC), HB-EGF, and epiregulin (EPR), which exhibit dual specificity, binding both EGFR and ErbB4; and the third group, the neuregulins (NRGs), forms two subgroups on the basis of their capacity to bind ErbB3 and ErbB4 (NRG-1 and NRG-2) or only ErbB4 (NRG-3 and NRG-4). ErbB2 has not known ligand. The ErbB ligands are synthesized as membrane-anchored precursors. These membrane-anchored peptides can signal to adjacent cells in a yuxtacrine fashion. However, in response to many physiological and pharmacological stimuli, active factors are released when the extracellular domain is proteolytically cleaved by transmembrane metalloproteases belonging to “a disintegrin and metalloproteinases” (ADAM) family, such as ADAM17 (also known as TNFα converting enzyme or TACE), in a process known as “ectodomain shedding”. The soluble growth factors can bind their receptors in an autocrine or paracrine manner (Berasain and Avila, 2014; Hynes and MacDonald, 2009).

EGFR becomes **activated** by receptor overexpression (frequent in cancer) as well as ligand-dependent and ligand-independent mechanisms. **Ligand binding** to the receptor induces a stabilizing conformational change of the receptor ectodomain that allows for receptor homodimerization, which leads to auto- or transphosphorylation by the intrinsic tyrosine-kinase activity on specific and several residues in the cytoplasmic domains. In fact, their activation requires the formation of an asymmetric dimer in which an activator kinase domain allosterically activates a receiver kinase, in a manner analogous to the activation of CDKs by cyclins. Moreover, asymmetric interaction of the yuxtamembrane domains was also described upon ligand-induced rearrangements of the receptor structure, leading to kinase domains interactions and activation. The phosphorylated sites serve as docking sites for various proteins involved in the activation and regulation of numerous intracellular signaling cascades (Jorissen et al., 2003; Morandell et al., 2008; Scaltriti and Baselga, 2006). **Ligand-independent** receptor activation occurs in some tumors that display forms of the EGFR that have a deletion of the extracellular domain that result in constitutive receptor activation, such an in glioblastoma (Endres et al., 2014; Frederick et al., 2000).

Interestingly, EGFR can interact with other molecules to become activated, which is known as **crosstalk**, which implies very different mechanisms including physical interactions, as well as again ligand-dependent and ligand-independent activations. Accordingly, the EGFR activation by heterologous ligands as a consequence of the primary activation of another receptor is named **transactivation**. However, it has also been described the ligand-independent transactivation of EGFR (Berasain et al., 2011; Jorissen et al., 2003; Scaltriti and Baselga, 2006).

Within the ones needing **physical interactions**, the simplest and most obvious EGFR crosstalk involves its heterodimerization with other members of the family, its three known homologues ErbB2, ErbB3 and ErbB4, in a ligand-dependent fashion. Differences in the C-terminal domains of these proteins result in changes to the repertoire of signaling molecules that interact with the heterodimers, thus leading to an expansion in the number of possible signaling pathways stimulated by a single ligand (Jorissen et al., 2003; Morandell et al., 2008; Scaltriti and Baselga, 2006). However, it has been also reported the physical interaction or heterodimerization of EGFR with other TKRs such as PDGF (Saito and Berk, 2001), IGF1R (Morgillo et al., 2006) and c-Met (Jo et al., 2000), and with multiple G-protein coupled receptors (GPCRs) (Liebmann and Böhmer, 2000), as well as with integrins (Comoglio et al., 2003), which was extensively reviewed by Berasain et al. (Berasain et al., 2011). In the **absence of physical interactions**, many GPCRs, cytokine receptors, nuclear hormone receptors and death receptors are able to induce **ligand-independent** EGFR activation. EGFR is used in these cases as a scaffold protein, and specific residues in the cytoplasmic tail of EGFR are phosphorylated by non-receptor kinases such as Jak and Src, providing docking sites for cytoplasmic signaling molecules. Finally, the **ligand-dependent** EGFR transactivation involves the activity of the already mentioned ADAM family of transmembrane metalloproteases, mainly ADAM17/TACE and ADAM10, and the shedding of EGFR ligands. This transactivation can be triggered by GPCRs, cytokine receptors, integrins and other TKRs. Different mechanisms has been proposed to mediate ADAM activation, such as the elevation of the intracellular levels of Ca^{2+} or reactive oxygen species (ROS) and the activation of kinases such as protein kinase C (PKC), ERK, or c-Src (Berasain et al., 2011). In addition, bile acids have been shown to transactivate EGFR (Werneburg et al., 2003).

3.2. EGFR signaling pathway

As already mentioned, activation of the receptor leads to the phosphorylation of key tyrosine residues within the COOH-terminal portion of EGFR and, as a result, provides specific docking sites for cytoplasmic proteins containing Src homology 2 and phospho-tyrosine-binding domains (Scaltriti and Baselga, 2006). These proteins bind to specific phosphotyrosine residues and initiate intracellular signaling via several pathways (**Figure XI**).

First, we found the **Ras/Raf/MAPK pathway**. This is a critically important route that regulates cell proliferation and survival. Following EGFR phosphorylation, the complex formed by the adaptor proteins Grb2 (growth factor receptor protein 2) and Sos binds directly, or through association with the adaptor molecule Shc (Src homology 2 domain containing transforming protein), to specific docking sites on the receptor. This interaction leads to a conformational modification of Sos, now able to recruit Ras-GDP, resulting in Ras activation (Ras-GTP). Ras-GTP activates Raf-1 that, through intermediate steps, phosphorylates the MAPK ERK1/2. Other MAPKs activated in EGFR signaling are JNK and p38. Activated MAPKs are imported into the nucleus where they phosphorylate specific transcription factors involved in cell proliferation. **PI3K/Akt pathway,** which is involved in cell growth, apoptosis resistance, invasion, and migration, is also activated by the activation of the EGFR. PI3K is a dimeric enzyme composed of a regulatory p85 subunit, responsible of the anchorage to ErbB receptor-specific docking sites, and a catalytic p110 subunit that generates the second messenger phosphatidylinositol-3,4,5-triphosphate, which is responsible for phosphorylation and activation of the protein serine/threonine kinase Akt. **Phospholipase Cγ** interacts directly with activated EGFR and hydrolyses phosphatidylinositol-4,5-diphosphate to give inositol-1,3,5-triphosphate, important for intracellular calcium release, and 1,2-diacylglycerol, cofactor in PKC activation, which can, in turn, result in JNK activation. **STAT proteins** are activated by direct interaction with EGFR via their Src homology 2 domains and, on dimerization, translocate to the nucleus and drive the expression of specific target genes. Finally, we find **Src kinase pathway**, which is a non-receptor tyrosine kinase critical in the regulation of cell proliferation, migration, adhesion, angiogenesis, and immune function. Src, which is located in the cytosol, activates a series of substrates, including focal adhesion kinase (FAK), PI3K, and STAT proteins. Although Src functions independently, it also cooperates with other receptor tyrosine kinases signaling, such as EGFR. Other receptor binding proteins are involved in the regulation of receptor signaling by **endocytosis**, such as Eps15 (EGFR pathway substrate 15), or by degradation, initiated by the binding in the C terminus of the ubiquitin ligase Cbl (Jorissen et al., 2003; Morandell et al., 2008; Scaltriti and Baselga, 2006).

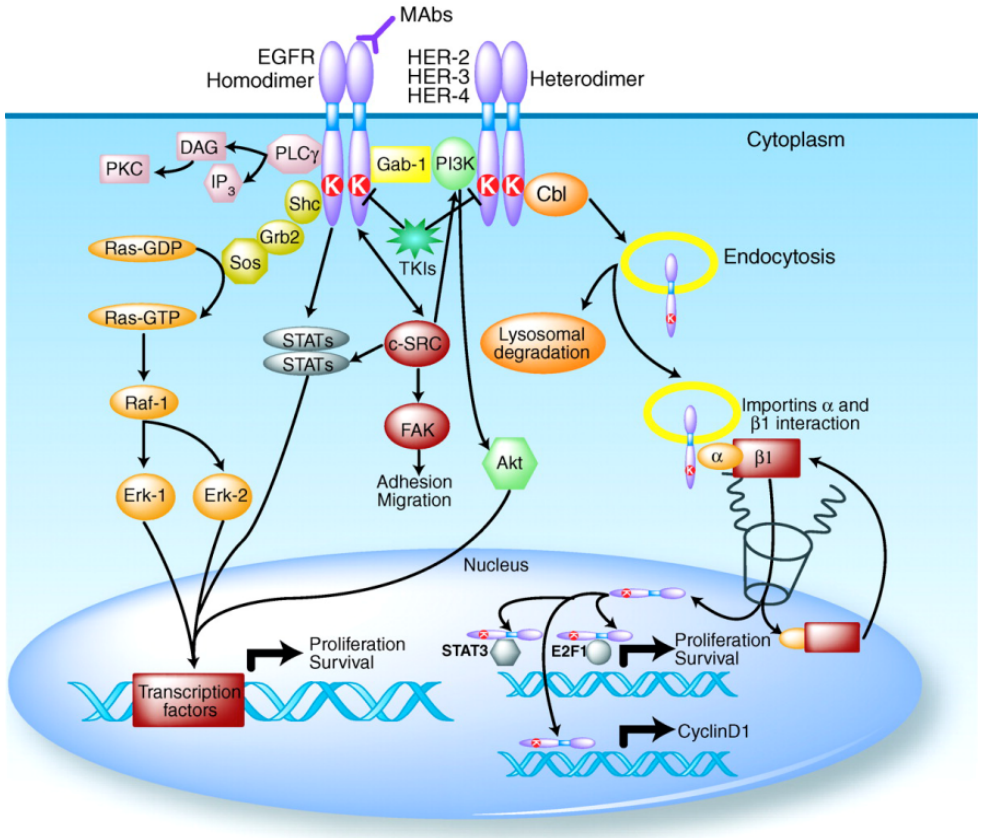

Figure XI. EGFR downstream signaling pathway (Scaltriti and Baselga, 2006).

There is also increasing evidence that the EGFR family of receptors has the ability to translocate to the nucleus where it may exert a variety of biological actions. For EGFR, part of the receptors may escape the internalization and lysosomal degradation route and translocate in the nucleus, where it functions as a transcription factor of the Cyclin D1 gene (Lin et al., 2001).

3.3. EGFR in cancer

The involvement of increased and/or aberrant EGFR activity in human cancers is well documented and cancer patients (most notably with gliomas and breast, pancreas and liver carcinoma) with altered EGFR activity tend to have a more aggressive disease, associated with a poor clinical outcome. There are quite a few mechanisms by which the tight regulation of the EGFR-ligand system can be abrogated. These include: 1) increased levels of EGFR protein, 2) increased production of ligands, 3) crosstalk with heterologous receptor systems, 4) defective downregulation of EGFR and 5) EGFR mutations giving rise to constitutively active variants (**Figure XII**) (Hynes and MacDonald, 2009; Jorissen et al., 2003; Zandi et al., 2007).

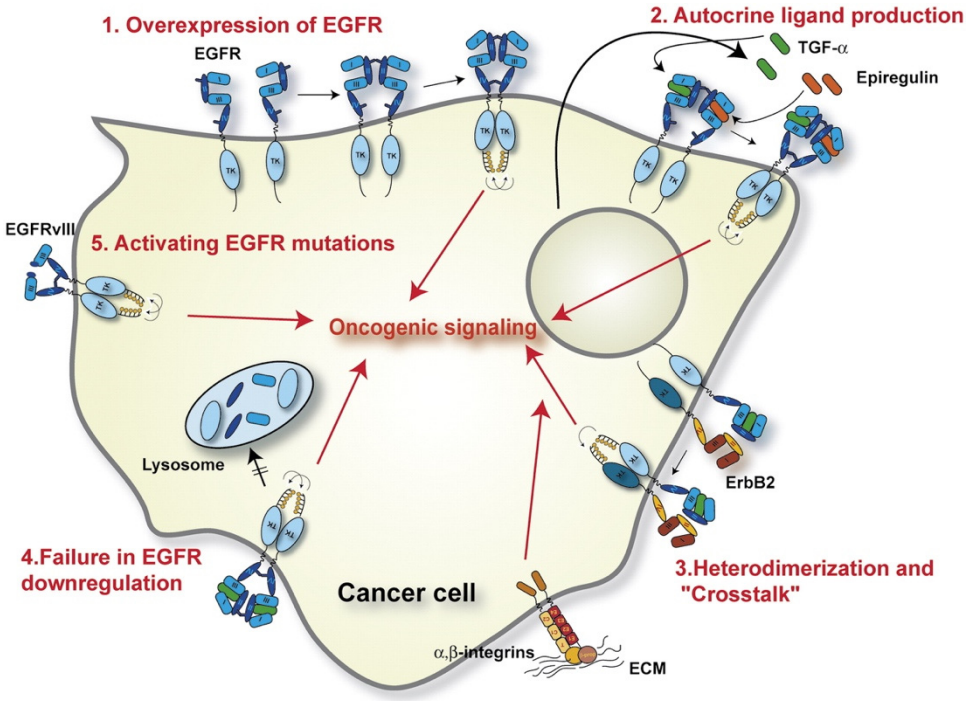

Figure XII. Mechanisms leading to EGFR oncogenic signaling (Zandi et al., 2007).

Various studies evaluated ErbB1 status in HCC and found this receptor frequently **overexpressed** in tumoral tissues. In fact, overexpression of EGFR occurs in 68% of human HCC, correlating with aggressive tumors with high proliferating activity, intrahepatic metastases, poor carcinoma differentiation and a bad prognosis related to poor patient survival. Although overexpression of EGFR is present in the majority of HCCs, this increased EGFR expression does not correlate with an increase in *EGFR* gene copy number (Buckley et al., 2008). This ability is likely due to constitutive receptor activation caused by spontaneous receptor dimerization as a result of high EGFR levels on the cell surface (Berasain and Avila, 2014; Komposch and Sibilia, 2016).

A number of **EGFR mutants** have been observed in tumors where gene amplification has occurred. The best characterized EGFR mutant is the 2-7Δ truncation (or EGFRvIII), in which amino acids encoded by exons 2-7 of the receptor (residues 2-273) are missing, resulting in a protein that lacks most of the extracellular domain. EGFRvIII is the most common EGFR mutation in human cancers, having been detected in 40%-50% of grade VI glioblastomas, and in up to 70% of medulloblastomas and a small proportion of breast and ovarian carcinomas. This mutant receptor is not activated by ligand; however, it is constitutively activated and has **defective downregulation behavior**, which results in constitutive long-term signaling. This variant is not present in normal tissues, and it has been found in up to 60% of HCC tissues examined. Other EGFR mutants have deletions, regions of sequence duplication or defective kinase regulatory signals (Berasain and Avila, 2014; Jorissen et al., 2003).

Overexpression of the ligands occurs in many epithelial cancers (Jorissen et al., 2003). In cancer patients, the autocrine production of TGF-α or EGF is associated with reduced survival (Hirai et al., 1998; Tateishi et al., 1990). Overexpression of EGFR ligands as well as ADAM17 has also been observed in human liver tumor cells and tissues from HCC patients (Berasain and Avila, 2014; Komposch and Sibilia, 2016). For example, mRNA levels of TGF-α in HCC tissues have been related to the prognosis of patients with liver cancer (Daveau et al., 2003). Many experimental studies have also showed the importance of EGFR ligands expression in liver cells. For instance, AR overexpression and ErbB1 define an autocrine loop capable of promoting cell proliferation, survival and resistance to cytotoxic drugs and TGF-β mediated apoptosis in human HCC cells (Berasain et al., 2007; Ortiz et al., 2008; Sancho et al., 2009). In animal models, it appears that overexpression of TGF-α is linked to hyperproliferative responses but does not generally lead to tumors in rodents (Jorissen et al., 2003).

Finally, as mentioned before, the **crosstalk** of EGFR pathway with other signaling systems that are also dysregulated in cancer is another mechanism of tumorigenesis. For example, it has been found a crosstalk in HCC between EGFR pathway and IGF-2/IGF-1R, through AR-mediated transactivation of the EGFR, and through the PI3K pathway (Desbois-Mouthon et al., 2006). Interestingly, c-Met associates with EGFR in tumor cells, and this association facilitates the phosphorylation of c-Met in the absence of HGF (Jo et al., 2000). Finally, a crosstalk between TGF-β and EGFR might switch the TGF-β role from tumor suppressor to tumor promoter. Due to the importance to this work, this specific crosstalk will be exposed in detail in **Section 4**.

Several data have shown that ErbB receptor family and its downstream pathway regulate migration and tumor invasiveness by modulating ECM components. In accordance, overexpression of EGF and its receptors has been demonstrated in many tumors, and was associated with higher incidence of distant **metastases** (Appert-Collin et al., 2015). In fact, activation of EGFR stimulates several proteins such as FAK, caveolin, E-cadherin and β-catenin, which play roles in migration and cytoskeletal reorganization (Nalesnik and

Michalopoulos, 2012). In cancer, epithelial-to-mesenchymal transition (EMT) induces tumor progression by affording properties such as invasiveness, the ability to metastasize, resistance to therapy and possibly the generation of stem-like cancer cells. Members of the ErbB receptor family play prominent roles during carcinogenesis, and most induce EMT when overexpressed both *in vitro* an *in vivo* (Al Moustafa et al., 2012).

All these observations have contributed to identify the EGFR signaling system as an ideal candidate for the targeted therapy of HCC. There are two classes of **anti-EGFR agents** that have shown clinical activity and achieved regulatory approval for the treatment of cancer. Firstly, monoclonal antibodies (mAbs) directed to the extracellular domain of the receptor, that prevent ligand binding, receptor activation and dimerization, ultimately inducing receptor downregulation, such as cetuximab or erbitux and panitumumab; secondly, low molecular weight, adenosine triphosphate (ATP)-competitive inhibitors of the tyrosine kinase of the receptor (TKIs), such as gefitibib, erlotinib and lapatinib. Several studies performed both in cultured HCC cell lines and *in vivo* experimental models demonstrated a potent antitumoral activity for both types of molecules (reviewed in Berasain and Avila, 2014; Komposch and Sibilia, 2016). Because of the promising results of EGFR inhibitors in animal models of HCC and their efficacy in other solid human tumors such as non-small cell lung carcinomas and colorectal cancers (Baselga and Arteaga, 2005; Marshall, 2006), it was hypothesized that targeting the EGFR signaling pathway might be beneficial also in HCC. Unfortunately, no responses were found to cetuximab or gefitinib, while erlotinib showed only a modest activity in advanced HCC patients. Thus, although an important challenge is the identification of EGFR-dependent tumors that may therefore be sensitive to EGFR inhibitors, the inhibition of receptor activation may be required but is not enough to achieve clinical benefit with anti-EGFR therapy (Berasain and Avila, 2014; Komposch and Sibilia, 2016; Scaltriti and Baselga, 2006).

4. Transforming Growth Factor-beta (TGF-β)

Transforming growth factor-β (TGF-β) signaling pathway is altered in several human diseases including cardiovascular, Marfan syndrome, Loeys-Dietz syndrome, Parkinson's disease, fibrosis, wound healing and immune disorders, as well as in several types of cancer. Regarding its role in tumorigenesis, TGF-β typically exerts tumor-suppressing activities in normal cells and in early-stage carcinomas through its ability to induce cell cycle arrest and apoptosis. However, as carcinomas continue to evolve and finally acquire metastatic phenotypes, the tumor suppressing functions of TGF-β are overpowered by the TGF-β oncogenic properties, which promote carcinoma growth, invasion, and metastasis. Our group has been focused on the study of the role of TGF-β in the liver. More precisely, we have been studying the relevance of this signaling pathway on cell death, proliferation, differentiation and migration in liver physiology and pathology, focusing on the mechanisms that regulate the **dual role of TGF-β**, and determine its final effects.

4.1. TGF-β in liver disease

Chronic liver diseases (CLDs) are leading cause of morbidity and mortality worldwide. During CLD, hepatocyte damage, wound healing and tissue remodeling progress, resulting in fibrosis and, ultimately, leading to cirrhosis and HCC, which are end-stage CLD. Although the complex hepatic response accompanying CLD is still not well defined, it is now clear that TGF-β plays a central role as from initial liver injury through inflammation and fibrosis, right up to end-stage cirrhosis and HCC (Dooley and ten Dijke, 2012; Fabregat et al., 2016; Giannelli et al., 2016).

4.1.1. TGF-β in HCC

The key for understanding the complicated role of TGF-β in cancer resides in knowing that it acts as a **tumor suppressor** during the **early stages** of tumorigenesis, but it also **promotes invasiveness and metastasis** in **advanced tumor** cells when cells become resistant to its suppressive effects (**Figure XIII**). Several components of TGF-β suppressor signaling have been found inactivated in pancreatic, colorectal, head-and-neck, ovarian and other tumors. Although mutations and deletions of TGF-β signaling-related genes are found in some cancers, they are rare in HCC (Fabregat et al., 2014).

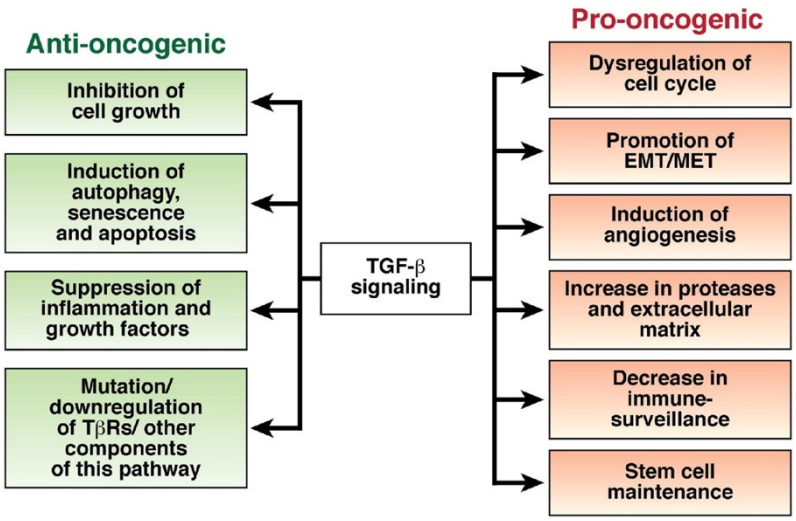

Figure XIII. TGF-β signaling exerts both anti-oncogenic and pro-oncogenic activities in carcinogenesis (Achyut and Yang, 2011).

As it has just stated, TGF-β exerts suppressive effects. However, it also modulates processes such as cell migration and invasion, immune regulation and microenvironment modification. Furthermore, TGF-β mediates liver fibrogenesis (Fabregat et al., 2014) which leads to cirrhosis, a condition that frequently develops in HCC as mentioned in a previous section (**Section 2.1**). In these cases, cancer cells grow embedded in a cirrhotic environment enriched with **extracellular matrix** that is, in turn, mediated by the cytokine. In these conditions, TGF-β signaling promotes HCC progression by two mechanisms: first, via an intrinsic activity in the tumor as an autocrine or paracrine growth factor and, second, via an extrinsic activity in the stroma. In the **stroma**, TGF-β induces microenvironment changes, including generation of cancer-associated fibroblasts (CAFs), which play a relevant role in facilitating the production of growth factors and cytokines that contribute to cell proliferation, invasion and neoangiogenesis. In fact, sources of TGF-β in tumors include the cancer cells themselves as well as various cells of the tumor stroma. In addition, due to its **immunosuppressive actions**, TGF-β contributes to tumor cell evasion from immune surveillance. On the other hand, the intrinsic effects are mostly observed in highly invasive tumor conditions, where TGF-β signaling may stimulate tumor proliferation and survival, and cells that survive to TGF-β suppressor effects undergo **EMT** favoring tumor metastasis (Fabregat et al., 2016; Giannelli et al., 2016).

All these different effects of TGF-β **in liver cells** are evidenced in a study by Coulouarn and col., where they define different liver gene signatures in response to TGF-β based on the response of mice hepatocytes to this cytokine. The **"early" TGF-β signature** is associated to suppressor genes, whereas the termed **"late" TGF-β signature** is associated to EMT, migration and invasion (Coulouarn et al., 2008). Interestingly, the early response pattern is associated with longer, and the late response pattern with shorter, survival in human HCC patients. In addition, tumors expressing the late TGF-β-responsive genes displayed invasive

phenotype, increased tumor recurrence and accurately predicted liver metastasis. Of importance, this study also discriminated HCC cell lines by degree of invasiveness (Coulouarn et al., 2008).

In normal cells, the cytostatic effects of TGF-β are often dominant over the opposing mitogenic signals; however, carcinoma-derived cells are usually refractory to growth inhibition by the cytokine. Malignant cells can circumvent the suppressive effects of TGF-β either through **inactivation of core components** of the pathway (such as TGF-β receptors or Smads transcriptors factors) or by downstream alterations that **disable just the tumor-suppressive arm** of this pathway. When the latter mode is used, cancer cells can then freely use the remaining TGF-β regulatory functions to their advantage, acquiring invasion capabilities, producing autocrine mitogens, or releasing pro-metastatic cytokines (Massagué, 2008; Seoane, 2006). In **HCC**, alterations at TGF-β receptors or SMAD2/3/4 levels are rare. Nevertheless, it has been shown, for example, that TGF-β-mediated SMAD-dependent cytostasis could be altered in HCC, as different cell lines express high amounts of SMAD7 and a reduced SMAD3 signaling (Dzieran et al., 2013), and reduced TβRII expression has been associated with more aggressive features of HCC (Mamiya et al., 2010). However, these alterations are not so frequent and, in fact, expression of TGF-β is upregulated in a great percentage of HCC patients (Massagué, 2008). Hence, other ways to disrupt TGF-β signaling may exist, probably altering just downstream signals in the tumor-suppressive branch, which would promote, or facilitate, the tumorigenic arm. In accordance to this idea, HCC cells overexpress a specific set of microRNAs (miRNAs) that would allow the escape from TGF-β-induced apoptosis (Huang et al., 2008; Li et al., 2010; Petrocca et al., 2008). Most importantly, overactivation of survival signals in HCC cells, such as MAPK/ERKs, PI3K/Akt or NF-κB, would impair the TGF-β suppressor arm observed in liver tumor cells. It is worthy to mention that, during hepatocarcinogenesis, an increase in the activity of the metalloprotease TACE/ADAM17 may promote the anti-apoptotic arm of the TGF-β signaling (Caja et al., 2007). Apart from the already mentioned crosstalk with the EGFR pathway (which will be deeply discussed in **Section 4.3**), crosstalk between TGF-β and other growth factors and chemokine pathways has been found in the tumor microenvironment. During liver tumorigenesis, TGF-β activates the β-catenin pathway, through induction of the PDGF signaling (Fischer et al., 2007), which mediates EMT, migration and survival in HCC cells. Interestingly, a crosstalk between TGF-β and chemokine signaling has been recently reported, as TGF-β induces the expression of the chemokine receptor CXCR4 in HCC cells, which is required for TGF-β-induced cell migration and cell survival (Bertran et al., 2013). Finally, the crosstalk between EMT and apoptosis would also explain the resistance to TGF-β-induced suppressor effects observed in HCC cells. Indeed, a mesenchymal-like phenotype correlates with resistance to drug therapy (Fernando et al., 2015).

4.2. TGF-β signaling pathway

In humans, the **TGF-β superfamily** represents 33 or more secreted diverse developmental factors, including bone morphogenic proteins (BMPs), growth and differentiation factors (GDFs), activins, TGF-β's, nodal, myostatin and anti-mullerian hormone (AMH), that mediate such diverse processes as cell proliferation, differentiation, motility, adhesion, organization and programmed cell death. Most members of this family exist in variant forms, with the TGF-β cytokine consisting of three isoforms: TGF-β1, TGF-β2 and TGF-β3. TGF-β, and most of its family members, are synthesized within the cell as pro-peptide precursors containing a pro-domain, named Latency-Associated peptide (LAP), and the mature domain, and are secreted into the ECM. They need to be cleaved to form active signaling molecules by the proteolytic cleavage of several ECM-associated polypeptides (Heldin et al., 2012).

The bioactive TGF-β molecule is a dimer, and once cleaved, it binds to its receptors triggering the formation of a heterotetrameric complex of type I and type II serine/threonine kinase receptors, in which the constitutively active type II receptor phosphorylates and activates the type I receptor. There are several types of both type I and type II receptors, but TGF-β preferentially signals through activin receptor-like kinase 5 (ALK5) type I receptor (TβRI) and the TGF-β type II receptor (TβRII). In addition, endoglin and betaglican, also called accessory receptors, bind TGF-β with low affinity and present it to the TβRI and TβRII. Activated receptor complexes mediate **canonical TGF-β signaling** through phosphorylation of the Receptor-associated **SMADs** (R-SMADs) at their carboxy-terminal. Humans express eight SMAD proteins that can be classified into three groups: Receptor-associated SMADs (R-SMADs), Cooperating SMADs (Co-SMADs) and Inhibitory SMADs (I-SMADs). Among the R-SMADs, SMAD2 and 3 mediate the TGF-β branch of signaling, whereas the BMP branch exclusively utilizes SMAD1, 5 and 8. Upon TGF-β stimulation, the R-SMADs SMAD2 and 3 are phosphorylated, losing their affinity to cytoplasmic retention proteins such as SARA (Smad anchor for receptor activation), thereby exposing their nuclear import signal. Then, they associate with the Co-SMAD SMAD4, forming a complex that translocates to the nucleus where, in collaboration with other transcription factors, binds and regulates promoters of different target genes (**Figure XIV**). Among these genes we find the I-SMADs SMAD6 and SMAD7, producing a negative feedback regulation of the TGF-β signaling. The SMAD binding partners include the forkhead, homeobox, zinc-finger, bHLH, and AP1 family of transcription factors. The coactivators and repressors recruited by the SMAD complex are cell- and context-specific, therefore determining the specific genes induced within particular cells, explaining the diverse set of biological responses exerted by TGF-β signaling (Drabsch and ten Dijke, 2012; Morrison et al., 2013; Padua and Massagué, 2009).

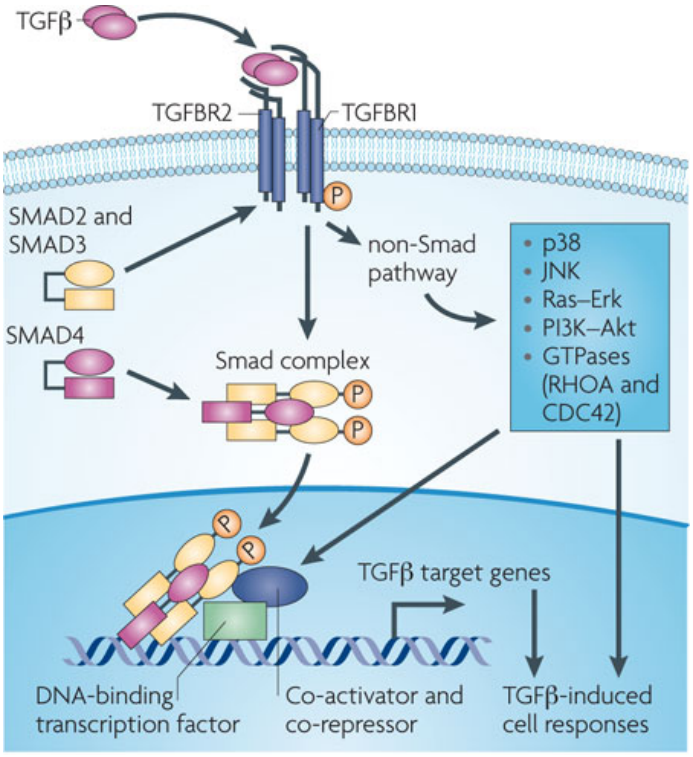

Figure XIV. TGF-β signaling is transduced through Smad and non-Smad pathways (Ikushima and Miyazono, 2010).

In addition to the canonical SMAD pathway, TGF-β is able to use **non-SMAD effectors** to mediate some of its biological responses, including non-receptor tyrosine kinases proteins such as Src and FAK, mediators of cell survival (e.g., NF-kB, PI3K/Akt pathways), MAPK (ERK1/2, p38 MAPK, and JNK among others), and Rho GTPases like Ras, RhoA, Cdc42 and Rac1. Interestingly, these pathways can also regulate the canonical SMAD pathway (Drabsch and ten Dijke, 2012; Heldin et al., 2012; Morrison et al., 2013).

4.3. TGF-β biological functions

As mentioned above, TGF-β is secreted by several cell types and plays essential roles in the regulation of different cellular processes, including cell proliferation, morphogenesis and differentiation, migration, extracellular matrix production, cytokine secretion or cell death, which are essential for the **homeostasis** of tissues and organs. To better contextualize the work presented here, this section will summarize the main functions exerted by TGF-β, especially in liver, on which our group has focused its efforts during the last decades.

4.3.1. TGF-β and Growth inhibition

In normal epithelial cells, as well as in endothelial, neuronal and hematopoietic cells, TGF-β regulates the expression of several genes promoting **cell cycle arrest** in the G_1 phase of the cell cycle, in a **Smad dependent** manner, through a diverse array of mechanisms, leading to pRb dephosphorylation. In these cells, TGF-β rapidly induces two CDK inhibitors, $p21^{CIP1}$ (which inhibits Cyclin E/A-cdk2 complexes) and $p15^{INK4B}$ (which inhibits Cyclin D-cdk4/6 complexes), mobilizes and activates $p27^{KIP1}$ (that targets also Cyclin E/A-Cdk2 complexes) and down-regulates Myc, Id1, Id2 and Id3, all four transcription factors involved in proliferation and inhibition of differentiation. Thus, TGF-β mediates a dual effect on the cell cycle by simultaneously inhibiting the CDK functions and eliminating proliferative drivers (Drabsch and ten Dijke, 2012; Massagué, 2008; Padua and Massagué, 2009; Seoane, 2006). Some of the mechanisms involved in the transcriptional regulation of the TGF-β cytostatic gene responses have been already elucidated. For example, TGF-β induces $p21^{CIP1}$ via a Smad3/4-FoxO complex that interacts with a specific region of the $p21^{CIP1}$ promoter (Seoane et al., 2004) and Myc downregulation is mediated by an E2F4/5-Smad3-Smad4 complex (Chen et al., 2002). TGF-β also represses the expression of the Cdc25A tyrosine phosphatase, responsible for de-phosphorylating and activating G_1 phase CDKs (Iavarone and Massagué, 1997; Nagahara et al., 1999). Besides the canonical Smad-dependent gene responses involved in the cytostatic program, TGF-β can also promote cell cycle arrest through **Smad-independent** pathways. For instance, the binding of TGFβ receptor complex to the regulatory subunit of the protein phosphatase PP2A facilitates the de-phosphorylation and inhibition of p70 S6 kinase and contributes to the anti-proliferative response (Petritsch et al., 2000). Moreover, TGF-β can also induce JNK and p38 to stabilize $p21^{CIP1}$ (Kim et al., 2002).

In **hepatocytes**, TGF-β is also known to induce cell cycle arrest at low doses (Sánchez et al., 1996), and to counteract proliferative signals induced by EGF or insulin (Carr et al., 1986; Sánchez et al., 1998).

In normal cells, the cytostatic effects of TGF-β are often dominant over the opposing mitogenic signals; however, **carcinoma-derived cells** are usually refractory to growth inhibition by the cytokine, as it has been previously introduced. In certain cases, such as colorectal, pancreatic, ovarian, gastric, and head and neck carcinomas, this is due to the disruption of

TGF-β signaling caused by **mutational inactivation** in the core TGF-β pathway components, such as microsatellite instability leading to mutations in TβRII, inactivating mutations in Smad2 and 4, or with lower incidence, mutations in the TβRI. Nevertheless, many other tumors (such as breast and prostate cancers, gliomas, melanomas and hematopoietic neoplasias), preferentially disable the tumor-supressive action of TGF-β by losing the tumor-supressive arm of the signaling pathway. For example, a subset of gliomas present homozygous deletion of *p15INK4b* (Jen et al., 1994), whereas certain other tumors overexpress c-MYC or Cyclin D1, which may blunt the effect of TGF-β-induced CDK inhibitors (Massagué, 2008; Seoane, 2006). Moreover, in some other cases the lack of the TGF-β anti-proliferative response is due to **overactivation of non-Smad pathways** that can lead to aberrant expression or post-transcriptional modification of the TGF-β pathway components. Indeed, in our group it has been described that TGF-β induces survival signals in both fetal and transformed hepatocytes, but not in adult hepatocytes, through the transactivation of the EGFR pathway. This specific action of TGF-β will be discussed in **Section 4.3.4**.

4.3.2. TGF-β and Apoptosis

In addition to its role in regulating the cell cycle, TGF-β also participates in the maintenance of tissue homeostasis through its influence on apoptotic pathways. TGF-β is a well-known **inducer of apoptosis**, although it involves different mechanisms that might occur differently, depending on cell-autonomous and environmental factors and, paradoxically, it can simultaneously induce **both pro- and anti-apoptotic signals**. There have been several Smad-dependent and -independent mechanisms described for a variety of cell lines, and this signal ultimately leads in activation of pro-apoptotic caspases as well as changes in the expression, localization and activation of both pro- and anti-apoptotic members of the BCL-2 family (Padua and Massagué, 2009).

Specifically, in **hepatocytes** TGF-β modulates the expression of different members of BCL-2 family. Nevertheless, as it happens with the role of TGF-β controlling cell proliferation, TGF-β can also exert both pro- and anti-apoptotic functions. In this sense, some reports have shown that TGF-β induces the downregulation of anti-apoptotic proteins as BCL-X_L (Herrera et al., 2001a). However, other reports have shown that TGF-β can also enhance the expression of BLC-X_L (Valdés et al., 2004). In addition, TGF-β also induces the expression of pro-apoptotic proteins, like BMF, BIM and BAX (Ramjaun et al., 2007; Teramoto et al., 1998; Yu et al., 2008).

Moreover, in epithelial cells, such as fetal hepatocytes, TGF-β-induced apoptosis is coincident with **ROS production** (Sánchez et al., 1996, 1997) through two different mechanisms: the induction of a nicotinamide adenine dinucleotide phosphate (NADPH) oxidase (NOX) system, (more precisely induction of NOX4) to increase extra-mitochondrial ROS (Carmona-Cuenca et al., 2008; Herrera et al., 2004a), or depletion of antioxidant proteins which increase mitochondrial ROS (Franklin et al., 2003; Herrera et al., 2004a). Thus, TGF-β-induced ROS production is necessary for the apoptotic process in hepatocytes (Sánchez et al., 1996)

and it is required for an efficient mitochondrial-dependent execution of apoptosis (Herrera et al., 2001a, 2001b).

4.3.3. TGF-β during liver regeneration.

A biological situation more relevant to this work, in which TGF-β actions are critical regulators, is **liver regeneration**, as it was already mentioned in a previous section **(Section 1.3).** Although a reduced response to the cytostatic and cytotoxic effects of TGF-β are observed in regenerating hepatocytes, through the upregulation of anti-apoptotic and anti-oxidant signals (Herrera et al., 2004b), TGF-β has been thought as a natural stimulus that terminates liver regeneration, preventing uncontrolled hepatocyte proliferation (Michalopoulos, 2007). Indeed, the same miRNAs shown to regulate TGF-β signaling during liver development might regulate TGF-β1/SMAD3 activation in the termination stage of liver regeneration (Yuan et al., 2011). Thus, a perfect spacio-temporal orchestration of TGF-β signaling at different stages of the process is required, although it is still unclear. In that sense, NOX4 could be one candidate mediating this situation, because as mentioned before it is necessary for the TGF-β apoptotic process in hepatocytes. Another potential mediator is the phosphatase PTP1B that binds Met and EGFR (the two main proliferating pathways during liver regeneration) and decreases their activation. PTP1B deficiency results in enhanced EGF- and HGF-mediated signaling in hepatocytes and livers submitted to PH resulting in accelerated regeneration (Revuelta-Cervantes et al., 2011), and also confers resistance on TGF-β-induced suppressor effects in hepatocytes (Ortiz et al., 2012). Thus, a proper balance of all these signals might be a good determinant of the efficiency of liver regeneration.

4.3.4. TGF-β-mediated anti-suppressor signals. Specific crosstalk with EGFR pathway.

As it has been pointing out, TGF-β can exert a **dual role:** apart from its pro-suppressor arm, it can induce survival signals, which are in a great extent due to the **transactivation of the EGFR pathway** (**Figure XV**).

TGF-β is able to activate survival pathways, for example activating Akt signaling inducing an increase in anti-apoptotic proteins (Song et al., 2006; Valdés et al., 2004; Wilkes et al., 2005). However, usually, Akt activation is transient and then, the survival signals might be related to the capacity of TGF-β to transactivate c-Src and EGFR pathways. Interestingly, the inhibition of the EGFR increases the apoptotic response to TGF-β (Murillo et al., 2005; Park et al., 2004). Furthermore, EGF is an important survival signal counteracting TGF-β-induced apoptosis in hepatocytes (Fabregat et al., 1996, 2000), a process that requires activation of the PI3K/Akt axis to counteract TGF-β-induced upregulation of NOX4, oxidative stress and mitochondrial-dependent apoptosis (Carmona-Cuenca et al., 2006, 2008).

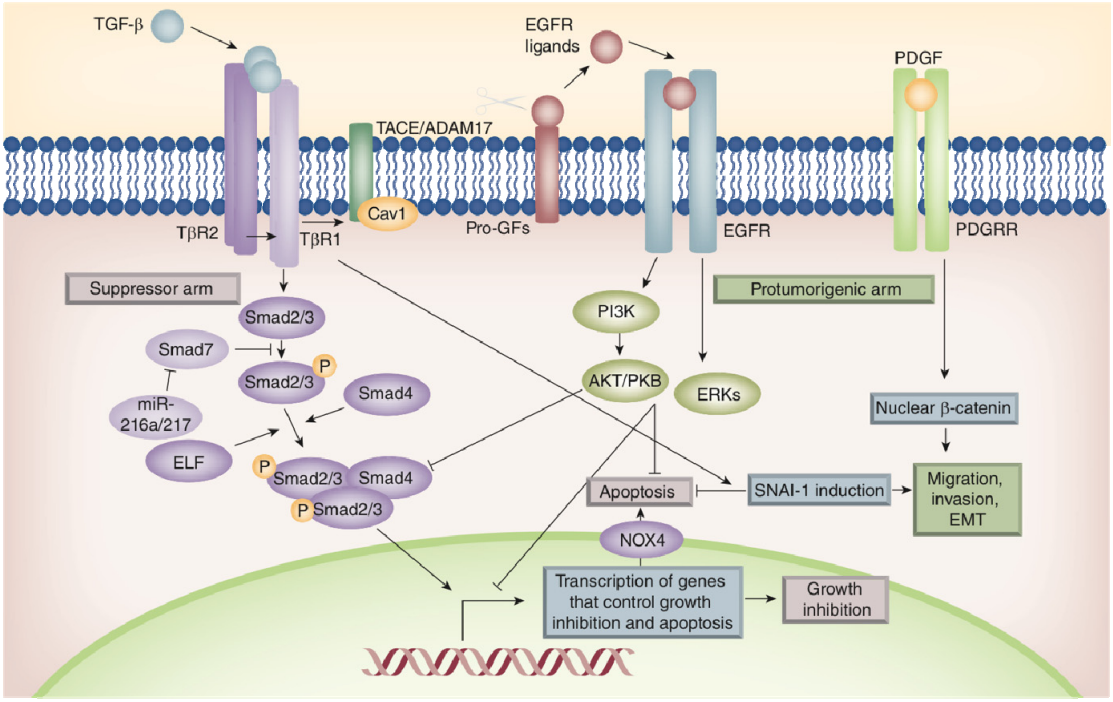

Figure XV. Diagram of the TGF-β crosstalk with EGFR and other growth factors, which may contribute to its pro-tumorigenic actions during liver tumorigenesis. The autocrine loop of EGFR activated by TGF-β in liver cells requires the activity of the metalloprotease TACE/ADAM17, which is responsible for the shedding of the EGF family of growth factors (Moreno-Càceres and Fabregat, 2016).

Moreover, TGF-β is able to mediate the production of EGFR ligands, which eventually confers resistance to its pro-apoptotic effects in hepatocytes (Carmona-Cuenca et al., 2006; Murillo et al., 2007) and HCC cells (Caja et al., 2011a), and the inhibition of the EGFR pathway enhances TGF-β induced apoptosis (Sancho et al., 2009). The autocrine loop of EGFR activated by TGF-β in liver cells requires the activity of the metalloprotease TACE/ADAM17 (Caja et al., 2007; Murillo et al., 2005), for which recently it has been described that Caveolin-1 is required (Moreno-Càceres et al., 2014).

Importantly, the capacity of hepatocytes to survive to TGF-β is also dependent on their differentiation status (Sánchez et al., 1999). Thus, rat hepatoma cells respond to TGF-β inducing survival signals, whereas adult hepatocytes do not (Caja et al., 2007). In the same way, different features of HCC cell lines, like the activation of the EGFR or MEK/ERK pathways, may provoke different outcomes after TGF-β exposure (Caja et al., 2009, 2011a).

In liver, our group has described that another member of the NADPH oxidase family, NOX1, plays an anti-apoptotic role. In fact, TGF-β-mediated early activation of NOXes mediates upregulation of EGFR ligands through a NF-κB-dependent mechanism (Murillo et al., 2007). Moreover, NOX1 promotes autocrine growth of liver tumor cells through the upregulation of the EGFR pathway in a Src dependent manner via upregulation of EGFR ligands expression

(Sancho and Fabregat, 2010). This proliferation can be impaired by the addition of the NOX inhibitor VAS2870 (Sancho and Fabregat, 2011).

Transactivation of the EGFR by TGF-β is also seen in other cellular models such as in airway epithelial cells where the TGF-β/EGFR crosstalk helps in the maintenance of tissue homeostasis (Ito et al., 2011). This process has also been widely regarded as a pro-tumorigenic mechanism apart from its physiological role. For instance, TGF-β induces shedding of the pro-HB-EGF and transactivation of the EGFR through a mechanism dependent on ADAMs activity in gastric cancer cells. Indeed, both ADAMs inhibition and an ADAM17 knockout suppressed EGFR-mediated TGF-β survival effects (Ebi et al., 2010). This can also be seen in breast cancer cells (Wang et al., 2008). Finally, TGF-β-mediated H_2O_2 production has been also considered to transactivate EGFR in SCC13 and A431 human carcinoma cells; in this case no metalloproteases were described but neither denied (Lee et al., 2010).

4.3.5. TGF-β and metastasis. The Epithelial-to-mesenchymal transition (EMT)

The paradoxical switch in TGF-β function during tumorigenesis has been linked to its ability to induce **epithelial-to-mesenchymal (EMT) programs.** EMT reflects an evolutionarily conserved cascade in which polarized epithelial cells adopt: mesenchymal cell characteristics together with enhanced chemoresistance and evasion from host immunosurveillance, expanded stem-like and tumor initiating activities, elevated resistance to apoptotic stimuli, and acquired migratory, invasive, and metastatic phenotypes (Morrison et al., 2013; Thiery, 2003).

Epithelial cells show apical-basal polarity, adhere and communicate with each other through specialized intercellular junctions and are positioned on a basement membrane that helps to define their physiology. In this way, epithelia function as permeable barriers that delineate tissues and organs. The transition of epithelial cells into mesenchymal cells, either in development or pathological situations, follows a common and conserved program with hallmarks. However, it has also inherent flexibility and variability depending on the cell type, tissue context and signals that activate the EMT program. Additionally, cells that have undergone EMT acquire resistance to senescence and apoptosis (Lamouille et al., 2014).

In all tissue contexts, EMT arises from various key events. It starts with the **dissolution of epithelial cell-to-cell contacts** (tight junctions, adherens junctions and desmosomes) and **loss of apical-basal polarity** (formed by PAR, Crumbs and Scribble complexes)**.** In addition, the expression of epithelial junction proteins, such as E-cadherin, ZO-1 and occludin, is downregulated at the level of gene expression, concomitantly with increases in the expression of mesenchymal adhesion proteins like N-cadherin. SNAIL transcription factors (such as SNAIL or SNAIL1, and SLUG or SNAIL2), zinc-finger E-box-binding (ZEB) transcription factors (such as ZEB1 and ZEB2) and basic helix-loop-helix (bHLH) transcription factors (such as TWIST) potently regulate this **epithelial to mesenchymal switch in gene expression**. Additionally, **actin cytoskeleton**, as well as microfilaments, microtubules and intermediate filaments

(vimentin and α-smooth muscle actin (α-SMA)) are dramatically modified and reorganized promoting phenotypic changes to enable cells to acquire a **front-rear polarity** and **directional motility**. The reorganization in the actin cytoskeleton is mainly regulated by Rho GTPases, including RhoA, Cdc42 and Rac1. Finally, **remodeling of the ECM** and changes in **cell interactions to the ECM** are essential. Thus, integrin complexes enable cells to receive signals from ECM proteins and, therefore, cells during EMT downregulate some epithelial integrins, but activate the expression of others. Additionally, cells enhance **ECM protein degradation** and enable invasion through increasing the expression and secretion of matrix metalloproteinases (MMPs), such as MMP2 and MMP9. Also, cells that undergo EMT are efficiently capable of synthesizing components of the ECM to reconstitute their microenvironment following cell invasion. Importantly, EMT can also be reverted through a process called **mesenchymal-to-epithelial transition (MET),** occurring after migration and homing into new sites within an embryo, during tumor progression or healing of fibrotic tissue (**Figure XVI**) (Heldin et al., 2012; Lamouille et al., 2014; Morrison et al., 2013; Moustakas and Heldin, 2016; Nalluri et al., 2015).

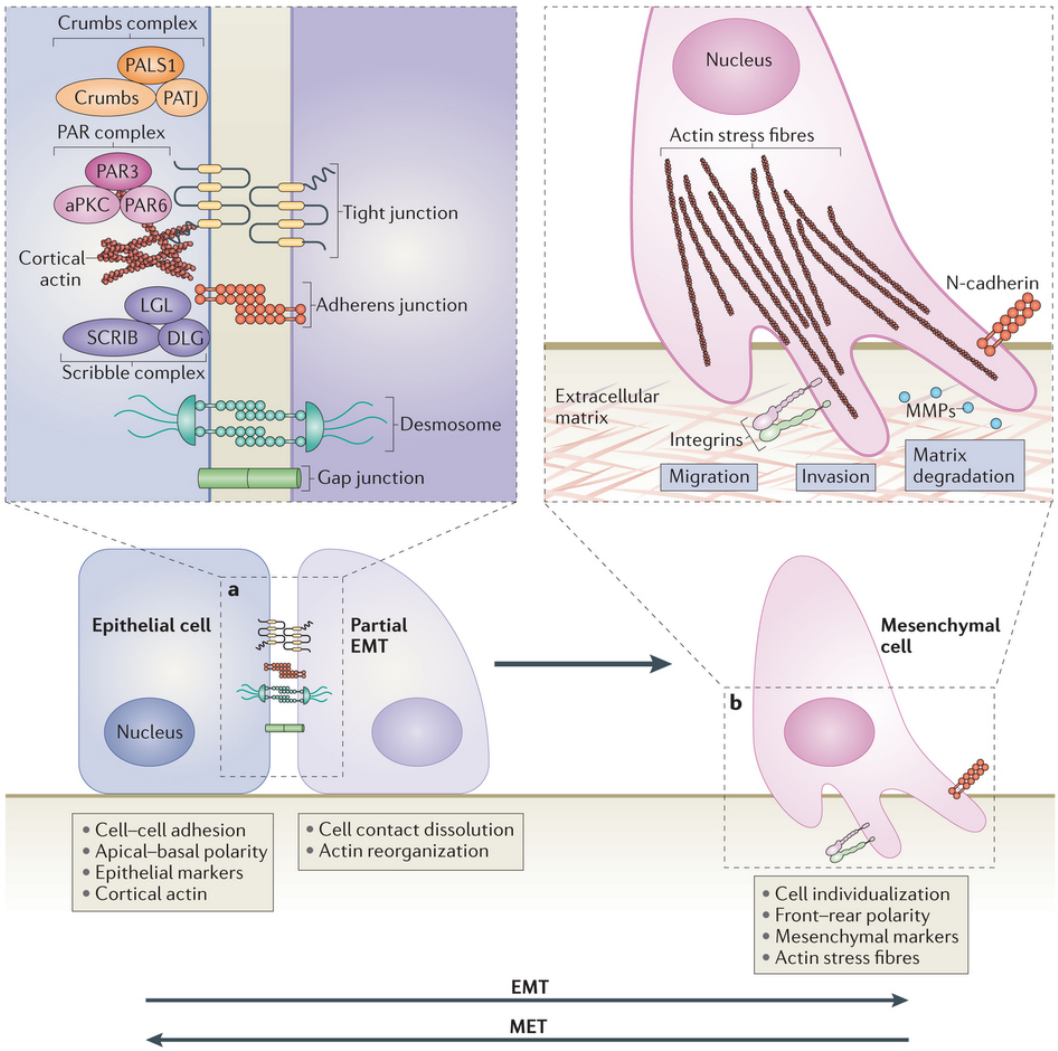

Figure XVI. The different stages during EMT (epithelial-to-mesenchymal transition) and the reverse process MET (mesenchymal-to-epithelial transition) (Lamouille et al., 2014).

In **cancer**, epithelial cells undergo EMT, which favors intravasation of cells to both lymph and blood vessels and consequent dissemination far from the primary tumor. At secondary loci, cells may undergo a MET process to be able to colonize secondary sites and form metastasis. It is worth to mention that cancer cells may undergo EMT in different extents: it is possible that some cells retain epithelial features at the same time that are acquiring some mesenchymal ones, and other cells become fully mesenchymal (Kalluri and Weinberg, 2009).

Regarding **TGF-β-induced EMT**, it should be noted that both canonical and non-canonical TGF-β pathways participate in driving EMT programs by the cytokine. Indeed, Smad3 and 4 function as positive regulators of EMT programs, while Smad2 functions as a negative regulator of EMT, by regulating different transcription of target genes. Through the activation of PI3K/Akt/mTOR pathway and small GTPases, including RhoA, TGF-β induces increased motility and invasion, and changes in protein synthesis and actin reorganization. MicroRNAs, as well as epigenetic changes and alternative splicing, also regulate the EMT program induced by the cytokine (Heldin et al., 2012; Katsuno et al., 2013; Morrison et al., 2013).

In the **liver**, TGF-β induces an EMT process in fetal hepatocytes that survive to its apoptotic effects (Sánchez et al., 1999). To induce EMT, TGF-β is known to upregulate the transcription factors SNAIL and SLUG, which in turn repress the expression of epithelial markers, while activating the expression of mesenchymal ones (Katsuno et al., 2013). Interestingly, EMT-inducing factors such as SNAIL or TWIST might help TGF-β to also promote cell dedifferentiation and expression of cell surface presumptive cancer stem cell markers (Mani et al., 2008). In accordance, fetal hepatocytes that undergo EMT become refractory to apoptotic effects of TGF-β showing characteristics of liver progenitor cells (Valdés et al., 2002). Indeed, TGF-β may contribute to transdifferentiation of fetal hepatocytes into liver progenitors, which later on will be able to differentiate both in mature hepatocytes and cholangiocytes (Caja et al., 2011b; del Castillo et al., 2008). It is important to note that in the absence of the cytokine, cells that underwent a TGF-β-induced EMT revert to an epithelial phenotype (Bertran et al., 2009). As it has been mentioned before, TGF-β is able to induce both pro-apoptotic and survival signals at the same time in hepatocytes, and the balance between them is what decides the final cell fate. There is a close link between apoptosis and EMT, not only because initially the EMT process depends on the ability of cells to overcome TGF-β induced apoptosis, but also because EMT induces survival signals that rescue from apoptosis (Bertran et al., 2009; Valdés et al., 2002, 2004). For instance, SNAIL overexpression has been shown to confer resistance to TGF-β induced pro-apoptotic effects (Franco et al., 2010; Vega et al., 2004). Interestingly, fetal hepatocytes and hepatoma cells that have undergone a TGF-β-mediated EMT express high levels of TGF-α and HB-EGF which might confer survival through the activation of the EGFR pathway (Caja et al., 2007; Del Castillo et al., 2006).

4.4. Targeting TGF-β in HCC

The major problem facing targeting TGF-β is its complex role in the liver, regarding cell proliferation, carcinogenesis, immune modulation and EMT (Fabregat et al., 2016).

Several different strategies have been proposed for inhibiting the TGF-β pathway in human cancer, including the use of chimeric proteins, monoclonal antibodies, small molecules and antisense oligonucleotides (Fabregat et al., 2014). Recently, it has been shown that the TGF-βRI kinase inhibitor Galunisertib, but not a monoclonal inhibitor of TGFβRII (D10), blocks the canonical and non-canonical pathways (Dituri et al., 2013; Fransvea et al., 2011; Giannelli et al., 2016). Biomarkers would be extremely useful in the proper selection of patients who might benefit from receiving the drug in clinical trial, although so far no biomarkers have been validated for this purpose. Recently, an inverse correlation between circulating TGF-β and E-cadherin levels has been reported in patients with HCC, that resembles the EMT process, as documented *in vitro* (Dituri et al., 2014; Giannelli et al., 2016). Thus, a phase II clinical trial using Galunisertib in patients with advanced HCC to test safety, time to progression and overall survival is currently ongoing. Preliminary data show that patients with higher levels of circulating TGF-β are more likely to respond to therapy with Galunisertib (NCT01246986 http://clinicaltrials.gov).

Besides intervention with the TGF-β canonical and non-canonical pathway, the inhibition of the signaling events collaborating with its cascade could be of interest. In this context, the switch from tumor-suppressive to pro-oncogenic TGF-β actions could be directed by its crosstalk with TKRs, such as EGFR. As this receptor is necessary for the activation of Akt, which confers resistance to TGF-β mediated apoptosis, interference with EGFR signaling by employing approved targeted drugs in TGF-β/Smad-positive HCC patients might be effective (Fabregat et al., 2016; Giannelli et al., 2016).

5. Cell migration

The current **metastasis** paradigm suggests that the primary tumor starts off benign but over time slowly acquires changes that provide a few rare cells within the tumor the ability to metastasize. Cancer metastasis is a highly complex multistep process that involves alterations in growth, angiogenesis, dissemination, invasion and survival, which leads to a subsequent attachment and growth of new cancer cell colonies (Budhu et al., 2005). The initial steps of local invasion include the activation of signaling pathways that control cytoskeletal dynamics in tumor cells and the turnover of cell-to-matrix and cell-to-cell junctions, followed by active tumor cell migration into the adjacent tissue (Friedl and Alexander, 2011).

Cell migration is a highly organized process and highly dependent on the actin cytoskeleton dynamics. Actin cytoskeleton is composed of microfilaments scattered throughout the cell from the apical to the basal regions, and it is a major component of the whole cytoskeleton. Globular actin (G-actin) is polymerized and compiled in an ATP-dependent process to form a helical filamentous structure known as F-actin (Stanley et al., 2014).

As mentioned in the previous section, acquiring a mesenchymal phenotype is the way through which epithelial cells can invade local and distant sites, but it is not the only one, since they can move also as a collective group, maintaining epithelial features. In **cancer**, it is now well recognized that tumor cells have multiple forms of movement. They can disseminate as individual cells, referred to as **"individual cell migration"**, or expand in solid cell strands, sheets, files or clusters, called **"collective migration"** (Figure XVII). In fact, in many tumors, both single cells and collectives are simultaneously present (Friedl and Wolf, 2003). Two modes of individual cell migration have been characterized: an elongated **"mesenchymal-like"** mode and a rounded **"ameboid"** mode of cell migration. **Mesenchymal migration**, such as the acquired after an EMT process, has been largely studied in two-dimensional systems and is typical of single cells migrating individually while adhering to a surface. It is characterized by cell polarization, requirement for extracellular proteolysis, and low actomyosin contractility. Cells largely depend on actin polymerization and depolymerization, that provoke sequential accumulations of actin at the front of the cell, including protrusions such as filopodia, lamellipodia, and membrane ruffles. Concomitantly, adhesion disassembly at the cell rear and the contraction of actomyosin then allows the cell to achieve directed cell movement. In addition, adhesion of these protrusions links the actin cytoskeleton to the extracellular matrix. Actin stress fibers are connected to focal adhesions and with them form a cellular network that is both a generator and a sensor of mechanical force (Sanz-Moreno and Marshall, 2010; Stanley et al., 2014). On the contrary, in **ameboid migration**, cells do not strongly adhere to the extracellular matrix. Instead, they adopt a rounded morphology and rely on actin-myosin contractility for propulsion, migrating independently of ECM degradation. This enables cells to migrate at relatively high velocities and to actively migrate through three-dimensional environments (Sahai and Marshall, 2003; Sanz-Moreno and Marshall, 2010; Stanley et al.,

2014). In addition to individual movement, cells can migrate collectively by a coordinated movement. Similarly to single-cell migration, collective cell movement results from actomyosin polymerization and contractility coupled to cell polarity; however, in the collective movement, cells remain coupled by cell-to-cell junctions at the leading edge as well as in lateral regions inside the moving cell group, and the leading cells generate movement through the use of cellular protrusion (similar to mesenchymal migration) (Ilina and Friedl, 2009; Stanley et al., 2014).

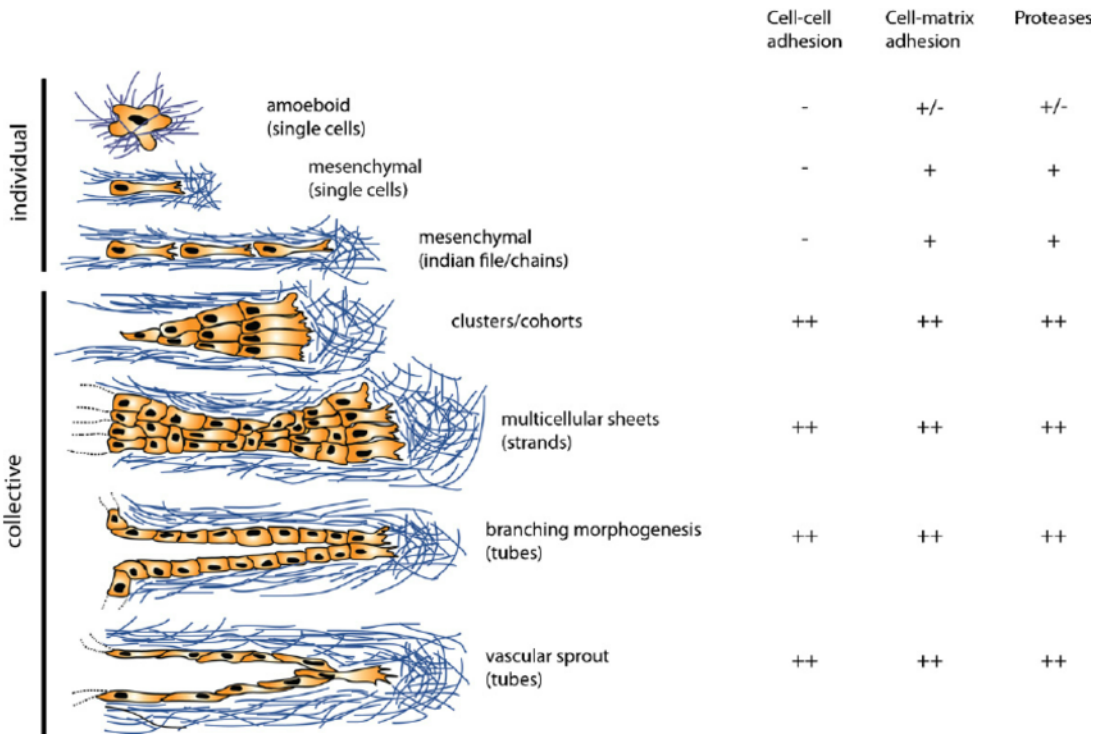

Figure XVII. Different types of cancer cell migration (Spano et al., 2012).

Cancer invasion is a cyclic process in which the cell changes shape, produces morphological asymmetry, and then translocates the cell body. For this, the **cytoskeleton** serves as the cell's engine, and the **cell surface receptors** act as its transmission (Friedl and Alexander, 2011). The orchestrated remodeling of the actin cytoskeleton requires spatial and temporal changes in adhesion to the ECM. Indeed, integrin receptors and their ligands are important regulators of the actin cytoskeleton since when active, integrins bind ECM and it occurs the recruitment of scaffold proteins, such as paxillin, and signaling proteins, such as the tyrosine kinase FAK which in turn associate with additional molecules, forming the **focal adhesion (FA) complexes** (Friedl and Wolf, 2003). Interestingly, the adhesion size and distribution reflect the contractile state of the cell. Thus, nascent adhesions initially form in the lamellipodium or filopodium and either disassemble or elongate at the convergence of the lamellipodium and lamellum. Adhesion maturation to focal complexes and focal adhesions is accompanied by the bundling and cross bridging of actin filaments and increase in adhesion size (Parsons et al., 2010; Wiesner et al., 2006). **Rho GTPases family** plays a key role in integrating intracellular signals

downstream of mechano-sensors, promoting re-organization of the actin cytoskeleton that is needed for the change in cell shape and, eventually, the mode of migration in a given environment. Rho GTPases family is composed of more than 20 small intracellular proteins that are key regulators of cell migration through their actions on actin assembly and actomyosin contractility, and they are grouped into eight subfamilies, though the best studied are Rac (composed of 4 members, Rac1, Rac2, Rac3 and RhoG), Rho (composed of 3 members, RhoA, RhoB and RhoC) and Cdc42 (composed of 5 members, Cdc42, TC10, TCL, Chip and Wrch-1) subfamilies (Sadok and Marshall, 2014).

5.1. Plasticity in cell migration

The ability of cells to transition into mesenchymal cells (EMT) and back (MET), either partially or fully, illustrates an inherent plasticity of the epithelial phenotype. In fact, the plasticity of the epithelial phenotype enables cells to transition through multiples rounds of EMT and MET (Lamouille et al., 2014). This implies that mechanisms of cell migration are plastic and allow the rapid adaptation to the environment which often results in transitions between different modes of migration (Friedl and Alexander, 2011; Friedl and Wolf, 2003). Thus, acquisition of an invasive phenotype is a result of a multistep process of cancer-associated EMT, as it has been explained. Incomplete or partial EMT can induce the collective migration in which cells retain cell-to-cell adhesions and migrate collectively in a coordinated manner. Cells that undergo complete EMT lose contact with the cell cohort or detach from the epithelial sheet, establish front-rear migratory polarity and migrate individually in the mesenchymal mode. Mesenchymally migrating cells may re-differentiate by MET and re-establish an epithelium. Alternatively, by losing dependency on ECM and by increasing actomyosin contractility, mesenchymal cells can undergo mesenchymal-to-ameboid transition (MAT) and invade in an ameboid mode (Gandalovičová et al., 2016; Panková et al., 2010). The ameboid phenotype could also be achieved by an increase in Rho activity in collectively migrating cells, which then undergo the collective-to-ameboid transition (CAT); however, this is less frequent than MAT. The ameboid and mesenchymal modes of invasion are often inter-convertible, and ameboid cells can also revert to mesenchymal mode by ameboid-to-mesenchymal transition (AMT) (**Figure XVIII**) (Gandalovičová et al., 2016).

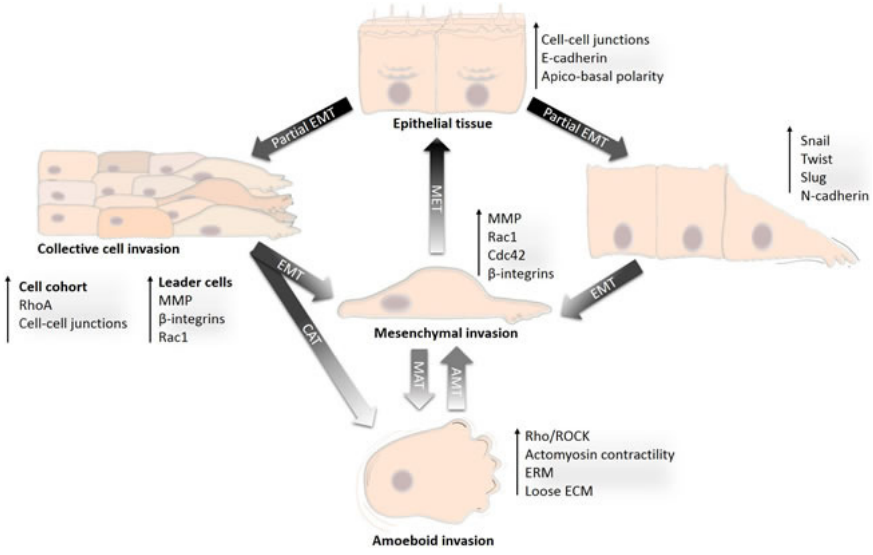

Figure XVIII. Plasticity in the development of tumor cell migration modes from differentiated epithelium (Gandalovičová et al., 2016).

Although TGF-β has been extensively described to drive a mesenchymal-migration through an EMT process, very little is known about its potential participation in other types of movement in the liver, which could be relevant when considered as a target for HCC patients.

II. HYPOTHESIS

Considering the crosstalk between the TGF-β and the EGFR pathways observed in liver cells in *in vitro* assays, when we started this work we wondered whether the interaction among these pathways would also be relevant *in vivo*. We hypothesized that overactivation of the EGFR during liver regeneration and/or hepatocarcinogenesis could be counteracting TGF-β suppressor actions. Furthermore, since TGF-β has been proposed as mediator of migration and invasion of liver tumor cells, we hypothesized that activation of the EGFR by TGF-β could be mediating some of these effects.

III. OBJECTIVES

OBJECTIVE 1: Analysis of the *in vivo* relevance of the crosstalk between the TGF-β and EGFR pathways during liver regeneration and hepatocarcinogenesis.

1.1. Characterization of a new experimental animal model for the study of the catalytic activity of the EGFR in liver physiology and pathology: mice expressing specifically in the liver a truncated form of the human EGFR, which lacks the catalytic intracellular domain.

1.2. Analysis of liver regeneration after 2/3 partial hepatectomy in the previous mentioned animal model. Comparison with WT mice. Status of TGF-β pathway under these conditions.

1.3. Analysis of diethylnitrosamine (DEN)-induced hepatocarcinogenesis in the previous mentioned animal model. Comparison with WT mice. Status of the TGF-β pathway under these conditions.

OBJECTIVE 2: Analysis of the crosstalk between the TGF-β and EGFR pathways in the regulation of cell adhesion and migration of HCC cells.

2.1. Analysis of the phenotype of different HCC cell lines: epithelial *versus* mesenchymal. Correlation with the autocrine production of TGF-β.

2.2. TGF-β effects on the epithelial-mesenchymal phenotype, adhesion and migration of liver tumor cells. Analysis of different types of migration and potential mechanisms involved.

2.3. Attenuation of the EGFR pathway in *in vitro* models of HCC cells by shRNA technology. Impact on the TGF-β-induced effects on cell adhesion and migration.

OBJECTIVE 3: Translational relevance of the results obtained in objectives 1 and 2. Analysis in tumoral and non-tumoral tissues from HCC patients.

IV. MATERIAL AND METHODS

1. Animal experimentation

1.1. Ethics statement

The use of animals complied with the institutional and European legislation concerning vivisection, the use of genetically modified organisms, animal care and welfare (European Directive 2010/63/UE adopted by the European Parliament and the Council of the EU on September 22, 2010). All mouse lines were maintained in a C57BL/6 background in the University Complutense of Madrid (UCM) animal facility allowed food and water ad libitum and routinely screened for pathogens in accordance with FELASA (Federation of European Laboratory Animal Science Associations) procedures. The experimental protocol for partial hepatectomy and diethylnitrosamine-induced hepatocarcinogenesis was approved by the Institutional Committee for Animal Care and Use (CEA -UCM 87/2012, Madrid, Spain).

1.2. Generation of transgenic EGFR mice

A complementary DNA coding for a truncated form of the human EGFR, lacking the kinase domain in its intracytosolic region (amino acids 654-1186), was cloned in a transference bacterial artificial chromosome clone RP23-279P6 (kindly provided by Prof. Dr. Günther Schütz, Molekularbiologie der Zelle I, Deutsches Krebsforschungszentrum (DKFZ) Heidelberg, Germany) carrying Albumin locus and Chloramphenicol resistance gene. The truncated EGFR was introduced just in the ATG starting codon of the albumin gene, surrounded by 160 kb of the albumin chromosomal genomic sequence, as described (Warming et al., 2005). Linearized bacterial artificial chromosome DNA was then microinjected into the pronuclei of mouse B6CBAF2 zygotes according to reported protocols (Giraldo and Montoliu, 2001), which were later transferred to pseudopregnant recipient females, finally obtaining transgenic mice Alb-Δ654-1186EGFR (from now abbreviated as ΔEGFR) (**Figure XIX**). Six different founder mice were bred with C57BL/6 wild-type (WT) mice. Three of them gave littermates and showed germline transmission of the transgene, so they were established and named as 1000 (>100 copies of the transgene), 2000 (10-20 copies of the transgene) and 4000 (<10 copies of the transgene) line. The ΔEGFR F1 mice obtained were interbred to generate stable transgenic mouse lines, which were kept heterozygous. Transgenic lines are archived in the European Mouse Mutant Archive as B6CBA-Tg(Alb-deltaEGFR). Genotyping was assessed by polymerase chain reaction (PCR) as specified in the European Mouse Mutant Archive. Using specific primers that exclusively detect expression of the human EGFR gene, we demonstrated the transgene expression in ΔEGFR mice by quantitative real-time polymerase chain reaction (qRT-PCR) analysis.

These experiments were carried out by Jose Carlos Segovia, María García Bravo and Esther Grueso, in collaboration with Lluis Montoliu and Almudena Fernández, and with Aránzazu Sánchez and Adoración Martínez Palacián, performed in Cell Differentiation and Cytometry Unit, Hematopoietic Innovative Therapies Division, Centro de Investigaciones Energéticas, Medioambientales y Tecnológicas (CIEMAT), Centro de Investigación Biomédica en Red de Enfermedades Raras (CIBERER), Advanced Therapies Mixed Unit, CIEMAT/IIS Fundación Jiménez Díaz, Department of Molecular and Cellular Biology, National Centre for Biotechnology (CNB-CSIC), and the Department of Biochemistry and Molecular Biology II, School of Pharmacy, Complutense University of Madrid (UCM) (Madrid, Spain).

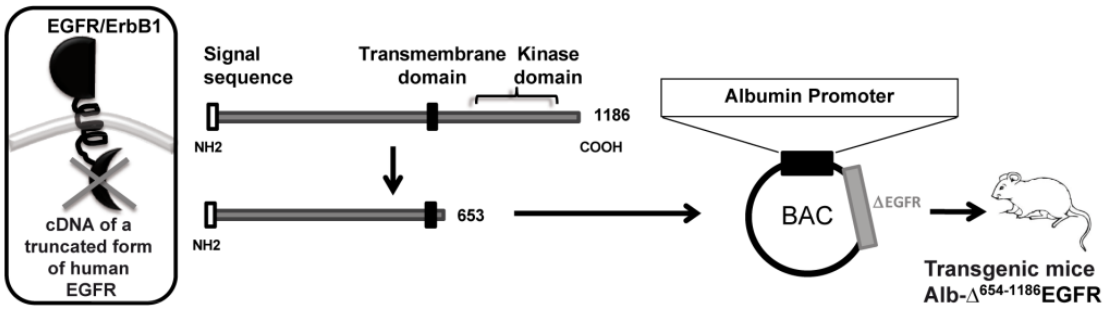

Figure XIX. Diagram representing the generation of the transgenic model of Alb-Δ654-1186EGFR (abbreviated as ΔEGFR) mice. A complementary DNA coding for a truncated form of the human *EGFR* that had a deletion in its intracytosolic region (amino acids 654-1186) was cloned in a transference plasmid under the control of a specific hepatocyte promoter formed by the albumin locus just before ATG of the albumin mouse gene.

1.3. Partial hepatectomy

Animals used in this study were C57BL/6 mice, aged 8 to 12 weeks. Partial hepatectomies (PH) were performed by removal of two-thirds of the adult mouse liver, as described by Higgins and Anderson (Higgins and Anderson, R., 1931). Briefly, after cleaning the animal with 70% Ethanol, an incision was made just above the sternum bone and opened a little bit up and down. Next, a “V” incision was made on the muscle layer just delimiting the bone. By pushing with four fingers from down to up surrounding the opened area, the central and left lobe of the liver got out of the body. A ligature surrounding the two lobes was performed and the two lobes were removed simply by cutting them. Finally, both incisions were closed sewing them. Mice were euthanized at 6, 12, 24, 48 and 72 hours and 7 days after surgery. Tissue samples were immediately frozen in liquid nitrogen for RNA and protein extraction, cryopreserved in optimal cutting temperature (OCT) compound or fixed in 4% paraformaldehyde (PFA) overnight and paraffin embedded for immunohistochemical analysis. Livers from sham-operated mice were used as control.

These experiments were performed by Aránzazu Sánchez, Margarita Fernández and Eva Crosas-Molist in the Department of Biochemistry and Molecular Biology II, School of Pharmacy, Complutense University of Madrid (UCM, Spain). Samples were collected by María García Álvaro, Annalisa Addante and Laura Almalé.

1.4. Diethylnitrosamine-induced hepatocarcinogenesis in mice

Male mice at day 15 of age received intraperitoneal injections of diethylnitrosamine (DEN) (10 mg/kg) diluted in saline buffer. After 9 and 12 months, mice were sacrificed and their livers removed. Tissue samples were immediately frozen in liquid nitrogen for RNA and protein extraction, cryopreserved in OCT compound or fixed in 4% PFA overnight and paraffin embedded for immunohistochemical analysis.

These experiments were performed by Aránzazu Sánchez in the Department of Biochemistry and Molecular Biology II, School of Pharmacy, Complutense University of Madrid (UCM, Spain). Samples were collected by María García Álvaro, Annalisa Addante and Laura Almalé.

1.5. Analysis of serum parameters

For serum biochemical analysis, total blood was withdrawn from the carotid artery under isoflurane anesthesia, allowed to clot at room temperature (RT) and centrifuged for 10 min at 1800rpm in a microcentrifuge. Serum was stored at -20ºC. Alkaline phosphatase (ALP), alanine aminotransferase (ALT), aspartate aminotransferase (AST) and total bilirubin (BIL T) were measured in a Clinical Analysis Laboratory (Complutense University, Madrid, Spain) using gold-standard methods and a Cobas Integra 400 Plus Chemistry Analyzer (Roche).

These experiments were performed by Aránzazu Sánchez, Margarita Fernández, Daniel Caballero Díaz and Judit López Luque in Department of Biochemistry and Molecular Biology II, School of Pharmacy, Complutense University of Madrid (UCM, Spain).

2. Cell culture

2.1. Cell models

2.1.1. Generation of transgenic ΔEGFR hepatocyte cell lines

To generate immortalized hepatocytes, pools of four to six livers from WT and ΔEGFR neonates (5-7 days old) were used. Isolation of the cells (by collagenase dispersion) and immortalization were performed as described (Valverde et al., 2003). Briefly, viral Bosc-23 packaging cells were transfected at 70% confluence with 3 µg/6 cm-dish of the puromycin-resistance retroviral vector pBabe encoding SV40 Large T antigen (LTAg) (kindly provided by J. de Caprio, Dana Farber Cancer Institute, Boston, MA). Then, primary cultures of neonatal hepatocytes isolated from WT and ΔEGFR mice were infected at 60% confluence with polybrene (4 µg/ml)-supplemented virus for 48 hours and maintained in culture medium for 72 hours, before selection with puromycin (0,5-1 µg/ml) for one week. Pools of infected cells rather than individual clones were selected to avoid potential clone-to-clone variations. Immortalized cell lines were further cultured for at least two weeks with arginine-free medium supplemented with 10% Fetal Bovine Serum (FBS) and ornithine to avoid growth of non-parenchymal cells.

These experiments were performed by Ángela M. Valverde and Águeda González Rodríguez in Instituto de Investigaciones Biomédicas “Alberto Sols” (CSIC/UAM), and Centro de Investigación Biomédica en Red de Diabetes y Enfermedades Metabólicas Asociadas (CIBERDEM), ISCIII, (Madrid, Spain).

2.1.2. Human liver tumor cell lines

HepG2, Hep3B and PLC/PRF/5 cell lines were obtained from the European Collection of Authenticated Cell Cultures (ECACC). Huh7 and HLF cells were from the Japanese Collection of Research Bioresources (JCRB Cell Bank) and were kindly provided by Dr. Perales (University of Barcelona, Spain) and Dr. Giannelli (University of Bari, Italy), respectively. SNU449 cells were from the American Tissue Culture Collection (ATCC). The molecular characteristics of human liver tumor cells are shown in **Table I**.

Cell line	Tumor type	Morphology / differentiation grade	P53 status	Other characteristics
HepG2	Human caucasian hepatoblastoma	Epithelial	Wild type	Mutation in NRAS
PLC/PRF/5	Human liver hepatocarcinoma	Epithelial / Well differentiated	Mutated pR249S	
Huh7	Human liver hepatocarcinoma	Epithelial / Well differentiated	Mutated pY220S	
Hep3B	Human negroid hepatocarcinoma	Epithelial / Well differentiated	Deleted	Deficient in functional pRB; mutations within hFas gene
SNU449	Human asian hepatocarcinoma	Diffusely spreading cells / Poorly differentiated	Mutated pK139R pA161T	Aneuploid; mutations in *CDKN2A*
HLF	Human hepatoma (non-differentiated)	Diffusely spreading cells / Poorly differentiated	Mutated pG244A	

Table I. Molecular characteristics of the human liver tumor cell lines used.

2.2. Culture conditions

2.2.1. Cell culture on plastic

For cell culture, ΔEGFR hepatocyte cell lines were grown in DMEM medium from Lonza (Ref. BE12-604F, Verviers, Belgium), supplemented with 10% FBS which was from Gibco by Life Technologies (Ref. 10500-064, Pasley, UK), Penicillin (120 mg/ml), Streptomycin (100 mg/ml) and Amphotericin (2.5 mg/ml), and maintained in a humidified atmosphere of 37ºC, 5% CO_2.

Human liver tumor cell lines were cultured as following for both maintenance of the cell lines and experiments in 2D. Hep3B cells were grown in MEM medium from Sigma-Aldrich (Ref. M2279, St. Louis, MO, USA), supplemented with non-essential aminoacids and supplemented with 10% FBS from Sera Laboratories (Ref. EU-000-F, Brazil EU Grade), in a humidified atmosphere at 37ºC, 5% CO_2. Huh7 and PLC/PRF/5 were grown in DMEM medium, and SNU449 and HLF in RPMI medium from Sigma-Aldrich (Ref. R8758, St. Louis, MO, USA), both media supplemented with 10% FBS from Sera Laboratories (Cinder Hill, UK), in a humidified

atmosphere at 37ºC, 5% CO_2. Cell lines were never used in the laboratory for longer than 4 months after receipt or resuscitation.

All cell lines needed to be split at sub-confluent cultures (70-80%) by trypsinization (Trypsin-EDTA 0.05%). For the indicated experiments, cells were serum-starved during 8 to 12 hours before treatments. After this time, it is considered that cells lose the proliferative stimuli obtained from FBS components. This is useful for evaluating the effect of compounds alone.

2.2.2. Cell culture on thick layers of collagen I

Fibrillar type I Bovine dermal collagen solution (Ref. 5005 PureCol, Advanced BioMatrix, San Diego, CA, USA) was prepared at 1.7mg/mL in DMEM according to the manufacturer's protocol. Volume used differed according to the culture plate: 100 μL per well in 96-well plates, 300μL per well in 24-well plates. After collagen gel polymerization (4 hours at 37ºC, 10% CO_2), cells were seeded on top of the collagen in medium containing 10% FBS and allowed to adhere for 24 hours.

2.3. Treatments used

For experiments with transgenic ΔEGFR hepatocyte cell lines, cells at 60% confluence were serum-starved for 16 hours and treated with different factors: human recombinant TGF-β_1 (2ng/ml) from Calbiochem (Ref. 616455, La Jolla, CA, USA), or HB-EGF (20 ng/ml) from Sigma-Aldrich (Ref. E4643, St. Louis, MO, USA).

For experiments with HCC cell lines, response to TGF-β, in terms of migration and adhesion, was analyzed by adding human recombinant TGF-β_1 (2ng/mL) (Ref. 616455, Calbiochem, La Jolla, CA, USA) to the culture (complete medium, 10% FBS) for 72 hours. For experiments analyzing the response to EGF, cells at 60% confluence were serum-starved for 16 hours and treated with EGF (20ng/mL) (Ref. E9644, Sigma-Aldrich, St. Louis, MO, USA). For experiments analyzing the response to TGF-β_1, in terms of EGFR transactivation, cells at 60% confluence were serum-starved for 16 hours and treated with TGF-β_1 (2ng/mL) for 30 min, 1.5 hours or 3 hours.

Pictures of cells on culture were taken with an Olympus 70iX microscope and a Spot 4.3 digital camera and software. Representative images were edited in Adobe Photoshop software.

3. Knock-down assays

For stable transfection of short hairpin RNA (shRNA), cells at 50–60% confluence were transfected with MAtra-A reagent (IBA GmbH, Goettingen, Germany) at a dilution of 1:600 in complete media, according to the manufacturer's recommendation (15 minutes on the magnet plate), using 2μg/mL of shRNA plasmid. Hep3B and PLC/PRF/5 cell lines were stable silenced for EGFR. Four different shRNA plasmids were transfected, separately and combined, as well as a control unspecific shRNA. Pools of transfected cells rather than individual clones were selected to avoid potential clone-to-clone variations, and the best-silenced pools of transfected cells were selected (from now on denominated as clones). After 24 hours, media was changed to complete media, and selection of transfected cells was done in all cases with puromycin (InvivoGen Therapeutics, France), for at least 50 days prior to experiments. At the beginning, selection was done at a dose of 0.5μg/mL of puromycin and this dose was gradually increased until reaching 2μg/mL, which is the one used for maintaining the silenced clones. shRNA plasmids transfected were selected from Mission SH, Sigma-Aldrich (Madrid, Spain) and sequences are indicated in **Table II**. The cell line and the clone used for experiments are indicated in each figure.

shRNA (gene)	Plasmid number	Sequence (5'-3')
Human EGFR	#1	CCGGCCTCCAGAGGATGTTCAATAACTCGAGTTATTGAACATCCTCTGGAGGTTTTTG
	#2	CCGGGTGGCTGGTTATGTCCTCATTCTCGAGAATGAGGACATAACCAGCCACTTTTTG
	#3	CCGGGCTGCTCTGAAATCTCCTTTACTCGAGTAAAGGAGATTTCAGAGCAGCTTTTTG
	#4	CCGGCGCAAAGTGTGTAACGGAATACTCGAGTATTCCGTTACACACTTTGCGTTTTTG

Table II. shRNA sequences.

Generation of Hep3BshEGFR was performed by Laia Caja, and PLCshEGFR was carried out by Judit López Luque, both at Fabregat's laboratory in the Molecular Oncology Laboratory (IDIBELL).

4. Analysis of cell proliferation

4.1. Analysis of cell viability by Trypan blue

Analysis of cell viability in transgenic ΔEGFR hepatocyte cell lines was performed by trypan blue staining. At the desired times of treatment, cells were trypsinized collecting the media (where dead cells were present). After 5 minutes centrifugation at 1200rpm, cells were resuspended in 50μl of phosphate-buffered saline (PBS) + 1:10 v/v Trypan blue. Viable and non-viable (blue dyed) cells were counted in a Neubauer chamber, counting eight squares/condition, in duplicates. Results are expressed as percentage of viable and non-viable cells.

4.2. Crystal violet staining

Crystal violet staining allows quantifying the amount of cells that survive after a toxic process, being useful when working with adherent cells that detached after undergoing a toxic process. It is useful as well for quantifying the changes in the cell number along time when cells are cultured under certain conditions (Drysdale et al., 1983). The method consists on cell staining with a colorant, crystal violet. HCC cells were seeded in 24-well plates and cultured under basal conditions or treated with TGF-β (medium supplemented with 10% FBS).

After the time of culture required, cell medium was removed, cells were washed twice with PBS and the remaining viable adherent cells were stained with 300μl/well of crystal violet solution (0.2%(w/v) in 2% ethanol) for 30 minutes. Following this, the staining solution was removed, and the wells were washed several times with PBS or distilled water until the dye excess was eliminated. The plate was air-dried, and the stained cells were lysed by adding 300μl of 10% Sodium Dodecyl Sulfate (SDS) during 30 minutes, in motion. This lead to a cellular rupture that released the dye incorporated by the remaining cells and stained the SDS proportionally to the number of still attached cells. By spectrophotometric analysis, the absorbance was measured in a wavelength of 595nm. Results were then calculated as the percentage of viable cells at the indicated times relative to time zero.

4.3. Analysis of DNA content by flow cytometry

After incubation in p60 dishes under basal conditions or with different stimuli, in our case HCC cells were treated with TGF-β, cell media was recovered in a 15mL tube, so detached cells were taken, and remaining cells on the plate were washed twice with PBS, which was also recovered in the tube. Then, cells were detached using Trypsin-EDTA (0.05%) and added to the

recovered media for centrifugation at 1500rpm for 5 minutes. The pellet was resuspended in 200μL of PBS 1X and added drop by drop into an eppendorf tube containing 500μL of cold (stored at -20ºC) 100% ethanol, in constant motion (gently applied with a vortex), in order to fix the cells. At this point, samples can be stored at -20°C. To collect the fixed cells, samples were centrifuged at 2500rpm during 5 minutes at 4°C. The pellet was air-dried and resuspended in 250μL PBS containing 0.1mg/mL of RNAse. After incubation during 30 minutes at 37°C, propidium iodide (PI) was added at a final concentration of 0.05%. Following this process, PI incorporation was directly proportional to the amount of DNA contained by each cell. Finally, this suspension was analyzed in a Gallios cytometer from Beckman-Coulter. Cell cycle analyses were carried out using Kaluza version 1.1 software developed by Beckman-Coulter. DNA content: 2C: G_0/G_1 phases; 4C: G_2/M phases; >2C and <4C: S phase. Cells with a DNA content lower than 2C (hypodiploid cells) suffered DNA fragmentation, a well-known hallmark of the apoptotic process. Cells with a DNA content higher than 4C (tetraploid cells) suffered endoreduplication, altered cytokinesis, or nuclei fusion.

5. Analysis of cell death

5.1. Analysis of caspase-3 activity

For the analysis of Caspase-3 activity, after incubation of cells with the desired stimuli, in our case cells were treated with TGF-β, media was preserved and cells were scrapped. Cells and media were collected together in a 15mL tube, which was then centrifuged at 2500rpm for 5 minutes. Indeed, this pellet contained those cells that were attached to the tissue culture dish and those that were dead and floating in the media. The pellet was resuspended in 30 to 100μL of Lysis Buffer, Table III. The solution was then transferred to an eppendorf tube, which was incubated for 20 minutes on ice and vortexed every 5 minutes in order to optimize cell lysis. After this time, eppendorf tubes were centrifuged at 13000rpm during 10 minutes at 4°C. The supernatant was stored at -20 or -80°C until caspase-3 activity was quantified.

When Caspase-3 activity was analyzed in tissues, small pieces of frozen tissues were pulverized mechanically in a mortar, previously sterilized at 200ºC for 4 hours to inactivate RNAses. Tissue powder was then transferred to an eppendorf tube and resuspended in 200μL of Lysis Buffer (Table III), incubated for 20 minutes on ice with a vortex mix every 5 minutes. From this point, the same procedure was used for both, cells and tissue samples.

In both cases, to determine Caspase-3 activity, first we determined the protein concentration by Bradford Reagent as detailed in **Material and Methods 7.2.** Then, a mix containing 20μg of protein (in a final volume of 25μL), 125μL of Reaction Buffer 2X (Table IV) and 2μL of fluorigenic substrate for Caspase-3, Ac-DEVD-AMC (Ref. 556449, BD Biosciences Pharmigen, Franklin Lakes, NJ, USA) was prepared. This substrate, once it is cleaved by caspase-3, releases the AMC fragment that is fluorigenic and can be quantified spectrofluorimetrically. After 2 hours of incubation at 37°C and protected from light, fluorescence was measured in a Microplate Fluorescence Reader Fluostar Optima (Centres Científics i Tecnològics de la UB, CCiTUB) using an exciting wavelength of 360nm and an emission wavelength of 440nm. A unit of Caspase-3 activity is the amount of active enzyme necessary to produce an increase in 1 fluorescence unit in the spectrofluorimeter. Results were represented as arbitrary units/h/μg protein.

Tris-HCl pH 8	5mM
EDTA	20mM
Triton-X-100	0.5%

Table III. Caspase-3 Lysis Buffer.

Glycerol	20%
Hepes pH 7.5	40mM
DTT	4mM

Table IV. Caspase-3 Reaction Buffer 2X.

6. Analysis of gene expression

6.1. RT-PCR

RNeasy Mini Kit (Qiagen, Valencia, CA, USA) was used following Manufacturer's protocol for total RNA isolation. When RNA was isolated from cells, p60 culture plates were washed with PBS and cells were scrapped in 350μl of a solution containing RLT Buffer (from the Kit) previously adding 10μl/mL of β-Mercaptoethanol. When RNA was isolated from tissues, small pieces of frozen tissues were pulverized mechanically in a mortar, previously sterilized at 200ºC for 4 hours to inactivate RNAses, then tissue powder was transferred to an eppendorf tube and resuspended in 600μL of RLT with 10μL/mL of β-Mercaptoethanol.

Reverse transcription (RT) was carried out with random primers using 1μg of total RNA from each sample for complementary DNA synthesis using High Capacity RNA to cDNA Master Mix Kit (Applied Biosystems, Foster City, CA, USA) following Manufacturer's instructions.

6.2. Quantitative Real Time PCR (qRT-PCR)

For quantitative Real Time PCR, RNA was obtained as explained in the above section. Expression levels were determined in duplicates in an ABIPrism7700 System, using the SYBR® Green PCR Master Mix (Applied Biosystems, Foster City, CA, USA) in a 96-well plate in a final volume of 25μL, for the primers detailed in bold in **Table V.** In that case, reaction was prepared using 25μL of SYBR® Green PCR Master Mix, 2.5μL specific primers (10μM) and 50ng of cDNA plus RNAse free water up to 50μL per duplicate. For the other primers in **Table V** and **Table VI**, expression was determined in a LightCycler® 480 Real Time PCR System, using the LightCycler® 480 SYBR Green I Master Mix (Roche Diagnostics GmbH, Mannheim, Germany), in a 384-well plate, in a final volume of 10μL. In this case, reaction was prepared using 10μL of LightCycler® 480 SYBR Green I Master Mix, 2μL specific primers (5μM) and 40ng of cDNA in a final volume of 20μL per duplicate. The levels of mRNA for each gene were determined following Manufacturers' protocols and were normalized with a housekeeping gene (18S for ABIPrism7700 SYBR Green System, L32 for LightCycler 480 SYBR Green System, and SFRS4 for human samples from HCC patients in the LightCycler 480 SYBR Green System).

Gene (mouse)	Forward	Reverse
18S	CGAGACTCTGGCATGCTAA	CGCCACTTGTCCCTCTAAG
A2m	TGTCACTCATCCTGTTGTCC	TCCTTCTTCGTGTCCTGGTT
Acaca	CTGCAGAAACTCATCCTCT	TCGAACATACACCTCCAGA
Acacb	TCCCCAGAGAAGTACCCCAA	CCATGCCCACCTCGTTACAA
Bclxl	GGAAAGCGTAGACAAGGAGATG	GCATTGTTCCCGTAGAGATCC
Bim	GAGATACGGATTGCACAGGAG	CGGAAGATAAAGCGTAACAGTTG
Bmf	AGTTCCATCGGCTTCATACG	CCCTTCCCTGTTTTCTTGTC
Ccna2	GAATGTCAACCCCGAAAAACTG	TGCTCATCGTTTATAGGAAGGTC
Ccnb2	TCCTAAAGCCAAGAGCCATG	TGGTACTTTGGTGTTCTGAGG
Ccnd1	CATCTACACTGACAACTCTATCCG	TCTGGCATTTTGGAGAGGAAG
Cdkn1a	TTCCGCACAGGAGCAAAGTG	AAGTCAAAGTTCCACCGTTCTCG
Cdkn2b	GGCAAGTGGAGACGGTG	GTTGGGTTCTGCTCCGTG
Egfr	CTCCATGCTTTCGAGAACCTAG	ATGATCACATCCCCATCACTG
Erbb2	ACCTCTCCTACATGCCTATCTG	ATGAATGTCACTGGGCTGG
Erbb3	GGGCTATGAGACGCTACTTG	ACAGTTCCAAAGACACCAGAG
Erbb4	ACTCCAATAGGAATCAGTT	AGGAGTCATCAAACATCTC
Fasn	GGATGGCCGCGGTTTAAATA	CCTCCATGGCTCTTCTCTGTC
G6pdx	TGAGGAGTCGGAGCTGGATC	AGTTCATCACTCCGGACAAAG
Hgf	GAGTCTGAGTTATGTGCTGGG	AGGACGATTTGGGATGGC
Il1b	CTGGGAAACAACAGTGGTCA	CTGCTCATTCACGAAAAGGG
Il6	AGTCAATTCCAGAAACCGCT	CTGTGAAGTCTCCTCTCCGG
L32	ACAATGTCAAGGAGCTGGAG	TTGGGATTGGTGACTCTGATG
Met	GACCTCAGTGCTCTAAATCCAG	TCCAGCAAAGTCCCATGATAG
Nox1	TCCTTCGCTTTTATCGCTCC	TCGCTTCCTCATCTGCAATTC
Nox2	TCCTATGTTCCTGTACCTTTGTG	GTCCCACCTCCATCTTGAATC
Nox4	TCCAAGCTCATTTCCCACAG	CGGAGTTCCATTACATCAGAGG
Tgfa	CTGGGTATCCTGTTAGCTGTG	GTACTGAGTGTGGGAATCTGG
Tgfb	CCTGAGTGGCTGTCTTTTGA	CGTGGAGTACATTATCTTTGCTG
Tnfa	ACGTCGTAGCAAACCACCAA	ATCGGCTGGCACCACTAGTT
uPA	GTCGTCAAATGGAGGGAAGA	GCCTGTGTCTGAGGGTAATG

Table V. Mouse primers sequences used in an ABIPrism7700 SYBR Green System (**bold**) or in a LightCycler 480 SYBR Green System quantitative PCR.

Gene (human)	Forward	Reverse
CDC42	CAGGGCAAGAGGATTATGACAG	GTTATCTCAGGCACCCACTT
CDH1	CCCAATACATCTCCCTTCACAG	CCACCTCTAAGGCCATCTTTG
CDH2	CCCAAGACAAAGAGACCCAG	GCCACTGTGCTTACTGAATTG
EGFR	AGATCATTTTCTCAGCCTCCAG	GACATAACCAGCCACCTCC
L32	AACGTCAAGGAGCTGGAAG	GGGTTGGTGACTCTGATGG
RAC1	GCTTTTCCCTTGTGAGTCCTG	CCTTCAGTTTCTCGATCGTGTC
RHOA	AGCTGGGCAGGAAGATTATG	CGTTGGGACAGAAATGCTTG
RHOC	CAAGACGAGCACACCAGG	AGCACTCAAGGTAGCCAAAG
SFRS4	TGGAACTGAAGTCAATGGGAG	CTGCTCTTACGGGAATGTCTG
SNAI1	GCTGCAGGACTCTAATCCAGAGTT	GACAGAGTCCCAGATGAGCATTG
SNAI2	ACACATTAGAACTCACACGGG	TGGAGAAGGTTTTGGAGCAG
TGFB1	AAGTGGACATCAACGGGTTC	GTCCTTGCGGAAGTCAATGT
TWIST1	CTCAGCTACGCCTTCTCG	ACTGTCCATTTTCTCCTTCTCTG
VIM	GGAAGCCTAACTACAGCGAG	CAGAGTCCCAGATGAGCATTG
ZEB1	ACCCTTGAAAGTGATCCAGC	CATTCCATTTTCTGTCTTCCGC
ZEB2	AGGCATATGGTGACGCACAA	CTTGAACTTGCGGTTACCTGC

Table VI. Human primers sequences used in a LightCycler 480 SYBR Green System quantitative PCR.

7. Analysis of protein expression

7.1. Cell lysis

For protein lysis from cells in culture, after incubation with different factors or after cell culture under basal conditions, cell culture dishes were placed on ice. The media was collected into tubes, 2mL of cold PBS was added to each dish, and cells were scrapped and collected into the tube. To make sure that most of the cells were collected, other 2mL of cold PBS were added to the dish and collected into the tube. Cells were then centrifuged at 2500rpm during 10 minutes at 4°C. The pellet was resuspended in 60-100μL of RIPA Lysis Buffer (Table VII) and transferred to an eppendorf tube, being the lysis performed during 1 hour with rotation at 4°C. Then, tubes were centrifuged at 13000rpm during 10 minutes at 4°C, and the supernatants were collected and stored at -20°C or -80°C until they were processed.

When protein was isolated from tissues, small pieces of frozen tissues were pulverized mechanically in a mortar, previously sterilized at 200ºC for 4 hours to inactivate RNAses, then tissue powder was transferred to an eppendorf tube and resuspended in 100-250μL of RIPA Lysis Buffer (Table VII). The lysis is performed during 1 hour with rotation at 4ºC. The, tubes were centrifuged at 13000rpm during 10 minutes at 4ºC, and the supernatants were collected in new eppendorf tubes, which were again centrifuged at 13000rpm during 10 minutes at 4ºC. Finally, these superantants were collected in new eppendorfs tubes and stored at -80ºC until they were processed.

Sodium Deoxycholate	0.5%
TRIS-HCl pH 7.5	30mM
SDS	0.1%
Triton-X-100	1%
NaCl	150mM
EDTA	5mM
Glycerol	10%
PMSF	1mM
Leupeptin	5μg/mL
Na_3VO_4	0.1mM
DTT	0.5mM
β-Glycerolphosphate	20mM

Table VII. RIPA Lysis Buffer.

7.2. Protein quantification by Bradford's method

Protein quantification was done following the spectrophotometric method described by M. Bradford in 1976. For each measurement, a standard curve of protein concentration was prepared with Bovine Serum Albumin (BSA) in a range from 0 to 2μg/mL. The reaction was prepared mixing 200μL of distilled water, 2μL of protein extract and 50μL of Bradford Reagent (Ref. B6916, Sigma-Aldrich, St. Louis, MO, USA). Absorbance was measured at 595nm.

7.3. Protein quantification by BCA commercial kit

If SDS was a component of the Lysis Buffer, Bradford method could not be used. Instead, we used the commercial Pierce™ BCA Protein Assay kit (Ref. 23227, Thermo Scientific, Rockford, IL, USA). For each measurement, a standard curve of protein concentration was prepared with BSA in a range from 0 to 2μg/mL. The reaction was prepared by mixing Solution A and Solution B in a ratio of 50:1. Then, 200μL of this mix were added to 10μL of 1:10 diluted sample, into a 96-well plate. After 30 minutes of incubation at 37°C, absorbance was measured at 595nm.

7.4. Protein quantification by Bio-Rad commercial kit

Another alternative when Bradford method could not be used is the commercial kit Bio-Rad protein assay dye reagent concentrate (Ref. 500-0006, Bio-Rad Laboratories GmbH, Munich, Germany). For each measurement, a standard curve of protein concentration was prepared with BSA in a range from 0 to 0.2μg/mL. The reaction was prepared by mixing the Concentrate Solution and distilled water in a ratio of 1:5. Then, 200μL of this mix were added to 10μL of 1:10 diluted sample, into a 96-well plate. Absorbance was measured at 595nm, and no previous incubation at 37ºC is needed.

7.5. Protein immunodetection by Western blot

Protein separation by their molecular weight was done by denaturalizing polyacrylamide gels. Protein samples were prepared by mixing 30 to 100μg of protein with Laemmli loading buffer, and were denaturalized by heating them at 95°C for 5 minutes. Once the samples were boiled, they were spun and saved at 4°C. Acrylamide gels consist of two different parts: the stacking and the resolving gel. The first part was always prepared at the same acrylamide concentration, as its function was to gather proteins. However, the resolving part is prepared at

different concentrations of acrylamide depending on the size of the proteins to be studied, as its function is to sort these proteins by their size after denaturalization: a gel of 12-15% acrylamide for proteins with low molecular weight, and gels of 8-10% acrylamide for proteins with high molecular weight. Once the gel was ready, it was assembled into the gel holder and immersed into the tank, which was filled with an electrophoresis buffer (25mM Tris-HCl; 0.1% SDS; 0.2M glycine; pH 8,3). Then, samples were carefully loaded into the gel, together with a molecular weight standard in order to know the molecular weight of the proteins studied. Finally, they were submitted to electrophoresis at a constant voltage.

Once finished the electrophoresis, proteins were transferred to an Amersham Hybond PVDF membrane (GE Healthcare, Life Science, Germany) through the passage of electrical current using semi-dry equipment. Previously to the protein transfer, the PVDF membrane was first immersed into methanol for 1 minute following the manufacturer's instructions. Then, the PVDF membrane and the Wattman paper were soaked in transfer buffer (48mM Tris-HCl; Glycine 39mM; SDS 0.04%; Methanol 20%; pH 8.3) for 5 minutes, and the equipment was assembled as follows from bottom to top: 3 Wattman papers - PVDF membrane - Acrylamide gel - 3 Wattman papers. An electrical current of 0.3 A was applied during 0.5-1 hour. After this time, the membrane was stained into a solution of 0.5% red Ponceau in 1% acetic acid while singing to confirm that proteins had uniformly been transferred into the membrane. Then, the membrane was washed several times in PBS-Tween 0.05% (PBS-T).

For blotting the desired protein, the membrane was incubated in 5% non-fat dry milk or 5% BSA (depending on the primary antibody to be used) in PBS-T for 1 hour at RT for blocking unspecific bindings. After this time, it was incubated with the primary antibody (see antibodies and conditions in **Table VIII**) in 0.5 % milk or 5% BSA in PBS-T during 16 hours at 4°C in motion. After that, the membrane was washed 3 times during 10 minutes with PBS-T, and subsequently incubated with the secondary antibody (from GE Healthcare: anti-Mouse (NA931V) and anti-Rabbit (NA934V), conjugated with peroxidase) at a dilution of 1:3000 in 0.5% milk-PBS-T during 1 hour at RT in motion. The membrane was washed again 3 times in PBS-T. To visualize the antibody hybridized to the protein of study, the membrane was incubated with a chemiluminescent solution, ECL TM Western blotting detection reagent (GE Healthcare, Life Science, UK) and exposed to an Amersham HyperfilmTM ECL (GE Healthcare, Life Science, UK).

In almost all the cases, hybridized antibody could be removed with the stripping process consisting in soaking the membrane during 30 minutes at 50°C with stripping solution (62.5nM TRIS-HCl pH 6.8; SDS 0.05%; β-Mercaptoethanol 20%), in motion.

Densitometric analysis of protein bands' intensity was performed using ImageJ software (National Institutes of Health (NIH), Bethesda, MD, USA).

Primary antibody	Secondary antibody	Working conditions	Reference number
β-Actin (clone AC-15)	Anti-mouse	1:5000	Sigma-Aldrich (A5441)
Bcl-$x_{S/L}$ (S-18)	Anti-rabbit	1:1000	Santa Cruz (sc-634)
Bim	Anti-rabbit	1:1000	BD Pharmigen (BD-559685)
Cyclin D1 (M-20)	Anti-rabbit	1:500	Santa Cruz (sc-718)
EGFR (V279) (human&mouse origin)	Anti-rabbit	1:500	Cell signaling (#3265)
EGFR (human origin)	Anti-rabbit	1:1000	Cell signaling (#2232)
Met (SP260)	Anti-rabbit	1:1000	Santa Cruz (sc-162-R)
Nox1 (Mox1 (H-75))	Anti-rabbit	1:500	Santa Cruz (sc-25545)
Nox2 (Gp91-phox (54.1))	Anti-mouse	1:1000	Santa Cruz (sc-130543)
Nox4*	Anti-rabbit	1:1000	SIGMA-Genosys
Phospho-Akt (Ser473)(D9E)XP	Anti-rabbit	1:1000	Cell signaling (#9271)
Phospho-EGFR (Tyr1068)(D7A5)	Anti-rabbit	1:1000	Cell signaling (#3777)
Phospho-Met (Tyr1234/1235)(D26)	Anti-rabbit	1:500	Cell signaling (#3077)
Phospho-p44/42 MAPK (Thr202/Tyr204)	Anti-rabbit	1:1000	Cell signaling (#9101)
Phospho-Smad3 (Ser423/Ser425)	Anti-rabbit	1:1000	Millipore (07-1389)
Smad3 (clone EP568Y)	Anti-rabbit	1:1000	Millipore (04-1035)

Table VIII. Primary antibodies used for Western blotting.

* Rabbit anti-NOX4 polyclonal antiserum was created by Sigma-Genosys against a peptide corresponding to the C-terminal loop region (amino acids 499-511), according to our order. We licensed the antibody to be commercially exploited by Merck Millipore (Billerica, MA) (Catalogue number. ABC459).

8. Immunocytochemistry

8.1. Immunofluorescence in 2D cultured cells

Epifluorescence microscopy studies were performed on cells seeded on gelatin-coated glass coverslips. For **F-actin staining**, under basal conditions or after treatment, cells were washed with PBS and fixed with 4% PFA in PBS for 20 minutes at RT, then washed 3 to 5 times with PBS and finally, incubated with phalloidin conjugated (Phalloidin-TRITC) diluted 1:500 in 1% BSA in PBS for 1 hour. To detect **E-cadherin** and **vimentin**, cells were fixed with cold methanol (stored at -20ºC) during 2 minutes, washed 3 to 5 times with PBS, and then incubated with the corresponding primary antibody. For **vinculin** and **ZO-1** staining, cells were fixed with 4% PFA in PBS during 20 minutes and washed 3 to 5 times with PBS. Primary antibodies, detailed in **Table IX**, were diluted in PBS-BSA 1% and incubated during 1 hour at room temperature. Then, after several washes with PBS, samples were incubated with fluorescent-conjugated secondary antibodies (anti-mouse Alexa Fluor® 488 or anti-rabbit Alexa Fluor® 488 from Molecular Probes (Eugene, OR, USA)), using 1:200 dilution in PBS-BSA 1% during 1 hour at room temperature. Finally, cells were washed 3 times for 5 minutes each with PBS, adding DAPI (40'6-diamidino-2-phenylindole) (Sigma-Aldrich, St. Louis, MO, USA) or DRAQ5 (Biostatus, UK) in the third last wash for nuclear DNA staining, when necessary. At the end, samples were embedded using MOWIOL® 4-88 reagent (Calbiochem, La Jolla, CA, USA).

Cells were visualized in a Nikon eclipse 80i microscope with the appropriate filters. Representative images were taken with a Nikon DS-Ri1 digital camera and using NIS-Elements BR 3.2 (64-bit) software.

Vinculin with F-actin staining (for focal adhesions studies) from cells seeded on gelatin-coated glass coverslips was visualized on a Leica TCS SP5 spectral confocal microscope (Centres Científics i Tecnològics de la UB, CCiTUB) with a HCX PL APO λ blue 40x 1.4 oil objective lens and excited with the 488nm (for Vinculin) and the 555nm (for F-actin) laser line of an Argon laser. Acquisition software was LEICA application suite advanced fluorescence (LAS AF). Confocal Z-slice images were analyzed using ImageJ software (National Institutes of Health (NIH), Bethesda, MD, USA).

Representative images were edited in Adobe Photoshop software.

8.2. Immunofluorescence in cells cultured on thick layers of collagen

For **F-actin and DRAQ5 immunostaining** of cells seeded on top of a thick collagen I matrix in a 24-well plate, the cells were fixed during 15 minutes at RT by adding 600μL of PFA 12% to the cells seeded on 300μL of matrix (final concentration of PFA is 4% considering

collagen matrix volume) and washed 3 times with PBS during 5 minutes. Afterwards, cells were finally stained for F-actin during 1 hour at RT with phalloidin conjugated (Phalloidin-TRITC) diluted 1:500 in blocking solution (PBS-BSA 4%), and washed again for 3 times with PBS during 5 minutes. During the last wash, nuclei were stained with a DRAQ5 (Biostatus, UK) 1:1000 solution, and stored with PBS at 4ºC until visualization.

For **pMLC2 (phospho-Myosin Light Chain 2) immunostaining** of cells seeded on top of a thick collagen I matrix in a 96-well plate, the cells were fixed during 15 minutes at RT by adding 50μL of PFA 12% to the cells seeded on 100μL of matrix (final concentration of PFA is 4% considering collagen matrix volume) and washed 3 times with PBS during 5 minutes. Afterwards, cells were permeabilized during 10 minutes using a solution containing 0.3% Triton X-100 in PBS-BSA 4% and washed again 3 times with PBS during 5 minutes. Next, samples were blocked in a PBS-BSA 4% solution during 20 minutes, and finally immunostained with the specific primary antibodies diluted in blocking solution. For pMLC2 staining, primary antibody was diluted 1:200 into blocking solution and incubated overnight at 4ºC, in motion. The day after, cells were washed 5 times with PBS for 5 minutes and incubated during 2 hours at RT with secondary anti-rabbit Alexa Fluor® 488 from Molecular Probes (Eugene, OR, USA) diluted 1:500 in blocking solution. Cells were washed 5 times with PBS during 5 minutes, and finally stained for F-actin during 1 hour at room temperature with phalloidin conjugated (Phalloidin-TRITC) diluted 1:500 in blocking solution, and washed again for 3 times with PBS during 5 minutes. During the last wash, nuclei were stained with a DRAQ5 (Biostatus, UK) 1:1000 solution.

In all incubations with primary and secondary antibodies, as well as for DRAQ5 staining, dilutions were calculated considering the volume of the collagen matrix. The antibodies are detailed in **Table IX**.

For the imaging, collagen gels with immunostained cells were transferred to glass-bottomed dishes and visualized on a Leica TCS SP5 spectral confocal microscope (Centres Científics i Tecnològics de la UB, CCiTUB) with a HCX PL APO λ blue 40x 1.4 oil objective lens. Acquisition software was LEICA application suite advanced fluorescence (LAS AF). Confocal Z-slice images were analyzed using ImageJ software (National Institutes of Health (NIH), Bethesda, MD, USA). pMLC2 fluorescence signal was quantified calculating the pixel intensity in each image relative to the number of cells, determined with DRAQ5 staining, using ImageJ. Representative images were edited in Adobe Photoshop software.

Primary antibody	Secondary antibody	Working conditions	Reference number
E-cadherin	Anti-mouse	1:50	BD Transduction (C20820)
Phospho-Myosin Light Chain 2 (Ser19)	Anti-rabbit	1:200	Cell signaling (#3671)
Phalloidin-TRITC	---------	1:500	Sigma-Aldrich (P1951)
Vimentin (cloneV9)	Anti-mouse	1:50	Sigma-Aldrich (V 6630)
Vinculin	Anti-mouse	1:100	Sigma-Aldrich (V9131)
ZO-1	Anti-rabbit	1:50	Invitrogen (61-7300)

Table IX. Primary antibodies used for Immunocytochemistry

9. Immunohistochemistry

9.1. Paraffin embedding

After fresh tissue was surgically recovered, it was rinsed with PBS and included into a cassette for paraffin embedding. Then, it was fixed with tamponed formaldehyde (4%) during 12-16 hours. After fixing the samples, they were washed 3-4 times with PBS, and immersed in PBS-30% sacarose, PBS-20% sacarose and PBS-10% sacarose, consecutively. After fixing the samples, those were dehydrated by bathing them in subsequent alcohols as indicated on **Table X**. Then, dehydrated samples were finally embedded in paraffin at 65ºC and taken to 4ºC for solidification.

Step	Time
Rinse with tap water	30 minutes
Ethanol 70%	60 minutes
Ethanol 96%	60 minutes
Ethanol 96% (new)	60 minutes
Ethanol 96% (new)	Overnight
Ethanol 100%	60 minutes
Ethanol 100% (new)	90 minutes
Ethanol 100% (new)	90 minutes
Xylene	90 minutes
Xylene-Paraffin (50%-65ºC)	90 minutes
Paraffin (65ºC)	Overnight

Table X. Samples dehydratation for paraffin-embedding.

9.2. Immunohistochemistry on paraffin-embedded tissues

Paraffin-embedded samples were cut into 4μm-thick sections using a microtome. Then after, slices were placed in poly-lysinated slides (for poly-lysing, slides were incubated for 20 minutes with poly-L-Lysine at 4ºC and let 16 hours of air-drying at 37ºC). Next, paraffin was removed and samples rehydrated. For this, sample slides were placed at 50ºC during 30 minutes and then soaked in subsequent alcohols as indicated in **Table XI**. Then after, sample slides were stained with Hematoxylin and Eosine (H&E) for tissue structure study or used for immunohistochemistry (IHC).

Step	Time
Xylene	10 minutes
Xylene (new)	10 minutes
Xylene (new)	10 minutes
Ethanol 100%	5 minutes
Ethanol 100% (new)	5 minutes
Ethanol 100% (new)	5 minutes
Ethanol 96%	5 minutes
Ethanol 96% (new)	5 minutes
Ethanol 96% (new)	5 minutes
Ethanol 70%	5 minutes
Distilled water	5 minutes

Table XI. Samples hydratation for IHC.

For **H&E staining**, Hematoxylin solution, Harris modified (Ref. HHS32, Sigma-Aldrich, St. Louis, MO), was used. Samples were stained for 1 minute and washed abundantly with tap water. Next, samples were stained with Eosin solution (Ref. HT110232, Sigma-Aldrich, St. Louis, MO) for 6 minutes and washed again abundantly with tap water. Finally, samples were dehydrated soaking them in subsequent alcohols as indicated in **Table XII** and slides were mounted in D.P.X. mountant (Ref. 360294H, BDH Prolabo, Germany) for preservation.

Step	Time
Ethanol 70%	5 minute
Ethanol 96%	5 minute
Ethanol 96% (new)	5 minute
Ethanol 96% (new)	5 minute
Ethanol 100%	5 minutes
Ethanol 100% (new)	5 minutes
Ethanol 100% (new)	5 minutes
Xylene	10 minutes
Xylene (new)	10 minutes
Xylene (new)	10 minutes

Table XII. Samples dehydratation after H&E staining.

For **IHC**, after rehydration, samples were rinsed during 5 minutes with distilled water and then covered with a mixture of citric acid (0.38mg/mL) and sodium citrate (2.45mg/mL), taken to boiling temperature and left boiling during 2 minutes to break the methylene bridges and expose

the antigenic sites in order to allow the antibodies to bind. Next, samples were left immersed in this mixtures for 20 minutes at RT (until the temperature is between 35-45ºC), and afterwards rinsed during 5 minutes with distilled water. At this point, we proceeded to inactivate the endogenous peroxidases of the samples, in order to minimize the background, by incubating the slides in 3% hydrogen peroxide during 10 minutes and then washing them, first during 5 minutes in distilled water, and then in PBS-Tween (0.1%) during 10 minutes. Afterwards, samples were covered during 2 hours in IHC-blocking solution: 2% BSA and 20% FBS in PBS-Tween (0.1%). Then, slides were incubated overnight with primary antibody (**Table XIII**) diluted in IHC-blocking solution, at 4ºC in a wet chamber.

Primary antibody	Secondary antibody	Working conditions	Reference number
Cleaved caspase-3 (Asp175)	Anti-rabbit	1:100	Cell signaling (#9661)
E-cadherin	Anti-mouse	1:50	BD Transduction (C20820)
F4/80	Anti-rabbit	1:100	Abcam (ab74383)
Ki67 (SP6)	Anti-rabbit	1:50	Abcam (ab16667)
Nox2 (Gp91-phox (54.1))	Anti-mouse	1:50	Santa Cruz (sc-130543)
Phospho-EGFR (Tyr1068)(1H12)	Anti-rabbit	1:50	Cell signaling (#2236)
Phospho-Smad2 (Ser 465/467)	Anti-rabbit	1:50	Cell signaling (#3101)
TGF-β1 (V)	Anti-rabbit	1:50	Santa Cruz (sc-146)

Table XIII. Primary antibodies used for Immunohistochemistry.

Next morning, slides were washed 3 times with PBS-Tween (0.1%) during 10 minutes and incubated during 1 hour with anti-mouse or anti-rabbit secondary peroxidase-conjugated antibodies (Ref. PK4001 for anti-rabbit and PK-4002 for anti-mouse, Vectastain ABC KIT, Vector laboratories Inc., Burlingame, CA, USA) following the manufacturer's indications; then, samples were washed 3 times with PBS-Tween (0.1%) during 10 minutes and incubated in ABC (Vectastain ABC KIT, Vector laboratories Inc., Burlingame, CA, USA) solution for 30 minutes, following the manufacturer's indications, until developing the peroxidase staining with diluted Diaminobenzidine (D.A.B) (Ref. K3468, DAKO, Inc., Carpinteria, CA, USA) for a maximum of 30 minutes and taking care not to obtain a saturated signal. Once we had acquired an optimum staining, the developing reaction was stopped by soaking the samples into tap water during 5 minutes.

The final steps consisted in a counterstaining with Mayer's Hematoxylin (Ref. MHS32, Sigma-Aldrich, St. Louis, MO, USA) following with sample dehydration as indicated in **Table XIV**, and mounting the slides in D.P.X. for preservation.

Step	Time
Filtered Hematoxylin (Mayer's)	5 minutes
Running tap water	Until desired staining
Ethanol 70%	5 minute
Ethanol 96%	5 minute
Ethanol 96% (new)	5 minute
Ethanol 96% (new)	5 minute
Ethanol 100%	5 minutes
Ethanol 100% (new)	5 minutes
Ethanol 100% (new)	5 minutes
Xylene	10 minutes
Xylene (new)	10 minutes
Xylene (new)	10 minutes

Table XIV. Hematoxylin counterstaining after IHC following samples dehydratation.

Tissues were visualized in a Nikon eclipse 80i microscope with the appropriate filters. Representative images were taken with a Nikon DS-Ri1 digital camera and using NIS-Elements BR 3.2 (64-bit) software. Representative images were edited in Adobe Photoshop software.

10. Lipid analysis

10.1. Oil red O staining

For analysis of lipid content staining by Oil Red O solution (Ref. 01391, Sigma-Aldrich, St. Louis, MO, USA), OCT tissue-blocks from partial hepatectomy were cut into 50-µm-thick sections. Firstly, sections were washed with distilled water, and after rinsing with 60% isopropanol and distilled water again, tissues were stained with freshly prepared Oil Red O working solution for 10 minutes at room temperature. The working solution of Oil Red O was prepared by diluting a stock solution, i.e. 0.5g of Oil Red O in 100mL of isopropanol, with distilled water at a ratio of 3:2 (v/v). After rinsing with 60% isopropanol and washing with distilled water for 5 minutes, tissues were stained with DAPI and mounted in MOWIOL® 4-88 reagent. Lipid droplets were visualized with a Nikon eclipse 80i microscope with the appropriate filters. Representative images were taken with a Nikon DS-Ri1 digital camera and using NIS-Elements BR 3.2 (64-bit) software. Representative images were edited in Adobe Photoshop software.

10.2. Analysis of triglyceride content

Frozen liver tissue (100mg) was homogenized using a tissue grinder in 1mL solution containing 5% NP-40 in water. The samples were slowly heated to 80-100ºC in a water bath for 2-5 minutes, and then cooled down to RT. This step was repeated one more time to obtain all triglyceride in a soluble state. Samples were then centrifuged for 2 minutes (maximum speed) to remove any insoluble material. Triglyceride (TG) content was determined using a commercially available kit: Trygliceride quantitative kit (Ref. K622-100, BioVision, Life Science, Milpitas, CA, USA) following the manufacturers' instructions and normalized to protein concentration of the homogenate. The kit permits to extract the endogenous glycerol in the livers, so as the obtained data only represents the triglyceride content.

11. Migration analysis

11.1. Wound healing assay

Cells were grown under basal conditions up to 90% confluence. Monolayers were scratched with a pipette tip, then culture dishes were washed 2-3 times with fresh medium and finally, cells were cultured for 72 hours at 37ºC in medium with 2% FBS to avoid proliferation interference and under basal conditions or adding TGF-β (2ng/ml). Representative phase contrast pictures were taken just after the scratch as a time zero. Then, cell migration was recorded by phase contrast microscopy (Olympus IX-70) 72 hours after wound scratch.

11.2. Real time migration assay

For real time monitoring of cell migration, xCELLigence System was used. For this, we used CIM plates (Ref. 05 665 817 001, ACEA Biosciences, Inc., San Diego, CA, USA) which have an upper chamber sealed at the bottom with a microporous polyethylene terephthalate (PET) membrane with a median pore size of 8μm and a lower chamber that serves as a reservoir for chemoattractant media. xCELLigence System measures electrical impedance across micro-electrodes integrated on the underside of the membrane providing quantitative information about cell migration. CIM plates were placed onto the Real-Time Cell Analyzer (RTCA) station (xCELLigence System, Roche, Mannheim, Germany) for monitoring cell migration (**Figure XX**).

First, both sides of the membrane were coated during 30 minutes with a collagen type IV solution (Ref. C7521, Sigma-Aldrich, St. Louis, MO, USA) (167μg/mL or, which is the same, 25.5μg/cm^2). Then, cells cultured under basal conditions or after 62 hours in the presence of TGF-β were trypsinized and counted. Afterwards, 100μL of a suspension containing 4x10^{5}cells/mL without FBS were seeded onto the top chamber of a CIM plate. The lower chamber contained medium with 10% FBS as a chemoattractant. Cell migration was continuously monitored throughout the experiments by measuring changes in the electrical impedance at the electrode/cell interface, as a population of cells migrated from the top to the bottom chamber. Continuous values every 15 minutes were represented as Cell Index (CI), a dimensionless parameter, which reflects a relative change in measured electrical impedance, and quantified as a slope (hours^{-1}) of the first eight hours.

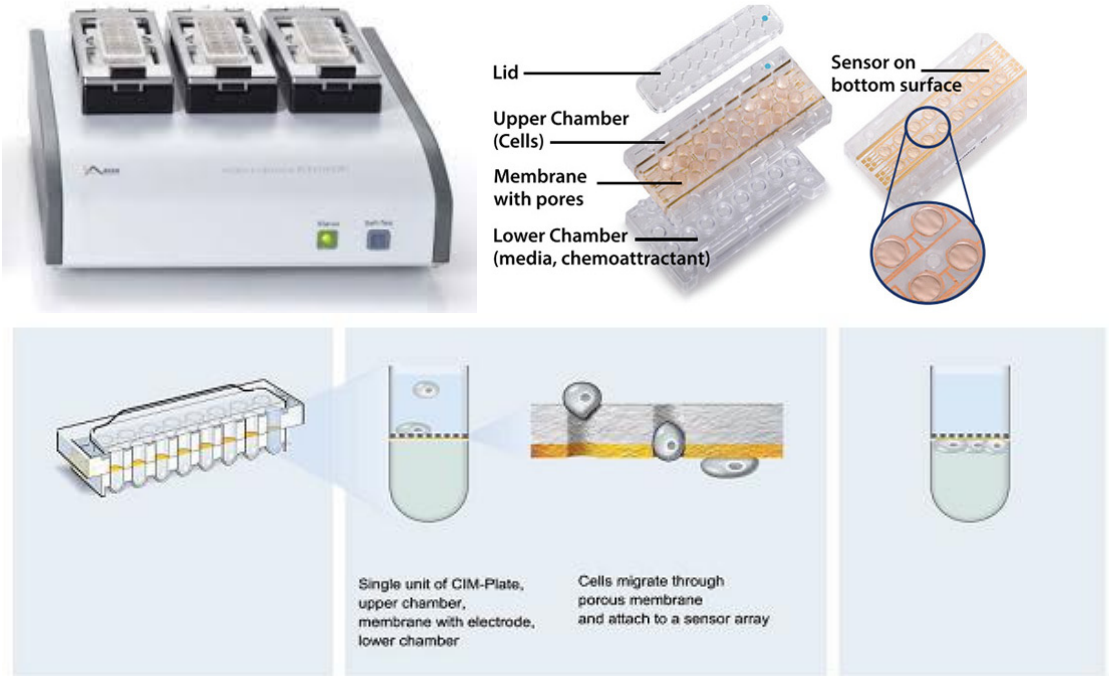

Figure XX. xCELLigence System for monitoring cell migration.

12. Real time adhesion assay

Cell adhesion was examined using a real time assay through the xCELLigence System. Cells were cultured under basal conditions or after 68 hours in the presence of TGF-β, then trypsinized and counted. Afterwards, $1.25x10^4$cells/well (final volume of 100μL) were seeded onto an E-plate 16 (Ref. 05 469 830 001, ACEA Biosciences, Inc., San Diego, CA, USA), which features microelectronic sensors integrated on the bottom of the plate. E-plates 16 were placed onto the Real-Time Cell Analyzer (RTCA) station (xCELLigence System, Roche, Mannheim, Germany) for monitoring cell adhesion (**Figure XXI**).

Cell adhesion was continuously monitored throughout the experiments by measuring changes in the electrical impedance at the electrode/cell interface every 5 minutes during several hours. To analyze cell adhesion to different extracellular matrix, wells were previously coated during 30 minutes with collagen type I (Ref. 354236, BD Biosciences, Bedford, MA, USA) (30μg/mL or, which is the same, $4.5\mu g/cm^2$), collagen IV (Ref. C7521, Sigma-Aldrich, St. Louis, MO, USA) (167μg/mL or, which is the same, $25.5\mu g/cm^2$) or fibronectin (Ref. 354008, BD Biosciences, Bedford, MA, USA) (10μg/mL or, which is the same, $1.5\mu g/cm^2$). Continuous values were represented as Cell Index (CI), a dimensionless parameter, which reflects a relative change in measured electrical impedance, and quantified as a slope ($hours^{-1}$) of the first four hours.

Figure XXI. xCELLigence System for monitoring cell adhesion.

13. Statistical analyses

Statistical analyses were performed as an estimation of the associated probability to a Student's *t* test (95% confidence interval) or as Two-way ANOVA method, depending on the involved conditions. In general, experiments were carried out at least 3 independent times with 2-3 technical replicates. Data were represented as mean ± standard error of the mean (SEM). Differences between groups were compared using Student's *t* test (when comparing two groups) or Two-way ANOVA with Tukey's multiple comparison post-hoc test (when comparing differences between groups considering two independent variables). Kaplan-Meier method using the log-rank test was used to estimate survival curves. For data from human samples, statistical significance was determined by Pearson correlation analysis. In all cases, statistical calculation was developed using GraphPad Prism software (GraphPad for Science Inc., San Diego, CA, USA). Differences were considered statistically significant at $p<0.05$ (* or #), $p<0.01$ (** or ##) and $p<0.001$ (*** or ###).

V. RESULTS

1. *In vivo* analysis of the crosstalk between the TGF-β and EGFR pathways during liver regeneration and hepatocarcinogenesis

1.1. Characterization of a new experimental animal model for the study of the catalytic activity of the EGFR in liver physiology and pathology

Related with the interest of the group to elucidate the specific crosstalk between EGFR and TGF-β pathways, we focused on the study of liver regeneration and hepatocarcinogenesis in a transgenic mouse model that had been previously generated in the group. It expresses a specific truncated form of the human EGFR, which lacks the catalytic intracellular domain in hepatocytes (amino acids 654-1186). This EGFR mutant is able to heterodimerize with the endogenous WT EGFR, which is also present in mouse hepatocytes of these animals, acting as a negative dominant mutant, capable of reducing WT EGFR tyrosine autophosphorylation and biological signaling in these Alb-Δ654-1186EGFR (abbreviated as ΔEGFR) mice (**Material and Methods** Figure XIX). Using specific primers that exclusively recognized the human EGFR (Figure 1A), we demonstrated the transgene expression in ΔEGFR mice by qRT-PCR analysis, which was also confirmed at the protein level by Western blot (Figure 1B).

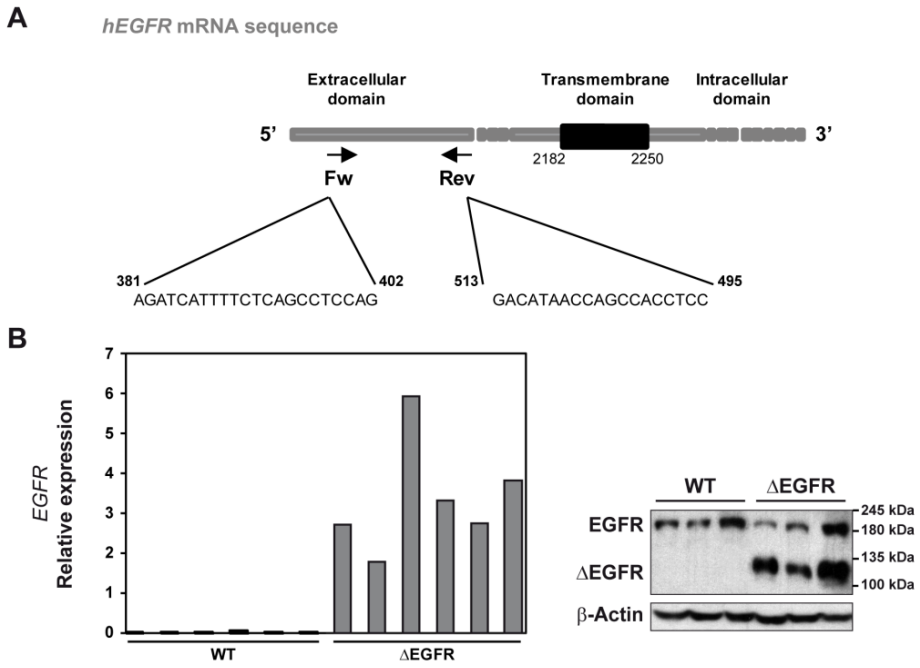

Figure 1. Analysis of the transgene expression in ΔEGFR livers. (A) Specific primers designed to detect the expression of the human *EGFR* transgene in ΔEGFR mice. **(B) Left:** Analysis of human *EGFR* mRNA expression levels by qRT-PCR in WT (N=6) and ΔEGFR mice (N=6) at basal conditions. **Right:** Analysis of endogenous and human EGFR protein levels by Western blot in WT (N=3) and ΔEGFR mice (N=3) under basal conditions. β-Actin was used as loading control.

In order to assess the downregulation of the EGFR pathway of this animal model *in vitro*, primary hepatocytes were isolated from WT and ΔEGFR mice and immortalized to create stable cell lines: HepWT, Hep1ΔEGFR and HepΔ2EGFR. We first confirmed EGFR mRNA expression levels by qRT-PCR, and we found that they were proportional to the copy number of the transgene in mice (Figure 2).

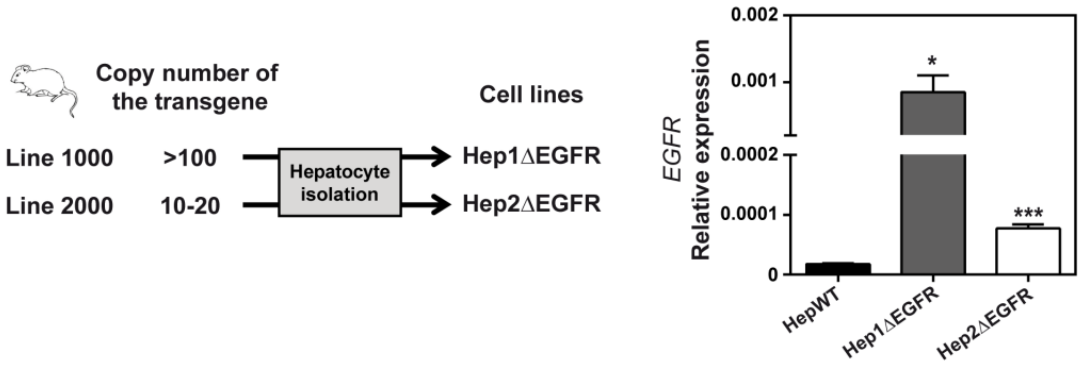

Figure 2. Analysis of the transgene expression in immortalized hepatocyte cell lines isolated from WT and ΔEGFR mice. Left: Primary hepatocytes were isolated and immortalized from WT mice and from the two ΔEGFR mouse lines that presented a higher transgene copy number. **Right:** Levels of human *EGFR* transcripts in mouse cell lines analyzed by qRT-PCR. Data in B are mean ± SEM of three independent experiments. Student's *t* test was used: *p<0.05 and ***p<0.001 compared to WT Hepatocytes (HepWT).

We analyzed cell morphology of these cell lines and we detected that Hep1ΔEGFR cell line (from line 1000, with the highest expression of the transgene) presented lower viability and decreased basal proliferative capacity compared to the WT one (Figure 3).

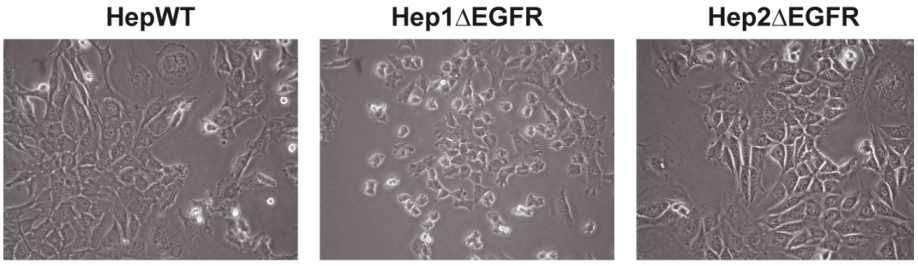

Figure 3. Cell morphology analysis of the different transgenic hepatocyte cell lines isolated from ΔEGFR mice. Representative bright-field images of cells cultured at basal conditions on top of plastic.

In Hep1ΔEGFR hepatocytes, the response to HB-EGF, one of the main ligands of EGFR, was significantly attenuated in terms of EGFR phosphorylation and signaling, as well as in terms of cell proliferation (Figure 4).

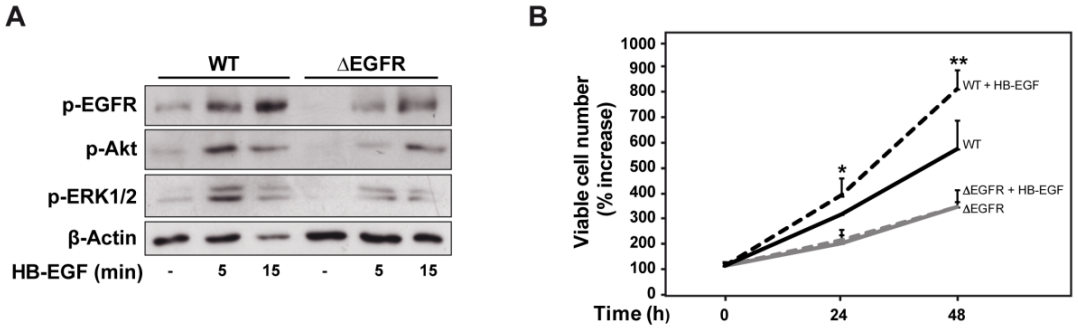

Figure 4. Characterization of transgenic hepatocyte cell lines from ΔEGFR mice. (A) Response to HB-EGF in terms of EGFR phosphorylation (FBS depleted medium) was attenuated in Hep1ΔEGFR hepatocytes by Western blot analysis. β-Actin was used as loading control. A representative experiment of five is shown. **(B)** Differences in the response to HB-EGF (FBS depleted medium) in terms of cell proliferation between WT and Hep1ΔEGFR hepatocytes. Cell number was analyzed by trypan blue staining. Data in B are mean ± SEM of two independent experiments performed in triplicates. Student's *t* test was used: *p<0.05 and **p<0.01.

It is known that TGF-β transactivates the EGFR in hepatocytes, which inhibits its pro-apoptotic activity (Caja et al., 2011a; Murillo et al., 2005). We could observe that hepatocytes isolated from ΔEGFR mice did not phosphorylate the EGFR after TGF-β treatment, which correlated with impairment in the activation of survival signals, such as ERK1/2 (**Figure 5A**), higher growth inhibition, and apoptosis (**Figure 5B-D**). Interestingly, ΔEGFR hepatocytes showed higher basal apoptosis compared to WT ones.

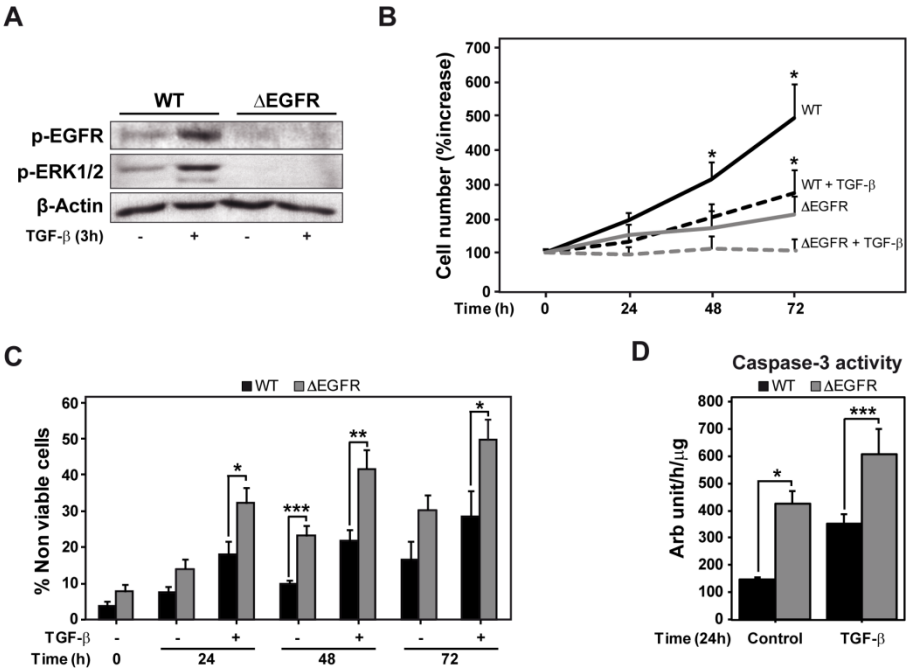

Figure 5. Hepatocytes from ΔEGFR mice show increased response to TGF-β-induced apoptosis. Immortalized HepWT and Hep1ΔEGFR cell lines were serum-starved during 16h and then treated with TGF-β (2ng/mL) at the indicated times. **(A)** Response to TGF-β in terms of phosphorylation of EGFR and ERKs analyzed by Western blot. β-Actin was used as loading control. A representative experiment of 3 is shown. **(B)** Analysis of viable cell number by trypan blue staining, shown as the percentage of increase versus time 0 hours. **(C)** Analysis of cell death shown as the percentage of non-viable cells, analyzed by trypan blue staining. **(D)** Caspase-3 activity, fluorimetric analysis. Data in B, C and D are mean ± SEM of at least 3 independent experiments. Student's *t* test was used: *p<0.05, **p<0.01 and ***p<0.001.

All these results indicate the suitability of the model to study the specific implication of the hepatocyte EGFR catalytic domain in liver physiology and pathology.

1.2. Analysis of liver regeneration after 2/3 partial hepatectomy in the previous mentioned animal model. Comparison with the WT mice. Status of the TGF-β pathway under these conditions

1.2.1. ΔEGFR mice show delayed hepatocyte proliferation after 2/3 PH

To explore the specific role of hepatocyte EGFR activity during liver regeneration, we performed two-thirds partial hepatectomy (2/3 PH) in WT and ΔEGFR mice. We observed that WT animals activated the EGFR pathway in the remaining liver after PH, analyzed by immunohistochemistry of the EGFR phosphorylation in hepatocytes from paraffined tissues. In contrast, ΔEGFR were not able to phosphorylate the EGFR (**Figure 6**).

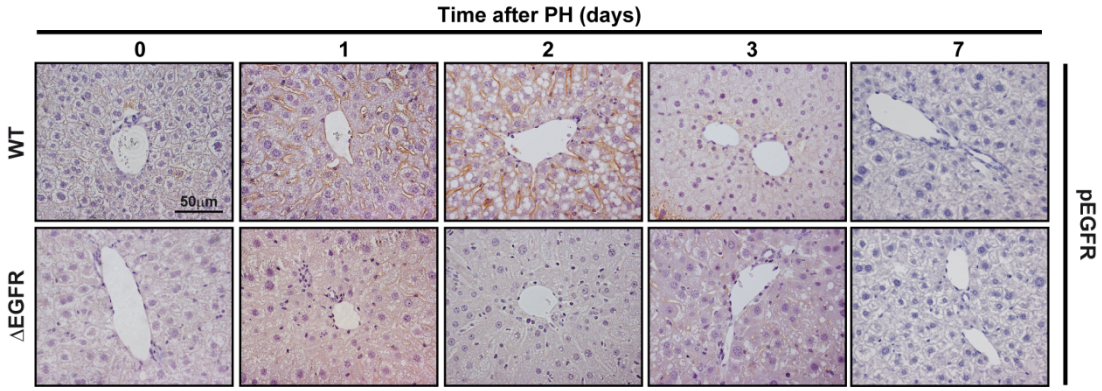

Figure 6. ΔEGFR transgenic livers are not able to phosphorylate EGFR after two-thirds partial hepatectomy. Immunohistochemical analysis of phospho-EGFR in paraffined tissues from WT and ΔEGFR transgenic mice at the indicated times after PH. Representative 40x images of at least 3 animals per condition are shown.

This was not due to differences in the expression of the endogenous EGFR or its ligand TGF-α, the EGFR ligand highly expressed in hepatocytes during liver regeneration (Mitchell et al., 2005) (**Figure 7A**), proving that the human ΔEGFR transgene indeed was acting as a negative dominant, inhibiting the hepatocyte response to EGFR ligands. Moreover, we did not find any compensatory increase in other members of the EGFR family (*Erbb2, Erbb3,* and *Erbb4*), due to inactivation of the EGFR function (**Figure 7B**).

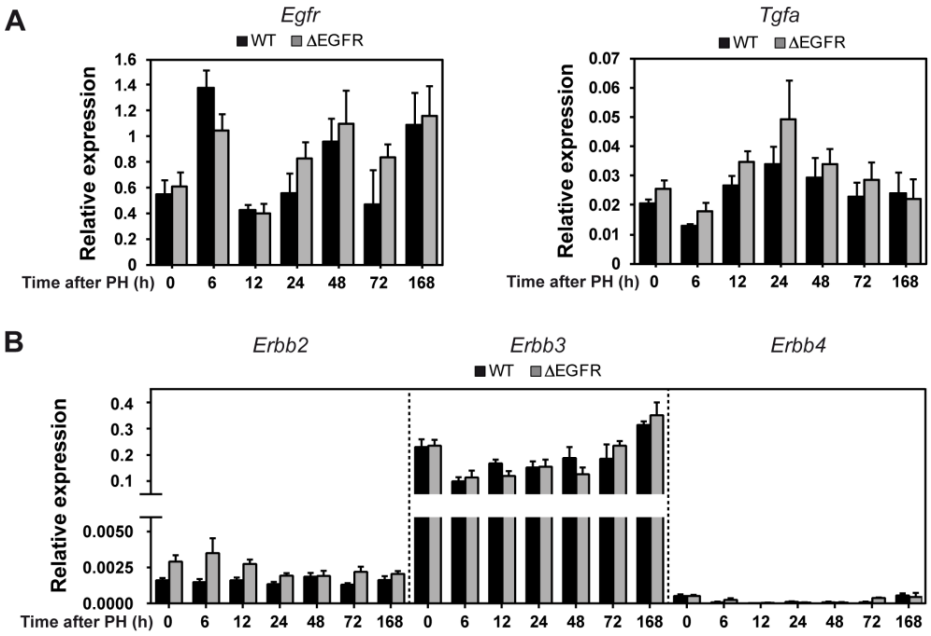

Figure 7. Expression of endogenous EGFR (*Egfr*) and TGF-α (*Tgfa*) is not altered in livers from ΔEGFR mice, and there is no compensation by other ErbB family members. Analysis of *Egfr* and *Tgfa* **(A)**, and *Erbb2*, *Erbb3* and *Erbb4* **(B)** expression by qRT-PCR in frozen liver tissues from WT and ΔEGFR mice submitted to PH and collected at the indicated times. Data are mean ± SEM of at least 4 animals per group. Student's *t* test was used. No significant differences were observed in any case.

Then, we moved to assess the effect of downregulating EGFR pathway on hepatic cellular proliferation. Thus, after 2/3 PH, immunohistochemical analysis of Ki67, a proliferative marker present in the nucleus during all active phases of the cell cycle (Scholzen and Gerdes, 2000), revealed that ΔEGFR livers displayed lower and delayed hepatocyte proliferation (Figure 8).

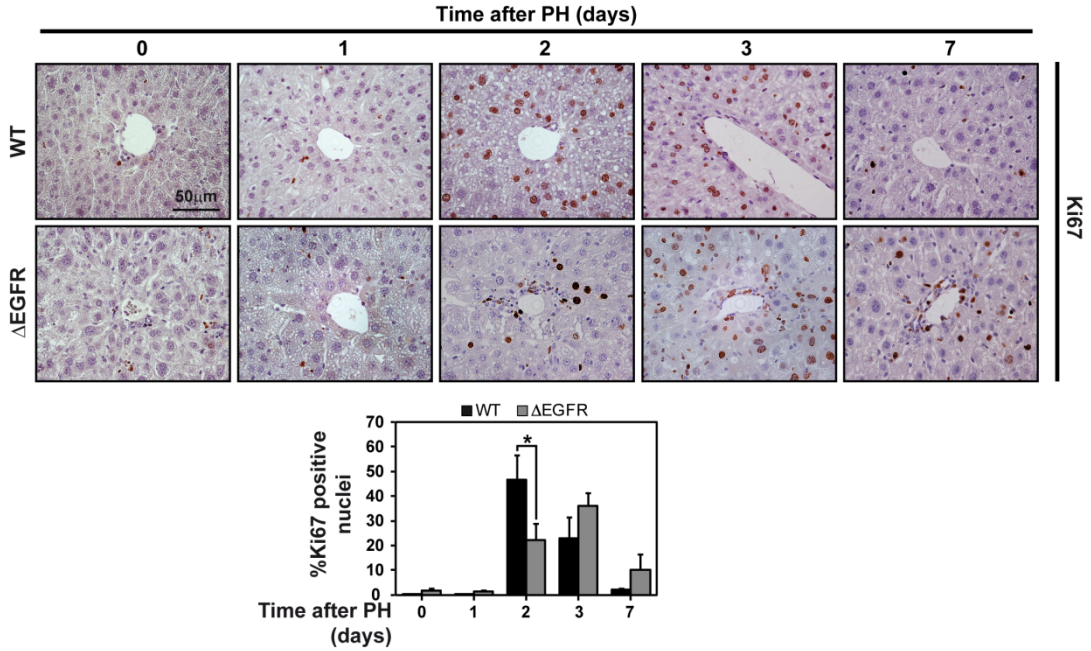

Figure 8. Hepatocyte proliferation induced after 2/3 partial PH is delayed in ΔEGFR transgenic mice. Immunohistochemical analysis of Ki67 in paraffined liver tissues from WT and ΔEGFR mice at the indicated times after PH **(upper)** and quantification of the percentage of Ki67-labeled nuclei **(lower)**. Representative 40x images of at least 4 animals per condition are shown. Data are mean ± SEM of at least 4 animals per group, and 10 fields per animal were quantified. Student's *t* test was used: *p<0.05.

Furthermore, while WT animals showed an early increase in the levels of intracellular signals that mediate hepatocyte proliferation, such as phospho-Akt and phospho-ERKs, ΔEGFR livers presented a significantly lower response (Figure 9).

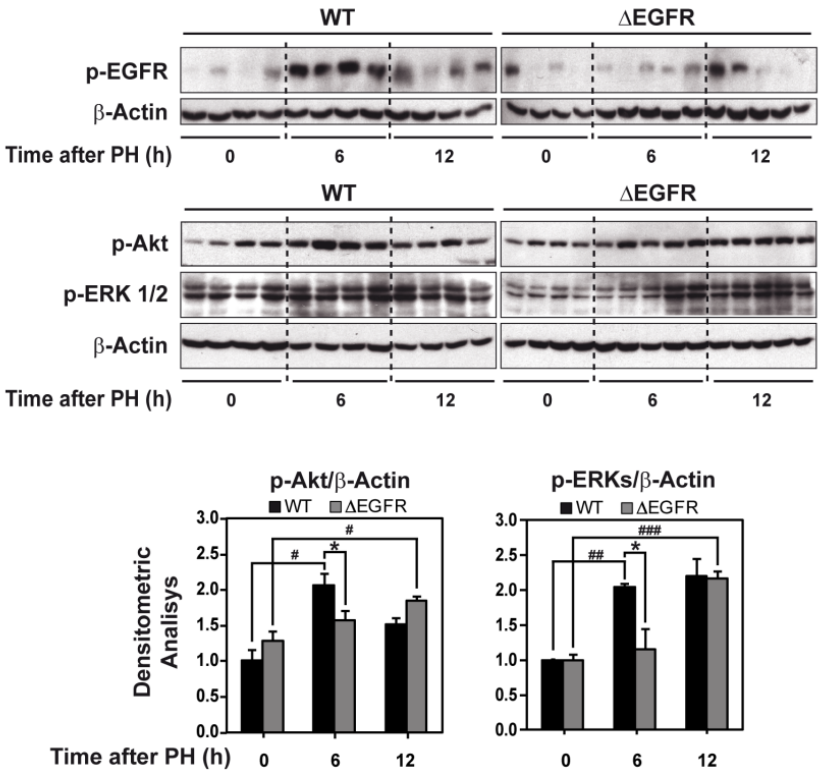

Figure 9. Lower and delayed response in terms of intracellular proliferative signals in ΔEGFR transgenic mice after two-thirds PH. Western blot analysis of the protein levels of phospho-EGFR, phospho-Akt, and phospho-ERKs as early proliferative signals **(upper)** and quantification of the densitometric analysis **(lower)**. β-Actin was used as loading control. Data are mean ± SEM of at least 4 animals per group. Student's *t* test was used: *p<0.05 compared to WT; #p<0.05, ##p<0.01, and ###p<0.001 compared to time 0 hours.

Moreover, we observed that the increase found in WT animals of Nox1 protein levels, the NADPH oxidase that is upregulated by EGF and mediates increase in proliferation (Sancho and Fabregat, 2010; Sancho et al., 2009), was delayed in transgenic mice, although we were not able to detect significant changes at the mRNA level, correlating with the delayed hepatocyte proliferation (Figure 10). It is worthy to mention that *Nox1* mRNA levels were barely detectable, which difficulties the analysis of its expression.

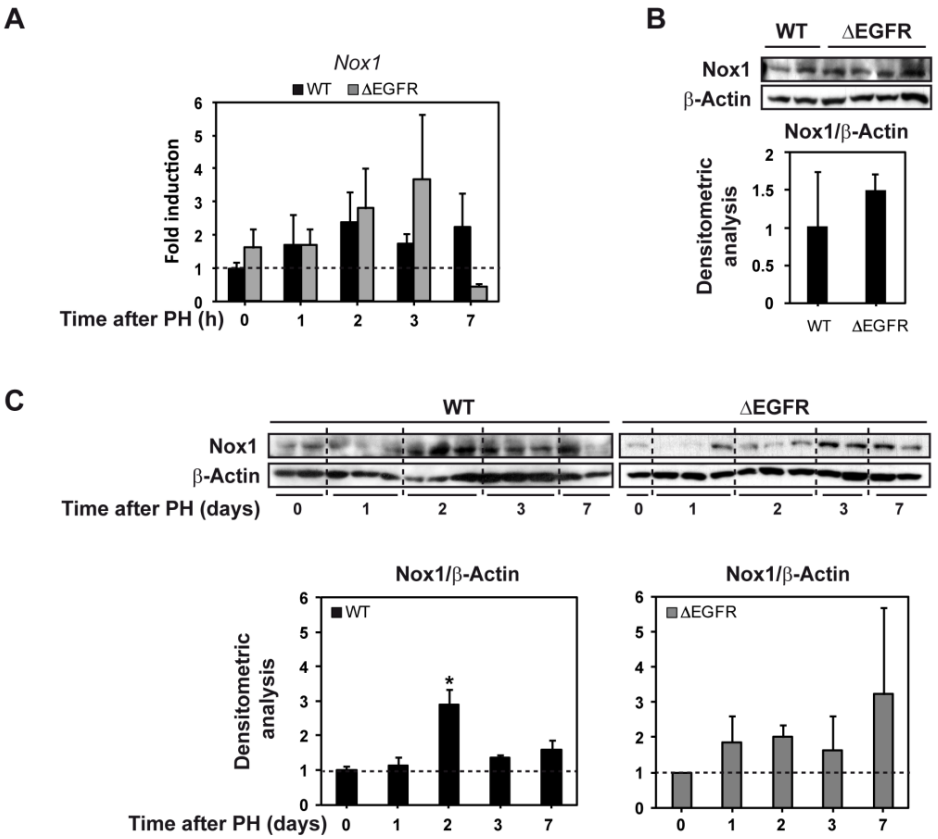

Figure 10. Upregulation of Nox1 after two-thirds PH is delayed in ΔEGFR transgenic mice. (A) Analysis of *Nox1* mRNA expression by qRT-PCR at the indicated times after PH. **(B)** Western blot analysis of Nox1 under basal conditions **(upper)** and quantification of the densitometric analysis **(lower). (C)** Western blot analysis of Nox1 at the indicated times after PH **(upper)** and its densitometric analysis **(lower).** β-Actin was used as loading control. Data in A are mean ± SEM of at least 4 animals per group. Data in B and C are also mean ± SEM. Student's *t* test was used: *p<0.05 compared to 0 hours.

Finally, cytokines, such as interleukin-6 (IL-6), tumor necrosis factor-α (TNF-α) and interleukin-1-beta (IL-1β), are considered relevant for priming hepatocytes to proliferate (Fausto et al., 2012; Michalopoulos, 2010; Riehle et al., 2011). We observed an increase of IL-6 (*Il6*), TNF-α (*Tnfa*) and IL-1β (*Il1b*) at short times after PH (6 hours) in WT mice, which was not detected in ΔEGFR animals, even decreasing the levels of some of these cytokines. However, we could not detect significant differences at longer times after PH between both animals. (**Figure 11A**). We further analyzed the inflammatory response performing an immunohistochemistry of F4/80, a specific marker of mice macrophages. Results showed a similar inflammatory response in both animals after PH (**Figure 11B**).

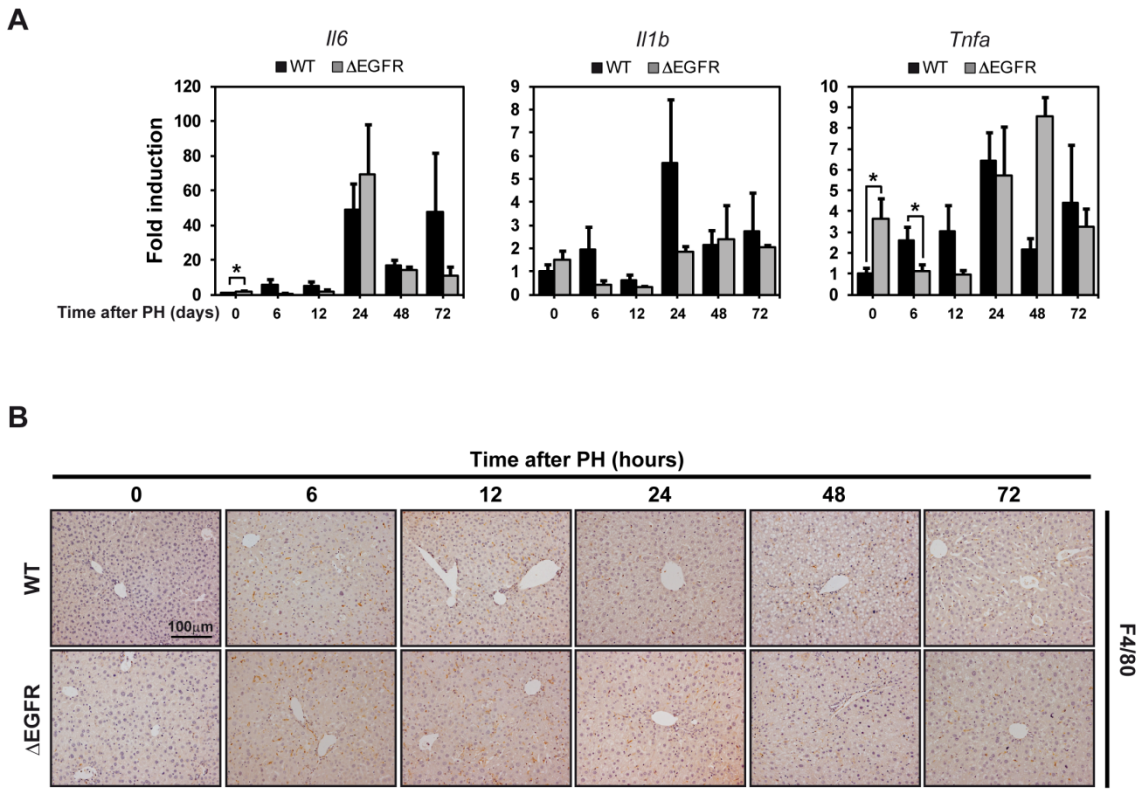

Figure 11. The analysis of inflammation show that ΔEGFR transgenic mice presented an altered cytokine profile in the early hours after PH. (A) qRT-PCR analysis of the levels of expression of the pro-inflammatory cytokines IL-6 (*Il6*), Il-1β (*Il1b*) and TNF-α (*Tnfa*) in WT and ΔEGFR livers at the indicated times after PH. **(B)** Immunohistochemical analysis of F4/80 in WT and ΔEGFR livers at different times after PH. Representative 20x images of at least 3 animals per condition are shown. Data in A are mean ± SEM of at least 4 animals per group. Student's *t* test was used: *p<0.05.

We finally analyzed the expression of Nox2, another NADPH oxidase, which is mainly expressed by other cell types different from hepatocytes, such as Kupffer cells, fibroblasts or Hepatic Stellate Cells (HSC). Although ΔEGFR livers expressed higher mRNA levels of *Nox2* after PH analyzed by qRT-PCR analysis (**Figure 12A**), differences were not significant, and we were not able to detect distinct protein levels neither by Western blot (**Figure 12C**) or by immunohistochemistry analyzed after PH (**Figure 12D**).

Interestingly, it is worthy to mention that, under basal conditions, ΔEGFR livers presented higher mRNA expression levels of almost all the cytokines analyzed (**Figure 11A**) and also higher mRNA and protein levels of Nox2 (**Figure 12A-B**).

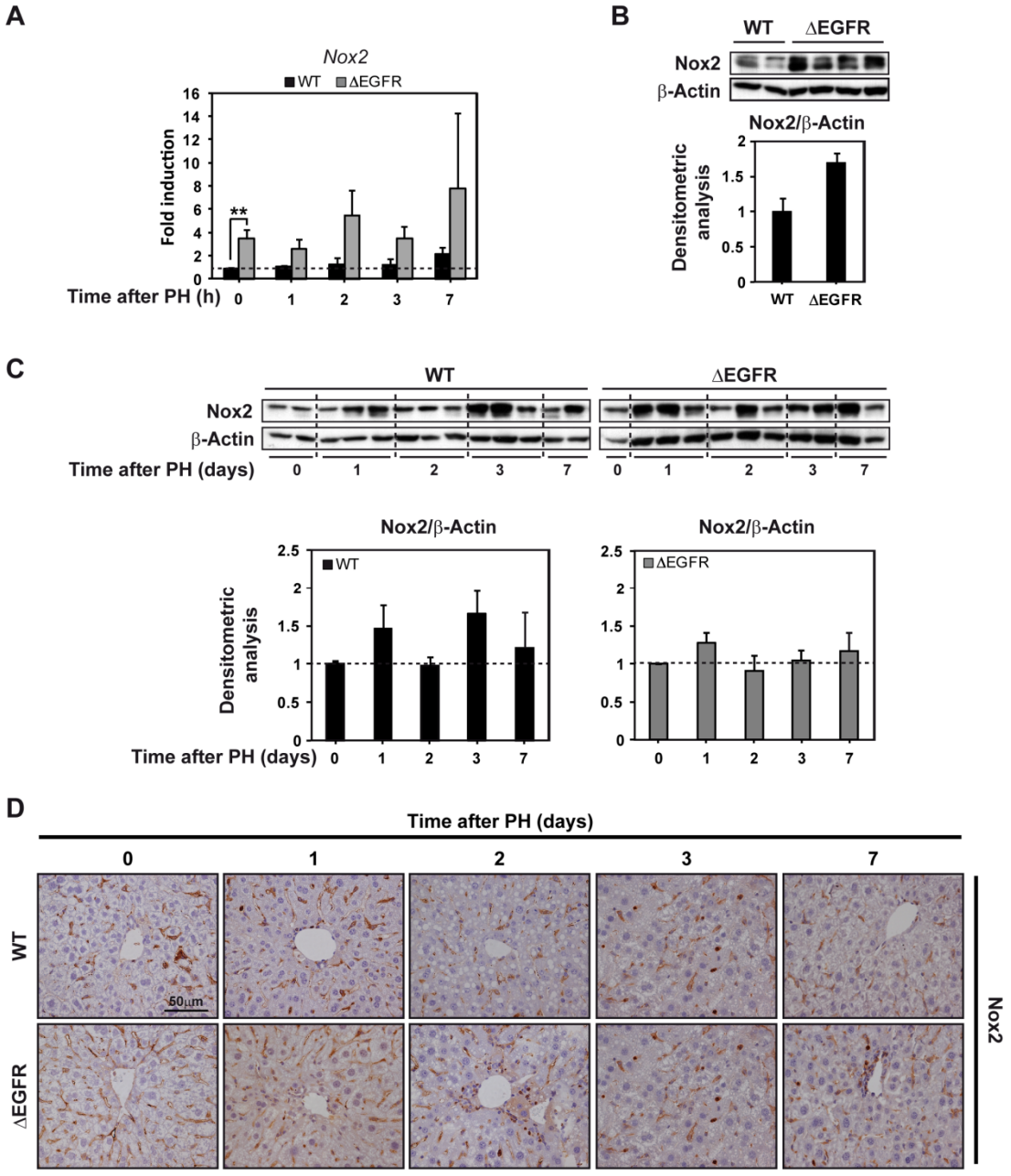

Figure 12. ΔEGFR transgenic mice presented similar levels of Nox2 after two-thirds PH. (A) Analysis of *Nox2* mRNA expression by qRT-PCR at the indicated times after PH. **(B)** Western blot analysis of Nox2 under basal conditions **(upper)** and quantification of the densitometric analysis **(lower). (C)** Western blot analysis of Nox2 at the indicated times after PH **(upper)** and its densitometric analysis **(lower).** β-Actin was used as loading control. **(D)** Immunohistochemical analysis of Nox2 in WT and ΔEGFR livers at different times after PH. Representative 40x images of at least 3 animals per condition are shown. Data in A are mean ± SEM of at least 4 animals per group. Student's *t* test was used: **p<0.01. Data in B and C are also mean ± SEM.

Altogether, these results indicated a critical role for EGFR catalytic activity during the early stages of liver regeneration.

1.2.2. ΔEGFR mice show higher activation of the TGF-β pathway under basal conditions and during liver regeneration after PH

As mentioned before, considering the relevant role played by EGF in counteracting the TGF-β suppressor effects (Fabregat et al., 2000), we wondered whether it was important *in vivo*. Results indicated that lower and delayed hepatocyte proliferation correlated with an overactivation of the TGF-β pathway. In that sense, ΔEGFR animals showed higher phosphorylation of Smad3, a hallmark of TGF-β activation, at basal levels and during all the times analyzed after PH compared to WT mice (Figure 13A-B). Interestingly, the decrease in Smad3 phosphorylation observed in WT animals at 12 hours after PH was not observed in ΔEGFR mice, which maintained a high activation of the pathway.

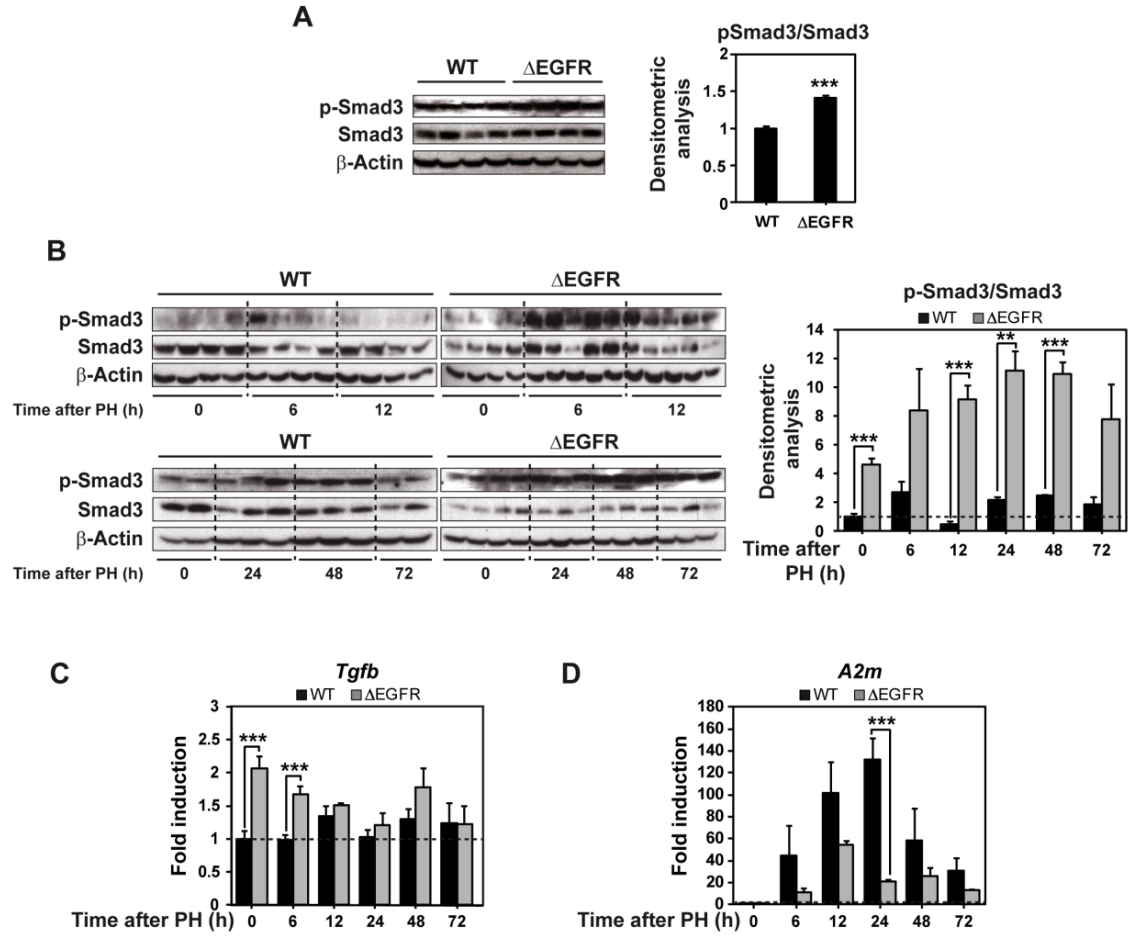

Figure 13. Overactivation of the TGF-β pathway in ΔEGFR mice under basal conditions and during liver regeneration after PH. Analysis of phospho-Smad3 and total Smad3 by Western blot at basal conditions **(A, left)** and at the indicated times after PH **(B, left)**. Densitometric analyses of Western blots are shown on the **right.** β-Actin was used as loading control. **(C)** qRT-PCR analysis of TGF-β1 (*Tgfb*) mRNA levels. **(D)** qRT-PCR analysis of α_2-macroglobulin (*A2m*) mRNA levels. Data in A and B are mean ± SEM. Data in C and D are also mean ± SEM of at least 4 animals per group. Student's *t* test was used: **p<0.01 and ***p<0.001.

Also, levels of TGF-β1 transcripts were significantly higher in ΔEGFR livers under basal conditions as well as at short times after PH compared with WT ones (**Figure 13C**). Furthermore, α_2-macroglobulin, a plasma protein that has previously been proposed as a binding protein for TGF-β that attenuates its effects (Arandjelovic et al., 2003), was upregulated in WT, but not to the same extent in ΔEGFR animals after PH (**Figure 13D**). Indeed, the EGFR pathway may upregulate α_2-macroglobulin, which could in turn counteract TGF-β activity. Altogether suggested a stronger activation of the TGF-β pathway in ΔEGFR livers compared with WT ones.

As *in vitro* experiments had indicated that EGF counteracts TGF-β-induced apoptosis inhibiting its effects on *Bim* and *Bmf*, two pro-apoptotic genes (Caja et al., 2011a), we wanted to know if this was also occurring *in vivo* in our model, analyzing potential changes in the expression of these genes between WT and ΔEGFR mice. *Bmf*, but not *Bim*, expression was downregulated after PH in both animals; but, interestingly, levels remained higher in ΔEGFR compared to WT mice between 6 and 48 hours after PH. The expression of *BclxL*, an anti-apoptotic Bcl-2 member known to be a TGF-β target gene in hepatocytes (Fabregat et al., 2000), increased early after PH in both animal models, although the increase in ΔEGFR mice was slightly lower (**Figure 14A**). Because *Bim* and *Bcl-xL* expression undergoes also post-transcriptional regulation, we analyzed their protein levels; but we could not find significant clear differences between WT and ΔEGFR mice (**Figure 14B**).

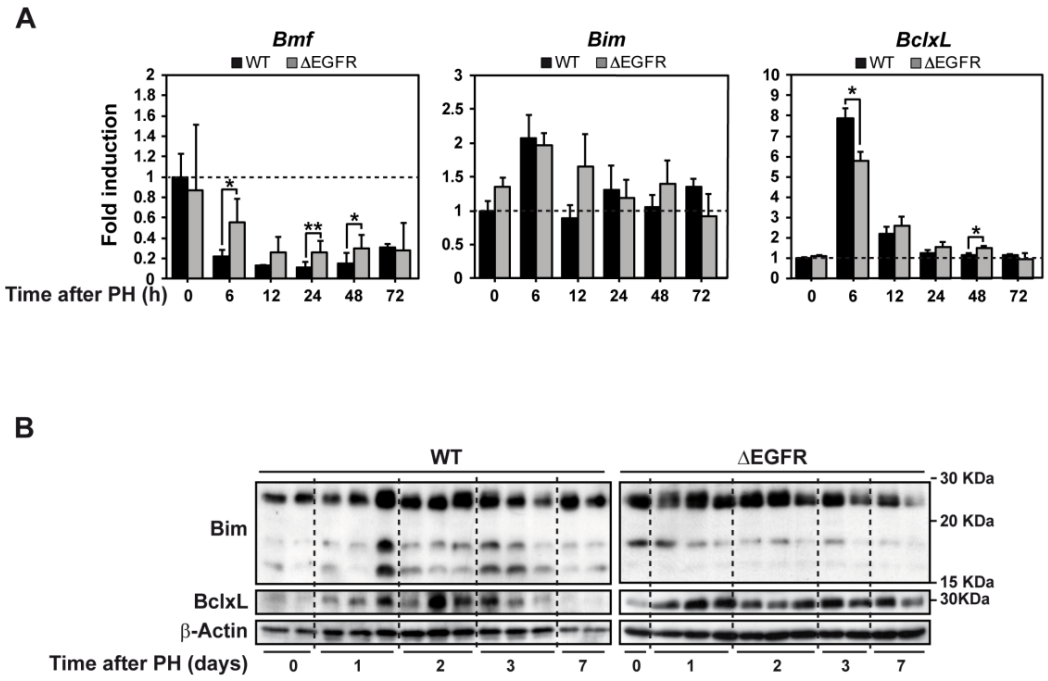

Figure 14. Analysis of the TGF-β-induced apoptotic pathway did not reveal significant changes in ΔEGFR mice during liver regeneration after PH. (A) qRT-PCR analysis of *Bmf*, *Bim* and *BclxL* mRNA levels at the indicated time after PH. **(B)** Analysis of Bim and BclxL by Western blot. β-Actin was used as loading control. Data in A are mean ± SEM of at least 4 animals per group. Student's *t* test was used: *p<0.05 and **p<0.01.

In spite of these differences, analysis of the active form of Caspase-3 by immunohistochemistry (Figure 15A) or Caspase-3 activity in tissues (Figure 15B) did not revealed differences between WT and ΔEGFR livers at any of the times analyzed.

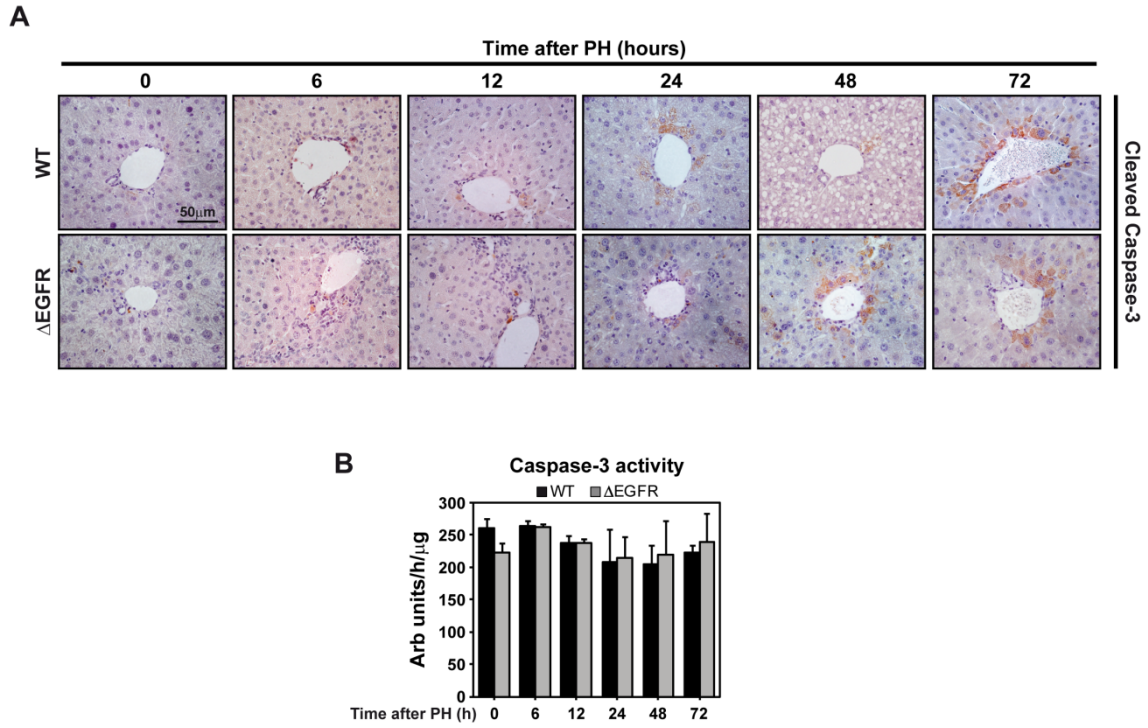

Figure 15. ΔEGFR mice do not show higher apoptosis during liver regeneration after 2/3 PH. (A) Immunohistochemical analysis of cleaved (active) Caspase-3 in WT and ΔEGFR livers at different times after PH. Representative 40x images of at least 3 animals per condition are shown. **(B)** Analysis of Caspase-3 activity in parallel protein extracts. Fluorimetric assay was performed. Data in B are mean ± SEM of at least 3 animals per group, performed in duplicates. Student's *t* test was used. No significant differences were observed in any of the cases.

Additionally, we searched for changes in the levels of Nox4, the NADPH oxidase whose expression is up-regulated by TGF-β and mediates its apoptotic actions, an effect that is impaired by EGF (Carmona-Cuenca et al., 2008). *Nox4* expression significantly decreased after PH, as we have recently described (Crosas-Molist et al., 2014), but no significant differences were observed between WT and ΔEGFR animals (Figure 16A). The analysis of Nox4 at the protein level fully agreed with the changes observed at the mRNA level (Figure 16B-C).

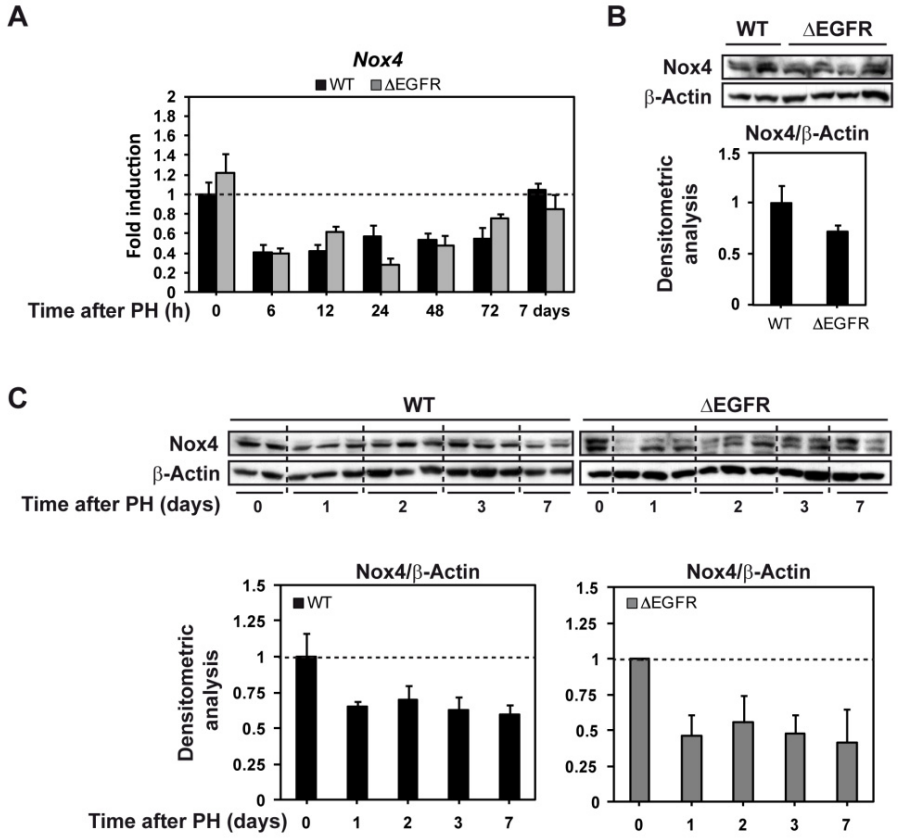

Figure 16. Downregulation of Nox4 after two-thirds PH is not altered in ΔEGFR transgenic mice. **(A)** Analysis of *Nox4* mRNA expression by qRT-PCR at the indicated times after PH. **(B)** Western blot analysis of Nox4 under basal conditions **(upper)** and quantification of the densitometric analysis **(lower).** **(C)** Western blot analysis of Nox4 at the indicated times after PH **(upper)** and its densitometric analysis **(lower).** β-Actin was used as loading control. Data in A are mean ± SEM of at least 4 animals per group. Data in B and C are also mean ± SEM. Student's *t* test was used. No significant differences were observed in any of the cases.

As the observed delay in the hepatocyte proliferative response was not associated with apoptosis, we next focused on the study of the cell cycle, mainly focusing in the expression of cell cycle negative regulators modulated by TGF-β, such as *Cdkn2b* (the gene encoding $p15^{INK4B}$) and *Cdkn1a* (the gene encoding $p21^{WAF1/CIP1}$) (Lee and Bae, 2002). On the one hand, we found a significant increase in the expression of *Cdkn2b* (p15), at 6 hours after PH in ΔEGFR mice that was not observed in WT animals. On the other hand, levels of *Cdkn1a* (p21) transcripts increased at short times after PH in both animals, but whereas in WT animals the levels slowly returned to basal ones, in ΔEGFR mice levels remained high, being the differences particularly relevant 72 hours after PH. These results suggest that high levels of p15 could be responsible for the delay in the early proliferative response of ΔEGFR hepatocytes to PH, whereas high levels of p21 at later times could slow the proliferation during the entire regenerative process. Interestingly, both p15 and p21 levels were increased in non-hepatectomized ΔEGFR livers compared with WT ones. Indeed, a functional EGFR pathway may be necessary to counteract the cytostatic effects of TGF-β in hepatocytes, a process that is particularly crucial after two-thirds PH of the liver (Figure 17A).

Moreover, we also checked the expression of different cyclins, positive regulators of cyclin-dependent kinases (CDKs), which govern cell cycle transitions. We first analyzed the expression of *Cyclin D1* by qRT-PCR, which is involved in the entrance into the cell cycle through the transition from G_0 to G_1-phase and G_1 progression (Ehrenfried et al., 1997), and which concentration is maintained during all the cell cycle. We observed that its expression is increased in WT animals during liver regeneration, presenting a peak 48 hours after PH. ΔEGFR mice also presented a maximum of its expression 48 hours after PH, although it was maintained until 72 hours. Interestingly, we could observe that ΔEGFR mice expressed higher levels of *Cyclin D1* under basal conditions and almost at all the times analyzed after PH. Protein levels of Cyclin D1 were also analyzed by Western blot, presenting a substantially good correlation with mRNA levels (**Figure 17B**). The expression of *Cyclin E1*, important in the transition from G_1 to S-phase, is up-regulated in both animals presenting the maximum expression also 48 hours after PH, without showing differences between both animals. Finally, *Cyclin A2*, whose expression is increased in S-phase and maintained until G_2-phase, and *Cyclin B2*, implicated in the transition from G_2 to M-phase (Ehrenfried et al., 1997), presented a clear induction 48 hours after PH in WT mice. Interestingly, this upregulation was clearly delayed until 72 hours in ΔEGFR mice (**Figure 17C**).

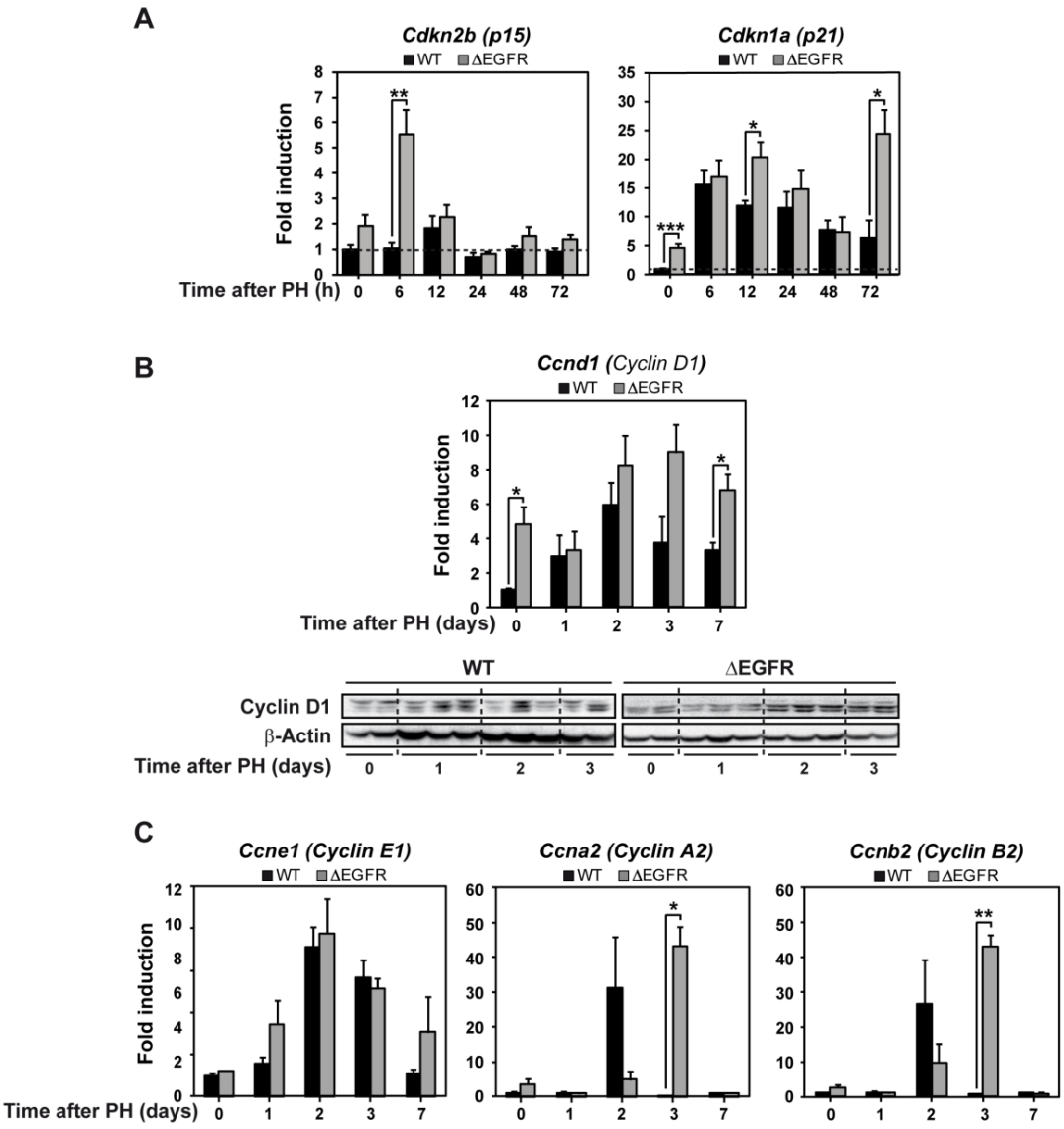

Figure 17. ΔEGFR transgenic mice show an amplification of the cytostatic effects of TGF-β through the induction of cell cycle negative regulators, resulting in a delay in the progression through the cell cycle. (A) Analysis of *Cdkn2b (*p15*)* and *Cdkn1a (*p21*)* mRNA expression by qRT-PCR at the indicated times after PH. **(B)** Analysis of Cyclin D1 *(Ccnd1*) by qRT-PCR **(upper)** and by Western blot **(lower)** at the indicated time after PH. β-Actin was used as loading control. **(C)** Analysis of Cyclin E1 (*Ccne1*), Cyclin A2 (*Ccna2*) and Cyclin B2 (*Ccnb2*) mRNA expression by qRT-PCR at the indicated times after PH. Data in A, B and C are mean ± SEM of at least 4 animals per group. Student's *t* test was used: *p<0.05, **p<0.01 and ***p<0.001.

All these results indicate that delayed hepatocyte proliferation was not associated to apoptosis but with an amplification of the cytostatic effects of TGF-β through the induction of cell cycle negative regulators, resulting in a delay in the progression through the cell cycle. Thus, this demonstrates that the major role of EGFR during liver regeneration after PH is not cell survival but counteracting the TGF-β cytostatic effects in hepatocytes, probably because apoptosis is not relevant in a model where there is no hepatocyte damage.

1.2.3. Regulation of lipid metabolism after two-thirds PH is altered in ΔEGFR mice

Histological analysis by hematoxylin and eosin showed the presence of vacuolated cells in WT livers 48 hours after PH, which is known as hepatocellular fat accumulation, whereas ΔEGFR livers did not show this appearance (Figure 18A). In order to confirm that they were deposits of lipids, we performed oil red O staining, confirming the accumulation of lipid drops (Figure 18B), which correlated with an increase in triglycerides levels in WT, but not in ΔEGFR livers (Figure 18C).

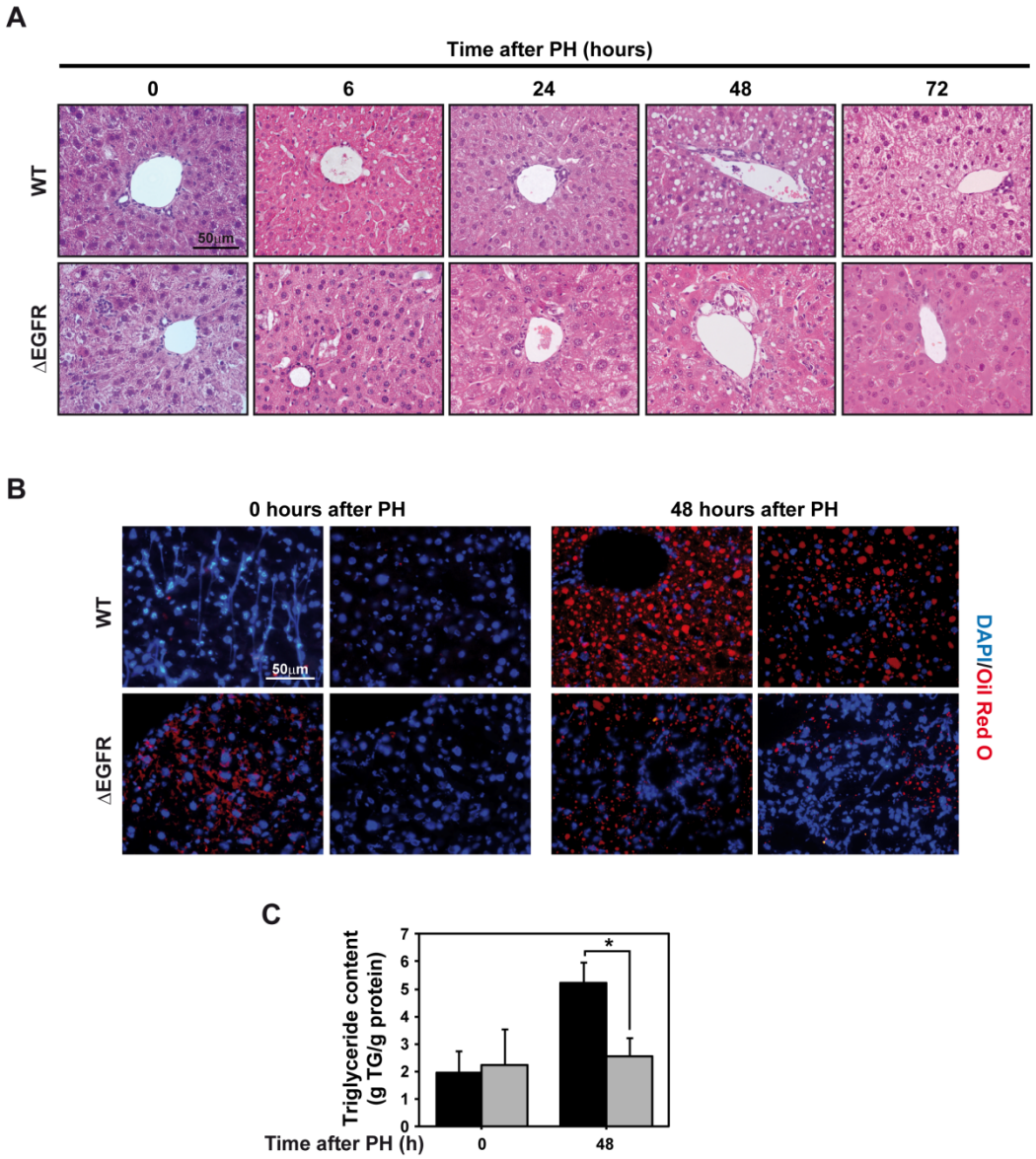

Figure 18. The increase in lipid content during liver regeneration after PH is almost absent in ΔEGFR mice. (A) Histological analysis of the livers from WT and ΔEGFR mice by hematoxylin and eosin staining. **(B)** Immunohistochemical analysis of the lipid content by oil red O staining performed in frozen liver sections. In A and B representative 40x images of at least 3 animals per condition are shown. **(C)** Analysis of triglyceride content in WT and ΔEGFR livers at basal conditions and 48 hours after PH. Data in C are mean ± SEM of at least 4 animals per group. Student's *t* test was used: *p<0.05. Abbreviations: DAPI, 40'6-diamidino-2-phenylindole; TG, triglyceride.

We then decided to analyze different regulatory genes of lipid metabolism. We observed that the increase in lipid accumulation in WT livers was coincident with an upregulation of the mRNA levels of fatty acid synthase (*Fasn*), a key enzyme involved in *de novo* fatty acid synthesis, and glucose-6-phosphate dehydrogenase (*G6pdx*), the regulatory enzyme of the pentose-phosphate cycle, responsible for NADPH production. However, the upregulation of these enzymes was altered in ΔEGFR animals. Moreover, we also found a different kinetic mRNA expression in ΔEGFR livers of acetyl-coenzyme A carboxylase alpha (*Acaca*), that catalyzes the generation of malonyl-CoA from acetyl-CoA, and of acetyl-coenzyme A carboxylase beta (*Acacb*), localized in the mitochondrial membrane, and which is known to control fatty acid oxidation by means of the ability of malonyl-CoA to inhibit carnitine/palmitoyl-transferase 1 (CPT1) (Figure 19).

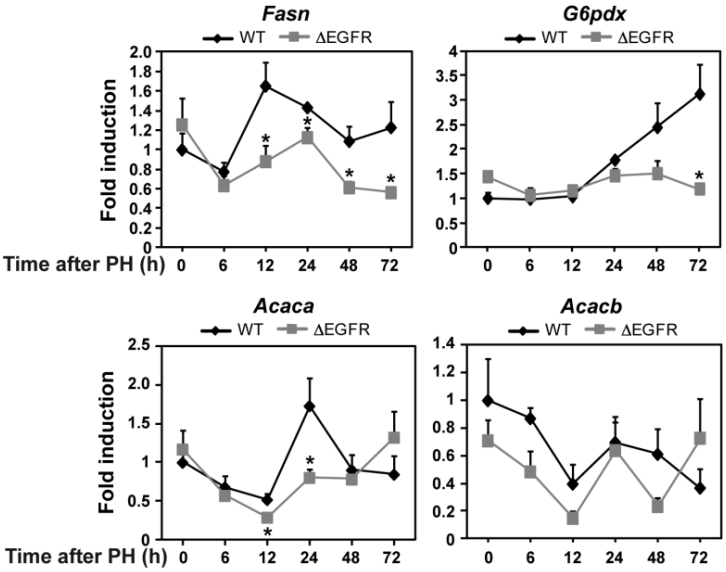

Figure 19. ΔEGFR mice show differences in lipid metabolic expression changes during liver regeneration. qRT-PCR analysis of the levels of expression of fatty acid synthase (*Fasn)*, glucose-6-phosphate dehydrogenase *(G6pdx)*, acetyl-coenzyme A carboxylase alpha (*Acaca*) and acetyl-coenzyme A carboxylase beta (*Acacb*) at the indicated times after PH. Data are mean ± SEM of at least 4 animals per group. Student's *t* test was used: *p<0.05.

These results suggest that the EGFR pathway regulates lipid metabolism in regenerating hepatocytes after PH, revealing a new function for EGFR kinase activity.

1.2.4. ΔEGFR mice are able to regenerate the liver showing an overactivation of the HGF/Met pathway

Regardless of the described alterations, ΔEGFR mice showed only a slight, but not significant, increase in the mortality after PH (Figure 20A). Remaining animals overcame liver

injury, analyzed by serum parameters (Table XV) and were able to fully regenerate the liver with a similar kinetic to WT animals, analyzed by the liver/body weight ratio (Figure 20B).

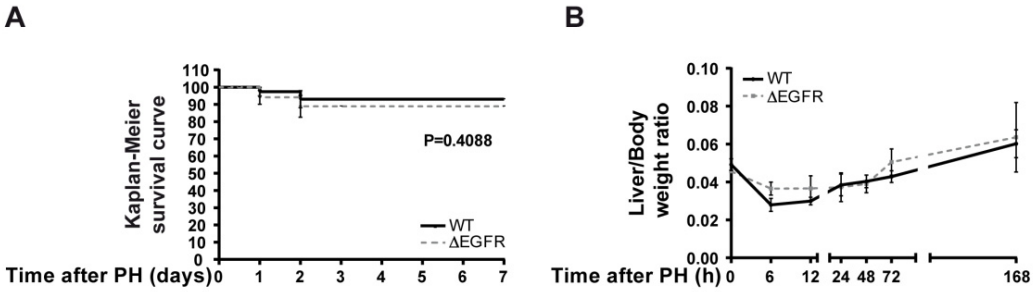

Figure 20. ΔEGFR livers are able to regenerate after PH and do not show significant increase in the mortality after PH. (A) Kaplan-Meier survival curve. **(B)** Remaining animals fully regenerate the liver analyzed by the Liver/body weight ratio. Data in B are mean ± SEM of at least 4 animals per group. Student's *t* test was used. No significant differences were observed in any of the cases.

	Wild Type			ΔEGFR		
Parameters*	Pre-Operatory (n=3)	24h PH (n=4)	48h PH (n=5)	Pre-Operatory (n=4)	24h PH (n=4)	48h PH (n=5)
ALP (U/L)	59.90 ± 4.65	156.26 ± 34.80	247.78 ± 114.69	113.70 ± 34.18	166.15 ± 43.36	328.38 ± 153.14
ALT (U/L)	31.00 ± 3.46	2830.20 ± 776.69	277.80 ± 51.10	808.00 ± 487.19	4332.00 ± 1617.32 #	648.40 ± 241.82
AST (U/L)	111.33 ± 31.39	5458.40 ± 1775.61 #	540.60 ± 117.49	2022.50 ± 1268.99	4524.25 ± 1389.27	1361.60 ± 460.00
BIL T (mg/dl)	0.04 ± 0.01	1.02 ± 0.56	0.59 ± 0.28	0.21 ± 0.13	1.32 ± 0.50	2.47 ± 1.44

*ALP: Alkaline phosphatase; ALT: Alanine aminotransferase; AST: Aspartate aminotransferase; BIL T: Bilirubin total

Table XV. Serum biochemical analysis at the indicated times after PH. ALP, ALT, AST and total bilirubin (BIL T) were measured using gold-standard methods and a Cobas Integra 400 Plus Chemistry Analyzer (Roche). Dara are mean ± SEM of at least 3 animals per group. Two-Way ANOVA test was used: #p<0.05 compared to pre-operatory condition.

Hence, we focused on identifying other potential mitogenic signals that could be overactivated in ΔEGFR mice. We observed that ΔEGFR mice expressed higher mRNA levels of *Hgf* than WT mice, both under basal conditions and shortly after PH (Figure 21A, left). Interestingly, we also found differences in the expression of urokinase-type plasminogen activator (*uPA*), which mediates the release of HGF from the extracellular matrix during liver regeneration (Shimizu et al., 2001). Thus, *uPA* mRNA levels were elevated in ΔEGFR livers, compared with WT mice, being this difference particularly significant at 6 hours after PH (Figure 21A, right). Moreover, the increase in *Hgf* expression correlated with higher levels of c-Met phosphorylation in ΔEGFR livers analyzed by Western blot (Figure 21B). Notably, levels of phosphorylated c-Met remained high 72 hours after PH in ΔEGFR livers. Finally, we analyzed *Met* expression by qRT-PCR. It is worth noting that, although mRNA levels decreased after PH in both WT and ΔEGFR livers (Figure 21C), the decrease in protein levels was only observed in

WT animals, whereas ΔEGFR mice maintained, or even increased, c-Met at all time points analyzed (Figure 21B). This suggests that a post-transcriptional regulation of c-Met may allow the maintenance of high protein levels after PH in ΔEGFR mice, resulting in a sustained activation of this pathway. All these results indicate that the HGF/c-Met pathway is overactivated in ΔEGFR livers after PH, which could justify the delayed but efficient regeneration in these animals.

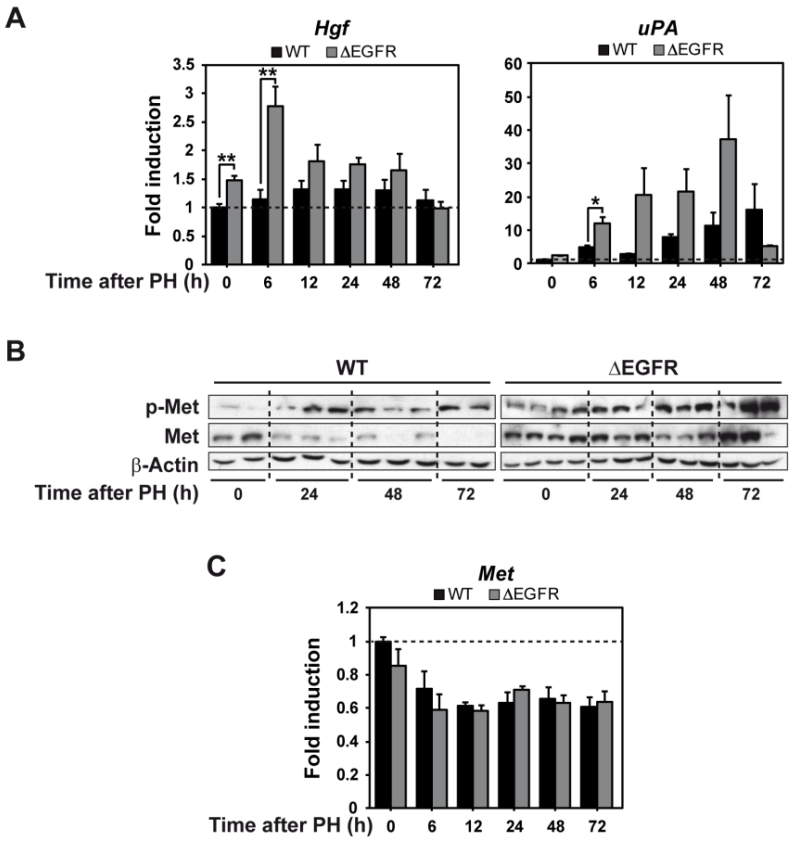

Figure 21. ΔEGFR livers that are able to regenerate after PH show overactivation of the HGF/Met pathway. (A) qRT-PCR analysis of the mRNA levels of *Hgf* **(left)** and urokinase-type plasminogen activator (*uPA)* **(right)**. **(B)** Analysis of phospho-Met and total Met by Western blot at the indicated times after PH in WT and ΔEGFR livers. β-Actin was used as loading control. **(C)** qRT-PCR analysis of the mRNA levels of *Met*. Data in A and C are mean ± SEM of at least 4 animals per group. Student's *t* test was used: *p<0.05 and **p<0.01.

It is also worth mentioning that hepatocyte size significantly decreased at short times after PH in both WT and ΔEGFR animals, analyzed performing an immunohistochemistry of E-cadherin in order to quantify the hepatocyte size (Figure 22). However, ΔEGFR mice showed a quick recovery, as after 24 hours the hepatocyte size in ΔEGFR livers was significantly higher than that observed in WT ones. This hypertrophy could also contribute to the maintenance of liver functions and the low percentage of failure observed in ΔEGFR mice.

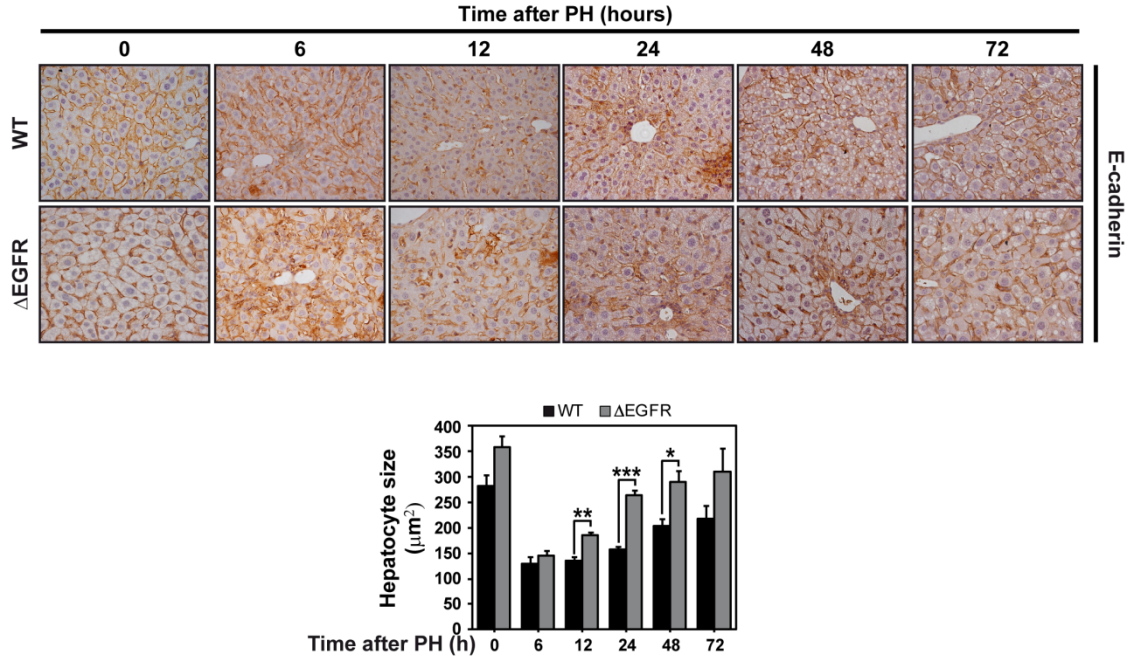

Figure 22. ΔEGFR mice show increased hepatocyte size. Upper: Immunohistochemical analysis of E-cadherin in WT and ΔEGFR livers at different times after PH, as a strategy to label the cell membranes and observe/quantify the cell size. Representative 40x images of at least 3 animals per condition are shown. **Lower:** Quantification of hepatocyte size at the indicated times using ImageJ software. Data are mean ± SEM of at least 3 animals per group, and 3 fields per animal were quantified. Student's *t* test was used: *p<0.05, **p<0.01 and ***p<0.001.

1.3. Analysis of DEN-induced hepatocarcinogenesis in the previous mentioned animal model. Comparison with the WT mice. Status of the TGF-β pathway under these conditions

Our results also indicate that EGFR catalytic activity is critical in the early pre-neoplastic stages of the liver, since ΔEGFR mice showed a delay in the appearance of diethylnitrosamine (DEN)-induced tumors. In that sense, when 15-day-old WT and ΔEGFR mice were submitted to an acute treatment with DEN, at 9 months of age, WT animals developed macroscopically visible tumors, which were barely observed in ΔEGFR mice (**Figure 23A-B**). Consistently, the liver/body weight ratio significantly increased in WT, but not in ΔEGFR mice (**Figure 23C**). However, 12 months after DEN injection, ΔEGFR animals presented macroscopic tumors, and the liver/body weight ratio increase was quite similar in both phenotypes (**Figure 23A-C**).

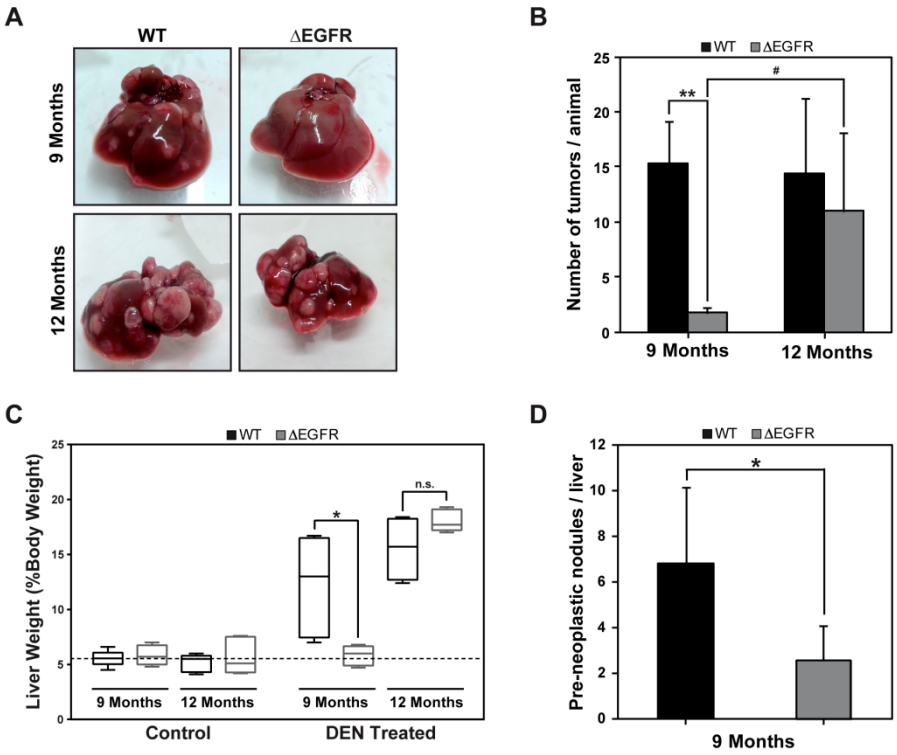

Figure 23. ΔEGFR mice show a delay in the appearance of DEN-induced tumors. WT and ΔEGFR male mice were treated at day 15 of age with phosphate-buffered saline (PBS) or DEN, and livers were collected at 9 and 12 months of age. **(A)** Representative images of livers from DEN-treated mice at the time of sacrifice. **(B)** Quantification of macroscopic tumors per animal. **(C)** Analysis of liver/body weight ratio in WT and ΔEGFR mice. **(D)** Appearance of microscopic pre-neoplastic lesions at 9 months of age. Data in B, C and D are mean ± SEM of at least 4 animals per group. Student's *t* test was used: *p<0.05 and **p<0.01 compared to WT mice; #p<0.05 compared to 9 months. Abbreviation: n.s., no significance.

We then moved to analyze the proliferative state in tissues at 9 months after DEN treatment. Immunohistological and proliferative analysis, through Ki67 staining, revealed the appearance of early pre-neoplastic lesions detectable only under the microscope. Moreover, the number of lesions at 9 months of age in WT mice was much higher than that observed in ΔEGFR mice (**Figure 23D**). The analysis of cell proliferation rate by Ki67 immunohistochemistry

showed lower proliferative rate in the neoplastic areas in ΔEGFR tumors at 9 months compared with WT ones, but a similar proliferative rate at 12 months after DEN injection (Figure 24). These results suggest that lack of the catalytic activity of the EGFR delays the appearance of pre-neoplastic nodules, but it is not able to prevent hepatocarcinogenesis.

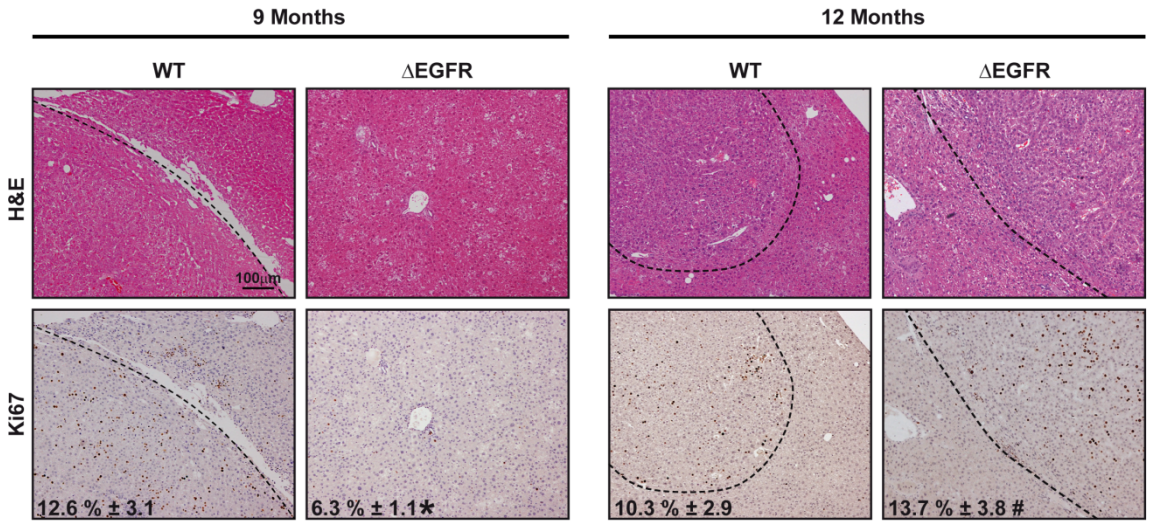

Figure 24. DEN-treated ΔEGFR mice showed lower proliferative rate in the pre-neoplastic areas at 9 months of age. (A) Representative 20x images of H&E and immunohistochemical analyses of proliferation (Ki67 staining) in pre-neoplastic areas in livers from WT and ΔEGFR mice. Quantification of Ki67-positive cells (percentage) is in the bottom of each image. Data are mean ± SEM of at least 4 animals per group, and 3 fields per animal were quantified. Student's *t* test was used: *p<0.05 compared to WT mice; #p<0.05 compared to 9 months. Abbreviation: H&E, hematoxylin and eosin.

In spite of the role observed for the EGFR pathway in inhibiting TGF-β effects during liver regeneration, we could not find significant differences between both animals at 9 months after DEN injection in terms of *Tgfb1* mRNA levels or downstream effectors of the TGF-β pathway, i.e., Smads phosphorylation analyzed by immunohistochemistry (Figure 25).

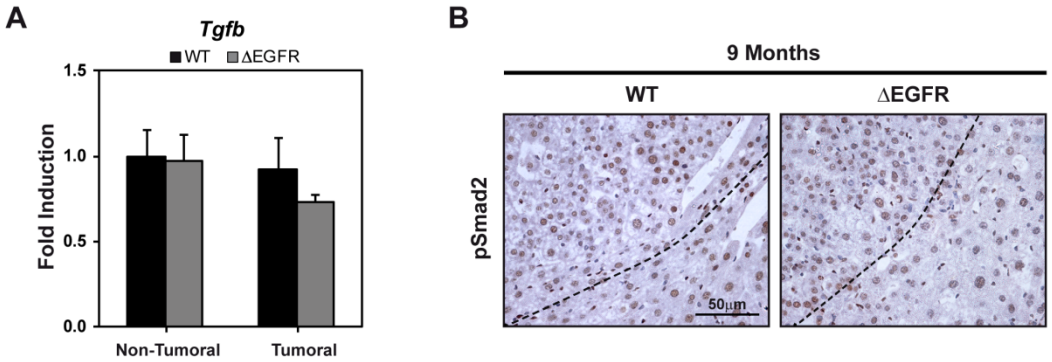

Figure 25. DEN-treated ΔEGFR mice did not show differences in TGF-β pathway. (A) Analysis of *Tgb1* mRNA expression by qRT-PCR in tumoral and non-tumoral areas in liver tissues from 9-month DEN-treated WT and ΔEGFR mice. Data are mean ± SEM of at least 4 animals per group. Student's *t* test was used. No significant differences were observed in any of the cases. **(B)** Immunohistochemical analysis of phospho-Smad2 in liver tissues from 9-month DEN-treated WT and ΔEGFR mice. Representative 40x images of at least 3 animals per condition are shown.

Although we could not find differences in the canonical TGF-β pathway, it is interesting to remark that the mRNA levels of *Nox4* were increased in the non-tumoral tissue of ΔEGFR animals when compared with WT ones (**Figure 26**).

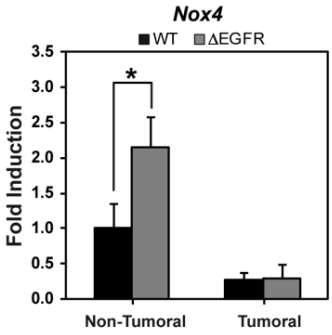

Figure 26. DEN-treated ΔEGFR mice presented higher expression of *Nox4* in non-tumoral areas. Analysis of *Nox4* mRNA expression by qRT-PCR in tumoral and non-tumoral areas in liver tissues from 9-month DEN-treated WT and ΔEGFR mice. Data are mean ± SEM of at least 4 animals per group. Student's *t* test was used: *p<0.05 compared to WT mice.

This work is being continued by Daniel Caballero, PhD investigator in our group, which has demonstrated that EGFR is required for the inflammatory process induced by DEN in the livers. Other mitogenic signals, such as HGF, may replace the EGF-induced growth once the tumor is formed. These results suggest that lack of the catalytic activity of the EGFR delays the appearance of tumors but cannot fully prevent the hepatocarcinogenic process.

Overall, our studies demonstrate that EGFR catalytic activity is critical during the initial phases of both liver regeneration and carcinogenesis and provide key mechanistic insights into how this kinase acts to regulate liver pathophysiology.

2. Analysis of the crosstalk between the TGF-β and EGFR pathways in the regulation of cell adhesion and migration of HCC cells

2.1. Analysis of the phenotype of different HCC cell lines: epithelial *versus* mesenchymal. Correlation with the autocrine production of TGF-β

In the group, we have analyzed the phenotype of different HCC cells, according to the expression of epithelial, such as E-cadherin, and mesenchymal, such as vimentin, proteins. Furthermore, phalloidin staining revealed the different organization of F-Actin depending on the HCC line analyzed (Figure 27A). While the most epithelial ones tend to form clusters (such as PLC/PRF/5) or parenchymas (such as Hep3B), the most mesenchymal ones are mainly found as individual cells (such as SNU449). Interestingly, as more mesenchymal the cells were, the higher expression of *Tgfb1* was observed, indicating a correlation between autocrine activation of the TGF-β pathway and the acquisition of mesenchymal properties (Figure 27B).

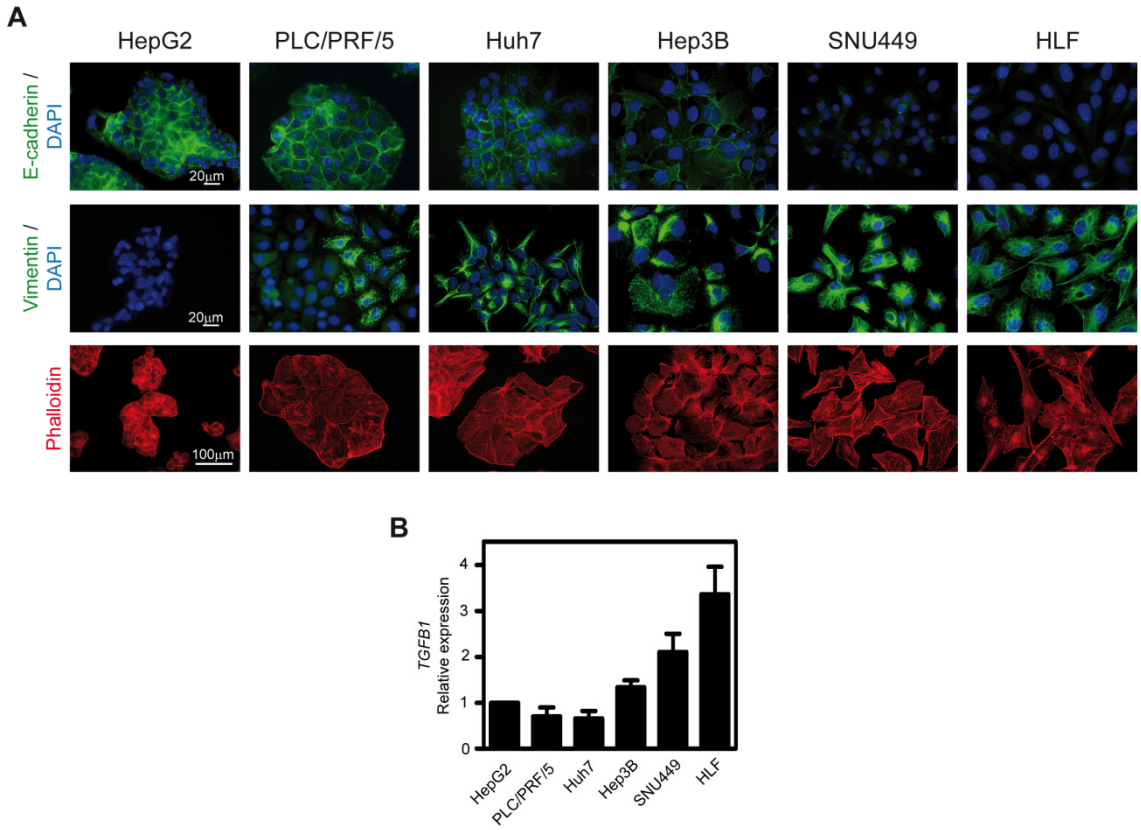

Figure 27. Autocrine TGF-β expression in HCC cells correlate with a mesenchymal-like phenotype. HepG2, PLC/PRF/5, Huh7, Hep3B, SNU449 and HLF were cultured under standard conditions in 10% FBS. **(A)** Immunofluorescence of E-cadherin (green), vimentin (green), Phalloidin (red) and DAPI (blue). Representative 20x and 40x images are shown. **(B)** *TGFB1* expression levels determined by qRT-PCR. Data in B are mean ± SEM of 5 independent experiments.

2.2. TGF-β effects on the epithelial-mesenchymal phenotype, adhesion and migration of liver tumor cells. Analysis of different types of migration and potential mechanisms involved

Considering the different phenotypes observed in liver tumor cells depending on TGF-β autocrine levels, we then decided to study the effect of exogenous TGF-β on the migratory capacity of different HCC cell lines: PLC/PRF/5 (low autocrine TGF-β expression with an epithelial-like phenotype), SNU449 (high autocrine TGF-β expression and mesenchymal-like phenotype) and Hep3B (a mix between both phenotypes).

We first performed wound healing assays and phase contrast analysis of morphology to macroscopically analyze the effects of TGF-β in those cells. Results revealed a high autocrine migratory capacity for SNU449. On the contrary, Hep3B presented also a basal migratory capacity, although not to the same extent as it was observed in SNU449. However, the presence of exogenous TGF-β in the medium induced a more migratory capacity in Hep3B and PLC/PRF/5. In the case of Hep3B, an individual migration was observed, with a more elongated phenotype and protrusions in the cells located in the migration front. In PLC/PRF/5, TGF-β induced an individual migration in some cells, which separate from the cluster structure, as well as collective migration in others, where the group of cells seemed to move together maintaining its multicellular structure. In the case of SNU449, only a slight difference was observed upon TGF-β treatment, as their migration capacity was very high under basal conditions. In that case, all the cells showed an individual mode of migration (**Figure 28**).

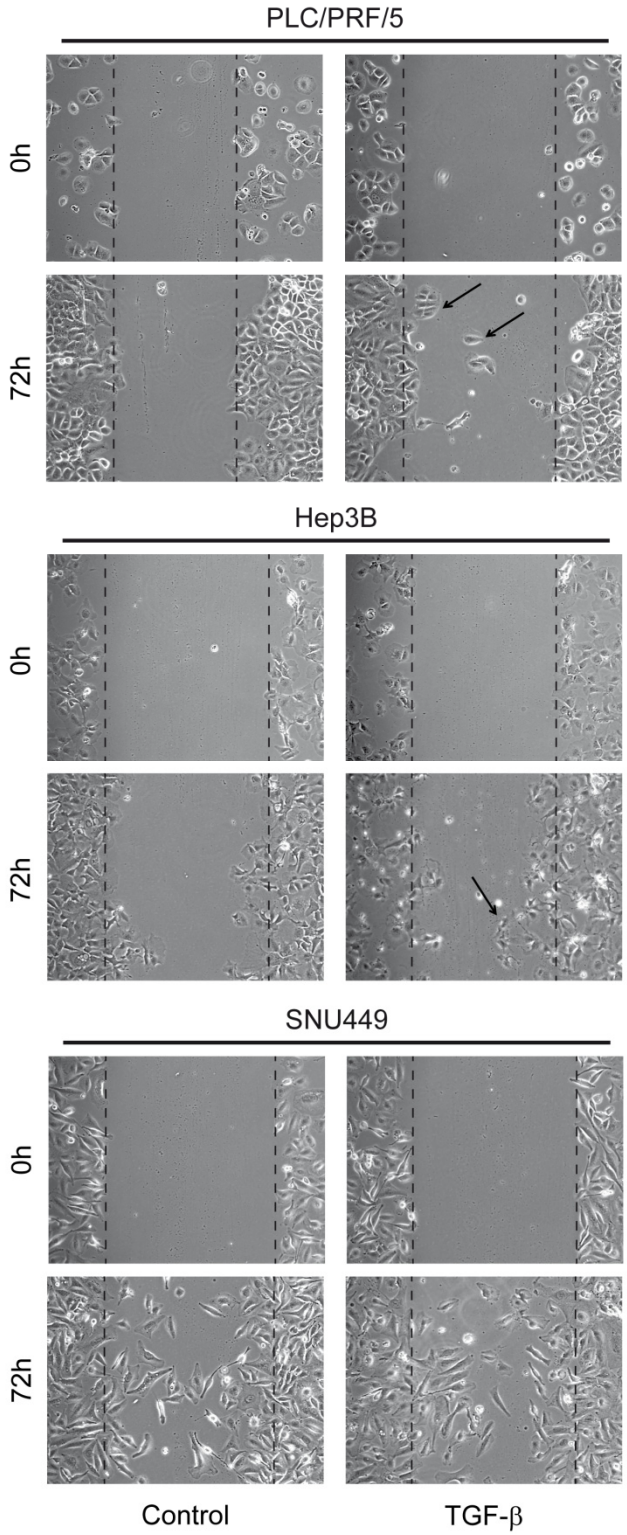

Figure 28. Different TGF-β-induced modes of migration in PLC/PRF/5, Hep3B and SNU449 cells. Wound healing assays after TGF-β treatment (2ng/mL) during 72 hours, cultured with 2% of FBS in the medium. Representative bright-field images are shown.

In order to quantify this migration capacity upon TGF-β treatment, we performed a real time monitoring of cell migration, through xCELLigence System. We corroborated that cells with high TGF-β autocrine expression presented higher migratory capacity (**Figure 29A**). Moreover,

exogenous TGF-β induced an increase in migration in the case of PLC/PRF/5 and Hep3B, but no in SNU449 (Figure 29B).

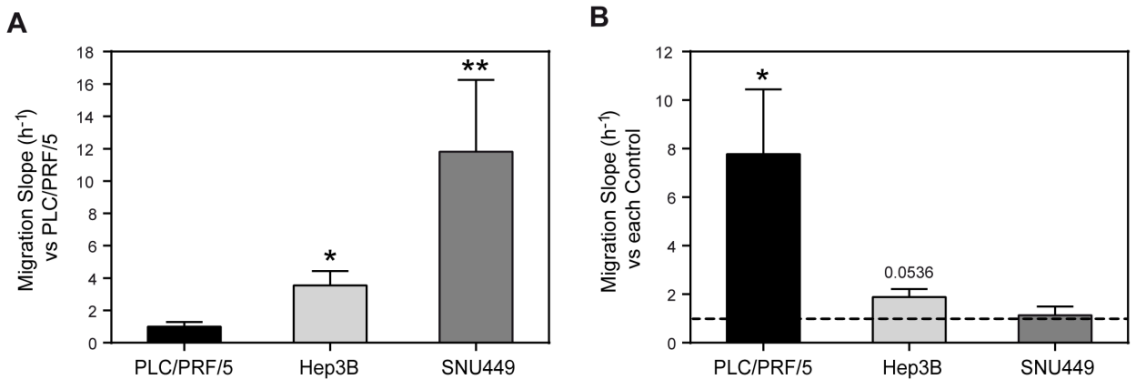

Figure 29. Different TGF-β-induced migration capacity in PLC/PRF/5, Hep3B and SNU449 cells. The mentioned HCC cell lines under basal conditions or treated with TGF-β (2ng/mL) during 64 hours, were trypsinized and plated in the xCELLigence system for a real time migration assay. Migration was then assessed during 8 hours. **(A)** Basal migration (untreated) of PLC/PRF/5, Hep3B and SNU449 HCC cell lines, expressed as relative to PLC/PRF/5. **(B)** Migration induced in these HCC cell lines after TGF-β treatment, represented as the increase in migration relative to untreated conditions of each HCC cell line. Data in A and B are mean ± SEM of 3 independent experiments performed in biological triplicates. Student's *t* test (versus PLC/PRF/5 in A and versus untreated conditions of each HCC cell line in B) was used: *p<0.05 and **p>0.01.

We then decided to study the changes in cell-to-cell contacts. On the one hand, immunocytochemical analysis revealed that E-cadherin, a well-known protein characteristic of epithelial cells and forming part of adherens junctions, was present only in PLC/PRF/5 and Hep3B cells, but not in SNU449, as it was described (Figure 30). A significant downregulation of its expression was observed in Hep3B after TGF-β treatment, while it increased in those PLC/PRF/5 cells that maintained the cluster structure. On the other hand, ZO-1, present in tight junctions, also showed changes after TGF-β treatment. Under basal conditions, only PLC/PRF/5 and some Hep3B cells expressed ZO-1. After TGF-β treatment, PLC/PRF/5 and Hep3B showed lower presence of ZO-1 in the cell membrane, which indicates lower cell-to-cell contact areas. Finally, SNU449, as in the case of E-cadherin, did not express ZO-1 neither under basal conditions nor after TGF-β treatment (Figure 30).

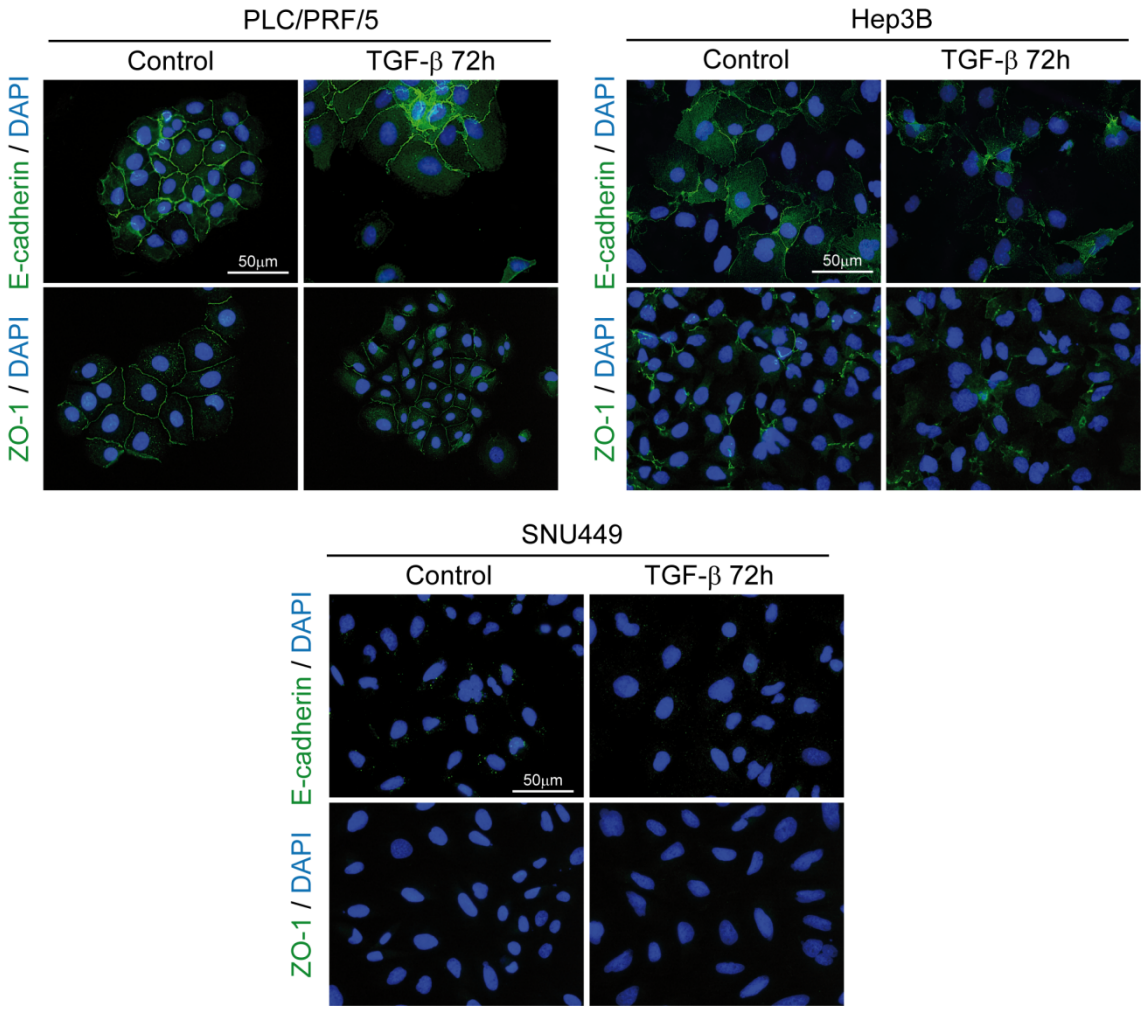

Figure 30. TGF-β promotes the disruption of cell-to-cell contacts in PLC/PRF/5 and Hep3B HCC cells. Immunostaining of E-cadherin and ZO-1 (green), and DAPI (blue: nuclei) 72 hours after TGF-β treatment (2ng/mL) in PLC/PRF/5, Hep3B and SNU449 cells cultured under standard conditions in 10% FBS. Representative 40x images are shown.

Finally, analysis of the morphology revealed a change in the cytoskeleton organization after TGF-β treatment. Indeed, the increase of F-actin forming more stress fibers was observed in all HCC cell lines analyzed compared to their basal conditions (**Figure 31A**). Also, upon TGF-β treatment, the percentage of individual cells was significantly increased in PLC/PRF/5 and Hep3B cells, but not in SNU449, as 90% of the cells were already individual under basal conditions (**Figure 31B**). A more detailed analysis of F-actin staining permitted to observe diverse actin-rich structures in HCC cells. In the case of PLC/PRF/5, under basal conditions, actin cytoskeleton was structured mainly as cortical F-actin, although with the presence of few and thin stress fibers (+). After TGF-β treatment, some of the cells which separate from the cluster adopted an elongated shape ($) with increased the number of long stress fibers along the cell (+), while others acquired a more rounded shape (*) with the presence of stress fibers mainly in the cortical area. On the contrary, those cells that maintained the cluster structure seemed to be more compacted. Regarding Hep3B cells, they showed long and thin stress fibers (+), as well as lamellipodia (≈), under basal conditions. After TGF-β treatment, they also

increased the presence of long but thin stress fibers (+) and showed membrane ruffles (^). Finally, SNU449 presented high amount of robust and thick stress fibers (+) in untreated conditions, which increased after TGF-β treatment. In that case, we could also observe cells with an elongated shape ($) and stress fibers along the body, and others with a more rounded shape (*) and stress fibers disposed in the cortical ring. Moreover, some of the cells presented filopodia (#) (Figure 31A).

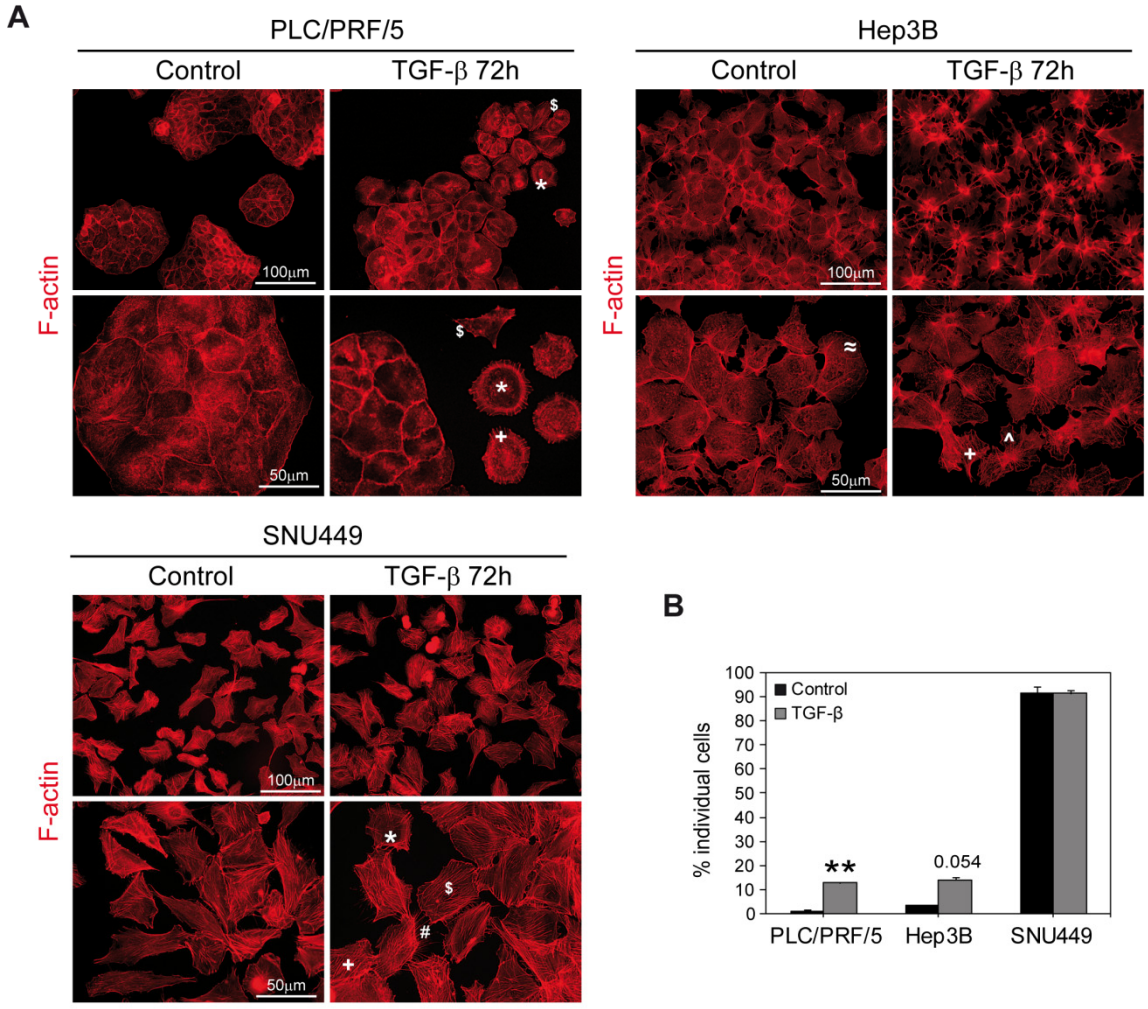

Figure 31. TGF-β treatment induced a reorganization of actin cytoskeleton increasing the presence of stress fibers in all HCC cell lines analyzed. PLC/PRF/5, Hep3B and SNU449 were cultured on plastic under standard conditions in 10% FBS and treated with TGF-β (2ng/mL) for 72 hours. **(A)** Immunostaining of F-actin (red). Symbols indicate different actin-rich structures and different phenotypes: + stress fibres, ^ membrane ruffles, ≈ lamellipodia, # filopodia, * rounded shape, $ elongated shape. Representative 20x and 40x images are shown. **(B)** Quantification of the percentage of individual cells. Data are mean ± SEM of at least 3 independent experiments, and 3 fields per condition were quantified. Student's *t* test was used: **p<0.01 compared to untreated control conditions of each HCC cell line.

In conclusion, we observed that TGF-β is able to induce rearrangements of the actin cytoskeleton, inducing or increasing the presence of different actin-rich structures, which are important to induce migration in all HCC lines. However, it exerts different changes in terms of cell-to-cell contacts, which could lead to different modes of migration.

2.3. Attenuation of the EGFR pathway in *in vitro* models of HCC cells by shRNA technology. Impact on the TGF-β-induced effects on cell adhesion and migration

Apart from proliferation and apoptosis there is almost no *in vitro* data of the crosstalk between the EGFR and the TGF-β pathways in terms of migration/invasion in liver tumor cells. Thus, once studied the TGF-β effects in different HCC cell lines, the next purpose was to clarify if the EGFR pathway could be implicated in these observed effects. For this purpose, we analyzed the effects of targeting knock-down the EGFR in two HCC cell lines with very different modes of migration, like PLC/PRF/5 and Hep3B.

2.3.1. Molecular and functional analysis of PLC/PRF/5 and Hep3B cells where the EGFR was targeted knock-down

In order to address this purpose, we obtained HCC cell lines where the EGFR was targeted knock-down with specific shRNA. Cells were transfected with different plasmids of EGFR shRNA, with the pool of two of them, or with a control unsilencing plasmid (sh-). We evaluated the EGFR levels by Western blot and the best and stable silenced clones were selected for future experiments: PLC/PRF/5shEGFR#pool and Hep3BshEGFR#3 (Figure 32A).

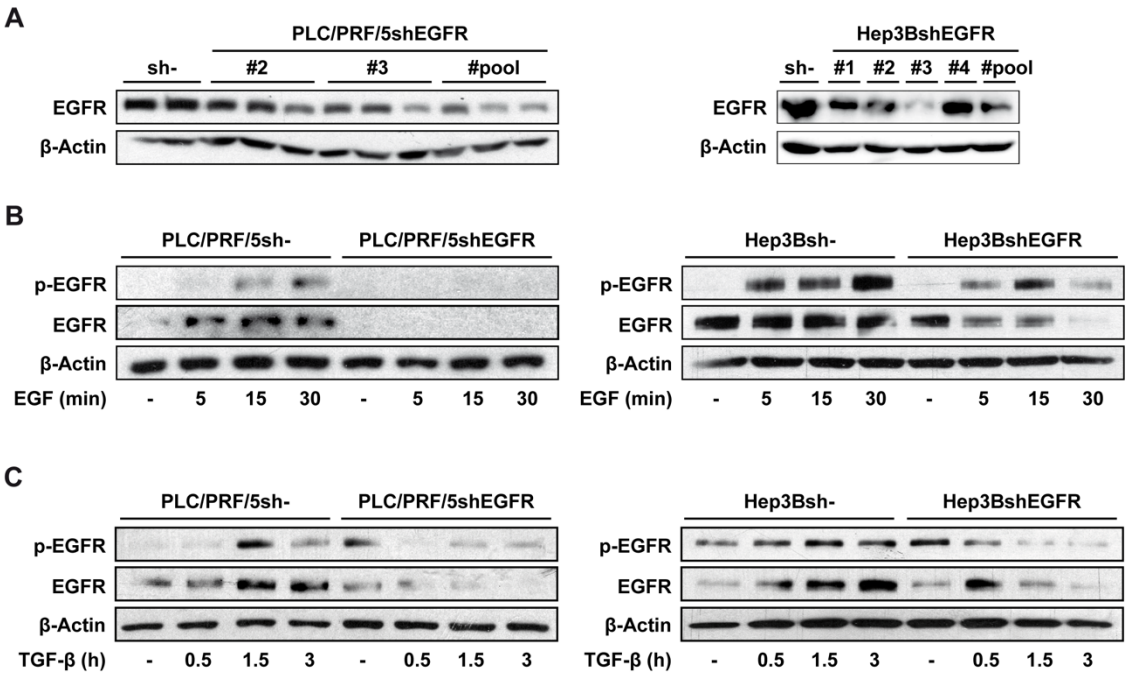

Figure 32. Molecular and functional analysis of the stable EGFR silencing in PLC/PRF/5 and Hep3B HCC cell lines. Human HCC cells PLC/PRF/5 and Hep3B were stably transfected either with an unsilencing shRNA (sh-) or with different plasmids against EGFR, separately and pooled. Best-silenced clones were selected for further experiments: PLC/PRF/5shEGFR#pool and Hep3BshEGFR#3. **(A)** Analysis of EGFR protein levels by Western blot of different passages per clone in PLC/PRF/5 cells, and only one passage in Hep3B cells. **(B)** Analysis of the response to EGF treatment (20ng/mL) in terms of EGFR phosphorylation. **(C)** Analysis of the EGFR transactivation by TGF-β treatment (2ng/mL) in terms of EGFR phosphorylation. β-Actin was used as loading control. In B and C representative experiments of at least 3 independent experiments are shown.

To further confirm the EGFR silencing, we decided to analyze the loss of EGFR function evaluating the response to EGF in terms of EGFR phosphorylation. As expected, EGF was not able to induce to the same extent the phosphorylation of EGFR in PLC/PRF/5shEGFR and Hep3BshEGFR cells (**Figure 32B**). Furthermore, TGF-β was able to transactivate the EGFR in both cell lines, effect that was not observed when EGFR was silenced (**Figure 32C**).

Unexpectedly, EGFR silencing provoked *per se* a change in morphology, as an apparent increase in the amount of individual cells was observed in both cell lines by contrast phase microscopy (**Figure 33**).

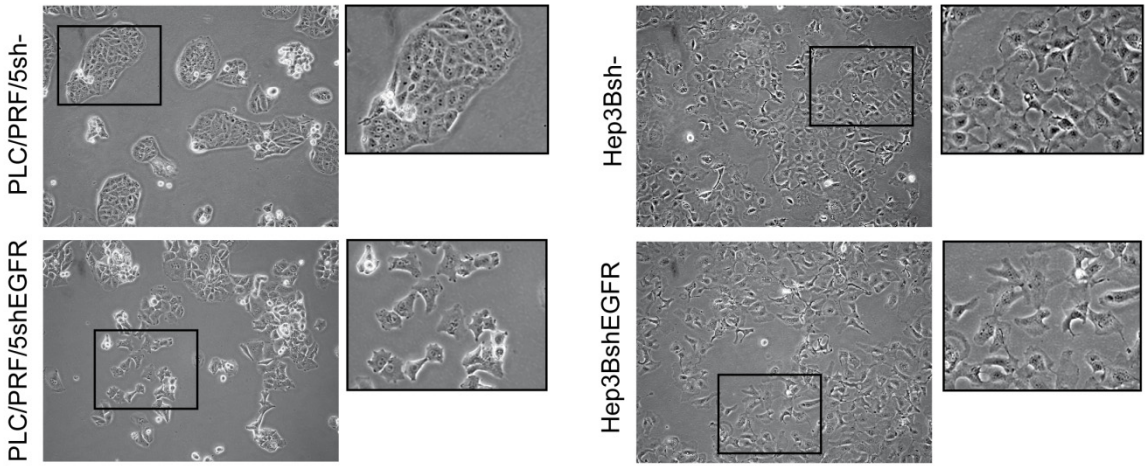

Figure 33. Cell morphology analysis of the stable EGFR silencing in PLC/PRF/5 and Hep3B HCC cell lines. Representative bright-field images of cells cultured under basal conditions on top of plastic.

As it has been explained, EGFR is involved in cell proliferation and survival, and TGF-β induces apoptosis and cell cycle arrest. For this reason, we examined the effects of silencing the EGFR in HCC cells on cell viability and how it affected to the response to TGF-β. Our purpose was to be sure about the viability of the cells in the next experiments. In the proliferation assay, where the increase in cell number upon time was assessed by crystal violet staining, Hep3B cells showed a tendency to a lower growth in EGFR silenced cells, being this decrease much more pronounced when TGF-β was present, effect also observed in PLC/PRF/5 silenced cells (**Figure 34A**). However, no relevant cell death was observed. Indeed, analysis of hypodiploid cells by flow cytometry showed that TGF-β treatment, both in PLC/PRF/5 and Hep3B cells, did not induce massive cell death ($SubG_0$) in any condition; a small percentage of cells underwent apoptosis in the EGFR silenced cells (**Figure 34B**), but not a significant decrease compared to the initial cell number was observed. It is worthy to point out that we are working in the presence of 10% FBS, where cells are mostly protected from cell death.

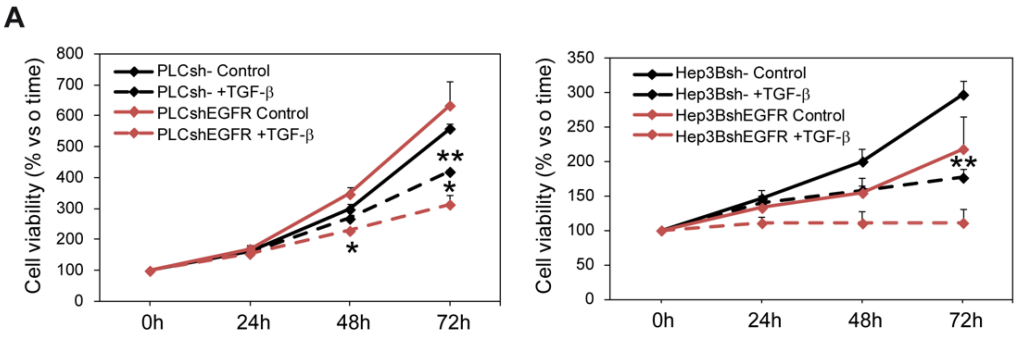

B

	SubG0
PLCsh- Control	1.9 ± 0.3
PLCsh- TGFbeta	1.4 ± 0.2
PLCshEGFR Control	2.6 ± 1
PLCshEGFR TGFbeta	4.5 ± 0.2 ##

	SubG0
Hep3Bsh- Control	1.2 ± 0.1
Hep3Bsh- TGFbeta	5.6 ± 1.1 *
Hep3BshEGFR Control	1.5 ± 0.3
Hep3BshEGFR TGFbeta	7.6 ± 0.9 *

Figure 34. Analysis of the TGF-β pro-suppressor effects after EGFR silencing in PLC/PRF/5 and Hep3B HCC cell lines in the presence of 10% of FBS. (A) Analysis of proliferation in unsilenced and silenced cells after 72 hours of TGF-β treatment (2ng/mL). Number of viable cells analyzed by crystal violet at the indicated times. Results are expressed as percentage of increase relative to zero time. Data are mean ± SEM of 3 independent experiments performed in triplicates. Student's *t* test was used: *p<0.05 and **p<0.01 versus control untreated cells in each cell line (silenced or unsilenced) in each time point. **(B)** Percentage of hypodiploid cells analyzed by flow cytometry in unsilenced and silenced cells after 72 hours of TGF-β treatment (2ng/mL). Data are mean ± SEM of 3 independent experiments. Student's *t* test was used: *p<0.05 compared to control untreated cells in each cell line (silenced or unsilenced); ##p<0.01 compared to unsilenced cells in each condition (untreated or treated).

2.3.2. Role of the EGFR pathway in the modulation of the epithelial-mesenchymal phenotype induced by TGF-β in PLC/PRF/5 and Hep3B cells

Once we have confirmed the model, we then moved to analyze the effects of TGF-β after silencing the EGFR in terms of EMT markers, cell-to-cell contacts, morphology and actin cytoskeleton.

To begin with, we analyzed the expression of some well-accepted **EMT markers**, performing qRT-PCR analysis of the expression of E-cadherin (*CDH1*), an epithelial marker, and vimentin (*VIM*), an intermediate filament, as a mesenchymal one. Furthermore, we also analyzed N-cadherin (*CDH2*) as another mesenchymal marker. First, in the case of unsilenced PLC/PRF/5, N-cadherin and vimentin mRNA levels were upregulated after TGF-β treatment, as expected. Moreover, E-cadherin mRNA levels were also increased, as it was observed by immunofluorescence in those cells that retained the cluster structure, although the differences were not statistically significant (Figure 35A). Thus, this HCC cell line may be carrying out a partial EMT after TGF-β treatment, as it increased mesenchymal markers but also retained some epithelial ones. Interestingly, EGFR silencing decreased E-cadherin mRNA levels dramatically, and TGF-β was not able to re-induce their expression. Regarding N-cadherin, its mRNA levels were also dramatically downregulated after EGFR silencing, and again TGF-β was

not able to recuperate them. Finally, we could observe a decrease in the case of vimentin mRNA expression compared to unsilenced cells in control conditions. However, TGF-β treatment was able to increase its expression to the same extent as in unsilenced cells. Considering now Hep3B cells, we could observe a full EMT after TGF-β treatment, detecting a decrease in E-cadherin, and upregulation of N-cadherin and vimentin mRNA levels (Figure 35B). However, in this case, EGFR silencing did not provoke any change in any of them, and TGF-β was able to induce the EMT program, in terms of EMT markers, as well.

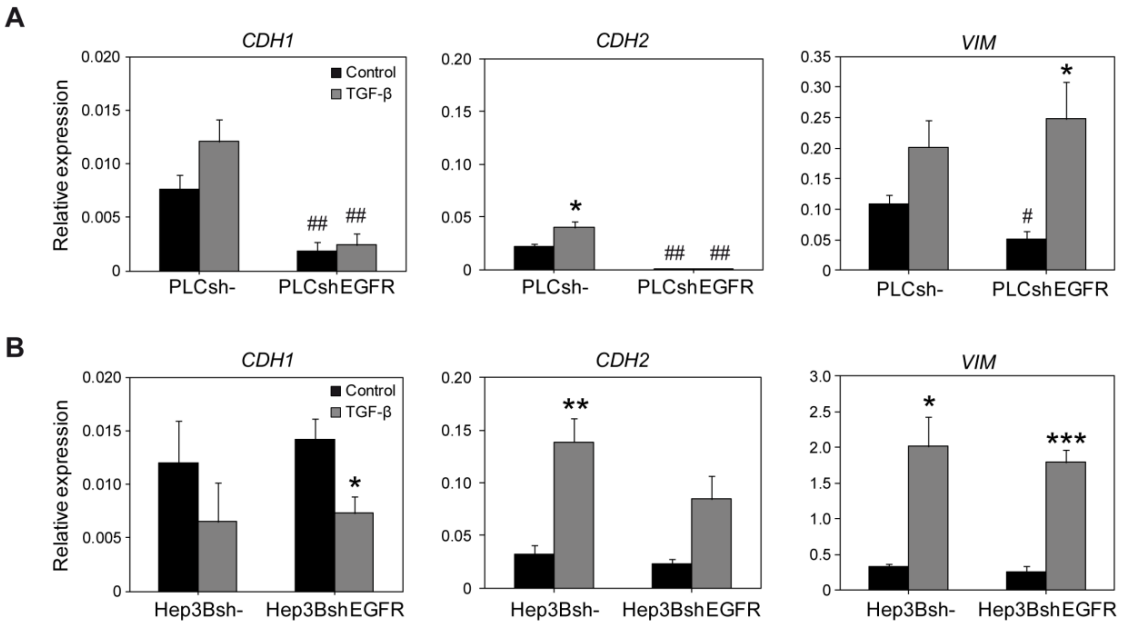

Figure 35. Role of the EGFR pathway in the TGF-β-induced EMT process in PLC/PRF/5 and Hep3B HCC cells in terms of EMT markers. qRT-PCR analysis of E-cadherin (*CDH1*), N-cadherin (*CDH2*) and vimentin (*VIM*) mRNA levels in EGFR silenced PLC/PRF/5 **(A)** and Hep3B cells **(B)** after 72 hours of TGF-β treatment (2ng/mL). Data in A and B are mean ± SEM of 3 independent experiments. Student's *t* test was used: *p<0.05, **p<0.01 and ***p<0.001 compared to control untreated cells in each cell line (unsilenced or silenced); #p<0.05 and ##p<0.01 compared to unsilenced cells in each condition (untreated or treated).

We also analyzed a battery of transcription factors implicated in the EMT process, such as SNAIL, SLUG, TWIST, ZEB1 and ZEB2. We confirmed that Hep3B cells, but not PLC/PRF/5, were undergoing a full EMT process as they increased the expression of *SNAI1, SNAI2, TWIST1* and *ZEB2* after TGF-β treatment. However, we could not observe differences in almost any of these transcription factors after EGFR silencing. Only in PLC/PRF/5 cells in the case of *ZEB2*, where silenced cells upregulated its expression, which was even increased after TGF-β treatment although it was not significant, and in the case of *TWIST1*, where EGFR silencing downregulated its expression (Figure 36A-B).

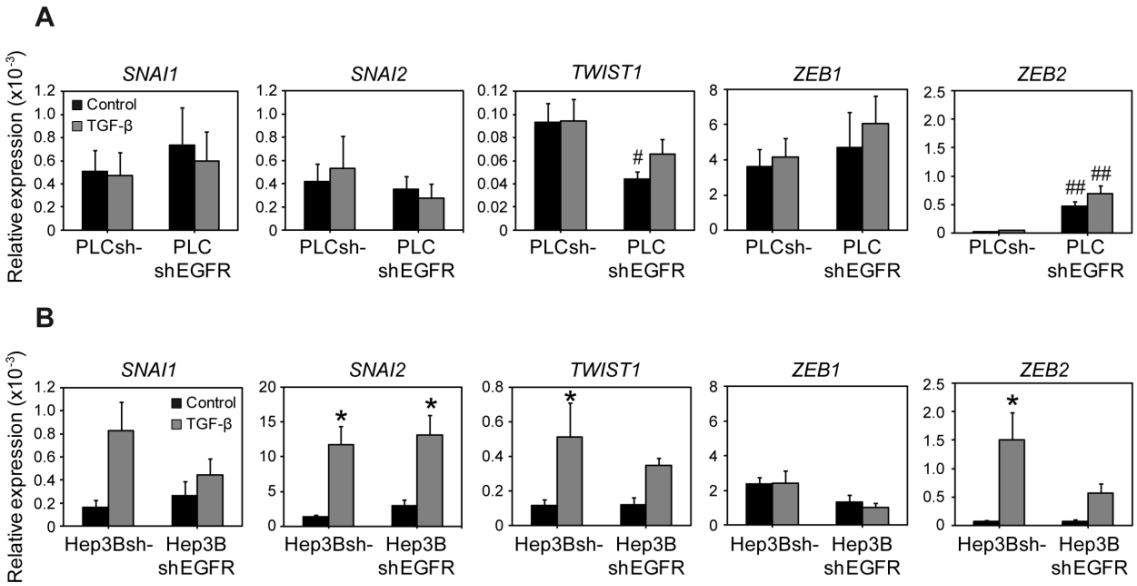

Figure 36. Role of EGFR pathway in the TGF-β-induced EMT process in PLC/PRF/5 and Hep3B cells in terms of EMT transcription factors. qRT-PCR analysis of SNAIL (*SNAI1*), SLUG (*SNAI2*), TWIST (*TWIST1)*, ZEB1 (*ZEB1*) and ZEB2 (*ZEB2*) mRNA levels in EGFR silenced PLC/PRF/5 **(A)** and Hep3B cells **(B)** after 72 hours of TGF-β treatment (2ng/mL). Data in A and B are mean ± SEM of 3 independent experiments. Student's *t* test was used: *p<0.05 compared to control untreated cells in each cell line (unsilenced or silenced); #p<0.05 and ##p<0.01 compared to unsilenced cells in each condition (untreated or treated).

After, we analyzed **cell-to-cell contacts** performing immunostainings of E-cadherin and ZO-1. Results in unsilenced PLC/PRF/5 cells confirmed that TGF-β treatment was able to increase the levels of E-cadherin in the cells that remain in the cluster structure, while the ones that separate lost their expression, and decreased the presence of ZO-1 in the cell membrane, the same that was observed in parental PLC/PRF/5 cells. Results after silencing the EGFR revealed almost a complete loss of E-cadherin and the disruption in tight junctions analyzed by ZO-1 immunostaining. TGF-β treatment was not able to increase the levels of E-cadherin in any cell, and the disruption of tight junctions was even more significant (**Figure 37A**). Regarding Hep3B, unsilenced cells also behaved as parental ones, decreasing E-cadherin and diminishing the staining of ZO-1 after TGF-β treatment. The silencing of EGFR provoked also a decrease in E-cadherin localized in cell-to-cell contacts and a decrease in tight junctions. Both effects were increased after TGF-β treatment, observing the disappearance of E-cadherin and almost of ZO-1 (**Figure 37B**).

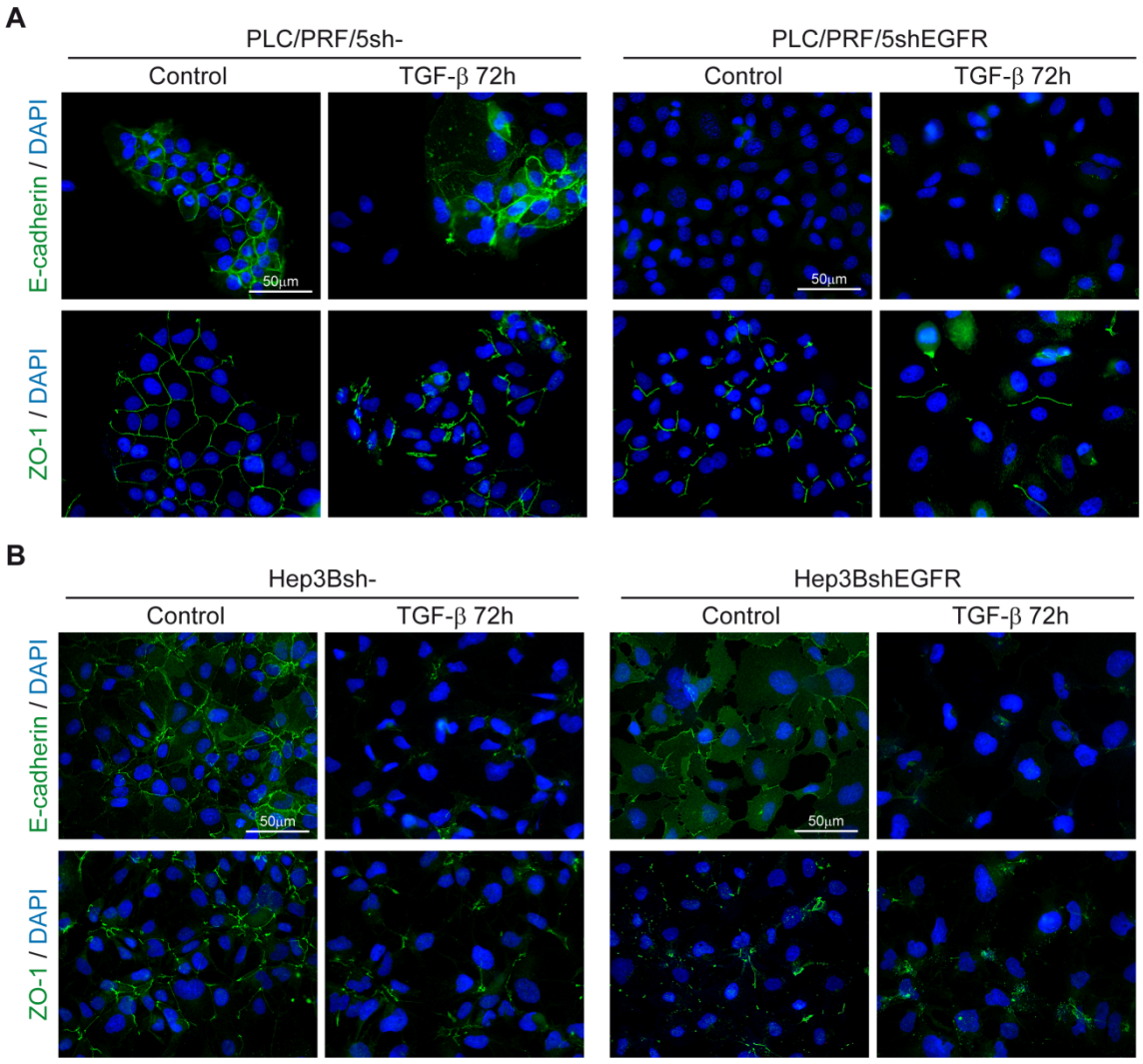

Figure 37. EGFR silencing together with TGF-β treatment promotes the disruption of cell-to-cell contacts in PLC/PRF/5 and Hep3B HCC cells. EGFR silenced PLC/PRF/5 **(A)** and Hep3B **(B)** cells were cultured on plastic. Immunostaining of E-cadherin and ZO-1 (green), and DAPI (blue: nuclei) after TGF-β treatment (2ng/mL) for 72 hours. Representative 40x images are shown.

Finally, we studied the **cytoskeleton organization** through F-actin staining. First, in the case of PLC/PRF/5, we confirmed the significant increase in the number of individual cells after EGFR silencing like we have previously observed by contrast phase microscopy, and less compactation in the remaining clusters. Moreover, after TGF-β treatment, there was a summatory effect as the number of individual cells was even higher, with a more rounded shape. On the contrary, in Hep3B cells we could not see an increase in individual cells after EGFR silencing, although the cells separate one from each other in the parenchyma, but maintaining some contacts between them. However, after TGF-β treatment there was an increase in the number of individual cells, but without difference compared with unsilenced treated cells (Figure 38A and B).

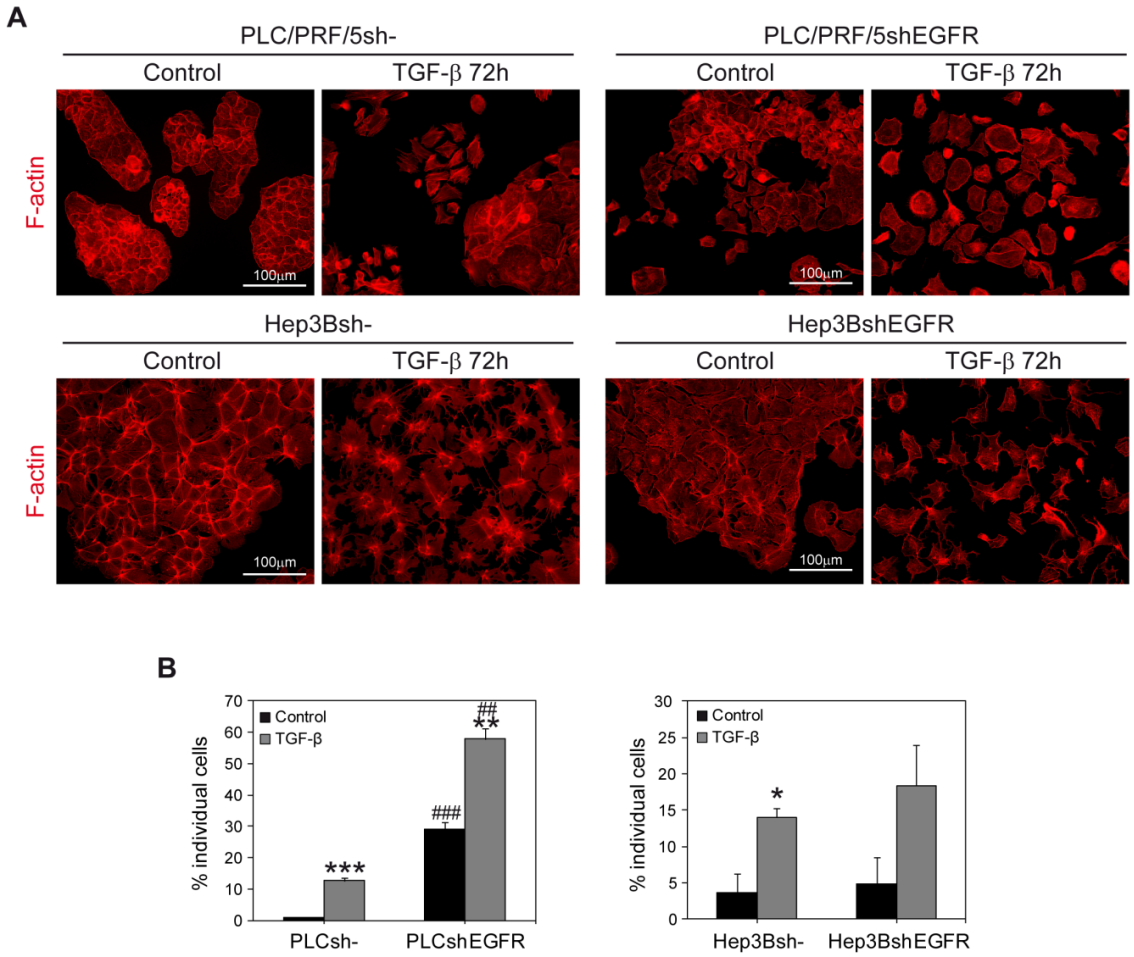

Figure 38. EGFR is important for maintaining parenchymal structures. EGFR silenced PLC/PRF/5 and Hep3B cells were cultured on plastic. **(A)** Immunostaining of F-actin (red) after TGF-β treatment (2ng/mL) for 72 hours. Representative 20x images are shown. **(B)** Quantification of the percentage of individual cells. Data in B are mean ± SEM of 2 independent experiments, and 3 fields per condition were quantified. Student's *t* test was used: *p<0.05, **p<0.01 and ***p<0.001 compared to control untreated cells in each cell line (unsilenced or silenced); ##p<0.01 and ###p<0.001 compared to unsilenced cells in each condition (untreated or treated).

Thus, EGFR might be implicated in the maintenance of parenchymal structures, which, at least in the case of PLC/PRF/5, might counteract the response to TGF-β.

2.3.3. EGFR silencing provokes a decrease in cell-to-matrix adhesion in PLC/PRF/5, but not in Hep3B cells

Cell movement is tightly related to cell shape and morphology since it determines the mode of migration that cells adopt to invade surrounding tissues. Among other characteristics, these types of movements differ on cell-to-matrix adhesion requirements. As it is known, TGF-β is able to induce changes in adhesion to the extracellular matrix (Lamouille et al., 2014; Nalluri et al., 2015). Thus, we decided to explore if EGFR silencing in the two HCC cell lines could be

modifying cell-to-matrix adhesion after TGF-β treatment. We decided to assess the adhesion through the xCELLigence System, after seeding the cells in special plates for this system without coating, but also using different extracellular matrix proteins for coating some wells of the plate: Collagen I, Collagen IV and Fibronectin. Results revealed that in PLC/PRF/5 unsilenced cells after TGF-β treatment, there is higher adhesive capacity in no coating and Collagen I coated wells, although it was not significant. Interestingly, EGFR silencing provoked a dramatic decrease in the adhesive capacity in all the different coatings, and TGF-β was not able to re-establish it, showing even a tendency to decrease the adhesion to some coatings, although it was not significant (Figure 39A). Regarding Hep3B cells, TGF-β treatment induced an increase in the adhesive capacity in all the coatings tested, although it was only significant in some of them. However, in that case, EGFR silencing was not able to significantly decrease cell-to-matrix adhesion. Moreover, TGF-β treatment in EGFR silenced cells was able to recuperate some of the adhesive capacity that had been lost when EGFR expression was attenuated (Figure 39B).

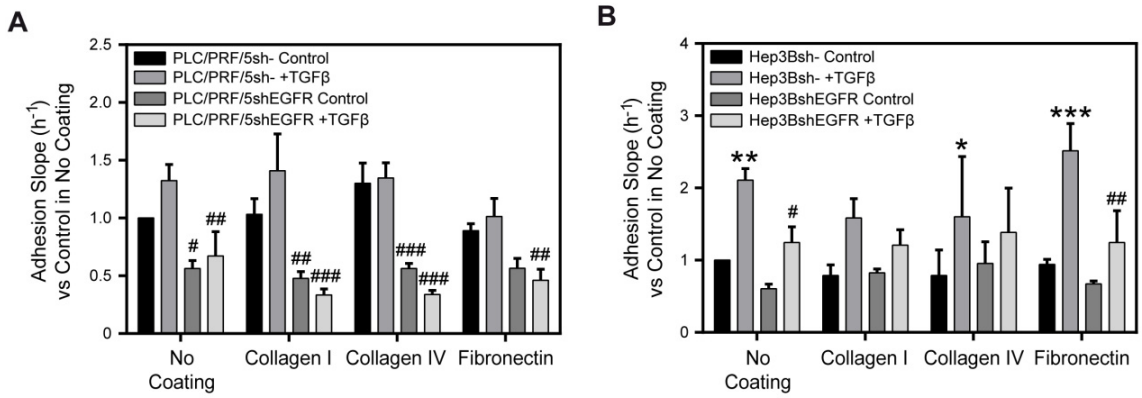

Figure 39. Stable silencing of EGFR provokes a decrease in cell-to-matrix adhesion in PLC/PRF/5, but not in Hep3B cells. Unsilenced and EGFR silenced PLC/PRF/5 **(A)** and Hep3B **(B)** cells were treated with TGF-β (2ng/mL) during 68 hours, then trypsinized and plated in the xCELLigence system for a real time adhesion assay. Adhesion was then assessed during 4 hours, and it is expressed as relative to PLC/PRF/5 or Hep3B unsilenced and untreated cells in no coating condition. Data are mean ± SEM of 3 independent experiments performed in biological duplicates. Two-way ANOVA was used: *p<0.05, **p<0.01 and ***p<0.001 compared to control untreated cells in each cell line (silenced or unsilenced); #p<0.05, ##p<0.01 and ###p<0.001 compared to unsilenced cells in each condition (treated or untreated).

These results suggested that TGF-β and EGFR might be regulating focal adhesions, which are large protein complexes through which the cytoskeleton of the cell connects to the extracellular matrix. Immunofluorescence analysis of vinculin, which is involved in the anchoring of actin to the plasma membrane, participating in cell-to-cell and cell-to-matrix adhesion, showed that focal adhesions in PLC/PRF/5 after EGFR silencing were drastically diminished compared to unsilenced cells (Figure 40A). This result confirmed the one observed in the xCELLigence system. Moreover, TGF-β treatment in unsilenced PLC/PRF/5 cells induced changes in the distribution of focal adhesion complexes within the cell surface. In that sense, the cells belonging to a cluster structure retained the staining of focal adhesion complexes

distributed within the cell body, like in untreated cells. On the contrary, in the cells separating from the cluster, the remaining focal adhesions were the ones on the edge of the cells. However, TGF-β was not able to promote these changes in EGFR silenced cells, as most of them showed vinculin staining homogeneously distributed in the cytoplasm, not forming part of well-structured focal adhesion complexes (**Figure 40A and Figure 41A**), confirming again the results obtained in the xCELLigence system. Finally, in the case of Hep3B cells the results were not so evident, as vinculin staining was much weaker even under basal conditions (**Figure 40B**). However, we could observe dislocalized vinculin staining within the cell when silencing EGFR, although we were also able to observe some cells with still structured focal adhesions. TGF-β treatment in unsilenced cells did not increase the number of focal adhesions dramatically, as we expected for the previous results from the xCELLigence system, although this effect was easily observed when EGFR was silenced, increasing the number of well-structured focal adhesion complexes (**Figure 40B and Figure 41B**). It is worthy to mention that in both cell lines there was a reduction in the presence of stress fibers in EGFR silenced cells under basal conditions, although it was clearly evident only in PLC/PRF/5 cells.

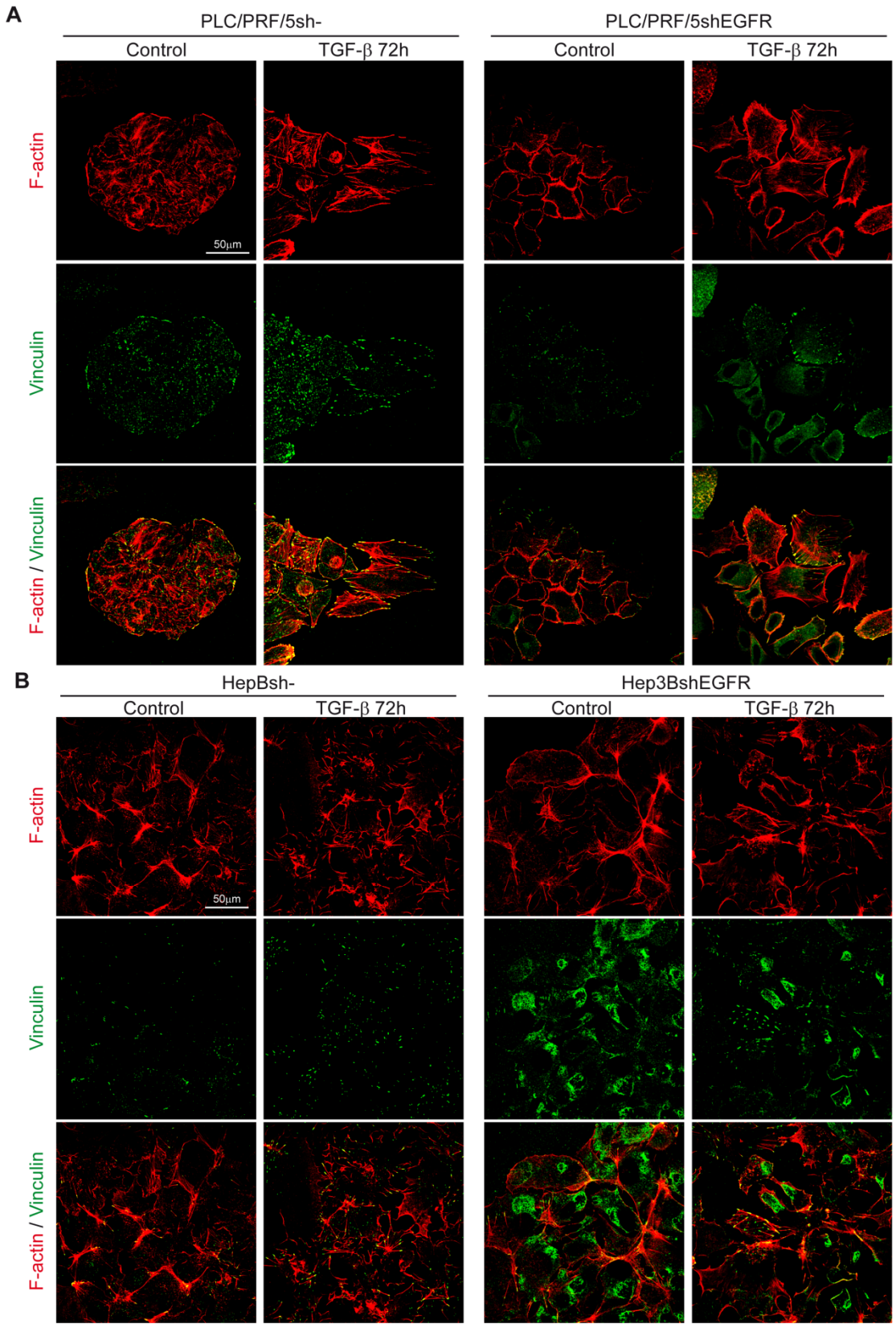

Figure 40. Stable silencing of EGFR disrupts focal adhesions in PLC/PRF/5, but not in Hep3B. Unsilenced and EGFR silenced PLC/PRF/5 **(A)** and Hep3B **(B)** cells were cultured on plastic. Immunostaining of vinculin (green) and F-actin (red) after TGF-β treatment (2ng/mL) for 72 hours. 3 independent experiments were performed and representative 40x confocal images of one stack from the cells' bottom are shown.

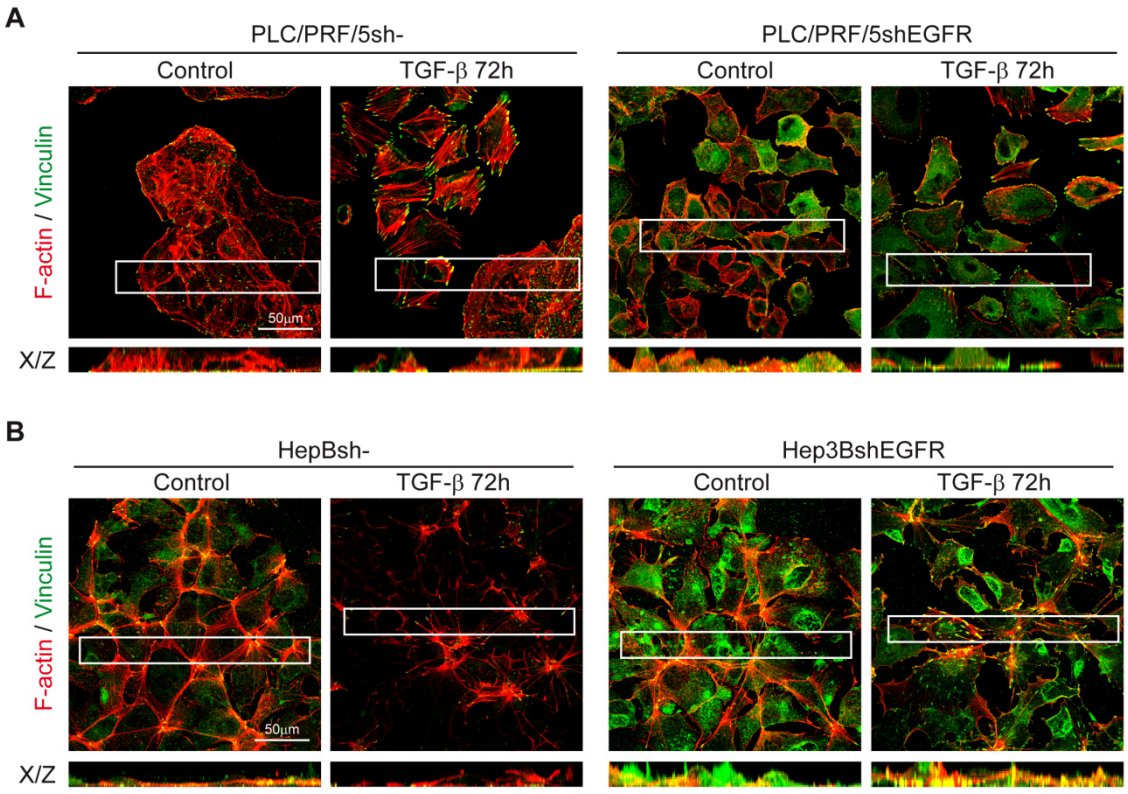

Figure 41. TGF-β treatment and EGFR silencing induced changes in the distribution of focal adhesion complexes within the cell in PLC/PRF/5 and Hep3B. Unsilenced and EGFR silenced PLC/PRF/5 **(A)** and Hep3B **(B)** cells were cultured on plastic. Immunostaining of vinculin (green) and F-actin (red) after TGF-β treatment (2ng/mL) for 72 hours. 3 independent experiments were performed and representative 40x confocal images of all the stacks from the cells are shown (0.25μm thick/stack). A detail of the X/Z axis is shown in the bottom of each image.

2.3.4. EGFR silencing promotes the disruption of parenchymal structures in PLC/PRF/5 but not in Hep3B cells when cultured on a matrix of collagen I

Considering the morphological differences, as well as the changes in cell-to-cell contacts and cell-to-matrix adhesion in PLC/PRF/5 and Hep3B after TGF-β treatment when EGFR was silenced, we hypothesized that this receptor could be regulating the kind of movement that HCC cells adopt to invade. Taking into account that mechanisms driving cell movement might differ between 2D and 3D environments, we decided to seed the cells on a matrix of bovine collagen I, one of the main components of the extracellular matrix that HCC cells have to invade and metastasize. On the one hand, PLC/PRF/5sh- also tended to form groups of cells, and only around 7% of the cells were individual. However, after TGF-β treatment this percentage was increased to almost 20%. When the effect of silencing EGFR was analyzed, results revealed that there was also a disruption of parenchymal structures, like in a 2D matrix, and most of the

cells became individual in a similar extent that after TGF-β treatment in unsilencing conditions. Noteworthy is that when the cells are both silenced for EGFR and treated with TGF-β, the percentage of individual cells is even increased, being the differences statistically significant (Figure 42A and C). On the other hand, in the case of unsilenced Hep3B, around 15% of the cells were individual, and this percentage was not increased after EGFR silencing. TGF-β treatment increased the number of individual cells up to 25% in unsilenced cells and up to 20% in silenced ones, although the increase was not significant (Figure 42B and C).

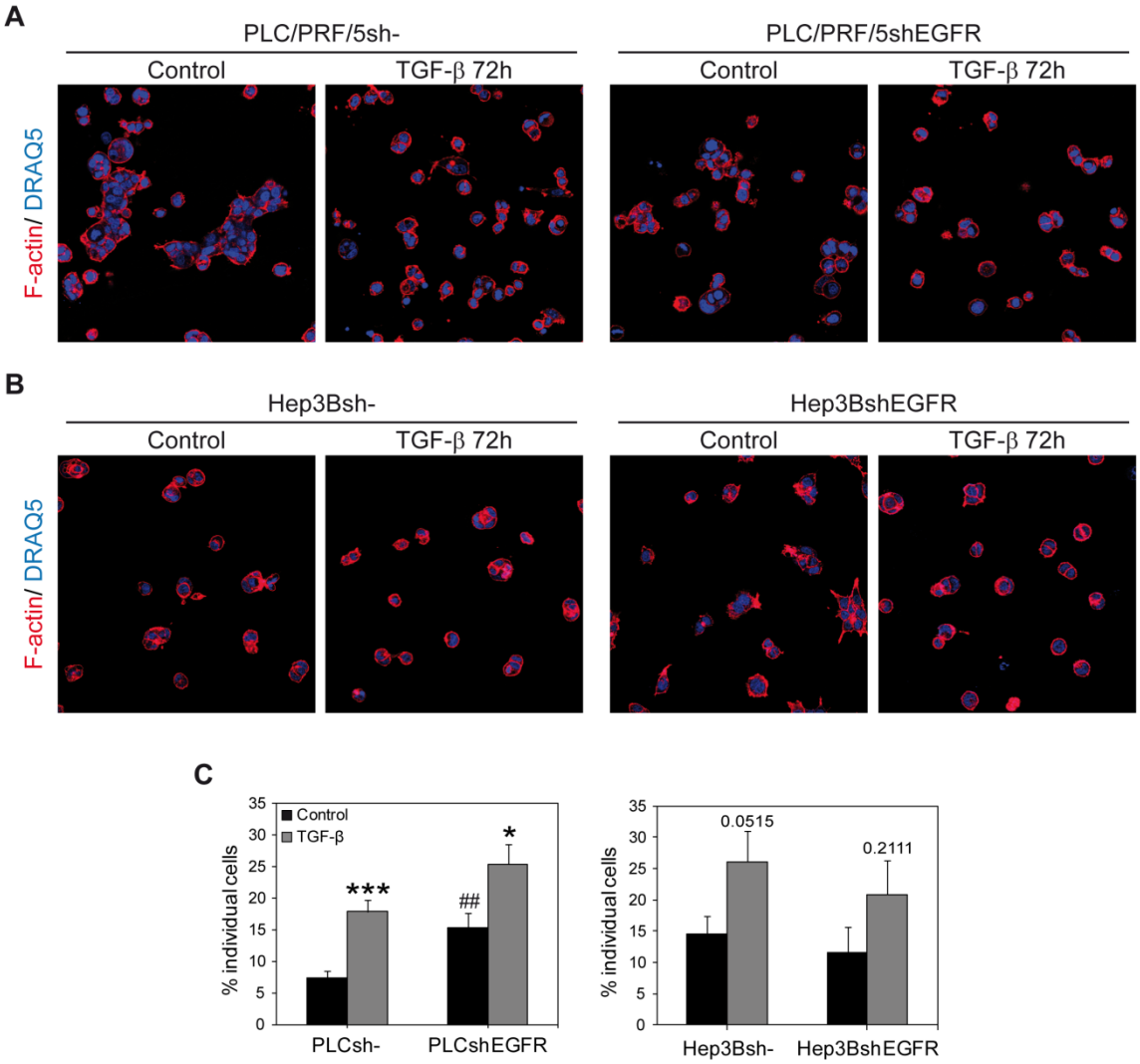

Figure 42. EGFR silencing also promotes the disruption of parenchymal structures in PLC/PRF/5 but not in Hep3B cells when cultured on top of a matrix of collagen I. Unsilenced and EGFR silenced PLC/PRF/5 and Hep3B cells were cultured on plastic and treated with TGF-β (2ng/mL) during 48 hours. Then cells were trypsinized and cultured on top of a bovine collagen I matrix for 24 hours more, up to a total of 72 hours with TGF-β treatment. Representative 40x confocal images of one stack of immunostaining of F-actin (red) and DRAQ5 (blue: nuclei) of PLC/PRF/5 **(A)** and Hep3B **(B)** are shown. **(C)** Quantification of the percentage of individual cells in PLC/PRF/5 **(left)** and Hep3B **(right).** Data are mean ± SEM of at least 2 independent experiments performed in duplicates, and 5 fields per condition were quantified. Student's *t* test was used: *p<0.05 and ***p<0.001 compared to control untreated cells in each cell line (unsilenced or silenced); ##p<0.01 compared to unsilenced cells in each condition (untreated or treated).

2.3.5. EGFR silencing induces actomyosin contractility in PLC/PRF/5 after TGF-β treatment, acquiring an ameboid-like phenotype, which is not observed in Hep3B cells

Cell movement is not only determined by cell shape but also by actomyosin contractility. Thus, an elongated “mesenchymal-like” mode of movement is characterized by cell polarization and low actomyosin contractility, while rounded “ameboid” mode of cell migration is driven by high levels of actomyosin contractility. Collective migration requires high contractility but differs from individual migration, as it is necessary to maintain cell-to-cell contacts. Considering this, we decided to study the contractility status of the cells after EGFR silencing and TGF-β treatment, in order to explain the differences observed between them. Actomyosin contractility was determined by analyzing the percentage of blebbing cells, as well as the immunostaining of pMLC2 (phospho-Myosin Light Chain 2), a downstream effector of the canonical Rho/ROCK signaling, in cells seeded on top of a thick collagen I matrix. Results revealed a correlation between actomyosin contractility and TGF-β treatment in PLC/PRF/5sh-, becoming more contractile after the treatment, since they showed a high percentage of cells with blebs and high levels of pMLC2 when analyzed by immunofluorescence. Moreover, EGFR silencing *per se* also increased the percentage of cells with blebs and the levels of pMLC2, effect that was even increased after TGF-β treatment (**Figure 43A, B and C**).

On the other hand, in Hep3Bsh- cells, we observed very low percentage of blebbing cells in all the conditions, although TGF-β and EGFR silencing were also able to increase this number, but never to the same extent of that found in PLC/PRF/5 cells. Moreover, TGF-β treatment did not increase the levels of pMLC2 neither in unsilenced nor silenced cells, although EGFR silencing was also able to increase it (**Figure 44A, B and C**).

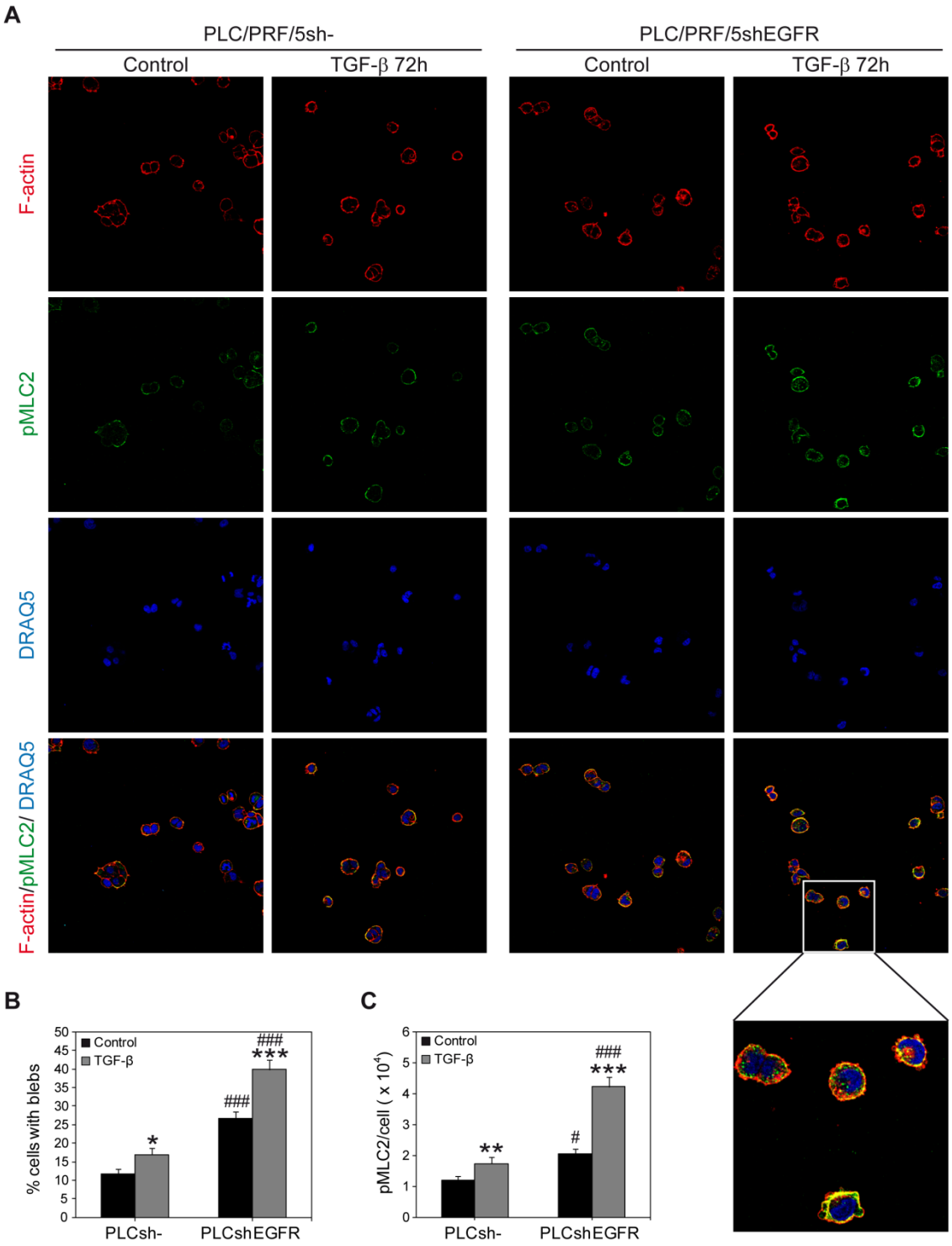

Figure 43. EGFR silencing significantly increases actomyosin contractility in PLC/PRF/5 when cultured on top of a matrix of collagen I. Unsilenced and EGFR silenced PLC/PRF/5 cells were cultured on plastic and treated with TGF-β (2ng/mL) during 48 hours. Cell were then trypsinized and cultured on top of a bovine collagen I matrix for 24 hours more, up to a total of 72 hours with TGF-β treatment. **(A)** Representative 40x confocal images of one stack of immunostaining of pMLC2 (green), F-actin (red), and DRAQ5 (blue: nuclei) are shown. **(B)** Quantification of the percentage of cells with blebs. **(C)** Quantification of pMLC2 immunostaining intensity per cell. Data in B and C are mean ± SEM of at least 3 independent experiments performed in duplicates and 5 fields per condition were quantified. Student's *t* test was used: *p<0.05, **p<0.01 and ***p<0.001 compared to control untreated cells in each cell line (unsilenced or silenced); #p<0.05 and ###p<0.001 compared to unsilenced cells in each condition (untreated or treated).

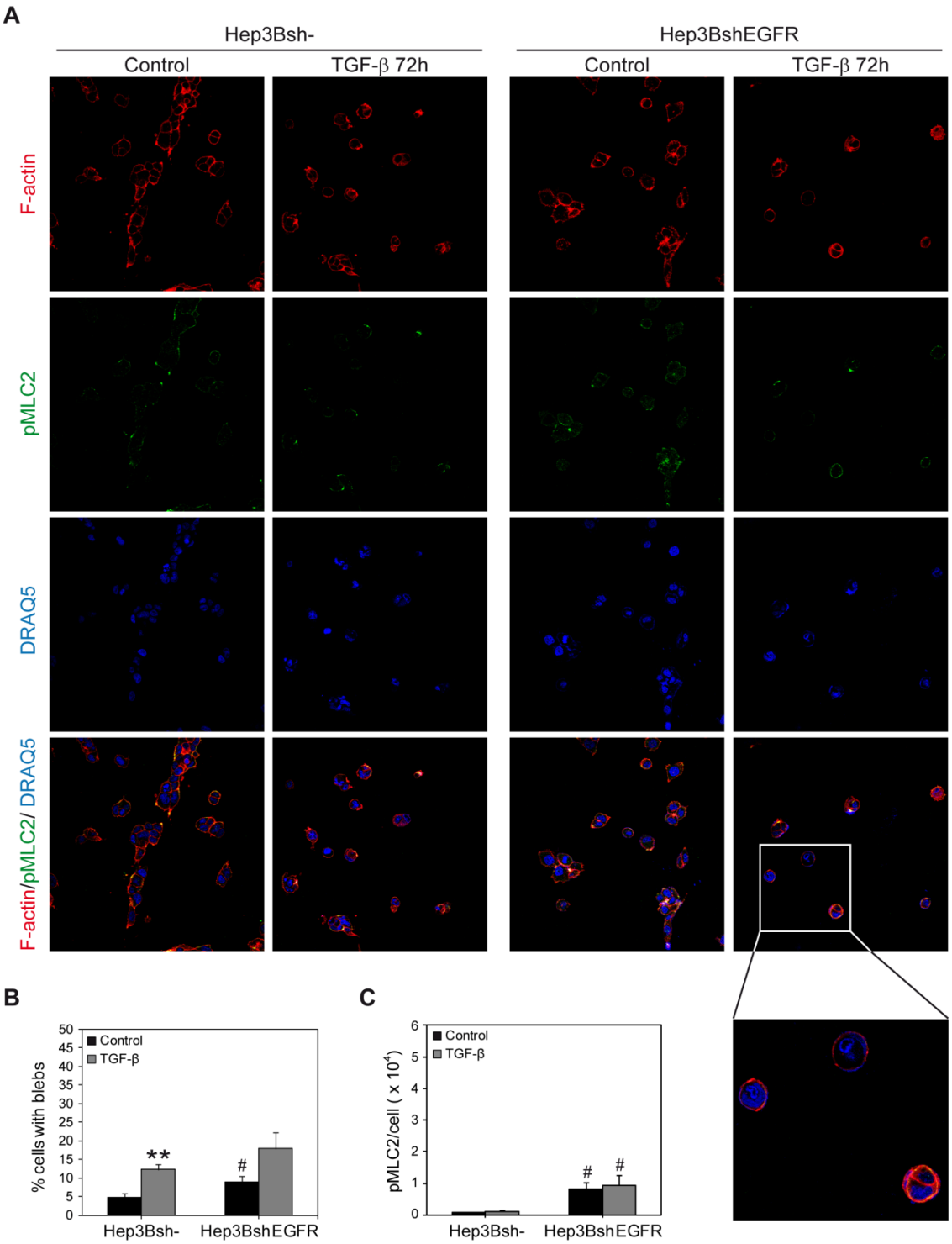

Figure 44. EGFR silencing does not induce high actomyosin contractility in Hep3B when cultured on top of a matrix of collagen I. Unsilenced and EGFR silenced Hep3B cells were cultured on plastic and treated with TGF-β (2ng/mL) during 48 hours. Cells were then trypsinized and cultured on top of a bovine collagen I matrix for 24 hours more, up to a total of 72 hours with TGF-β treatment. **(A)** Representative 40x confocal images of one stack of immunostaining of pMLC2 (green), F-actin (red), and DRAQ5 (blue: nuclei) are shown. **(B)** Quantification of the percentage of cells with blebs. **(C)** Quantification of pMLC2 immunostaining intensity per cell. Data in B and C are mean ± SEM of at least 2 independent experiments performed in duplicates and 5 fields per condition were quantified. Student's *t* test was used: **p<0.01 compared to control untreated cells in each cell line (unsilenced or silenced); #p<0.05 compared to unsilenced cells in each condition (untreated or treated).

Since EGFR suppresses the TGF-β-induced contractility in PLC/PRF/5, we analyzed expression levels of different Rho GTPases which have been reported to be important for sustaining bleb based migration and actomyosin contractility (Calvo et al., 2011; Gadea et al., 2008; Sanz-Moreno et al., 2008). EGFR silencing in PLC/PRF/5 cells allowed them to respond to TGF-β upregulating *RHOC*, *CDC42* and *RAC1*. Notably, Hep3B cells responded to TGF-β upregulating these three genes regardless the EGFR pathway was active or not (**Figure 45A and B**).

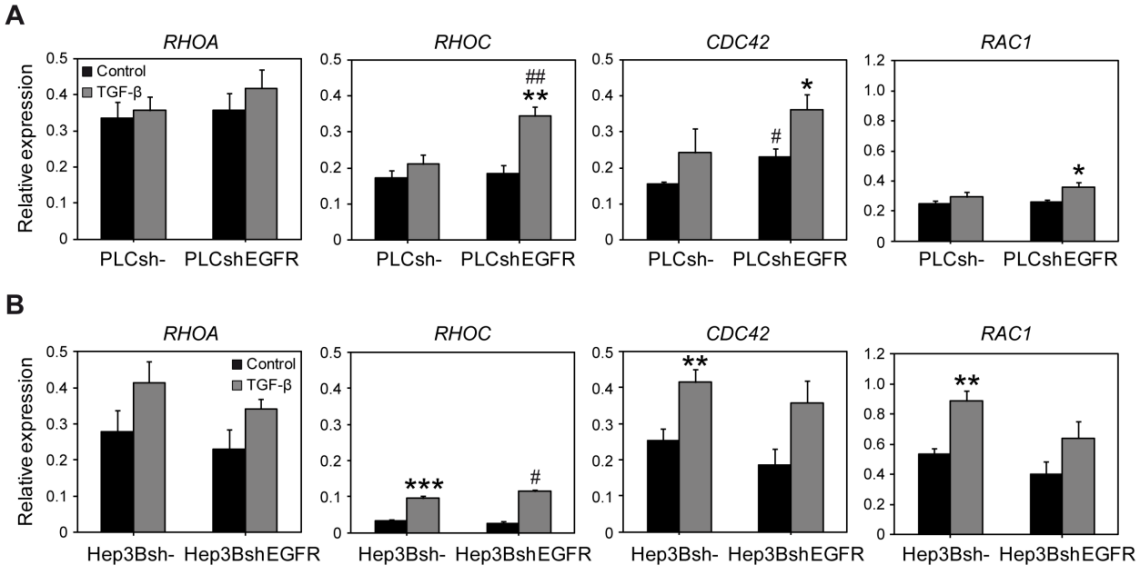

Figure 45. Rho GTPases transcriptional levels are regulated after TGF-β and EGFR silencing. qRT-PCR analysis of RHOA (*RHOA*), RHOC (*RHOC*), CDC42 (*CDC42*) and Rac1 (*RAC1*) mRNA levels in unsilenced and EGFR silenced PLC/PRF/5 **(A)** and Hep3B cells **(B)** after 72 hours of TGF-β treatment (2ng/mL) when cells were cultured on plastic. Data in A and B are mean ± SEM of 3 independent experiments. Student's *t* test was used: *p<0.05, **p<0.01 and ***p<0.001 compared to control untreated cells in each cell line (unsilenced or silenced); #p<0.05 compared to unsilenced cells in each condition (untreated or treated).

2.3.6. EGFR silencing increases TGF-β-induced migration in PLC/PRF/5, but not in Hep3B cells

Taking into account all the changes observed after EGFR silencing and TGF-β treatment in terms of EMT markers, cell-to-cell contacts, actin cytoskeleton organization, cell-to-matrix adhesion and contractility, we asked whether this was having a direct impact on the migratory capacity of both HCC cell lines. To achieve this purpose, we decided to perform a migration assay through the xCELLigence System. Results showed that EGFR silencing *per se* did not provoke a significant increase in the migration capacity in any of the cell lines. However, in the case of PLC/PRF/5 after TGF-β treatment, EGFR silenced cells acquired a high migratory capacity, being significant the differences compared to unsilenced cells (**Figure 46A**). Interestingly, in the case of Hep3B, TGF-β treatment was not able to increase the migratory

capacity after EGFR silencing (Figure 46B). In order to discard that this different effect found in Hep3B could be due to the absence of FBS in the upper chamber of the xCELLigence System where the cells are seeded **(see Material and Methods, Section 11, for more details)**, we performed a control experiment: we compared the established conditions to a different one where 10% of FBS was used in the upper chamber and 100% in the lower one. We observed the same pattern of migration in Hep3B cells upon TGF-β treatment and EGFR silencing, although the migratory capacity was increased in all the cases compared to the established conditions. This excluded the fact that lack of FBS could induce increased TGF-β-induced cell death that would compromise the migratory capacity of the cells (Figure 46C).

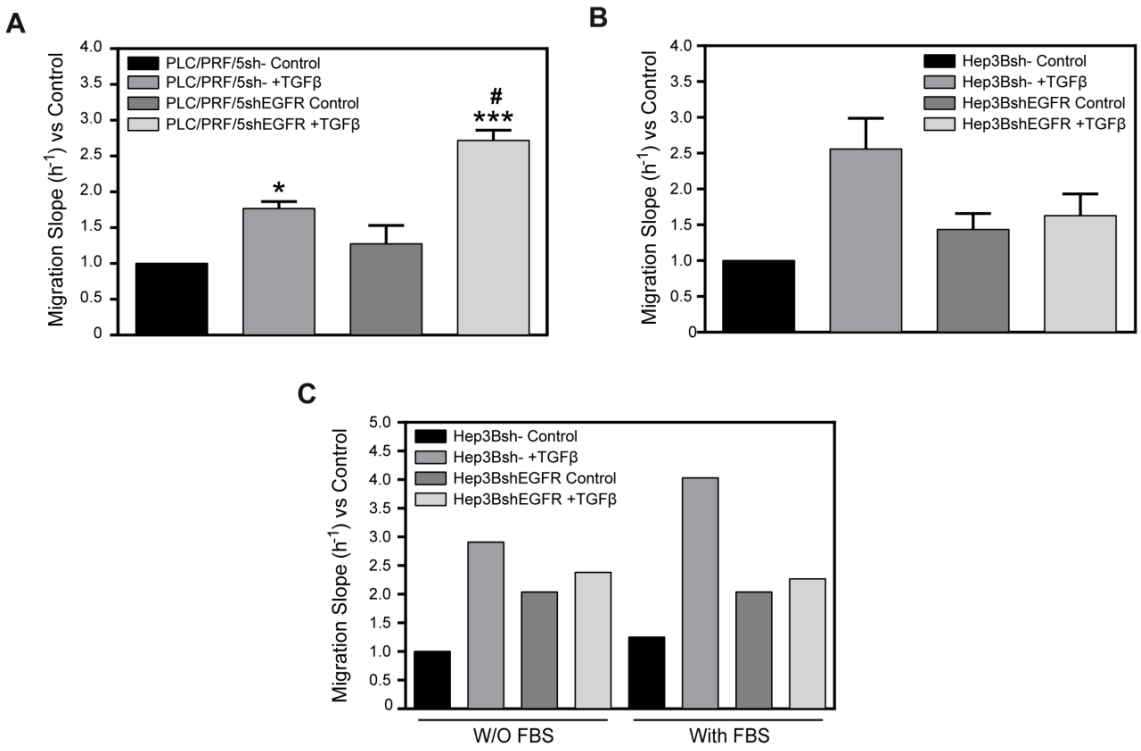

Figure 46. Stable silencing of EGFR induces a higher migratory capacity in PLC/PRF/5, but not in Hep3B, after TGF-β treatment. Unsilenced and EGFR silenced PLC/PRF/5 **(A)** and Hep3B **(B)** cells were treated with TGF-β (2ng/mL) during 64 hours, then trypsinized and plated in the xCELLigence system for a real time migration assay. Migration was then assessed during 8 hours, and it is expressed as relative to PLC/PRF/5 or Hep3B unsilenced and untreated cells. **(C)** The same migration assay was performed in Hep3B cells in the absence and presence of FBS in the upper chamber. Data in A and B are mean ± SEM of 3 independent experiments performed in biological quadruplicates. Student's *t* test was used: *p<0.05 and ***p<0.001 compared to control untreated cells in each cell line (silenced or unsilenced); #p<0.05 compared to unsilenced cells in each condition (treated or untreated).

Altogether these results suggest that in some HCC cells, EGFR may participate in the control of cell-to-cell contacts, cell-to-extracellular matrix adhesion and actomyosin contractility status, consequently acquiring different migratory capacity.

3. Translational relevance of the results obtained in objectives 1 and 2. Analysis in tumoral and non-tumoral tissues from HCC patients

We finally decided to examine the potential translational relevance of the previous results in a subset of HCC patients. Analysis of tissues from a cohort of 31 HCC patients from different etiologies, collected from surgeries in Bellvitge's Hospital by Dr. Emilio Ramos (co-director of the thesis), revealed that, in spite of the heterogeneity among HCC tumors, most tumoral tissues from HCC patients showed increased TGF-β expression and increased nuclear localization of phospho-Smad2 performed by immunohistochemistry, when compared with healthy or surrounding non-tumoral tissues (Figure 47). These results corroborate previous data (Giannelli et al., 2011; Murawaki et al., 1996), demonstrating that a relevant percentage of HCC tumors presents high levels of TGF-β.

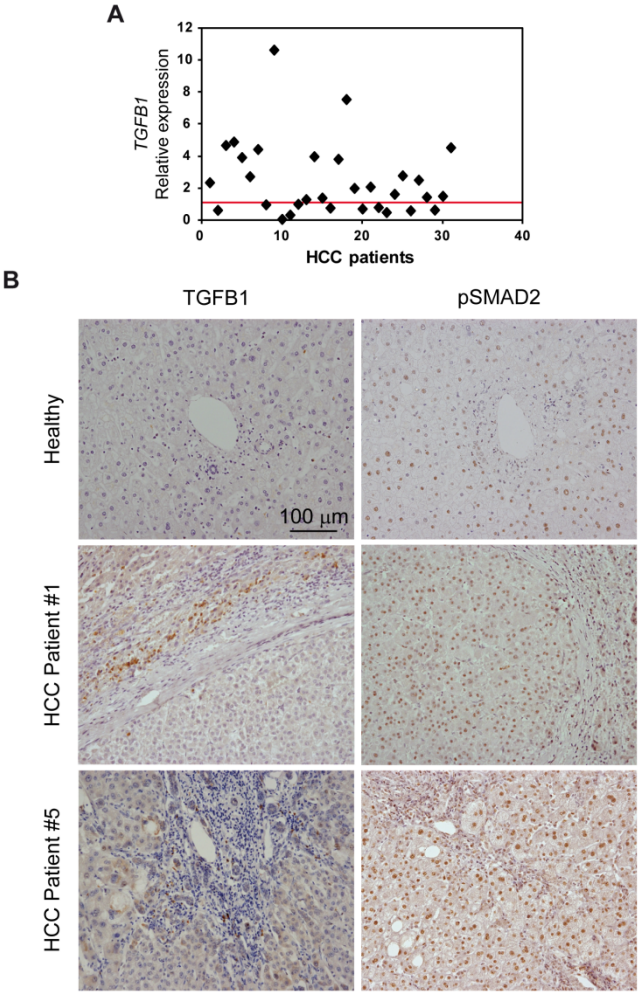

Figure 47. Activation of TGF-β pathway in tumor tissues from HCC patients. (A) *TGFB1* expression was analyzed by qRT-PCR and relative expression of each HCC tumor tissue *versus* its respective surrounding tissue was calculated (n=31). Red line represents cut-off (relative expression = 1). **(B)** Immunohistochemical analysis of TGF-β1 and phospho-Smad2 of serial sections in two representative HCC patients (1 and 5), compared with healthy tissue. Representative 20x images are shown.

We then moved to analyze *EGFR* expression in tumor and non-tumoral tissues from these HCC patients. Although the EGFR might be a relevant pathway involved in HCC, we observed that most of the tumor tissues presented lower *EGFR* expression levels than the surrounding non-tumoral tissue (**Figure 48A**). To extent the analysis to a higher number of patients, we used the Mas Liver database (n=115) from Oncomine (https://www.oncomine.org/). We found that HCC patients express lower *EGFR* mRNA expression when compared with normal tissue, in accordance with our data (**Figure 48B**), and also when comparing with cirrhotic patients. To complete the analysis, we used the TCGA database (n=212), from Oncomine as well, to look for changes in the number of copies in the *EGFR* locus. Surprisingly, we found higher *EGFR* DNA copy number in HCC patients compared with normal analysis (**Figure 48C**). We have no explanations for the lack of correlation between gene copy number and expression, but the fact that the *EGFR* expression could be lower in a great number of HCC tumors reinforces the relevance of our *in vitro* study. We next examined correlations between the changes in the expression of *TGFB1* and the *EGFR* genes in our cohort of HCC patients, but no correlation was found, indicating that the changes in the expression of both genes could be independent phenomena (**Figure 48D**).

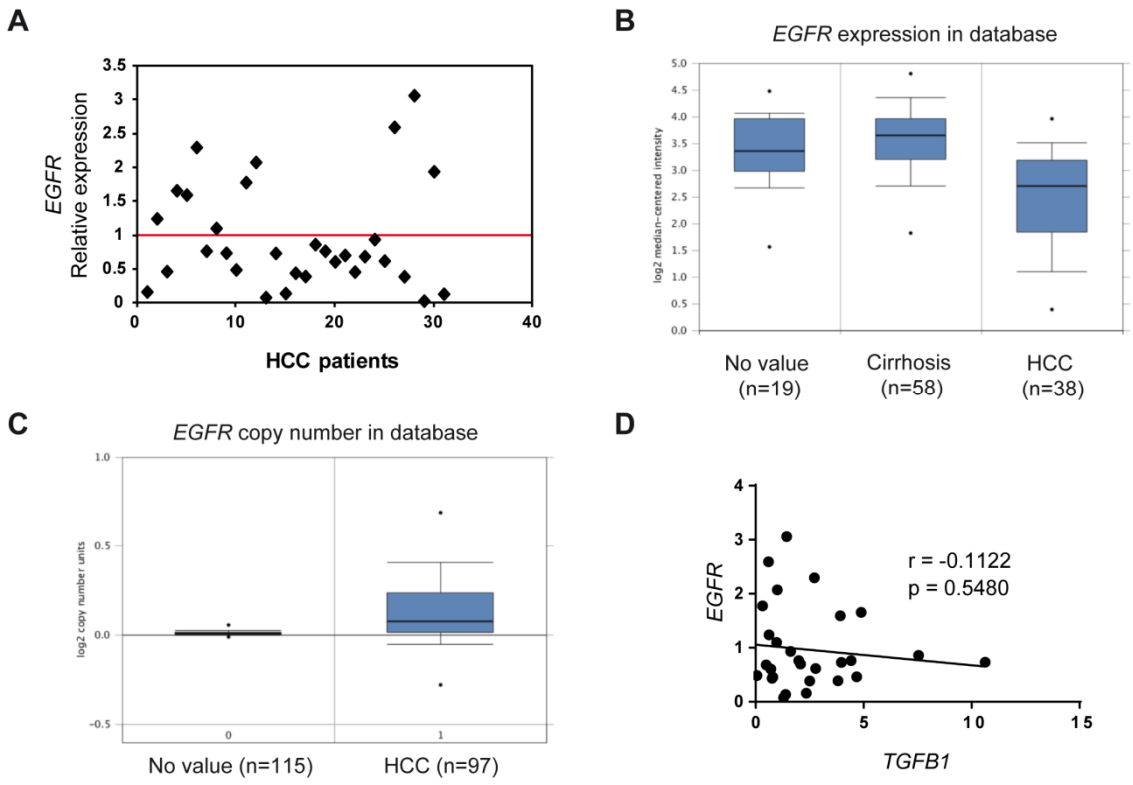

Figure 48. Tumoral tissue from HCC patients showed low *EGFR* expression. Absence of correlation between *TGFB1* and *EGFR* in samples from HCC patients. (A) *EGFR* expression was analyzed by qRT-PCR and relative expression of each HCC tumor tissue *versus* its respective surrounding tissue was calculated (n=31). Red line represents cut-off (relative expression = 1). **(B)** *EGFR* mRNA expression in the Mas Liver database from Oncomine (n=115). **(C)** *EGFR* copy number in the TCGA database from Oncomine (n=212). **(D)** Pearson correlation analysis among *TGFB1* and *EGFR* expression analyzed by qRT-PCR in the cohort of 31 samples from HCC patients. Each dot represents relative expression of each HCC tumor tissue *versus* its respective surrounding tissue.

With the aim of translating the *in vitro* observations to HCC patients, we decided to study E-cadherin (*CDH1*) as an epithelial marker, and vimentin (*VIM*) as a mesenchymal one. Most HCC patients showed low levels of *CDH1*, although it was not related to high or low *EGFR* expression, excluding that changes in *CDH1* expression are closely associated to *EGFR* expression (Figure 49A). However, regarding *VIM*, we observed that most samples from HCC patients presented high *VIM* expression and, interestingly, the percentage of them with *VIM* above the cut-off is higher in HCC patients with low *EGFR* (Figure 49B).

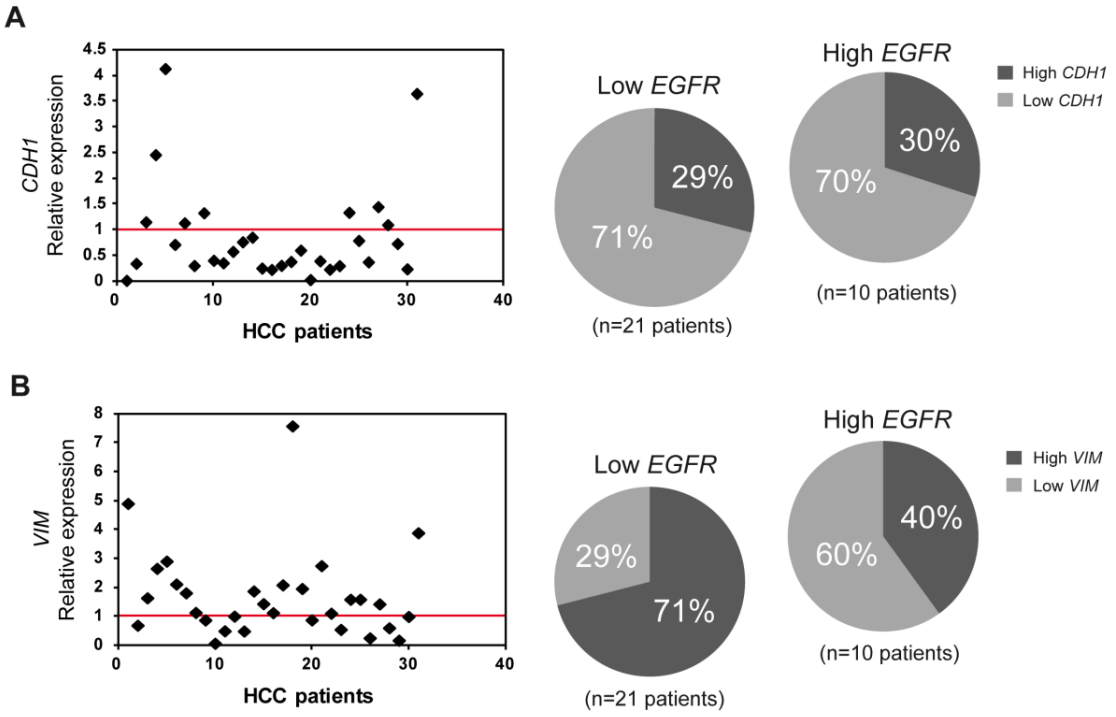

Figure 49. Vimentin (*VIM*), but not E-cadherin (*CDH1*), appears associated to low *EGFR* expression in samples from HCC patients. *CDH1* **(A, left)** and *VIM* **(B, left)** expression was analyzed by qRT-PCR and relative expression of each HCC tumor tissue *versus* its respective surrounding tissue was calculated (n=31). Red line represents cut-off (relative expression = 1). Percentage of patients with high or low relative expression of *CDH1* **(A, right)** and *VIM* **(B, right)** depending on high or low *EGFR* expression.

Moreover, as mentioned above, most HCC patients presented high *TGFB1* expression (Figure 47), which let us to consider to stratify patients taking into account only the ones with high *TGFB1* expression. A detailed analysis showed some patients, like Patient#01, presenting low *EGFR* expression, concomitantly with low *CDH1* and high *VIM* expressions, while others, like Patient#05, presented high expression of *EGFR*, concomitantly with high *CDH1* and high *VIM* expressions (Figure 50A). Immunohistochemistry of E-cadherin revealed different structure of the tumoral tissue among the patients that expressed higher and lower levels of E-cadherin. Given this fact, we decided to make a detailed individual analysis and to classify them in high and low *EGFR* expression. Interestingly, upon stratification, we could then observe association between *CDH1* and *EGFR*, as high *EGFR* expression was related with a higher percentage of

patients presenting also high *CDH1* expression, and *viceversa* (Figure 50B). Regarding *VIM*, the association observed previously (Figure 49B) was even more clear when considering only HCC patients expressing high levels of *TGFB1* (Figure 50C). Nonetheless, it is very important to keep in mind that these are very preliminary results as the number of samples from HCC patients analyzed is insufficient to finally establish firmed correlations. Thus, a higher number of patients must be used to validate all these preliminary data. We are, in fact, continuing analyzing more patients.

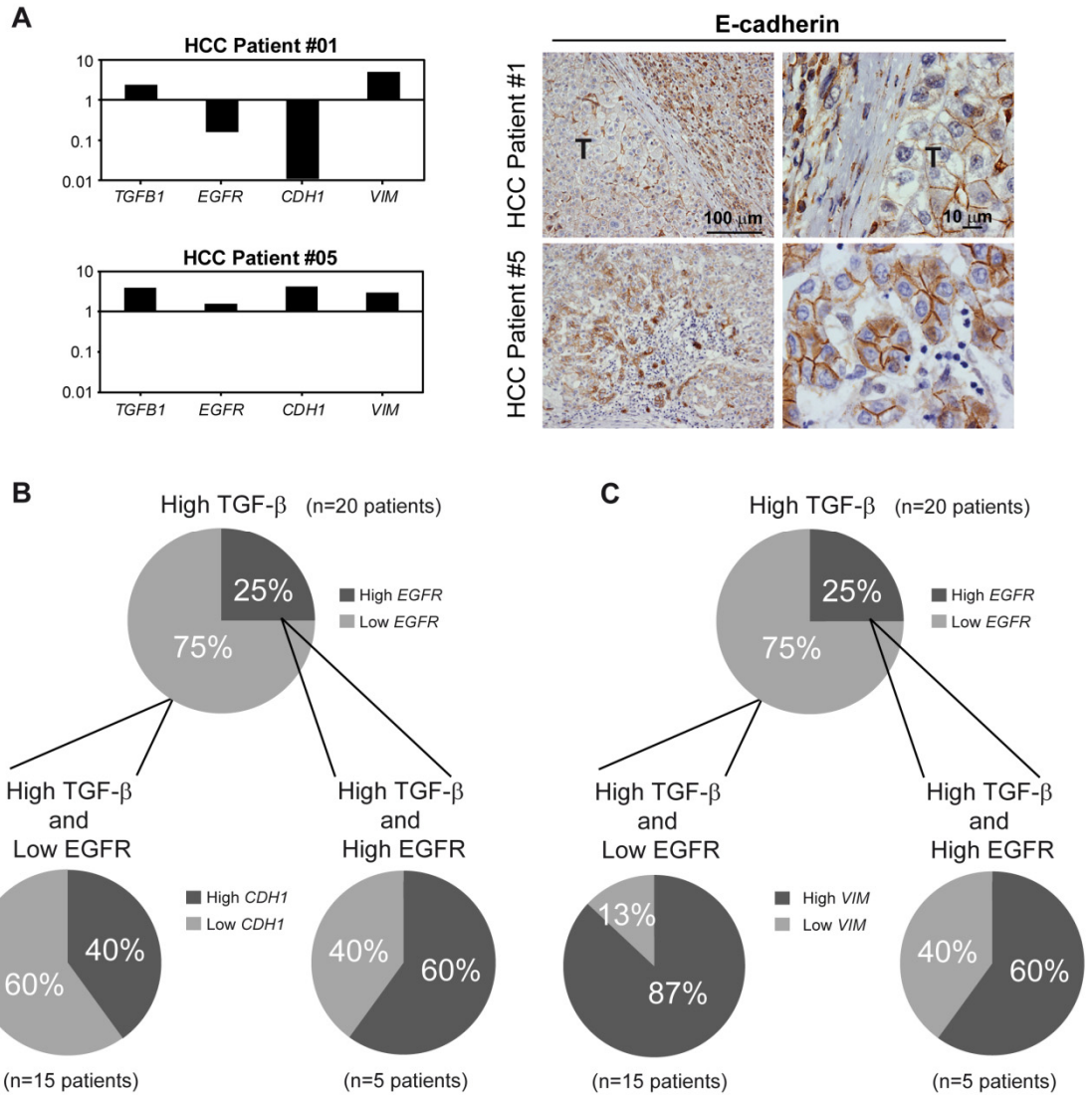

Figure 50. Selection of patients showing high *TGFB1* expression reveals association for both *CDH1* and *VIM* with *EGFR* expression (A) Left: Relative expression of *TGFB1, EGFR, CDH1* and *VIM* in 2 HCC patients (patient 1 and 5). Values are represented in a logarithmic scale for a better understanding of the changes observed. **Right:** Corresponding immunohistochemistry of E-cadherin of the previous 2 HCC patients. **(B and C, upper)** Considering only the patients with high *TGFB1* expression, we stratified them depending on their *EGFR* expression. A second analysis allowed to calculate the percentage of them with high or low relative expression of *CDH1* **(B, lower)** and *VIM* **(C, lower)**.

VI. DISCUSSION

HCC is the most often primary cancer of the liver and has fast become the second leading cause of cancer-related mortality worldwide (Bruix et al., 2014). In spite of the continuous achievements in new therapeutic approaches (such as radiofrequency ablation or chemotherapy) and in surgery techniques (such as liver transplantation and hepatic resection), patients with HCC have very poor prognosis (Connell et al., 2016; Grandhi et al., 2016). In fact, this is due to the recurrence in the appearance of new nodules or metastasis during liver regeneration after a hepatic resection or a chemotherapeutic treatment. This is the reason why it is very important to deeply study the molecular mechanisms related to liver regeneration and HCC and to find new biomarkers that could predict the response of each patient to a specific treatment approach. In that sense, EGFR and TGF-β pathways have been proposed as key players during liver regeneration and in many types of cancer such as HCC. However, there are still some undiscovered roles under their crosstalk during liver physiology and pathology.

1. Role of the EGFR catalytic activity during liver regeneration and hepatocarcinogenesis. Crosstalk with the TGF-β pathway

The purpose of the first part of the thesis was to study the crosstalk between the EGFR and TGF-β pathways *in vivo*, focusing in elucidating the specific role of the EGFR catalytic activity in a physiological (liver regeneration) and a pathological (hepatocarcinogenesis) situation of the liver, where proliferation of adult hepatocytes takes place. Results demonstrate that although EGFR signaling plays crucial roles in these processes, its absence only results in an overall **delay in both regeneration and carcinogenesis**, suggesting the existence of at least partial functional compensation by alternative routes.

First of all, we propose an essential role for EGFR in the **early phases of the regenerative response after PH** in mice, mediating a fast and efficient process. In a previous study, Natarajan et al. (Natarajan et al., 2007) generated a mouse model carrying a floxed *EGFR* allele to inactivate the EGFR in the adult liver. They proposed that EGFR is a critical regulator of hepatocyte proliferation in the initial phases of liver regeneration. We also observe this result in our animal model but, moreover, we associate these effects with the catalytic activity of the EGFR and provide new insights about the molecular mechanisms by which this occurs, particularly by observing an overactivation of the TGF-β pathway and alterations in lipid metabolism.

Inactivation of TGF-β signaling in hepatocytes results in an increased proliferative response after PH (Oe et al., 2004; Romero-Gallo et al., 2005). One of the main effects of TGF-β in liver cells is the induction of apoptosis through upregulation of *Bim* and *Bmf*, pro-apoptotic members of the Bcl-2 family. The EGF pathway counteracts TGF-β pro-apoptotic effects by impairing upregulation of both genes and upregulating *BclxL* and *Mcl-1*, two anti-apoptotic members of the Bcl-2 family (Caja et al., 2011a; Fabregat et al., 2000), an effect mediated by survival signals such as the PI3K/Akt and ERK pathways. However, in this work we cannot observe differences in terms of apoptosis, suggesting that the major role of EGF during liver regeneration after PH is not cell survival, probably because apoptosis is not relevant in a model where there is no hepatocyte damage. In contrast, the decrease and delay in the activation of the PI3K/Akt and ERK pathways at early times after PH in ΔEGFR animals, concomitant with high expression of the cyclin-dependent kinase inhibitor $p15^{INK4B}$ (*Cdkn2b*), suggest a relevant role for the EGFR pathway in priming hepatocytes to enter into the cell cycle. The delay could be related, at least partially, to the overexpression of *Tgfb1* and **overactivation of the TGF-β pathway** observed in animals with attenuated EGFR signaling. It is known that TGF-β expression increases rapidly after PH and it remains elevated until the end of regeneration (Braun et al., 1988). However, its inhibitory effects are surpassed in the regenerating liver by downregulation of TGF-β receptors (Chari et al., 1995), increasing the transcriptional repressors

SnoN and *Ski*, which antagonize TGF-β signaling (Macias-Silva et al., 2002), as well as being removed and inactivated through binding α-2-macroglobulin in the circulation (Arandjelovic et al., 2003; LaMarre et al., 1991). Although initially it was supposed that TGF-β could play a relevant role in mediating termination of liver regeneration, given its mito-inhibitory properties and its upregulated expression as regeneration advances, more recent results indicated that it is not necessary during this stage (Oe et al., 2004). In contrast, a higher and accelerated DNA synthesis peak after PH was found in a *Tgfbr2* knockout (R2LivKO) animal model, which presented a normal ending of liver regeneration, as other signals can contribute to it (Oe et al., 2004). Thus, in contrast to previous hypothesis, TGF-β could play an essential role in the first stages of liver regeneration, and EGFR pathway may be essential in regulating its expression and signaling.

Recently, oxidative stress is becoming crucial for many physiological and pathological processes, as reactive oxygen species (ROS) are known to regulate many different pathways. **NADPH oxidases (NOXes)** produce ROS, being involved in the regulation of cell growth, differentiation and death. Hepatocytes and liver tumor cells express *NOX1* and *NOX4* that play opposite roles in the control of cell proliferation and death in *in vitro* experiments. *NOX4* is transcriptionally upregulated by TGF-β, mediating apoptosis, and EGFR pathway counteracts this effect, acting at the transcriptional level on the *NOX4* promoter, impairing cell death (Caja et al., 2011a; Carmona-Cuenca et al., 2008; Sancho et al., 2009). By contrary, NOX1 is involved in regulating autocrine growth and protecting cells from TGF-β-induced pro-apoptotic signals, since it activates EGFR pathway. Furthermore, EGFR upregulates *NOX1* and also activates it, creating a loop of co-activation among the two pathways (Moreno-Càceres et al., 2016; Sancho and Fabregat, 2010). We found opposite regulation of Nox1 and Nox4 during liver regeneration after PH in mice. In fact, we have recently demonstrated that NOX4 negatively controls hepatocyte proliferation and its expression is downregulated during liver regeneration after PH in mice (Crosas-Molist et al., 2014). As ΔEGFR animals also presented a downregulation of Nox4 after PH as well as WT mice, it might indicate that other alternative pathways, not only EGFR, may contribute to its decrease. In this sense, it has been described that HGF may downregulate *NOX4* (Clavijo-Cornejo et al., 2013) and counteract TGF-β-induced *NOX4* upregulation (Martínez-Palacián et al., 2013). However, upregulation of Nox1 was delayed and attenuated in ΔEGFR mice, which indicates that this NADPH oxidase is target of the EGFR pathway in the liver and other signals are not so efficient in regulating its expression.

It is well known that after PH hepatocellular fat accumulation occurs, concomitant with upregulation of genes related to the adipogenic program (Shteyer et al., 2004), which has been suggested to be a mammalian target of rapamycin–dependent process (Obayashi et al., 2013). Increased *de novo* hepatic fatty acid production and catabolism of systemic adipose tissue might be the main sources of the lipid that accumulates in the regenerating liver. It is required to meet the increased energy demand for rapid cell proliferation and it is essential for the enhanced biosynthesis of membrane phospholipids during liver regeneration (Rudnick and

Davidson, 2012). Disruption of hepatic adipogenesis and lipid accumulation is associated with impaired or inefficient liver regeneration following PH (Kohjima et al., 2013; Shteyer et al., 2004). Interestingly, it has been found that EGFR plays a role in the regulation of liver and plasma lipid levels in adult male mice (Scheving et al., 2014). Our results show for the first time that EGFR pathway is required for **fat accumulation** and properly **regulation of key enzymes** related to the ***de novo* lipid synthesis** during liver regeneration. Recently, these results have been corroborated by Michalopoulos' group (Paranjpe et al., 2016), where they also observe a suppression of many enzymes associated with fatty acid synthesis when inhibiting EGFR. Moreover, they emphasize and corroborate our proposed dominant role of EGFR, but not MET, in the regulation of Acetyl-CoA Carboxylase. In addition, it has been described that sequential waves of hepatocyte proliferation are linked with hepatic fat accumulation waves during liver regeneration after PH (Zou et al., 2012). We observe this link in our model, as the delay in hepatocyte proliferation in ΔEGFR animals is coincident with the absence of this temporary hepatic fat accumulation, although we could not know if it is the cause or the consequence of this alteration. Further studies will be required to determine the precise EGFR molecular mechanisms mediating these effects during liver regeneration.

However, in spite of these alterations, most of the ΔEGFR mice survive to PH and no significant differences are observed in serum parameters related to liver injury or in the liver to body mass ratio. However, a higher mortality is seen in the first 48 hours after PH, as it was also suggested by Natarajan et al. in the mice carrying a floxed *EGFR* (Natarajan et al., 2007), but differences were not statistically significant. Our results are in agreement with a previous work of Michalopoulos's group, where the consequences of *in vivo* EGFR silencing on rat liver regeneration using EGFR-specific short hairpin RNAs were analyzed (Paranjpe et al., 2010). Despite suppression of hepatocyte proliferation, liver restoration occurred. Interestingly, **hepatocytes** in short hairpin EGFR–treated rats were considerably **larger** compared with short hairpin RNA-treated controls, an effect that we also observe in the ΔEGFR animals. In fact, the inhibition of cell cycle progression during liver regeneration has been shown to result in enlarged hepatocytes (Diril et al., 2012; Haga et al., 2005; Minamishima et al., 2002). In contrast to the work performed with shEGFR-treated rats, we do not find compensatory increases in the expression of *ErbB2* or *ErbB3*. Hypothetically, this could be due to the difference between the models. In the one from Michalopoulos' group, the shRNA contributes to the decrease of the protein levels of EGFR, which could promote compensation through the expression of other members of the family. In our model, the expression of endogenous EGFR is not affected, and the transgene expresses a truncated form that acts as a dominant negative decreasing only the catalytic active EGFR pathway.

However, we show that ΔEGFR mice presented **higher phosphorylation levels of c-Met** that could compensate the lack of EGFR-mediated proliferative signals, a possibility that was also suggested in the shEGFR-treated rats model (Paranjpe et al., 2010). Interestingly, we demonstrate **upregulation** not only of the **expression of *Hgf*** in ΔEGFR livers after PH but also

of its activator *uPA (*urokinase plasminogen activator*)*, whose deficiency was shown to retard liver regeneration by impairing HGF pathway (Shimizu et al., 2001). In this sense, the very recent above mentioned work of Michalopoulo's has demonstrated that only the combined elimination of Met (METKO) and the inhibition of the EGFR signaling pathway (with the EGFR inhibitor Canertinib) completely abolishes liver regeneration. In this work, they state that both pathways separately control many non-overlapping critical points, and the inhibition of only one of them had distinct alterations in different signaling pathways, allowing for compensation when only one of the signals is blocked (Paranjpe et al., 2016). Thus, even though the HGF/Met pathway is clearly overactivated in ΔEGFR animals, some EGFR functions seem not to be compensated by c-Met. In particular, early activation of PI3K/Akt and ERK signaling would require EGFR signaling. Interestingly, Factor et al. elegantly demonstrated that c-Met signaling in hepatocytes is essential for sustaining long-term ERK1/2 activation throughout liver regeneration, although alternative pathways may account for the early ERK1/2 activation (Factor et al., 2010). Thus, although different studies define c-Met as the main player in regenerating liver (Borowiak et al., 2004; Huh et al., 2004), other studies have shown that lack of EGFR signaling in *EGFR* mutant livers blocked G_1/S transition (Natarajan et al., 2007), emphasizing the requirement of simultaneous co-activation of parallel signaling pathways for full mitogenic signaling and efficient liver regeneration. Furthermore, our work show that compensation of the cytostatic effects of the TGF-β pathway and regulation of lipid metabolism after PH appear to be fully dependent on EGFR, and may be necessary for a more efficient liver regeneration but dispensable for restoring liver mass in the animals that survive the first hours after PH. In agreement with these results, lack of Nogo-B (reticulon 4B) produces overactivation of TGF-β pathway after PH in mice, coincident with a delay in hepatocyte proliferation, but did not affect the liver to body mass ratio in the regenerative process (Gao et al., 2013).

Cytokines like TNF-α and IL-6 are known to play a significant role in the early phases of liver regeneration, when the "priming" of hepatocytes takes place (Riehle et al., 2011). Lack of an early increase in both cytokines in ΔEGFR animals could also explain the delay in the entry of hepatocytes in G_1 phase. Moreover, **Cyclin D1** is required for G_0/G_1 transition of the cell cycle (Hinz et al., 1999) and, in contrast to other similar studies (Natarajan et al., 2007; Paranjpe et al., 2010), we do not observe a reduced and delayed expression in ΔEGFR mice after PH. On the contrary, high levels were maintained for longer times, which correlates with the delayed peak in proliferation in those animals, concomitant with a delay in Cyclin A2 (*Ccna2*) and B2 (*Ccnb2*) mRNA expression. Interestingly, higher basal levels of Cyclin D1 in ΔEGFR livers were also observed by Michalopoulo's et al. in mice treated with an EGFR inhibitor (Paranjpe et al., 2016). One hypothesis that could explain this observation is that higher TNF-α (*Tnfa*) expression levels under basal conditions in ΔEGFR livers could be leading to c-Jun expression and activation (Cienfuegos et al., 2014), which it has been shown to directly regulate Cyclin D1 (*Ccnd1*) expression in fibroblasts (Wisdom et al., 1999). However, in our model, overactivation of the TGF-β pathway increases $p15^{INK4B}$ (*Cdkn2b*) expression at short

times. This CDKI might be counteracting Cyclin D1 activity, pushing the balance towards a delay in the early proliferative response of ΔEGFR hepatocytes to PH. Another hypothesis for the sustained expression of Cyclin D1 during liver regeneration in ΔEGFR animals could be the increased levels of *Hgf*. It is known to induce the Janus Kinase (JAK) pathway, which activates transcription factors such as STAT-3 and NF-κB, able to stimulate the transcription of *Ccnd1*. Moreover, also HGF has been described to induce β-catenin translocation to the nucleus (Monga et al., 2002), where it can induce *Ccnd1* expression (Shtutman et al., 1999). However, in this case, high levels of $p21^{CIP1}$ (*Cdkn1a*) at short and later times could slow the proliferation during the entire regenerative process.

We also show here that attenuation of EGFR catalytic activity induces a significant **delay in the appearance of tumorigenic lesions in DEN-treated animals**. However, once tumors appear, the proliferative rate is similar in ΔEGFR and WT animals. Surprisingly, no significant differences are observed in the TGF-β pathway, or in the expression of apoptosis or cell cycle regulatory genes (data not shown), which could justify the delay in tumorigenesis. However, the delay in the appearance of tumors is coincident with a significant change in mRNA levels of *Nox4* in non-tumoral areas, where it is upregulated. This observation is in accordance to recent results published by Crosas-Molist et al., where NOX4 protein levels are lower in samples from HCC patients; furthermore, NOX4 negatively modulates liver tumor cell proliferation (Crosas-Molist et al., 2014). Thus, in this process, EGFR catalytic activity is not controlling *Tgfb1* expression, maybe no Smads phosphorylation, but could act on other downstream pathways that regulate *Nox4* expression. However, the more significant difference lies in the appearance of pre-neoplastic lesions. In agreement with this result, a previous study using gefitinib (an EGFR inhibitor) in DEN-induced hepatocarcinogenesis in mice revealed that the gefitinib-treated animals showed significantly lower numbers of HCC nodules but that the mean tumor size was not different between untreated and gefitinib-treated mice (Schiffer et al., 2005). Similar to what was found during liver regeneration, levels of *Hgf* are much higher in ΔEGFR animals (data not shown), which suggests that this cytokine might replace the mitogenic function of the EGFR ligands.

Parallel studies in our group have indicated that the delay in the appearance of tumoral lesions might be associated with **attenuation of the inflammatory process.** EGFR signaling has been proposed as a critical junction between inflammation-related signals and potent cell regulating machineries (Berasain et al., 2009). Our results indicate differences in the expression of IL-6 (*Il6*) and TNF-α (*Tnfa*) in the tumor surrounding tissue, which suggests that the transgene expression in hepatocytes affects the production of inflammatory cytokines by themselves or other surrounding cells. Interestingly, the EGFR pathway plays an essential role in liver macrophages to mediate the inflammatory process in DEN-induced HCC (Lanaya et al., 2014). Indeed, we cannot exclude that the overexpression of a truncated form of the EGFR that binds its ligands, but does not transduce the signal, may decrease the number of free EGFR ligands able to act on the non-parenchymal cells. Regardless of the mechanism and

considering together our results and others in the literature, there is no doubt that one of the most essential functions of the EGFR pathway during hepatocarcinogesis should be regulation of inflammation addressed by parenchymal and/or non-parenchymal cells.

In conclusion, ΔEGFR transgenic mouse model might be useful in deciphering the molecular mechanisms underlying the functions of EGFR signaling in the adult liver, in particular the ones specifically related to its tyrosine kinase-dependent functions in liver regeneration and carcinogenesis. Moreover, our results evidence the crosstalk between the EGFR and the TGF-β pathways in an *in vivo* model, providing new molecular mechanisms in adult hepatocytes for these two pathways.

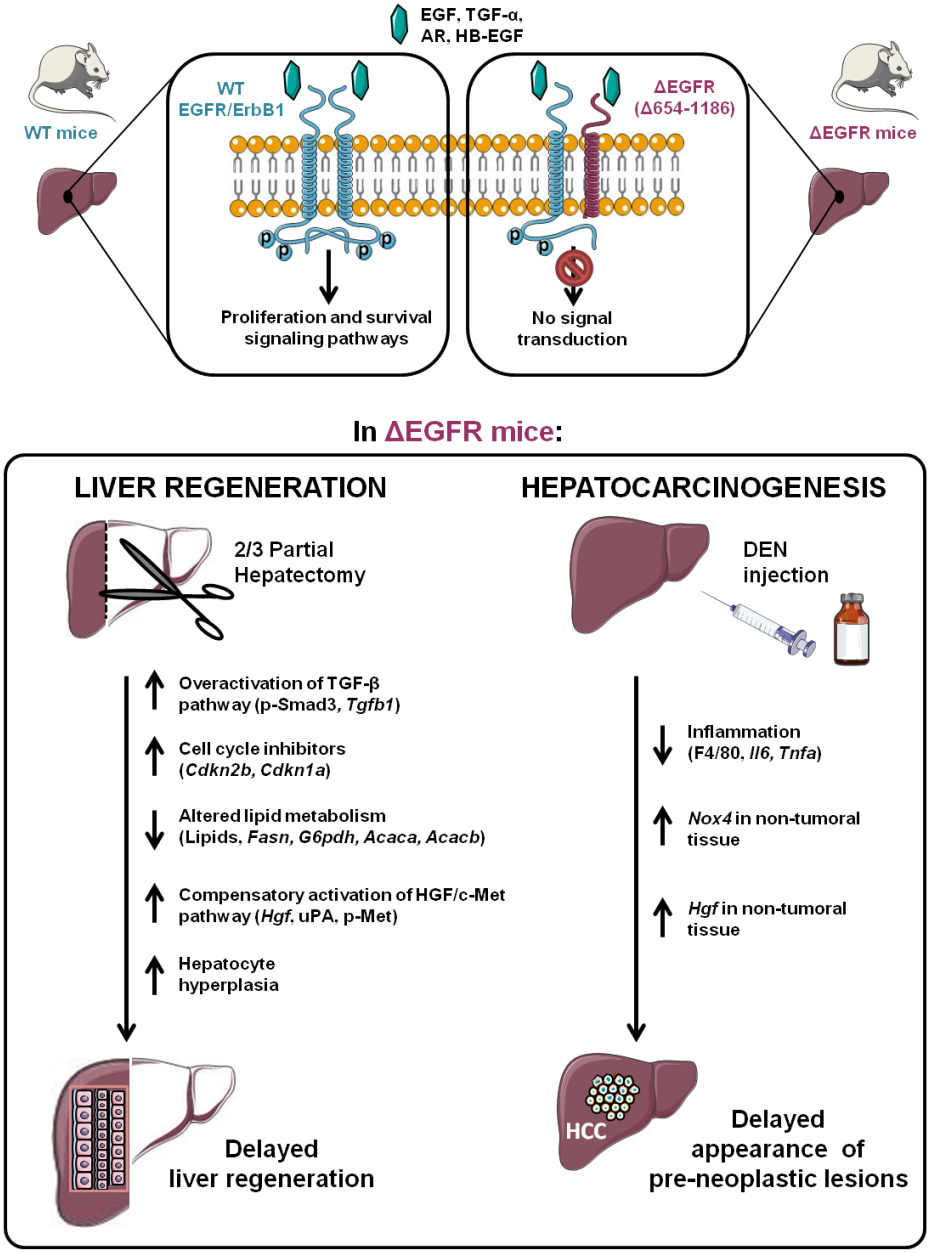

Figure XXII. Implications of ΔEGFR transgene expression in mice during liver regeneration after partial hepatectomy and DEN-induced hepatocarcinogenesis (Graphical abstract performed with Servier Medical Art).

2. Crosstalk between the TGF-β and EGFR pathways in the regulation of cell adhesion and migration of HCC cells

There is clear evidence that TGF-β is a liver tumor suppressor. However, tumor cells that overcome TGF-β suppressor effects become susceptible to respond to this cytokine inducing other effects that contribute to tumor dissemination (Moustakas and Heldin, 2012). Different studies have identified **overexpression of TGF-β in HCC**, which correlates with tumor progression and bad prognosis (Coulouarn et al., 2008). In our group, it has been described that overactivation of TGF-β pathway differs among different HCC cell lines tested and a strong correlation between TGF-β overactivation and mesenchymal-like and migratory phenotypes is observed (Bertran et al., 2013). This behavior permitted a classification according to the TGF-β signature proposed by C. Coulouarn (Coulouarn et al., 2008) in our used cell lines: early for PLC/PRF/5, late for SNU449, and an intermediate phenotype for Hep3B.

To spread within the tissues, tumor cells use migration mechanisms that are similar, if not identical, to those that occur in normal, non-neoplastic cells during physiological processes (Friedl and Wolf, 2003). Multiple environmental factors, such as chemokines, cytokines like **TGF-β,** and growth factors like **EGF**, can induce and regulate **tumor-cell motility**, thereby contributing to invasion. Actin cytoskeleton rearrangements, regulated mainly by Rho GTPases, play a crucial role in these events (Stanley et al., 2014). However, depending on the cell type and tissue environment, cells can migrate individually, when cell-to-cell junctions are absent, or collectively as strands, sheets or clusters, when cell-to-cell adhesions are retained (Friedl and Wolf, 2003). In this work, we studied the effect of TGF-β treatment on different HCC cell lines to determine the different types of movement. We observe that it increases the formation of stress fibers in all the cell lines analyzed. TGF-β provokes a mesenchymal-like migration in Hep3B cells, as we observe an individual elongated spindle-like shape, and the appearance of protrusions, such as lamellipodia and membrane ruffles at the leading edge. These protrusions are known to be actin-rich structures resulting from a localized activation a GTPases in some tumors like melanoma (Sanz-Moreno et al., 2008). The loss of cell-to-cell contacts inducing an individual migration upon TGF-β treatment was already observed by our group in human fetal hepatocytes, concomitant with reorganization of the actin cytoskeleton in stress fibers (Caja et al., 2011b). Also, it has been described that TGF-β induces rearrangements of the actin filament system in other cancers (Edlund et al., 2002). In contrast, in SNU449 and PLC/PRF/5, TGF-β treatment induces also the presence of cells with a rounded shape, and the formation of more stress fibers organized in a cortical ring around the cell, which let us to think about an ameboid-like migration. Thus, although TGF-β is well known to promote epithelial-to-mesenchymal transition (EMT) and contribute to metastasis in this way, our results demonstrate that it can also induce an ameboid-mode of migration, which was already proposed in melanoma cells (Cantelli et al., 2015). Interestingly, in the case of PLC/PRF/5, TGF-β is also able to maintain cluster structure of some cells contributing to a mixed phenotype in the cell culture, which

maintain cell-to-cell junctions and apparently facilitating its migration as cohorts, which was also observed by U. Hibner in a highly differentiated mouse hepatocyte cell line (Binamé et al., 2008). This phenomenon has been observed in other cellular contexts, such as in ovarian cancer (Gao et al., 2014) or in epithelial sheets of keratinocytes (Chapnick and Liu, 2014). Thus, TGF-β is able to induce diverse types of migration in HCC cells, which might be differently regulated.

It is known that EGFR system plays an essential role in cell proliferation, survival and migration and its altered activity has been implicated in the development and growth of many tumors including HCC. Interestingly, results presented here show that **EGFR** is also implicated in the maintenance of **cell-to-cell contacts** and **parenchymal structures** between HCC cells. It is observed an increase in the individualization or separation in PLC/PRF/5 and Hep3B cells, together with a disruption of cell-to-cell adhesion analyzed by E-cadherin and ZO-1, effect that is accentuated upon TGF-β treatment. In fact, it has been described by Erasmus et al. that EGFR co-precipitated with E-cadherin in keratinocytes when cell-to-cell junctions are formed, and in the absence of EGFR these cell-to-cell contacts are abolished (Erasmus et al., 2015). They observed that EGFR is necessary for actin recruitment to cadherin clusters, which could be a hypothesis to explain the decrease of actin stress fibers in PLC/PRF/5 and Hep3B when silencing EGFR. Moreover, it has been shown in NIH 3T3 fibroblasts that EGFR activity is required for integrin-induced stress fiber formation (Marcoux and Vuori, 2005), and EGFR blockade with Erlotinib diminishes the amount of actin stress fibers and the stress fiber diameter in lens epithelial cells (Wertheimer et al., 2014).

As the **EMT process** implies a reduction in cell-to-cell contacts, these results suggest that the EMT program could be altered when silencing EGFR. Considering our results, in the case of Hep3B cells, the ones carrying out a full EMT after TGF-β treatment, we cannot observe any difference in terms of EMT markers after EGFR silencing, suggesting that EGFR is dispensable in the TGF-β-induced EMT. However, we can observe that PLC/PRF/5 cells, that undergo a partial EMT in response to TGF-β, show decreased expression of E-cadherin (*CDH1*), N-cadherin (*CDH2*) and vimentin (*VIM*) after EGFR silencing, although maintaining the potential to increase the expression of *VIM* upon TGF-β treatment. It has been described in the literature that TGF-β signaling switches breast cancer cells from cohesive to single cell motility (Giampieri et al., 2009), and that it is not necessarily related to a more mesenchymal phenotype in terms of EMT markers and transcription factors. In fact, they observed that although vimentin expression is modulated by TGF-β signaling, it was observed also in a significant proportion of non-motile cells and collective-moving cells. Thus, changes in *VIM* expression may merely indicate increased TGF-β signaling, and not that expression of mesenchymal markers mandatory drives the switch to single cell motility.

3D matrix are known to be much more interesting to study the different modes of tumor cell migration, mainly focusing on distinguishing between the two modes of individual movement:

the elongated-protrusive manner or the rounded, “ameboid” mode (Sanz-Moreno and Marshall, 2010). Results presented here reveal that silencing EGFR correlated with increased **actomyosin contractility**, showing PLC/PRF/5 highest levels of pMLC2, readout of actomyosin contractility, correlating with membrane blebbing, characteristic of an ameboid-type of migration. This effect is even increased upon TGF-β treatment. However, this is not clearly observed in Hep3B cells, where the levels of pMLC2 are lower and do not colocalize with blebs. It is known that this rounded “ameboid” type of movement is driven by high actomyosin contractility through Rho signaling, whilst Rac signaling is required for actin assembly in an elongated-protrusive movement (Sanz-Moreno and Marshall, 2010). Our results show that PLC/PRF/5 express higher levels of Rho, mainly *RHOC*, whilst Hep3B presented higher levels of *RAC1* under basal conditions. Thus, the differences in the basal expression of Rho GTPases could explain the different response that it is observed between PLC/PRF/5 and Hep3B. Moreover, it is well known that high actomyosin contractility and ameboid-like migration is related to a decrease in **cell-to-matrix adhesion** (Friedl and Alexander, 2011). In fact, low adhesion induce fast ameboid migration of slow mesenchymal cells (Liu et al., 2015). Results presented here show a decrease in the capacity of adhesion to different matrixes when silencing EGFR in the case of PLC/PRF/5, and TGF-β treatment maintained it at low levels. On the contrary, Hep3B do not show a decrease in cell-to-matrix adhesion after EGFR silencing, and TGF-β is able to increase it as well as in unsilenced conditions. Thus, all these observations may indicate an **ameboid-TGF-β-induced** type of migration when EGFR is silenced in PLC/PRF/5, but not in Hep3B.

The phenotypic changes observed in both HCC cell lines have an effect on the **migratory capacity**, as PLC/PRF/5 increase it after EGFR silencing and upon TGF-β treatment, although this is not observed in the case of Hep3B. Considering the plasticity between the different modes of migration, altogether our results suggest that EGFR counteracts the TGF-β-ameboid-induced migration in PLC/PRF/5 cells, as when the receptor is silenced almost all the cells change its migration towards an ameboid movement. Interestingly, in primary melanoma explants, interference with β1-integrin, which is involved in cell-to-matrix adhesion, induced complex changes in cluster polarity and cohesion, including cluster disruption, and the detachment of individual cells by β1-integrin-independent “ameboid” crawling and migration (Hegerfeldt et al., 2002). This mechanism pattern would be similar to the process that we observe when silencing EGFR, which decreases cell-to-matrix adhesion, and upon TGF-β treatment in PLC/PRF/5 cells. However, Hep3B cells undergo full EMT in response to TGF-β, and the genetic program initiated does not seem to require the EGFR, neither the EGFR is able to counteract it. In contrast to our findings, many studies emphasize the role of the ErbB receptor family in inducing EMT. For instance, in oral squamous cell carcinoma cells, inhibition of EGFR induced a transition from a fibroblastic morphology to a more epithelial phenotype (Lorch et al., 2004), suggesting that EGFR mediates the initial steps of EMT. Also, ligand-independent, constitutively active forms of EGFR can increase motility and invasiveness of tumor cells and EGFR inhibitors have been shown to inhibit cancer cell migration *in vitro* (Liu et al., 2014b; Yue et al., 2012). However, interestingly, a work from Schaeffer et al. states that

enhanced migration is not a phenotypic requirement of EMT and, moreover, that migration and invasion can be uncoupled during carcinoma-associated EMT. Actually, they demonstrate that EGFR would be required for an enhanced migration once the cells have undergone EMT (Schaeffer et al., 2014). These results together with our observations suggest that different and additional mechanisms are probably involved in TGF-β and EGFR activation effects on EMT and cell migration, and although EGFR is not required for a TGF-β-induced EMT program, it might be necessary for a TGF-β-mesenchymal-induced migration.

Overexpression of EGFR occurs in 68% of human HCC correlating with **more aggressive liver tumors**, metastasis and poor patient survival (Ito et al., 2001). The interplay between EGFR and other receptors or factors, such as TGF-β, localizes it as a signal integrator of multiple stimuli originated from the stroma and cancer cells themselves. As EGFR inhibitors have been used in HCC treatment in animal models, such as erlotinib or gefitinib, obtaining successful results (Fuchs et al., 2014; Höpfner et al., 2004; Schiffer et al., 2005), and their efficacy has been observed in other solid human tumors, it was thought that targeting it might be useful in human HCC. Surprisingly, only modest results could be obtained in clinical studies. Accordingly, our results can put a bit of light on it, as they show different behavior depending on the HCC cell line studied when EGFR is silenced. Thus, in PLC/PRF/5 cells, TGF-β would induce a partial EMT, upregulating expression of both epithelial and mesenchymal markers, but when EGFR is silenced a collective-to-ameboid transition (CAT) is observed and a more migratory phenotype. However, Hep3B cells undergo a full EMT in response to TGF-β, downregulating epithelial markers and upregulating mesenchymal ones, which does not seem to depend on *EGFR* expression. Nonetheless, when EGFR is silenced, TGF-β is not able to induce a more migratory phenotype, analyzed through real time migration in the xCELLigence system. Thus, it is necessary to deeply study the specific mechanisms through which EGFR correlates with more aggressive liver tumors, as EGFR can be driving or counteracting the pro-tumorigenic effects of TGF-β, in order to try to identify which patients are targetable for its inhibition or not.

Altogether, these results show an interplay between the EGFR and the TGF-β pathways in terms of migration in HCC cells, regulating cytoskeleton dynamics, cell-to-cell and cell-to-matrix adhesion as well as actomyosin contractility. However, these effects are different between the cell lines, showing heterogeneity among them, which must be considered when studying the different mechanisms underlying both pathways.

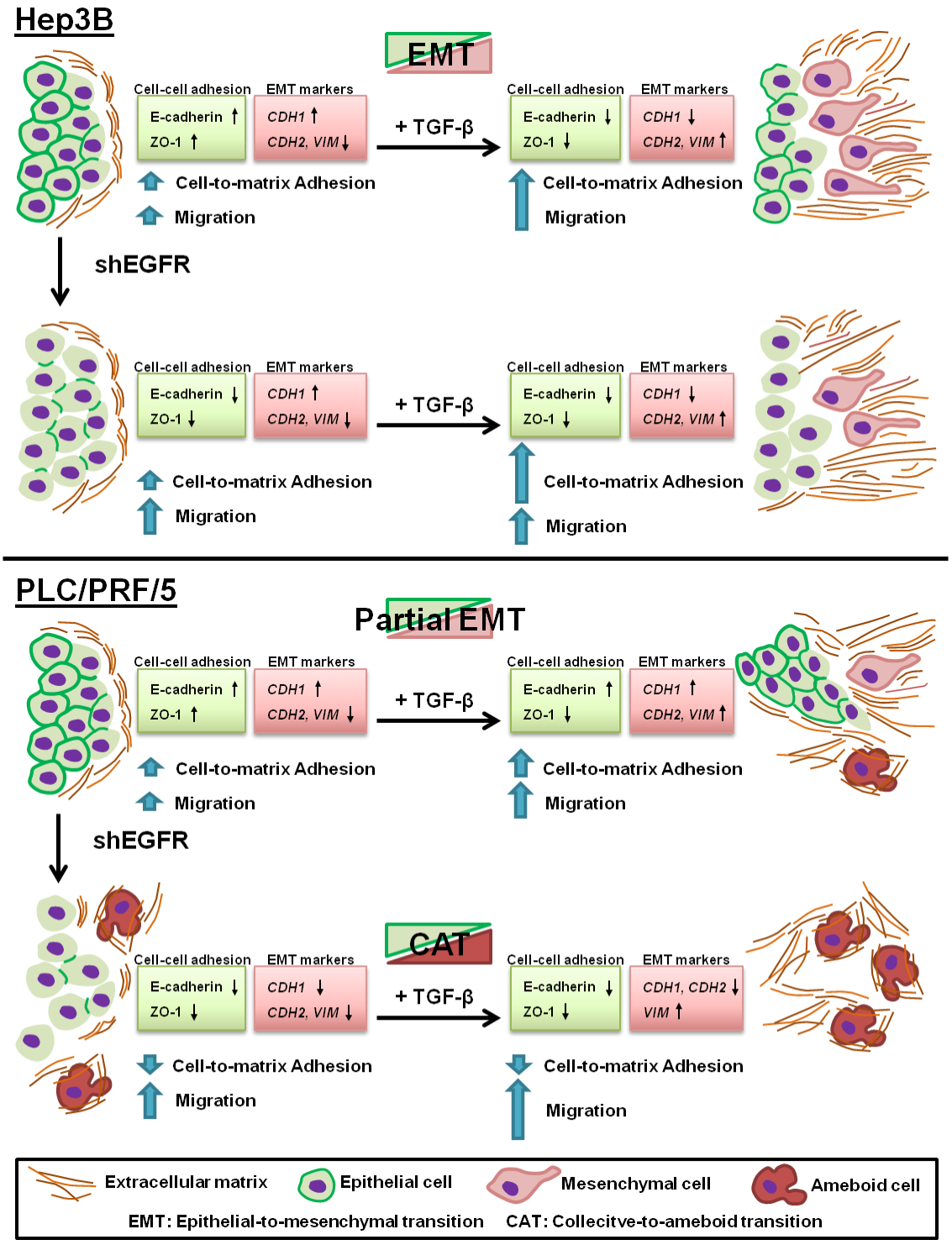

Figure XXIII. Consequences of EGFR silencing in PLC/PRF/5 and Hep3B HCC cells in the TGF-β-regulated adhesion and migration (Graphical abstract performed with Servier Medical Art).

3. Analysis of the expression of *TGFB1*, *EGFR* and EMT-related genes in tumoral and non-tumoral tissues from HCC patients

Hepatocellular carcinoma treatment is challenging, as the mechanisms underlying tumor progression are still largely unknown. To know if previous results observed *in vitro* have any relevance in patients, we studied a cohort of 31 samples from HCC patients from different etiologies, collected from surgeries in Bellvitge's Hospital. Studies of the TGF-β pathway reveal that, although we can observe a great diversity, most **tumoral tissues from HCC patients** in our cohort present **high expression of *TGFB1***, as well as high **activation of the pathway**, analyzed by immunohistochemistry of TGF-β1 and phospho-Smad2 nuclear staining. These findings correlate with *in vitro* data, as almost all the HCC cell lines studied express, to some extent, an autocrine production of TGF-β. These results are in accordance with the literature, where TGF-β in HCC patients has been reported to be overexpressed in both blood and urine, correlating with a worse prognosis and survival, and thus representing a marker of this cancer (Giannelli et al., 2011).

The EGFR signaling axis has been shown to play a key role during liver regeneration following acute and chronic liver damage, as well as in cirrhosis and HCC, highlighting its importance in the development of liver diseases (Komposch and Sibilia, 2016). However, clinical studies with EGFR inhibitors have shown only modest results in HCC. Surprisingly, contrary to what we expected, we observe a **low *EGFR* expression in tumor tissue from HCC patients**. We find similar data in a great number of databases when searching for *EGFR* expression, corroborating our results, and emphasizing the relevance of our *in vitro* studies when using shRNA technology for EGFR silencing in HCC cell lines. However, higher *EGFR* copy number is observed in databases, showing lack of correlation between gene copy number and expression. In fact, one of the main challenges within EGFR expression, as well as with other key players in cancer, is to select the best approximation to study the EGFR pathway to decide the best therapy. For example, EGFR immunohistochemical analysis has been used with varying degrees of success to predict response to anti-EGFR therapies. For instance, results from one study indicated a correlation between immunohistochemical overexpression of EGFR protein levels and increased *EGFR* copy number as measured by FISH (Tsiambas et al., 2009). However, many other studies like the one from Buckley et al. did not find correlation between increased EGFR expression by immunohistochemical analysis and the increase in *EGFR* gene copy number analyzed also by FISH in human HCC (Buckley et al., 2008). Altogether, it indicates that the analysis of the EGFR pathway in liver diseases appears to be a complex issue.

TGF-β-induced-EMT may play an important role in the progression and aggressiveness of HCC. In fact, many studies are focused on the expression of EMT markers to evaluate the

prognosis of HCC patients. It is generally well established that reduced E-cadherin protein expression alone (Chen et al., 2014) or concomitant with high vimentin protein expression (Zhai et al., 2014) indicates a poor prognosis for HCC patients. Moreover, it has been also observed that high phospho-Smad2 nuclear positivity correlated with E-cadherin(low)/vimentin(high) protein expression profile, closely associated with high-grade malignant behavior (Mima et al., 2013). More recently, Dituri et al. showed that circulating TGF-β was inversely correlated with E-cadherin (Dituri et al., 2014). Here we observe that most HCC patients' samples express **low *CDH1* and high *VIM*.** However, we observe heterogeneity among patients and high expression of *TGFB1* is not always associated to low *CDH1*. It is worthy to mention that, although a full mesenchymal pattern is related to poor outcome, it is not the more frequent phenotype found within HCC patients (Yamada et al., 2014), corroborating also the **heterogeneity** that we observe.

The crosstalk between the TGF-β and EGFR pathways in HCC tumors is poorly understood. According to our *in vitro* results, we expected to find association between low expression of *EGFR* and low expression of *CDH1*, but we could not find it. However, a detailed analysis in those samples from HCC patients expressing high *TGFB1* shows that a great percentage of tumors expressing low *EGFR* also present low *CDH1* and high *VIM*. These results suggest that **interactions between TGF-β and EGFR pathways** may exist **in HCC**.

In conclusion, our results suggest that gene profile (and, indeed, the tumor cell phenotype) in tumoral tissue from HCC patients that express high levels of *TGFB1* may depend on the expression of the *EGFR*. There is no apparent correlation among their expressions, but the levels of *EGFR* would determine the EMT profile of tumor cells. It is necessary to deep more into the connection among the pathways altered in HCC to advance in the design of new therapeutic tools.

FINAL DISCUSSION

Due to the EGFR role in promoting tumorigenesis or a more aggressive cancer phenotype, research has been focused on anti-EGFR treatments to diminish EGFR signaling as therapeutic strategies against tumorigenesis. However, most of clinical trials have failed to show beneficial effects, which demonstrates the necessity for a better understanding of the EGFR pathway in physiological and pathological processes of the liver. Results presented here suggest that EGFR is important and crucial in the first stages of liver regeneration and hepatocarcinogenesis. However, once HCC is already developed during carcinogenesis *in vivo*, or the tumorigenic capacity has been acquired in HCC cells *in vitro*, EGFR would be dispensable or even could be counteracting some tumorigenic abilities. In fact, this observation seems to be represented in samples from HCC patients in an advanced stage of HCC. Moreover, considering the specific crosstalk with the TGF-β pathway, it will be necessary to be cautious in the use of anti-EGFR therapy in this pathology, and the properly stratification of HCC patients who are incorporated in clinical trials is of huge importance to obtain positive results and to the benefit of patients.

VII. CONCLUSIONS

1. Mice expressing the truncated form of the EGFR in hepatocytes show a delay in the process of liver regeneration after 2/3 partial hepatectomy and in the appearance of tumors in a model of DEN-induced hepatocarcinogenesis.

2. Lack of EGFR catalytic activity promotes higher activation of the TGF-β pathway during liver regeneration, which correlates with induction of the expression of cell-cycle inhibitors, such as *Cdkn1a* and *Cdkn2b*.

3. EGFR signaling is required for fat accumulation and adipogenic gene expression during liver regeneration, suggesting a relevant role for EGFR in hepatic lipid metabolism.

4. In spite of these alterations, life of the transgenic mice is not significantly compromised and animals are able to fully regenerate the liver. Overactivation of the HGF/Met pathway and hyperplasia of the remaining cells may contribute to the success of the regenerative process.

5. During DEN-induced tumorigenesis, the delay in the appearance of tumors when EGFR catalytic activity is attenuated does not correlate with increased *Tgfb1* expression or overactivation of Smad signaling, but the expression of *Nox4*, target of TGF-β and inhibitor of liver cell proliferation, is significantly increased.

6. TGF-β effects on the EMT phenotype and migratory capabilities of HCC cells are heterogeneous. Hep3B cells respond to it inducing a full EMT, while PLC/PRF/5 cells undergo a partial EMT, increasing mesenchymal markers, but retaining cell-to-cell adhesion.

7. EGFR silencing decreases cell-to-cell adhesion in PLC/PRF/5 and Hep3B cells. However, it decreases cell-to-matrix adhesion only in PLC/PRF/5, but not in Hep3B cells.

8. EGFR silencing provokes a TGF-β-induced ameboid-like migration in PLC/PRF/5, but not in Hep3B cells, which correlates with high actomyosin contractility and advantages in cell migration.

9. Analyses in tumor tissues from HCC patients reveal that most of them present an activation of the TGF-β pathway and low *EGFR* expression. However, there is no correlation between *TGFB1* and *EGFR* expression, suggesting that they are independent parameters.

10. EMT-related gene profile in HCC patients that express high levels of TGF-β may depend on the expression of the *EGFR*, being low levels of *EGFR* associated to low expression of *CDH1* and high expression of *VIM*.

VIII. REFERENCES

Abdel-Misih, S.R.Z., and Bloomston, M. (2010). Liver anatomy. Surg. Clin. North Am. *90*, 643–653.

Abe, Y., Hines, I.N., Zibari, G., Pavlick, K., Gray, L., Kitagawa, Y., and Grisham, M.B. (2009). Mouse model of liver ischemia and reperfusion injury: method for studying reactive oxygen and nitrogen metabolites in vivo. Free Radic. Biol. Med. *46*, 1–7.

Achyut, B.R., and Yang, L. (2011). Transforming growth factor-β in the gastrointestinal and hepatic tumor microenvironment. Gastroenterology *141*, 1167–1178.

Al Moustafa, A.-E., Achkhar, A., and Yasmeen, A. (2012). EGF-receptor signaling and epithelial-mesenchymal transition in human carcinomas. Front Biosci Sch. Ed *4*, 671–684.

Ao, R., Zhang, D.-R., Du, Y.-Q., and Wang, Y. (2014). Expression and significance of Pin1, β-catenin and cyclin D1 in hepatocellular carcinoma. Mol. Med. Rep. *10*, 1893–1898.

Appert-Collin, A., Hubert, P., Crémel, G., and Bennasroune, A. (2015). Role of ErbB Receptors in Cancer Cell Migration and Invasion. Front. Pharmacol. *6*, 283.

Arandjelovic, S., Freed, T.A., and Gonias, S.L. (2003). Growth factor-binding sequence in human alpha2-macroglobulin targets the receptor-binding site in transforming growth factor-beta. Biochemistry (Mosc.) *42*, 6121–6127.

Baselga, J., and Arteaga, C.L. (2005). Critical update and emerging trends in epidermal growth factor receptor targeting in cancer. J. Clin. Oncol. *23*, 2445–2459.

Becker, A.K., Tso, D.K., Harris, A.C., Malfair, D., and Chang, S.D. (2014). Extrahepatic metastases of hepatocellular carcinoma: A spectrum of imaging findings. Can Assoc Radiol J *65*, 60–66.

Berasain, C., and Avila, M.A. (2014). The EGFR signalling system in the liver: from hepatoprotection to hepatocarcinogenesis. J. Gastroenterol. *49*, 9–23.

Berasain, C., Castillo, J., Perugorría, M.J., Prieto, J., and Avila, M.A. (2007). Amphiregulin: a new growth factor in hepatocarcinogenesis. Cancer Lett. *254*, 30–41.

Berasain, C., Perugorria, M.J., Latasa, M.U., Castillo, J., Goñi, S., Santamaría, M., Prieto, J., and Avila, M.A. (2009). The epidermal growth factor receptor: a link between inflammation and liver cancer. Exp. Biol. Med. Maywood *234*, 713–725.

Berasain, C., Ujue Latasa, M., Urtasun, R., Goñi, S., Elizalde, M., Garcia-Irigoyen, O., Azcona, M., Prieto, J., and Avila, M.A. (2011). Epidermal Growth Factor Receptor (EGFR) Crosstalks in Liver Cancer. Cancers Basel *3*, 2444–2461.

Bertran, E., Caja, L., Navarro, E., Sancho, P., Mainez, J., Murillo, M.M., Vinyals, A., Fabra, A., and Fabregat, I. (2009). Role of CXCR4/SDF-1 alpha in the migratory phenotype of hepatoma cells that have undergone epithelial-mesenchymal transition in response to the transforming growth factor-beta. Cell. Signal. *21*, 1595–1606.

Bertran, E., Crosas-Molist, E., Sancho, P., Caja, L., Lopez-Luque, J., Navarro, E., Egea, G., Lastra, R., Serrano, T., Ramos, E., et al. (2013). Overactivation of the TGF-β pathway confers a mesenchymal-like phenotype and CXCR4-dependent migratory properties to liver tumor cells. Hepatology *58*, 2032–2044.

Binamé, F., Lassus, P., and Hibner, U. (2008). Transforming growth factor beta controls the directional migration of hepatocyte cohorts by modulating their adhesion to fibronectin. Mol. Biol. Cell *19*, 945–956.

Böhm, F., Köhler, U.A., Speicher, T., and Werner, S. (2010). Regulation of liver regeneration by growth factors and cytokines. EMBO Mol. Med. *2*, 294–305.

Borowiak, M., Garratt, A.N., Wüstefeld, T., Strehle, M., Trautwein, C., and Birchmeier, C. (2004). Met provides essential signals for liver regeneration. Proc. Natl. Acad. Sci. U. S. A. *101*, 10608–10613.

Braun, L., Mead, J.E., Panzica, M., Mikumo, R., Bell, G.I., and Fausto, N. (1988). Transforming growth factor beta mRNA increases during liver regeneration: a possible paracrine mechanism of growth regulation. Proc. Natl. Acad. Sci. U. S. A. *85*, 1539–1543.

Bruix, J., Gores, G.J., and Mazzaferro, V. (2014). Hepatocellular carcinoma: clinical frontiers and perspectives. Gut *63*, 844–855.

Bruix, J., Reig, M., and Sherman, M. (2016). Evidence-Based Diagnosis, Staging, and Treatment of Patients With Hepatocellular Carcinoma. Gastroenterology *150*, 835–853.

Buckley, A.F., Burgart, L.J., Sahai, V., and Kakar, S. (2008). Epidermal growth factor receptor expression and gene copy number in conventional hepatocellular carcinoma. Am. J. Clin. Pathol. *129*, 245–251.

Budhu, A.S., Zipser, B., Forgues, M., Ye, Q.-H., Sun, Z., and Wang, X.W. (2005). The molecular signature of metastases of human hepatocellular carcinoma. Oncology *69*, 23–27.

Caja, L., Ortiz, C., Bertran, E., Murillo, M.M., Miró-Obradors, M.J., Palacios, E., and Fabregat, I. (2007). Differential intracellular signalling induced by TGF-beta in rat adult hepatocytes and hepatoma cells: implications in liver carcinogenesis. Cell. Signal. *19*, 683–694.

Caja, L., Sancho, P., Bertran, E., Iglesias-Serret, D., Gil, J., and Fabregat, I. (2009). Overactivation of the MEK/ERK pathway in liver tumor cells confers resistance to TGF-{beta}-

induced cell death through impairing up-regulation of the NADPH oxidase NOX4. Cancer Res. *69*, 7595–7602.

Caja, L., Sancho, P., Bertran, E., and Fabregat, I. (2011a). Dissecting the effect of targeting the epidermal growth factor receptor on TGF-β-induced-apoptosis in human hepatocellular carcinoma cells. J. Hepatol. *55*, 351–358.

Caja, L., Bertran, E., Campbell, J., Fausto, N., and Fabregat, I. (2011b). The transforming growth factor-beta (TGF-β) mediates acquisition of a mesenchymal stem cell-like phenotype in human liver cells. J. Cell. Physiol. *226*, 1214–1223.

Calvo, F., Sanz-Moreno, V., Agudo-Ibáñez, L., Wallberg, F., Sahai, E., Marshall, C.J., and Crespo, P. (2011). RasGRF suppresses Cdc42-mediated tumour cell movement, cytoskeletal dynamics and transformation. Nat. Cell Biol. *13*, 819–826.

Cantelli, G., Orgaz, J.L., Rodriguez-Hernandez, I., Karagiannis, P., Maiques, O., Matias-Guiu, X., Nestle, F.O., Marti, R.M., Karagiannis, S.N., and Sanz-Moreno, V. (2015). TGF-β-Induced Transcription Sustains Amoeboid Melanoma Migration and Dissemination. Curr. Biol. *25*, 2899–2914.

Capece, D., Fischietti, M., Verzella, D., Gaggiano, A., Cicciarelli, G., Tessitore, A., Zazzeroni, F., and Alesse, E. (2013). The inflammatory microenvironment in hepatocellular carcinoma: a pivotal role for tumor-associated macrophages. Biomed Res. Int. *2013*, 187204.

Carmona-Cuenca, I., Herrera, B., Ventura, J.-J., Roncero, C., Fernández, M., and Fabregat, I. (2006). EGF blocks NADPH oxidase activation by TGF-beta in fetal rat hepatocytes, impairing oxidative stress, and cell death. J. Cell. Physiol. *207*, 322–330.

Carmona-Cuenca, I., Roncero, C., Sancho, P., Caja, L., Fausto, N., Fernández, M., and Fabregat, I. (2008). Upregulation of the NADPH oxidase NOX4 by TGF-beta in hepatocytes is required for its pro-apoptotic activity. J. Hepatol. *49*, 965–976.

Carr, B.I., Hayashi, I., Branum, E.L., and Moses, H.L. (1986). Inhibition of DNA synthesis in rat hepatocytes by platelet-derived type beta transforming growth factor. Cancer Res. *46*, 2330–2334.

del Castillo, G., Alvarez-Barrientos, A., Carmona-Cuenca, I., Fernández, M., Sánchez, A., and Fabregat, I. (2008). Isolation and characterization of a putative liver progenitor population after treatment of fetal rat hepatocytes with TGF-beta. J. Cell. Physiol. *215*, 846–855.

Chapnick, D.A., and Liu, X. (2014). Leader cell positioning drives wound-directed collective migration in TGFβ-stimulated epithelial sheets. Mol. Biol. Cell *25*, 1586–1593.

Chari, R.S., Price, D.T., Sue, S.R., Meyers, W.C., and Jirtle, R.L. (1995). Down-regulation of transforming growth factor beta receptor type I, II, and III during liver regeneration. Am. J. Surg. *169*, 126-131-132.

Che, Y., Ye, F., Xu, R., Qing, H., Wang, X., Yin, F., Cui, M., Burstein, D., Jiang, B., and Zhang, D.Y. (2012). Co-expression of XIAP and cyclin D1 complex correlates with a poor prognosis in patients with hepatocellular carcinoma. Am. J. Pathol. *180*, 1798–1807.

Chen, C.-R., Kang, Y., Siegel, P.M., and Massagué, J. (2002). E2F4/5 and p107 as Smad cofactors linking the TGFbeta receptor to c-myc repression. Cell *110*, 19–32.

Chen, J., Zhao, J., Ma, R., Lin, H., Liang, X., and Cai, X. (2014). Prognostic significance of E-cadherin expression in hepatocellular carcinoma: a meta-analysis. PloS One *9*, e103952.

Cheng, A.-L., Kang, Y.-K., Chen, Z., Tsao, C.-J., Qin, S., Kim, J.S., Luo, R., Feng, J., Ye, S., Yang, T.-S., et al. (2009). Efficacy and safety of sorafenib in patients in the Asia-Pacific region with advanced hepatocellular carcinoma: a phase III randomised, double-blind, placebo-controlled trial. Lancet Oncol. *10*, 25–34.

Cienfuegos, J.A., Rotellar, F., Baixauli, J., Martínez-Regueira, F., Pardo, F., and Hernández-Lizoáin, J.L. (2014). Liver regeneration--the best kept secret. A model of tissue injury response. Rev Esp Enferm Dig *106*, 171–194.

Clavijo-Cornejo, D., Enriquez-Cortina, C., López-Reyes, A., Domínguez-Pérez, M., Nuño, N., Domínguez-Meraz, M., Bucio, L., Souza, V., Factor, V.M., Thorgeirsson, S.S., et al. (2013). Biphasic regulation of the NADPH oxidase by HGF/c-Met signaling pathway in primary mouse hepatocytes. Biochimie *95*, 1177–1184.

Comoglio, P.M., Boccaccio, C., and Trusolino, L. (2003). Interactions between growth factor receptors and adhesion molecules: breaking the rules. Curr. Opin. Cell Biol. *15*, 565–571.

Connell, L.C., Harding, J.J., and Abou-Alfa, G.K. (2016). Advanced Hepatocellular Cancer: the Current State of Future Research. Curr. Treat. Options Oncol. *17*, 43.

Coulouarn, C., Factor, V.M., and Thorgeirsson, S.S. (2008). Transforming growth factor-beta gene expression signature in mouse hepatocytes predicts clinical outcome in human cancer. Hepatology *47*, 2059–2067.

Crosas-Molist, E., Bertran, E., Sancho, P., López-Luque, J., Fernando, J., Sánchez, A., Fernández, M., Navarro, E., and Fabregat, I. (2014). The NADPH oxidase NOX4 inhibits hepatocyte proliferation and liver cancer progression. Free Radic. Biol. Med. *69*, 338–347.

Daveau, M., Scotte, M., François, A., Coulouarn, C., Ros, G., Tallet, Y., Hiron, M., Hellot, M.-F., and Salier, J.-P. (2003). Hepatocyte growth factor, transforming growth factor

alpha, and their receptors as combined markers of prognosis in hepatocellular carcinoma. Mol. Carcinog. *36*, 130–141.

Del Castillo, G., Murillo, M.M., Alvarez-Barrientos, A., Bertran, E., Fernández, M., Sánchez, A., and Fabregat, I. (2006). Autocrine production of TGF-beta confers resistance to apoptosis after an epithelial-mesenchymal transition process in hepatocytes: Role of EGF receptor ligands. Exp. Cell Res. *312*, 2860–2871.

Desbois-Mouthon, C., Cacheux, W., Blivet-Van Eggelpoël, M.-J., Barbu, V., Fartoux, L., Poupon, R., Housset, C., and Rosmorduc, O. (2006). Impact of IGF-1R/EGFR cross-talks on hepatoma cell sensitivity to gefitinib. Int. J. Cancer *119*, 2557–2566.

Diril, M.K., Ratnacaram, C.K., Padmakumar, V.C., Du, T., Wasser, M., Coppola, V., Tessarollo, L., and Kaldis, P. (2012). Cyclin-dependent kinase 1 (Cdk1) is essential for cell division and suppression of DNA re-replication but not for liver regeneration. Proc. Natl. Acad. Sci. U. S. A. *109*, 3826–3831.

Dituri, F., Mazzocca, A., Fernando, J., Peidrò, F.J., Papappicco, P., Fabregat, I., De Santis, F., Paradiso, A., Sabbà, C., and Giannelli, G. (2013). Differential Inhibition of the TGF-β Signaling Pathway in HCC Cells Using the Small Molecule Inhibitor LY2157299 and the D10 Monoclonal Antibody against TGF-β Receptor Type II. PloS One *8*, e67109.

Dituri, F., Serio, G., Filannino, D., Mascolo, A., Sacco, R., Villa, E., and Giannelli, G. (2014). Circulating TGF-β1-related biomarkers in patients with hepatocellular carcinoma and their association with HCC staging scores. Cancer Lett. *353*, 264–271.

Dooley, S., and ten Dijke, P. (2012). TGF-β in progression of liver disease. Cell Tissue Res. *347*, 245–256.

Drabsch, Y., and ten Dijke, P. (2012). TGF-β signalling and its role in cancer progression and metastasis. Cancer Metastasis Rev. *31*, 553–568.

Drysdale, B.E., Zacharchuk, C.M., and Shin, H.S. (1983). Mechanism of macrophage-mediated cytotoxicity: production of a soluble cytotoxic factor. J. Immunol. *131*, 2362–2367.

Dzieran, J., Fabian, J., Feng, T., Coulouarn, C., Ilkavets, I., Kyselova, A., Breuhahn, K., Dooley, S., and Meindl-Beinker, N.M. (2013). Comparative analysis of TGF-β/Smad signaling dependent cytostasis in human hepatocellular carcinoma cell lines. PloS One *8*, e72252.

Ebi, M., Kataoka, H., Shimura, T., Kubota, E., Hirata, Y., Mizushima, T., Mizoshita, T., Tanaka, M., Mabuchi, M., Tsukamoto, H., et al. (2010). TGFβ induces proHB-EGF shedding and EGFR transactivation through ADAM activation in gastric cancer cells. Biochem. Biophys. Res. Commun. *402*, 449–454.

Edlund, S., Landström, M., Heldin, C.-H., and Aspenström, P. (2002). Transforming growth factor-beta-induced mobilization of actin cytoskeleton requires signaling by small GTPases Cdc42 and RhoA. Mol. Biol. Cell *13*, 902–914.

Ehrenfried, J.A., Ko, T.C., Thompson, E.A., and Evers, B.M. (1997). Cell cycle-mediated regulation of hepatic regeneration. Surgery *122*, 927–935.

Endres, N.F., Barros, T., Cantor, A.J., and Kuriyan, J. (2014). Emerging concepts in the regulation of the EGF receptor and other receptor tyrosine kinases. Trends Biochem. Sci. *39*, 437–446.

Erasmus, J.C., Welsh, N.J., and Braga, V.M.M. (2015). Cooperation of distinct Rac-dependent pathways to stabilise E-cadherin adhesion. Cell. Signal. *27*, 1905–1913.

European Association For The Study Of The Liver, and European Organisation For Research And Treatment Of Cancer (2012). EASL-EORTC clinical practice guidelines: management of hepatocellular carcinoma. J. Hepatol. *56*, 908–943.

Fabregat, I., Sánchez, A., Alvarez, A.M., Nakamura, T., and Benito, M. (1996). Epidermal growth factor, but not hepatocyte growth factor, suppresses the apoptosis induced by transforming growth factor-beta in fetal hepatocytes in primary culture. FEBS Lett. *384*, 14–18.

Fabregat, I., Herrera, B., Fernández, M., Alvarez, A.M., Sánchez, A., Roncero, C., Ventura, J.J., Valverde, A.M., and Benito, M. (2000). Epidermal growth factor impairs the cytochrome C/caspase-3 apoptotic pathway induced by transforming growth factor beta in rat fetal hepatocytes via a phosphoinositide 3-kinase-dependent pathway. Hepatology *32*, 528–535.

Fabregat, I., Fernando, J., Mainez, J., and Sancho, P. (2014). TGF-beta signaling in cancer treatment. Curr. Pharm. Des. *20*, 2934–2947.

Fabregat, I., Moreno-Càceres, J., Sánchez, A., Dooley, S., Dewidar, B., Giannelli, G., Ten Dijke, P., and IT-LIVER Consortium (2016). TGF-β signalling and liver disease. FEBS J. *283*, 2219–2232.

Factor, V.M., Seo, D., Ishikawa, T., Kaposi-Novak, P., Marquardt, J.U., Andersen, J.B., Conner, E.A., and Thorgeirsson, S.S. (2010). Loss of c-Met disrupts gene expression program required for G2/M progression during liver regeneration in mice. PloS One *5*, e12739.

Fausto, N., and Campbell, J.S. (2003). The role of hepatocytes and oval cells in liver regeneration and repopulation. Mech. Dev. *120*, 117–130.

Fausto, N., and Campbell, J.S. (2010). Mouse models of hepatocellular carcinoma. Semin. Liver Dis. *30*, 87–98.

Fausto, N., Campbell, J.S., and Riehle, K.J. (2006). Liver regeneration. Hepatology *43*, S45-53.

Fausto, N., Campbell, J.S., and Riehle, K.J. (2012). Liver regeneration. J. Hepatol. *57*, 692–694.

Fernando, J., Malfettone, A., Cepeda, E.B., Vilarrasa-Blasi, R., Bertran, E., Raimondi, G., Fabra, À., Alvarez-Barrientos, A., Fernández-Salguero, P., Fernández-Rodríguez, C.M., et al. (2015). A mesenchymal-like phenotype and expression of CD44 predict lack of apoptotic response to sorafenib in liver tumor cells. Int. J. Cancer *136*, E161-172.

Fischer, A.N.M., Fuchs, E., Mikula, M., Huber, H., Beug, H., and Mikulits, W. (2007). PDGF essentially links TGF-beta signaling to nuclear beta-catenin accumulation in hepatocellular carcinoma progression. Oncogene *26*, 3395–3405.

Flores, A., and Marrero, J.A. (2014). Emerging trends in hepatocellular carcinoma: focus on diagnosis and therapeutics. Clin. Med. Insights Oncol. *8*, 71–76.

Flynn, J.F., Wong, C., and Wu, J.M. (2009). Anti-EGFR Therapy: Mechanism and Advances in Clinical Efficacy in Breast Cancer. J. Oncol. *2009*, 526963.

Forner, A., Llovet, J.M., and Bruix, J. (2012). Hepatocellular carcinoma. Lancet *379*, 1245–1255.

Franco, D.L., Mainez, J., Vega, S., Sancho, P., Murillo, M.M., de Frutos, C.A., Del Castillo, G., López-Blau, C., Fabregat, I., and Nieto, M.A. (2010). Snail1 suppresses TGF-beta-induced apoptosis and is sufficient to trigger EMT in hepatocytes. J. Cell Sci. *123*, 3467–3477.

Franklin, C.C., Rosenfeld-Franklin, M.E., White, C., Kavanagh, T.J., and Fausto, N. (2003). TGFbeta1-induced suppression of glutathione antioxidant defenses in hepatocytes: caspase-dependent post-translational and caspase-independent transcriptional regulatory mechanisms. FASEB J. *17*, 1535–1537.

Fransvea, E., Mazzocca, A., Santamato, A., Azzariti, A., Antonaci, S., and Giannelli, G. (2011). Kinase activation profile associated with TGF-β-dependent migration of HCC cells: a preclinical study. Cancer Chemother. Pharmacol. *68*, 79–86.

Frederick, L., Wang, X.Y., Eley, G., and James, C.D. (2000). Diversity and frequency of epidermal growth factor receptor mutations in human glioblastomas. Cancer Res. *60*, 1383–1387.

Friedl, P., and Alexander, S. (2011). Cancer invasion and the microenvironment: plasticity and reciprocity. Cell *147*, 992–1009.

Friedl, P., and Wolf, K. (2003). Tumour-cell invasion and migration: diversity and escape mechanisms. Nat. Rev. Cancer *3*, 362–374.

Fuchs, B.C., Hoshida, Y., Fujii, T., Wei, L., Yamada, S., Lauwers, G.Y., McGinn, C.M., DePeralta, D.K., Chen, X., Kuroda, T., et al. (2014). Epidermal growth factor receptor inhibition attenuates liver fibrosis and development of hepatocellular carcinoma. Hepatology *59*, 1577–1590.

Gadea, G., Sanz-Moreno, V., Self, A., Godi, A., and Marshall, C.J. (2008). DOCK10-mediated Cdc42 activation is necessary for amoeboid invasion of melanoma cells. Curr. Biol. *18*, 1456–1465.

Gandalovičová, A., Vomastek, T., Rosel, D., and Brábek, J. (2016). Cell polarity signaling in the plasticity of cancer cell invasiveness. Oncotarget *7*, 25022–25049.

Gao, J., Zhu, Y., Nilsson, M., and Sundfeldt, K. (2014). TGF-β isoforms induce EMT independent migration of ovarian cancer cells. Cancer Cell Int. *14*, 72.

Gao, L., Utsumi, T., Tashiro, K., Liu, B., Zhang, D., Swenson, E.S., and Iwakiri, Y. (2013). Reticulon 4B (Nogo-B) facilitates hepatocyte proliferation and liver regeneration in mice. Hepatology *57*, 1992–2003.

Giampieri, S., Manning, C., Hooper, S., Jones, L., Hill, C.S., and Sahai, E. (2009). Localized and reversible TGFbeta signalling switches breast cancer cells from cohesive to single cell motility. Nat. Cell Biol. *11*, 1287–1296.

Giannelli, G., Mazzocca, A., Fransvea, E., Lahn, M., and Antonaci, S. (2011). Inhibiting TGF-β signaling in hepatocellular carcinoma. Biochim. Biophys. Acta *1815*, 214–223.

Giannelli, G., Mikulits, W., Dooley, S., Fabregat, I., Moustakas, A., ten Dijke, P., Portincasa, P., Winter, P., Janssen, R., Leporatti, S., et al. (2016). The rationale for targeting TGF-β in chronic liver diseases. Eur. J. Clin. Invest. *46*, 349–361.

Gilgenkrantz, H., and Collin de l'Hortet, A. (2011). New insights into liver regeneration. Clin. Res. Hepatol. Gastroenterol. *35*, 623–629.

Giraldo, P., and Montoliu, L. (2001). Size matters: use of YACs, BACs and PACs in transgenic animals. Transgenic Res. *10*, 83–103.

Gordillo, M., Evans, T., and Gouon-Evans, V. (2015). Orchestrating liver development. Development *142*, 2094–2108.

Grandhi, M.S., Kim, A.K., Ronnekleiv-Kelly, S.M., Kamel, I.R., Ghasebeh, M.A., and Pawlik, T.M. (2016). Hepatocellular carcinoma: From diagnosis to treatment. Surg. Oncol. *25*, 74–85.

Haga, S., Ogawa, W., Inoue, H., Terui, K., Ogino, T., Igarashi, R., Takeda, K., Akira, S., Enosawa, S., Furukawa, H., et al. (2005). Compensatory recovery of liver mass by Akt-mediated hepatocellular hypertrophy in liver-specific STAT3-deficient mice. J. Hepatol. *43*, 799–807.

den Hartigh, J.C., van Bergen en Henegouwen, P.M., Verkleij, A.J., and Boonstra, J. (1992). The EGF receptor is an actin-binding protein. J. Cell Biol. *119*, 349–355.

Hegerfeldt, Y., Tusch, M., Bröcker, E.-B., and Friedl, P. (2002). Collective cell movement in primary melanoma explants: plasticity of cell-cell interaction, beta1-integrin function, and migration strategies. Cancer Res. *62*, 2125–2130.

Heindryckx, F., Colle, I., and Van Vlierberghe, H. (2009). Experimental mouse models for hepatocellular carcinoma research. Int. J. Exp. Pathol. *90*, 367–386.

Heldin, C.-H., Vanlandewijck, M., and Moustakas, A. (2012). Regulation of EMT by TGFβ in cancer. FEBS Lett. *586*, 1959–1970.

Hernandez-Gea, V., Toffanin, S., Friedman, S.L., and Llovet, J.M. (2013). Role of the microenvironment in the pathogenesis and treatment of hepatocellular carcinoma. Gastroenterology *144*, 512–527.

Herrera, B., Fernández, M., Alvarez, A.M., Roncero, C., Benito, M., Gil, J., and Fabregat, I. (2001a). Activation of caspases occurs downstream from radical oxygen species production, Bcl-xL down-regulation, and early cytochrome C release in apoptosis induced by transforming growth factor beta in rat fetal hepatocytes. Hepatology *34*, 548–556.

Herrera, B., Murillo, M.M., Alvarez-Barrientos, A., Beltrán, J., Fernández, M., and Fabregat, I. (2004a). Source of early reactive oxygen species in the apoptosis induced by transforming growth factor-beta in fetal rat hepatocytes. Free Radic. Biol. Med. *36*, 16–26.

Herrera, B., Alvarez, A.M., Sánchez, A., Fernández, M., Roncero, C., Benito, M., and Fabregat, I. (2001b). Reactive oxygen species (ROS) mediates the mitochondrial-dependent apoptosis induced by transforming growth factor (beta) in fetal hepatocytes. FASEB J. *15*, 741–751.

Herrera, B., Alvarez, A.M., Beltrán, J., Valdés, F., Fabregat, I., and Fernández, M. (2004b). Resistance to TGF-beta-induced apoptosis in regenerating hepatocytes. J. Cell. Physiol. *201*, 385–392.

Higgins, G.M., and Anderson, R. (1931). Experimental pathology of the liver. I. Restoration of the liver of the white rat following partial surgical removal. Arch Pathol *12*, 186–202.

Hinz, M., Krappmann, D., Eichten, A., Heder, A., Scheidereit, C., and Strauss, M. (1999). NF-kappaB function in growth control: regulation of cyclin D1 expression and G0/G1-to-S-phase transition. Mol. Cell. Biol. *19*, 2690–2698.

Hirai, T., Kuwahara, M., Yoshida, K., Kagawa, Y., Hihara, J., Yamashita, Y., and Toge, T. (1998). Clinical results of transhiatal esophagectomy for carcinoma of the lower thoracic esophagus according to biological markers. Dis. Esophagus *11*, 221–225.

Höpfner, M., Sutter, A.P., Huether, A., Schuppan, D., Zeitz, M., and Scherübl, H. (2004). Targeting the epidermal growth factor receptor by gefitinib for treatment of hepatocellular carcinoma. J. Hepatol. *41*, 1008–1016.

Huang, S., He, X., Ding, J., Liang, L., Zhao, Y., Zhang, Z., Yao, X., Pan, Z., Zhang, P., Li, J., et al. (2008). Upregulation of miR-23a approximately 27a approximately 24 decreases transforming growth factor-beta-induced tumor-suppressive activities in human hepatocellular carcinoma cells. Int. J. Cancer *123*, 972–978.

Huh, C.-G., Factor, V.M., Sánchez, A., Uchida, K., Conner, E.A., and Thorgeirsson, S.S. (2004). Hepatocyte growth factor/c-met signaling pathway is required for efficient liver regeneration and repair. Proc. Natl. Acad. Sci. U. S. A. *101*, 4477–4482.

Hynes, N.E., and MacDonald, G. (2009). ErbB receptors and signaling pathways in cancer. Curr. Opin. Cell Biol. *21*, 177–184.

Iavarone, A., and Massagué, J. (1997). Repression of the CDK activator Cdc25A and cell-cycle arrest by cytokine TGF-beta in cells lacking the CDK inhibitor p15. Nature *387*, 417–422.

Ikushima, H., and Miyazono, K. (2010). TGFbeta signalling: a complex web in cancer progression. Nat. Rev. Cancer *10*, 415–424.

Ilina, O., and Friedl, P. (2009). Mechanisms of collective cell migration at a glance. J. Cell Sci. *122*, 3203–3208.

Ito, J., Harada, N., Nagashima, O., Makino, F., Usui, Y., Yagita, H., Okumura, K., Dorscheid, D.R., Atsuta, R., Akiba, H., et al. (2011). Wound-induced TGF-β1 and TGF-β2 enhance airway epithelial repair via HB-EGF and TGF-α. Biochem. Biophys. Res. Commun. *412*, 109–114.

Ito, Y., Takeda, T., Sakon, M., Tsujimoto, M., Higashiyama, S., Noda, K., Miyoshi, E., Monden, M., and Matsuura, N. (2001). Expression and clinical significance of erb-B receptor family in hepatocellular carcinoma. Br. J. Cancer *84*, 1377–1383.

Janevska, D., Chaloska-Ivanova, V., and Janevski, V. (2015). Hepatocellular Carcinoma: Risk Factors, Diagnosis and Treatment. Open Access Maced. J. Med. Sci. *3*, 732–736.

Jen, J., Harper, J.W., Bigner, S.H., Bigner, D.D., Papadopoulos, N., Markowitz, S., Willson, J.K., Kinzler, K.W., and Vogelstein, B. (1994). Deletion of p16 and p15 genes in brain tumors. Cancer Res. *54*, 6353–6358.

Jo, M., Stolz, D.B., Esplen, J.E., Dorko, K., Michalopoulos, G.K., and Strom, S.C. (2000). Cross-talk between epidermal growth factor receptor and c-Met signal pathways in transformed cells. J. Biol. Chem. *275*, 8806–8811.

Jorissen, R.N., Walker, F., Pouliot, N., Garrett, T.P.J., Ward, C.W., and Burgess, A.W. (2003). Epidermal growth factor receptor: mechanisms of activation and signalling. Exp. Cell Res. *284*, 31–53.

Kalluri, R., and Weinberg, R.A. (2009). The basics of epithelial-mesenchymal transition. J. Clin. Invest. *119*, 1420–1428.

Kang, L.-I., Mars, W.M., and Michalopoulos, G.K. (2012). Signals and cells involved in regulating liver regeneration. Cells *1*, 1261–1292.

Katsuno, Y., Lamouille, S., and Derynck, R. (2013). TGF-β signaling and epithelial-mesenchymal transition in cancer progression. Curr. Opin. Oncol. *25*, 76–84.

Kim, G.-Y., Mercer, S.E., Ewton, D.Z., Yan, Z., Jin, K., and Friedman, E. (2002). The stress-activated protein kinases p38 alpha and JNK1 stabilize p21(Cip1) by phosphorylation. J. Biol. Chem. *277*, 29792–29802.

Kohjima, M., Tsai, T.-H., Tackett, B.C., Thevananther, S., Li, L., Chang, B.H.-J., and Chan, L. (2013). Delayed liver regeneration after partial hepatectomy in adipose differentiation related protein-null mice. J. Hepatol. *59*, 1246–1254.

Komposch, K., and Sibilia, M. (2016). EGFR Signaling in Liver Diseases. Int. J. Mol. Sci. *17*.

Kung, J.W.C., Currie, I.S., Forbes, S.J., and Ross, J.A. (2010). Liver development, regeneration, and carcinogenesis. J. Biomed. Biotechnol. *2010*, 984248.

Kwon, Y.J., Lee, K.G., and Choi, D. (2015). Clinical implications of advances in liver regeneration. Clin. Mol. Hepatol. *21*, 7–13.

LaMarre, J., Hayes, M.A., Wollenberg, G.K., Hussaini, I., Hall, S.W., and Gonias, S.L. (1991). An alpha 2-macroglobulin receptor-dependent mechanism for the plasma clearance of transforming growth factor-beta 1 in mice. J. Clin. Invest. *87*, 39–44.

Lamouille, S., Xu, J., and Derynck, R. (2014). Molecular mechanisms of epithelial-mesenchymal transition. Nat. Rev. Mol. Cell Biol. *15*, 178–196.

Lanaya, H., Natarajan, A., Komposch, K., Li, L., Amberg, N., Chen, L., Wculek, S.K., Hammer, M., Zenz, R., Peck-Radosavljevic, M., et al. (2014). EGFR has a tumour-promoting role in liver macrophages during hepatocellular carcinoma formation. Nat. Cell Biol. *16*, 972–981, 1–7.

Lee, J.-S. (2015). The mutational landscape of hepatocellular carcinoma. Clin. Mol. Hepatol. *21*, 220–229.

Lee, K.Y., and Bae, S.-C. (2002). TGF-beta-dependent cell growth arrest and apoptosis. J. Biochem. Mol. Biol. *35*, 47–53.

Lee, E., Yi, J.Y., Chung, E., and Son, Y. (2010). Transforming growth factorbeta(1) transactivates EGFR via an H(2)O(2)-dependent mechanism in squamous carcinoma cell line. Cancer Lett. *290*, 43–48.

Li, J., Fu, H., Xu, C., Tie, Y., Xing, R., Zhu, J., Qin, Y., Sun, Z., and Zheng, X. (2010). miR-183 inhibits TGF-beta1-induced apoptosis by downregulation of PDCD4 expression in human hepatocellular carcinoma cells. BMC Cancer *10*, 354.

Liebmann, C., and Böhmer, F.D. (2000). Signal transduction pathways of G protein-coupled receptors and their cross-talk with receptor tyrosine kinases: lessons from bradykinin signaling. Curr. Med. Chem. *7*, 911–943.

Lin, S.Y., Makino, K., Xia, W., Matin, A., Wen, Y., Kwong, K.Y., Bourguignon, L., and Hung, M.C. (2001). Nuclear localization of EGF receptor and its potential new role as a transcription factor. Nat. Cell Biol. *3*, 802–808.

Liu, M., Jiang, L., and Guan, X.-Y. (2014a). The genetic and epigenetic alterations in human hepatocellular carcinoma: a recent update. Protein Cell *5*, 673–691.

Liu, S.V., Subramaniam, D., Cyriac, G.C., Abdul-Khalek, F.J., and Giaccone, G. (2014b). Emerging protein kinase inhibitors for non-small cell lung cancer. Expert Opin. Emerg. Drugs *19*, 51–65.

Liu, Y.-J., Le Berre, M., Lautenschlaeger, F., Maiuri, P., Callan-Jones, A., Heuzé, M., Takaki, T., Voituriez, R., and Piel, M. (2015). Confinement and low adhesion induce fast amoeboid migration of slow mesenchymal cells. Cell *160*, 659–672.

Llovet, J.M. (2014). Liver cancer: time to evolve trial design after everolimus failure. Nat. Rev. Clin. Oncol. *11*, 506–507.

Llovet, J.M., and Bruix, J. (2008). Molecular targeted therapies in hepatocellular carcinoma. Hepatology *48*, 1312–1327.

Llovet, J.M., Ricci, S., Mazzaferro, V., Hilgard, P., Gane, E., Blanc, J.-F., de Oliveira, A.C., Santoro, A., Raoul, J.-L., Forner, A., et al. (2008). Sorafenib in advanced hepatocellular carcinoma. N. Engl. J. Med. *359*, 378–390.

Lorch, J.H., Klessner, J., Park, J.K., Getsios, S., Wu, Y.L., Stack, M.S., and Green, K.J. (2004). Epidermal growth factor receptor inhibition promotes desmosome assembly and strengthens intercellular adhesion in squamous cell carcinoma cells. J. Biol. Chem. *279*, 37191–37200.

Lu, L.-C., Hsu, C.-H., Hsu, C., and Cheng, A.-L. (2016). Tumor Heterogeneity in Hepatocellular Carcinoma: Facing the Challenges. Liver Cancer *5*, 128–138.

Macias-Silva, M., Li, W., Leu, J.I., Crissey, M.A.S., and Taub, R. (2002). Up-regulated transcriptional repressors SnoN and Ski bind Smad proteins to antagonize transforming growth factor-beta signals during liver regeneration. J. Biol. Chem. *277*, 28483–28490.

Malarkey, D.E., Johnson, K., Ryan, L., Boorman, G., and Maronpot, R.R. (2005). New insights into functional aspects of liver morphology. Toxicol. Pathol. *33*, 27–34.

Malhi, H., and Gores, G.J. (2008). Cellular and molecular mechanisms of liver injury. Gastroenterology *134*, 1641–1654.

Mamiya, T., Yamazaki, K., Masugi, Y., Mori, T., Effendi, K., Du, W., Hibi, T., Tanabe, M., Ueda, M., Takayama, T., et al. (2010). Reduced transforming growth factor-beta receptor II expression in hepatocellular carcinoma correlates with intrahepatic metastasis. Lab. Invest. *90*, 1339–1345.

Mani, S.A., Guo, W., Liao, M.-J., Eaton, E.N., Ayyanan, A., Zhou, A.Y., Brooks, M., Reinhard, F., Zhang, C.C., Shipitsin, M., et al. (2008). The epithelial-mesenchymal transition generates cells with properties of stem cells. Cell *133*, 704–715.

Mao, S.A., Glorioso, J.M., and Nyberg, S.L. (2014). Liver regeneration. Transl. Res. *163*, 352–362.

Marcoux, N., and Vuori, K. (2005). EGF receptor activity is essential for adhesion-induced stress fiber formation and cofilin phosphorylation. Cell. Signal. *17*, 1449–1455.

Marshall, J. (2006). Clinical implications of the mechanism of epidermal growth factor receptor inhibitors. Cancer *107*, 1207–1218.

Martínez-Palacián, A., del Castillo, G., Suárez-Causado, A., García-Álvaro, M., de Morena-Frutos, D., Fernández, M., Roncero, C., Fabregat, I., Herrera, B., and Sánchez, A. (2013). Mouse hepatic oval cells require Met-dependent PI3K to impair TGF-β-induced oxidative stress and apoptosis. PloS One *8*, e53108.

Massagué, J. (2008). TGFbeta in Cancer. Cell *134*, 215–230.

Michalopoulos, G.K. (2007). Liver regeneration. J. Cell. Physiol. *213*, 286–300.

Michalopoulos, G.K. (2010). Liver regeneration after partial hepatectomy: critical analysis of mechanistic dilemmas. Am. J. Pathol. *176*, 2–13.

Mima, K., Hayashi, H., Kuroki, H., Nakagawa, S., Okabe, H., Chikamoto, A., Watanabe, M., Beppu, T., and Baba, H. (2013). Epithelial-mesenchymal transition expression profiles as a prognostic factor for disease-free survival in hepatocellular carcinoma: Clinical significance of transforming growth factor-β signaling. Oncol. Lett. *5*, 149–154.

Minamishima, Y.A., Nakayama, K., and Nakayama, K.-I. (2002). Recovery of liver mass without proliferation of hepatocytes after partial hepatectomy in Skp2-deficient mice. Cancer Res. *62*, 995–999.

Mitchell, C., Nivison, M., Jackson, L.F., Fox, R., Lee, D.C., Campbell, J.S., and Fausto, N. (2005). Heparin-binding epidermal growth factor-like growth factor links hepatocyte priming with cell cycle progression during liver regeneration. J. Biol. Chem. *280*, 2562–2568.

Miyaoka, Y., Ebato, K., Kato, H., Arakawa, S., Shimizu, S., and Miyajima, A. (2012). Hypertrophy and Unconventional Cell Division of Hepatocytes Underlie Liver Regeneration. Curr. Biol. *22*, 1166–1175.

Monga, S.P.S., Mars, W.M., Pediaditakis, P., Bell, A., Mulé, K., Bowen, W.C., Wang, X., Zarnegar, R., and Michalopoulos, G.K. (2002). Hepatocyte growth factor induces Wnt-independent nuclear translocation of beta-catenin after Met-beta-catenin dissociation in hepatocytes. Cancer Res. *62*, 2064–2071.

Morandell, S., Stasyk, T., Skvortsov, S., Ascher, S., and Huber, L.A. (2008). Quantitative proteomics and phosphoproteomics reveal novel insights into complexity and dynamics of the EGFR signaling network. Proteomics *8*, 4383–4401.

Moreno-Càceres, J., Caja, L., Mainez, J., Mayoral, R., Martín-Sanz, P., Moreno-Vicente, R., Del Pozo, M.Á., Dooley, S., Egea, G., and Fabregat, I. (2014). Caveolin-1 is required for TGF-β-induced transactivation of the EGF receptor pathway in hepatocytes through the activation of the metalloprotease TACE/ADAM17. Cell Death Dis. *5*, e1326.

Moreno-Càceres, J. and Fabregat, I. (2016). Apoptosis in liver carcinogenesis and chemotherapy. Hepatic Oncology 10.2217/hep.15.27

Moreno-Càceres, J., Mainez, J., Mayoral, R., Martín-Sanz, P., Egea, G., and Fabregat, I. (2016). Caveolin-1-dependent activation of the metalloprotease TACE/ADAM17 by TGF-β in hepatocytes requires activation of Src and the NADPH oxidase NOX1. FEBS J. *283*, 1300–1310.

Morgillo, F., Woo, J.K., Kim, E.S., Hong, W.K., and Lee, H.-Y. (2006). Heterodimerization of insulin-like growth factor receptor/epidermal growth factor receptor and induction of survivin expression counteract the antitumor action of erlotinib. Cancer Res. *66*, 10100–10111.

Morrison, C.D., Parvani, J.G., and Schiemann, W.P. (2013). The relevance of the TGF-β Paradox to EMT-MET programs. Cancer Lett. *341*, 30–40.

Moustakas, A., and Heldin, C.-H. (2012). Induction of epithelial-mesenchymal transition by transforming growth factor β. Semin. Cancer Biol. *22*, 446–454.

Moustakas, A., and Heldin, C.-H. (2016). Mechanisms of TGFβ-Induced Epithelial-Mesenchymal Transition. J. Clin. Med. *5*, E63.

Murawaki, Y., Ikuta, Y., Nishimura, Y., Koda, M., and Kawasaki, H. (1996). Serum markers for fibrosis and plasma transforming growth factor-beta 1 in patients with hepatocellular carcinoma in comparison with patients with liver cirrhosis. J. Gastroenterol. Hepatol. *11*, 443–450.

Murillo, M.M., del Castillo, G., Sánchez, A., Fernández, M., and Fabregat, I. (2005). Involvement of EGF receptor and c-Src in the survival signals induced by TGF-beta1 in hepatocytes. Oncogene *24*, 4580–4587.

Murillo, M.M., Carmona-Cuenca, I., Del Castillo, G., Ortiz, C., Roncero, C., Sánchez, A., Fernández, M., and Fabregat, I. (2007). Activation of NADPH oxidase by transforming growth factor-beta in hepatocytes mediates up-regulation of epidermal growth factor receptor ligands through a nuclear factor-kappaB-dependent mechanism. Biochem. J. *405*, 251–259.

Nagahara, H., Ezhevsky, S.A., Vocero-Akbani, A.M., Kaldis, P., Solomon, M.J., and Dowdy, S.F. (1999). Transforming growth factor beta targeted inactivation of cyclin E:cyclin-

dependent kinase 2 (Cdk2) complexes by inhibition of Cdk2 activating kinase activity. Proc. Natl. Acad. Sci. U. S. A. *96*, 14961–14966.

Nalesnik, M.A., and Michalopoulos, G.K. (2012). Growth factor pathways in development and progression of hepatocellular carcinoma. Front. Biosci. Sch. Ed. *4*, 1487–1515.

Nalluri, S.M., O'Connor, J.W., and Gomez, E.W. (2015). Cytoskeletal signaling in TGFβ-induced epithelial-mesenchymal transition. Cytoskelet. Hoboken *72*, 557–569.

Natarajan, A., Wagner, B., and Sibilia, M. (2007). The EGF receptor is required for efficient liver regeneration. Proc. Natl. Acad. Sci. U. S. A. *104*, 17081–17086.

Obayashi, Y., Campbell, J.S., Fausto, N., and Yeung, R.S. (2013). Impaired lipid accumulation in the liver of Tsc2-heterozygous mice during liver regeneration. Biochem. Biophys. Res. Commun. *437*, 146–150.

Oe, S., Lemmer, E.R., Conner, E.A., Factor, V.M., Levéen, P., Larsson, J., Karlsson, S., and Thorgeirsson, S.S. (2004). Intact signaling by transforming growth factor beta is not required for termination of liver regeneration in mice. Hepatology *40*, 1098–1105.

Ortiz, C., Caja, L., Sancho, P., Bertran, E., and Fabregat, I. (2008). Inhibition of the EGF receptor blocks autocrine growth and increases the cytotoxic effects of doxorubicin in rat hepatoma cells: role of reactive oxygen species production and glutathione depletion. Biochem. Pharmacol. *75*, 1935–1945.

Ortiz, C., Caja, L., Bertran, E., Gonzalez-Rodriguez, Á., Valverde, Á.M., Fabregat, I., and Sancho, P. (2012). Protein-tyrosine phosphatase 1B (PTP1B) deficiency confers resistance to transforming growth factor-β (TGF-β)-induced suppressor effects in hepatocytes. J. Biol. Chem. *287*, 15263–15274.

Padua, D., and Massagué, J. (2009). Roles of TGFbeta in metastasis. Cell Res. *19*, 89–102.

Panková, K., Rösel, D., Novotný, M., and Brábek, J. (2010). The molecular mechanisms of transition between mesenchymal and amoeboid invasiveness in tumor cells. Cell. Mol. Life Sci. CMLS *67*, 63–71.

Paranjpe, S., Bowen, W.C., Tseng, G.C., Luo, J.-H., Orr, A., and Michalopoulos, G.K. (2010). RNA interference against hepatic epidermal growth factor receptor has suppressive effects on liver regeneration in rats. Am. J. Pathol. *176*, 2669–2681.

Paranjpe, S., Bowen, W.C., Mars, W.M., Orr, A., Haynes, M.M., DeFrances, M.C., Liu, S., Tseng, G.C., Tsagianni, A., and Michalopoulos, G.K. (2016). Combined systemic elimination

of MET and EGFR signaling completely abolishes liver regeneration and leads to liver decompensation. Hepatology.

Park, S.S., Eom, Y.-W., Kim, E.H., Lee, J.H., Min, D.S., Kim, S., Kim, S.-J., and Choi, K.S. (2004). Involvement of c-Src kinase in the regulation of TGF-beta1-induced apoptosis. Oncogene *23*, 6272–6281.

Parsons, J.T., Horwitz, A.R., and Schwartz, M.A. (2010). Cell adhesion: integrating cytoskeletal dynamics and cellular tension. Nat. Rev. Mol. Cell Biol. *11*, 633–643.

Pellicoro, A., Ramachandran, P., Iredale, J.P., and Fallowfield, J.A. (2014). Liver fibrosis and repair: immune regulation of wound healing in a solid organ. Nat. Rev. Immunol. *14*, 181–194.

Petritsch, C., Beug, H., Balmain, A., and Oft, M. (2000). TGF-beta inhibits p70 S6 kinase via protein phosphatase 2A to induce G(1) arrest. Genes Dev. *14*, 3093–3101.

Petrocca, F., Vecchione, A., and Croce, C.M. (2008). Emerging role of miR-106b-25/miR-17-92 clusters in the control of transforming growth factor beta signaling. Cancer Res. *68*, 8191–8194.

Ramakrishna, G., Rastogi, A., Trehanpati, N., Sen, B., Khosla, R., and Sarin, S.K. (2013). From cirrhosis to hepatocellular carcinoma: new molecular insights on inflammation and cellular senescence. Liver Cancer *2*, 367–383.

Ramjaun, A.R., Tomlinson, S., Eddaoudi, A., and Downward, J. (2007). Upregulation of two BH3-only proteins, Bmf and Bim, during TGF beta-induced apoptosis. Oncogene *26*, 970–981.

Rani, B., Cao, Y., Malfettone, A., Tomuleasa, C., Fabregat, I., and Giannelli, G. (2014). Role of the tissue microenvironment as a therapeutic target in hepatocellular carcinoma. World J. Gastroenterol. *20*, 4128–4140.

Revuelta-Cervantes, J., Mayoral, R., Miranda, S., González-Rodríguez, A., Fernández, M., Martín-Sanz, P., and Valverde, A.M. (2011). Protein Tyrosine Phosphatase 1B (PTP1B) deficiency accelerates hepatic regeneration in mice. Am. J. Pathol. *178*, 1591–1604.

Riehle, K.J., Dan, Y.Y., Campbell, J.S., and Fausto, N. (2011). New concepts in liver regeneration. J. Gastroenterol. Hepatol. *26*, 203–212.

Romero-Gallo, J., Sozmen, E.G., Chytil, A., Russell, W.E., Whitehead, R., Parks, W.T., Holdren, M.S., Her, M.F., Gautam, S., Magnuson, M., et al. (2005). Inactivation of TGF-beta signaling in hepatocytes results in an increased proliferative response after partial hepatectomy. Oncogene *24*, 3028–3041.

Rozga, J. (2002). Hepatocyte proliferation in health and in liver failure. Med. Sci. Monit. *8*, RA32-38.

Rudnick, D.A., and Davidson, N.O. (2012). Functional Relationships between Lipid Metabolism and Liver Regeneration. Int. J. Hepatol. *2012*, 549241.

Sadok, A., and Marshall, C.J. (2014). Rho GTPases: masters of cell migration. Small GTPases *5*, e29710.

Sahai, E., and Marshall, C.J. (2003). Differing modes of tumour cell invasion have distinct requirements for Rho/ROCK signalling and extracellular proteolysis. Nat. Cell Biol. *5*, 711–719.

Saito, Y., and Berk, B.C. (2001). Transactivation: a novel signaling pathway from angiotensin II to tyrosine kinase receptors. J. Mol. Cell. Cardiol. *33*, 3–7.

Sánchez, A., and Fabregat, I. (2009). Genetically modified animal models recapitulating molecular events altered in human hepatocarcinogenesis. Clin. Transl. Oncol. *11*, 208–214.

Sánchez, A., Alvarez, A.M., Benito, M., and Fabregat, I. (1996). Apoptosis induced by transforming growth factor-beta in fetal hepatocyte primary cultures: involvement of reactive oxygen intermediates. J. Biol. Chem. *271*, 7416–7422.

Sánchez, A., Alvarez, A.M., Benito, M., and Fabregat, I. (1997). Cycloheximide prevents apoptosis, reactive oxygen species production, and glutathione depletion induced by transforming growth factor beta in fetal rat hepatocytes in primary culture. Hepatology *26*, 935–943.

Sánchez, A., Pagan, R., Alvarez, A.M., Roncero, C., Vilaró, S., Benito, M., and Fabregat, I. (1998). Transforming growth factor-beta (TGF-beta) and EGF promote cord-like structures that indicate terminal differentiation of fetal hepatocytes in primary culture. Exp. Cell Res. *242*, 27–37.

Sánchez, A., Alvarez, A.M., López Pedrosa, J.M., Roncero, C., Benito, M., and Fabregat, I. (1999). Apoptotic response to TGF-beta in fetal hepatocytes depends upon their state of differentiation. Exp. Cell Res. *252*, 281–291.

Sancho, P., and Fabregat, I. (2010). NADPH oxidase NOX1 controls autocrine growth of liver tumor cells through up-regulation of the epidermal growth factor receptor pathway. J. Biol. Chem. *285*, 24815–24824.

Sancho, P., and Fabregat, I. (2011). The NADPH oxidase inhibitor VAS2870 impairs cell growth and enhances TGF-β-induced apoptosis of liver tumor cells. Biochem. Pharmacol. *81*, 917–924.

Sancho, P., Bertran, E., Caja, L., Carmona-Cuenca, I., Murillo, M.M., and Fabregat, I. (2009). The inhibition of the epidermal growth factor (EGF) pathway enhances TGF-beta-induced apoptosis in rat hepatoma cells through inducing oxidative stress coincident with a change in the expression pattern of the NADPH oxidases (NOX) isoforms. Biochim. Biophys. Acta *1793*, 253–263.

Sanz-Moreno, V., and Marshall, C.J. (2010). The plasticity of cytoskeletal dynamics underlying neoplastic cell migration. Curr. Opin. Cell Biol. *22*, 690–696.

Sanz-Moreno, V., Gadea, G., Ahn, J., Paterson, H., Marra, P., Pinner, S., Sahai, E., and Marshall, C.J. (2008). Rac activation and inactivation control plasticity of tumor cell movement. Cell *135*, 510–523.

Scaltriti, M., and Baselga, J. (2006). The epidermal growth factor receptor pathway: a model for targeted therapy. Clin. Cancer Res. *12*, 5268–5272.

Schaeffer, D., Somarelli, J.A., Hanna, G., Palmer, G.M., and Garcia-Blanco, M.A. (2014). Cellular migration and invasion uncoupled: increased migration is not an inexorable consequence of epithelial-to-mesenchymal transition. Mol. Cell. Biol. *34*, 3486–3499.

Scheving, L.A., Zhang, X., Garcia, O.A., Wang, R.F., Stevenson, M.C., Threadgill, D.W., and Russell, W.E. (2014). Epidermal growth factor receptor plays a role in the regulation of liver and plasma lipid levels in adult male mice. Am. J. Physiol. Gastrointest. Liver Physiol. *306*, G370-381.

Schiffer, E., Housset, C., Cacheux, W., Wendum, D., Desbois-Mouthon, C., Rey, C., Clergue, F., Poupon, R., Barbu, V., and Rosmorduc, O. (2005). Gefitinib, an EGFR inhibitor, prevents hepatocellular carcinoma development in the rat liver with cirrhosis. Hepatology *41*, 307–314.

Schlachterman, A., Craft, W.W., Hilgenfeldt, E., Mitra, A., and Cabrera, R. (2015). Current and future treatments for hepatocellular carcinoma. World J. Gastroenterol. *21*, 8478–8491.

Scholzen, T., and Gerdes, J. (2000). The Ki-67 protein: from the known and the unknown. J. Cell. Physiol. *182*, 311–322.

Schulze, K., Nault, J.-C., and Villanueva, A. (2016). Genetic profiling of hepatocellular carcinoma using next-generation sequencing. J. Hepatol. S0168-8278-5.

Seoane, J. (2006). Escaping from the TGFbeta anti-proliferative control. Carcinogenesis *27*, 2148–2156.

Seoane, J., Le, H.-V., Shen, L., Anderson, S.A., and Massagué, J. (2004). Integration of Smad and forkhead pathways in the control of neuroepithelial and glioblastoma cell proliferation. Cell *117*, 211–223.

Shimizu, M., Hara, A., Okuno, M., Matsuno, H., Okada, K., Ueshima, S., Matsuo, O., Niwa, M., Akita, K., Yamada, Y., et al. (2001). Mechanism of retarded liver regeneration in plasminogen activator-deficient mice: impaired activation of hepatocyte growth factor after Fas-mediated massive hepatic apoptosis. Hepatology *33*, 569–576.

Shteyer, E., Liao, Y., Muglia, L.J., Hruz, P.W., and Rudnick, D.A. (2004). Disruption of hepatic adipogenesis is associated with impaired liver regeneration in mice. Hepatology *40*, 1322–1332.

Shtutman, M., Zhurinsky, J., Simcha, I., Albanese, C., D'Amico, M., Pestell, R., and Ben-Ze'ev, A. (1999). The cyclin D1 gene is a target of the β-catenin/LEF-1 pathway. Proc. Natl. Acad. Sci. *96*, 5522–5527.

Sia, D., and Villanueva, A. (2011). Signaling pathways in hepatocellular carcinoma. Oncology *81*, 18–23.

Siriwardena, A.K., Mason, J.M., Mullamitha, S., Hancock, H.C., and Jegatheeswaran, S. (2014). Management of colorectal cancer presenting with synchronous liver metastases. Nat. Rev. Clin. Oncol. *11*, 446–459.

Si-Tayeb, K., Lemaigre, F.P., and Duncan, S.A. (2010). Organogenesis and development of the liver. Dev. Cell *18*, 175–189.

Song, K., Wang, H., Krebs, T.L., and Danielpour, D. (2006). Novel roles of Akt and mTOR in suppressing TGF-beta/ALK5-mediated Smad3 activation. EMBO J. *25*, 58–69.

Spano, D., Heck, C., De Antonellis, P., Christofori, G., and Zollo, M. (2012). Molecular networks that regulate cancer metastasis. Semin. Cancer Biol. *22*, 234–249.

Spear, B.T., Jin, L., Ramasamy, S., and Dobierzewska, A. (2006). Transcriptional control in the mammalian liver: liver development, perinatal repression, and zonal gene regulation. Cell. Mol. Life Sci. *63*, 2922–2938.

Stanley, A., Thompson, K., Hynes, A., Brakebusch, C., and Quondamatteo, F. (2014). NADPH oxidase complex-derived reactive oxygen species, the actin cytoskeleton, and Rho GTPases in cell migration. Antioxid. Redox Signal. *20*, 2026–2042.

Tabrizian, P., Roayaie, S., and Schwartz, M.E. (2014). Current management of hepatocellular carcinoma. World J. Gastroenterol. *20*, 10223–10237.

Tateishi, M., Ishida, T., Mitsudomi, T., Kaneko, S., and Sugimachi, K. (1990). Immunohistochemical evidence of autocrine growth factors in adenocarcinoma of the human lung. Cancer Res. *50*, 7077–7080.

Taub, R. (2004). Liver regeneration: from myth to mechanism. Nat. Rev. Mol. Cell Biol. *5*, 836–847.

Teramoto, T., Kiss, A., and Thorgeirsson, S.S. (1998). Induction of p53 and Bax during TGF-beta 1 initiated apoptosis in rat liver epithelial cells. Biochem. Biophys. Res. Commun. *251*, 56–60.

Thiery, J.P. (2003). Epithelial-mesenchymal transitions in development and pathologies. Curr. Opin. Cell Biol. *15*, 740–746.

Toffanin, S., Hoshida, Y., Lachenmayer, A., Villanueva, A., Cabellos, L., Minguez, B., Savic, R., Ward, S.C., Thung, S., Chiang, D.Y., et al. (2011). MicroRNA-based classification of hepatocellular carcinoma and oncogenic role of miR-517a. Gastroenterology *140*, 1618–1628.e16.

Tsiambas, E., Manaios, L., Papanikolopoulos, C., Rigopoulos, D.N., Tsounis, D., Karameris, A., Soultati, A., Koliopoulou, A., Kravvaritis, C., Sergentanis, T., et al. (2009). Chromogenic in situ hybridization analysis of Epidermal Growth Factor Receptor gene/chromosome 7 numerical aberrations in hepatocellular carcinoma based on tissue microarrays. Pathol. Oncol. Res. *15*, 511–520.

Utsunomiya, T., Shimada, M., Imura, S., Morine, Y., Ikemoto, T., and Mori, M. (2010). Molecular signatures of noncancerous liver tissue can predict the risk for late recurrence of hepatocellular carcinoma. J. Gastroenterol. *45*, 146–152.

Vacca, M., Degirolamo, C., Massafra, V., Polimeno, L., Mariani-Costantini, R., Palasciano, G., and Moschetta, A. (2013). Nuclear receptors in regenerating liver and hepatocellular carcinoma. Mol. Cell. Endocrinol. *368*, 108–119.

Valdés, F., Alvarez, A.M., Locascio, A., Vega, S., Herrera, B., Fernández, M., Benito, M., Nieto, M.A., and Fabregat, I. (2002). The epithelial mesenchymal transition confers resistance to the apoptotic effects of transforming growth factor Beta in fetal rat hepatocytes. Mol. Cancer Res. *1*, 68–78.

Valdés, F., Murillo, M.M., Valverde, A.M., Herrera, B., Sánchez, A., Benito, M., Fernández, M., and Fabregat, I. (2004). Transforming growth factor-beta activates both pro-apoptotic and survival signals in fetal rat hepatocytes. Exp. Cell Res. *292*, 209–218.

Valverde, A.M., Burks, D.J., Fabregat, I., Fisher, T.L., Carretero, J., White, M.F., and Benito, M. (2003). Molecular mechanisms of insulin resistance in IRS-2-deficient hepatocytes. Diabetes *52*, 2239–2248.

Vega, S., Morales, A.V., Ocaña, O.H., Valdés, F., Fabregat, I., and Nieto, M.A. (2004). Snail blocks the cell cycle and confers resistance to cell death. Genes Dev. *18*, 1131–1143.

Villanueva, A., Hernandez-Gea, V., and Llovet, J.M. (2013). Medical therapies for hepatocellular carcinoma: a critical view of the evidence. Nat. Rev. Gastroenterol. Hepatol. *10*, 34–42.

Wallace, M.C., and Friedman, S.L. (2014). Hepatic fibrosis and the microenvironment: fertile soil for hepatocellular carcinoma development. Gene Expr. *16*, 77–84.

Wang, K., Lim, H.Y., Shi, S., Lee, J., Deng, S., Xie, T., Zhu, Z., Wang, Y., Pocalyko, D., Yang, W.J., et al. (2013). Genomic landscape of copy number aberrations enables the identification of oncogenic drivers in hepatocellular carcinoma. Hepatology *58*, 706–717.

Wang, S.E., Xiang, B., Guix, M., Olivares, M.G., Parker, J., Chung, C.H., Pandiella, A., and Arteaga, C.L. (2008). Transforming growth factor beta engages TACE and ErbB3 to activate phosphatidylinositol-3 kinase/Akt in ErbB2-overexpressing breast cancer and desensitizes cells to trastuzumab. Mol. Cell. Biol. *28*, 5605–5620.

Warming, S., Costantino, N., Court, D.L., Jenkins, N.A., and Copeland, N.G. (2005). Simple and highly efficient BAC recombineering using galK selection. Nucleic Acids Res. *33*, e36.

Werneburg, N.W., Yoon, J.-H., Higuchi, H., and Gores, G.J. (2003). Bile acids activate EGF receptor via a TGF-alpha-dependent mechanism in human cholangiocyte cell lines. Am. J. Physiol. Gastrointest. Liver Physiol. *285*, G31-36.

Wertheimer, C., Liegl, R., Kernt, M., Docheva, D., Kampik, A., and Eibl-Lindner, K.H. (2014). EGFR-blockade with erlotinib reduces EGF and TGF-β2 expression and the actin-cytoskeleton which influences different aspects of cellular migration in lens epithelial cells. Curr. Eye Res. *39*, 1000–1012.

Whittaker, S., Marais, R., and Zhu, A.X. (2010). The role of signaling pathways in the development and treatment of hepatocellular carcinoma. Oncogene *29*, 4989–5005.

Wiesner, S., Lange, A., and Fässler, R. (2006). Local call: from integrins to actin assembly. Trends Cell Biol. *16*, 327–329.

Wilkes, M.C., Mitchell, H., Penheiter, S.G., Doré, J.J., Suzuki, K., Edens, M., Sharma, D.K., Pagano, R.E., and Leof, E.B. (2005). Transforming growth factor-beta activation of

phosphatidylinositol 3-kinase is independent of Smad2 and Smad3 and regulates fibroblast responses via p21-activated kinase-2. Cancer Res. *65*, 10431–10440.

Wisdom, R., Johnson, R.S., and Moore, C. (1999). c-Jun regulates cell cycle progression and apoptosis by distinct mechanisms. EMBO J. *18*, 188–197.

Wu, Y., Qiao, X., Qiao, S., and Yu, L. (2011). Targeting integrins in hepatocellular carcinoma. Expert Opin. Ther. Targets *15*, 421–437.

Yamada, S., Okumura, N., Wei, L., Fuchs, B.C., Fujii, T., Sugimoto, H., Nomoto, S., Takeda, S., Tanabe, K.K., and Kodera, Y. (2014). Epithelial to mesenchymal transition is associated with shorter disease-free survival in hepatocellular carcinoma. Ann. Surg. Oncol. *21*, 3882–3890.

Yu, J., Zhang, L., Chen, A., Xiang, G., Wang, Y., Wu, J., Mitchelson, K., Cheng, J., and Zhou, Y. (2008). Identification of the gene transcription and apoptosis mediated by TGF-beta-Smad2/3-Smad4 signaling. J. Cell. Physiol. *215*, 422–433.

Yuan, B., Dong, R., Shi, D., Zhou, Y., Zhao, Y., Miao, M., and Jiao, B. (2011). Down-regulation of miR-23b may contribute to activation of the TGF-β1/Smad3 signalling pathway during the termination stage of liver regeneration. FEBS Lett. *585*, 927–934.

Yue, P., Zhang, X., Paladino, D., Sengupta, B., Ahmad, S., Holloway, R.W., Ingersoll, S.B., and Turkson, J. (2012). Hyperactive EGF receptor, Jaks and Stat3 signaling promote enhanced colony-forming ability, motility and migration of cisplatin-resistant ovarian cancer cells. Oncogene *31*, 2309–2322.

Zandi, R., Larsen, A.B., Andersen, P., Stockhausen, M.-T., and Poulsen, H.S. (2007). Mechanisms for oncogenic activation of the epidermal growth factor receptor. Cell. Signal. *19*, 2013–2023.

Zhai, X., Zhu, H., Wang, W., Zhang, S., Zhang, Y., and Mao, G. (2014). Abnormal expression of EMT-related proteins, S100A4, vimentin and E-cadherin, is correlated with clinicopathological features and prognosis in HCC. Med. Oncol. *31*, 970.

Zhang, D.Y., and Friedman, S.L. (2012). Fibrosis-dependent mechanisms of hepatocarcinogenesis. Hepatology *56*, 769–775.

Zimmermann, A. (2004). Regulation of liver regeneration. Nephrol. Dial. Transplant. *19 Suppl 4:iv6-10.*, iv6-10.

Zou, Y., Bao, Q., Kumar, S., Hu, M., Wang, G.-Y., and Dai, G. (2012). Four waves of hepatocyte proliferation linked with three waves of hepatic fat accumulation during partial hepatectomy-induced liver regeneration. PloS One *7*, e30675.

IX. APPENDIX

HEPATOLOGY
Official Journal of the American Association for the Study of Liver Diseases

Overactivation of the TGF-β Pathway Confers a Mesenchymal-Like Phenotype and CXCR4-Dependent Migratory Properties to Liver Tumor Cells

Esther Bertran,[1] Eva Crosas-Molist,[1] Patricia Sancho,[1] Laia Caja,[1] Judit Lopez-Luque,[1] Estanislao Navarro,[1] Gustavo Egea,[2] Raquel Lastra,[3] Teresa Serrano,[4] Emilio Ramos,[3] and Isabel Fabregat[1,5]

Transforming growth factor-beta (TGF-β) is an important regulatory suppressor factor in hepatocytes. However, liver tumor cells develop mechanisms to overcome its suppressor effects and respond to this cytokine by inducing other processes, such as the epithelial-mesenchymal transition (EMT), which contributes to tumor progression and dissemination. Recent studies have placed chemokines and their receptors at the center not only of physiological cell migration but also of pathological processes, such as metastasis in cancer. In particular, CXCR4 and its ligand, stromal cell-derived factor 1α (SDF-1α) / chemokine (C-X-C motif) ligand 12 (CXCL12) have been revealed as regulatory molecules involved in the spreading and progression of a variety of tumors. Here we show that autocrine stimulation of TGF-β in human liver tumor cells correlates with a mesenchymal-like phenotype, resistance to TGF-β-induced suppressor effects, and high expression of CXCR4, which is required for TGF-β-induced cell migration. Silencing of the TGF-β receptor1 (TGFBR1), or its specific inhibition, recovered the epithelial phenotype and attenuated CXCR4 expression, inhibiting cell migratory capacity. In an experimental mouse model of hepatocarcinogenesis (diethylnitrosamine-induced), tumors showed increased activation of the TGF-β pathway and enhanced CXCR4 levels. In human hepatocellular carcinoma tumors, high levels of CXCR4 always correlated with activation of the TGF-β pathway, a less differentiated phenotype, and a cirrhotic background. CXCR4 concentrated at the tumor border and perivascular areas, suggesting its potential involvement in tumor cell dissemination. *Conclusion*: A crosstalk exists among the TGF-β and CXCR4 pathways in liver tumors, reflecting a novel molecular mechanism that explains the protumorigenic effects of TGF-β and opens new perspectives for tumor therapy. (HEPATOLOGY 2013;58:2032-2044)

Transforming growth factor-beta (TGF-β) is an important regulatory suppressor factor; however, paradoxically, it also modulates other processes that contribute to tumorigenesis, such as fibrosis, immune regulation, microenvironment modification, and cell invasion.[1] Indeed, in addition to its suppressor effects, TGF-β induces antiapoptotic signals in fetal hepatocytes and hepatoma cells,[2,3] through activation of the epidermal growth factor receptor (EGFR) pathway.[4] Cells that survive to TGF-β-induced apoptotic signals undergo epithelial-mesenchymal transition (EMT).[3,5,6] Upon progression of liver cancer, EMT is considered a key process that may drive intrahepatic metastasis.[7] TGF-β levels are increased in hepatocellular carcinoma (HCC) tissue, plasma, and urine and decreased in patients who

Abbreviations: CDH1, E-cadherin; CK-18, cytokeratin; CXCL12/SDF-1α, stromal cell-derived factor 1α; DEN, diethylnitrosamine; EGFR, the epidermal growth factor receptor; EMT, epithelial-mesenchymal transition; HCC, hepatocellular carcinoma; TGF-β, transforming growth factor-beta; TGFBR1, transforming growth factor-beta receptor-1

From the [1]Bellvitge Biomedical Research Institute (IDIBELL), L'Hospitalet de Llobregat, Barcelona, Spain; [2]Department of Cell Biology, Immunology and Neuroscience, University of Barcelona, Spain; [3]Department of Surgery, Liver Transplant Unit, University Hospital of Bellvitge, Barcelona, Spain; [4]Pathological Anatomy Service, University Hospital of Bellvitge, Barcelona, Spain; [5]Department of Physiological Sciences-II, University of Barcelona, Spain.

Received February 4, 2013; accepted June 15, 2013.

Supported by grants to I.F. from the Ministry of Economy and Competitiveness (MINECO), Spain (BFU2009-07219, BFU2012-35538, and ISCIII-RTICC RD06/0020) and AGAUR-Generalitat de Catalunya (2009SGR-312). E.C-M. was the recipient of a predoctoral fellowship from the FPU program, Ministry of Education, Culture and Sport, Spain.

underwent effective therapy for HCC.[8] Liver tumors expressing late TGF-β-responsive genes (antiapoptotic and EMT-related genes) display a higher invasive phenotype and increased tumor recurrence when compared to those that show an early TGF-β signature (suppressor genes).[9] Interestingly, blocking TGF-β up-regulates E-cadherin and reduces migration and invasion of HCC cells.[10]

Recent studies place chemokines and their receptors at the center not only of physiological cell migration, but also of pathological processes, such as metastasis in cancer.[11] In particular, CXCR4 and its ligand, stromal cell-derived factor 1α (SDF-1α) / chemokine (C-X-C motif) ligand 12 (CXCL12), have been revealed as important molecules involved in the spreading and progression of a variety of tumors.[12] Different data suggest that molecular strategies to inhibit the CXCR4/CXCL12 pathway could be of therapeutic use for the treatment of HCC.[13] CXCR4 is up-regulated in human HCC,[14] correlating with progression of the disease.[15] Its ligand CXCL12 stimulates human hepatoma cell growth, migration, and invasion.[14] We have recently described that TGF-β up-regulates CXCR4 in rat hepatoma cells[16] and sensitizes cells to respond to CXCL12, which mediates cell scattering and survival. These results suggest a crosstalk between the increased protumorigenic response to TGF-β and the establishment of a functional CXCR4/CXCL12 axis. Nothing is known about whether a similar situation occurs in human liver tumorigenesis.

The aim of this work was to analyze whether autocrine stimulation of TGF-β in human liver tumors may induce up-regulation, and/or intracellular reorganization, of CXCR4, which, concomitant with the EMT process induced by this factor, would contribute to the enhancement of cell migration and invasion.

Materials and Methods

Ethics Statement. Approval for experiments related to the study of liver carcinogenesis in experimental animal models was obtained from the General Direction of Environment and Biodiversity, Government of Catalonia, #4589, 2011. All animals received humane care and study protocols comply with the institution's guidelines. Human tissues were collected with the required approvals from the Institutional Review Board (Comité Ético de Investigación Clínica del Hospital Universitario de Bellvitge) and patient's written consent conformed to the ethical guidelines of the 1975 Declaration of Helsinki.

Cell Culture. Cell lines used in this study were from commercial sources. Hep3B, HepG2, and PLC/PRF/5 were obtained from the European Collection of Cell Cultures (ECACC). SNU449 were obtained from the American Tissue Culture Collection (ATCC). Huh7 and HLF cells were from the Japanese Collection of Research Bioresources (JCRB Cell Bank) and were kindly provided by Dr. Perales (University of Barcelona, Spain) and Dr. Giannelli (University of Bari, Italy), respectively. Cell lines were never used in the laboratory for longer than 4 months after receipt or resuscitation.

HepG2 and Hep3B were maintained in modified Eagle's medium (MEM) medium, PLC/PRF/5 and Huh7 in Dulbecco's modified Eagle's medium (DMEM) medium, SNU449 and HLF in RPMI medium. Neonatal mice hepatocytes were immortalized as described[17] and cultured in DMEM. All media (Lonza, Basel, Switzerland) were supplemented with 10% fetal bovine serum (FBS; Sera Laboratories International, Cinder Hill, UK) and cells maintained in a humidified atmosphere of 37°C, 5% CO_2. Analysis of cell viability was performed by Crystal violet staining.[3]

Immunofluorescence Staining. Fluorescence microscopy studies were performed as described[3] (further details in the Supporting Materials and Methods). Cells were visualized with a Nikon eclipse 80i microscope with the appropriate filters. Representative images were taken with a Nikon DS-Ri1 digital camera. ImageJ software (National Institutes of Health [NIH], Bethesda, MD) was used to analyze fluorescence from TIFF images captured using the same exposure conditions.

Immunohistochemistry. Human HCC tissues were obtained from the Pathological Anatomy Service, University Hospital of Bellvitge, Barcelona. Paraffin-embedded tissues were cut into 4-μm-thick sections, incubated with the specific primary antibody overnight at 4°C, and binding developed with the Vectastain ABC kit (Vector

Address reprint requests to: Isabel Fabregat, Bellvitge Biomedical Research Institute (IDIBELL), Gran Via de L'Hospitalet, 199, 08908 L'Hospitalet de Llobregat, Barcelona, Spain. E-mail: ifabregat@idibell.cat; fax: 34 932 607426.

View this article online at wileyonlinelibrary.com.

DOI 10.1002/hep.26597

Potential conflict of interest: Nothing to report.

Additional Supporting Information may be found in the online version of this article.

Laboratories, Burlingame, CA). Further information is supplied in the Supporting Materials and Methods.

Western Blot Analysis. Total protein extracts and western blotting procedures were carried out as described.[3] Source of antibodies are detailed in the Supporting Materials and Methods.

Analysis of Gene Expression. RNeasy Mini Kit (Qiagen, Valencia, CA) was used for total RNA isolation. Reverse transcription (RT) was carried out using the High Capacity Reverse Transcriptase kit (Applied Biosystems, Foster City, CA), and 500 ng of total RNA from each sample for complementary DNA synthesis. For details about semiquantitative and real-time polymerase chain reaction (PCR) reactions, see the Supporting Materials and Methods.

RNA Interference Assays. Cells at 70% confluence were transiently transfected with 50 nM small interfering RNA (siRNA) for 8 hours using TransIT-siQuest following the manufacturer's instructions (Mirus, Madison, WI). For stable transfection of short hairpin RNA (shRNA), cells at 50%-60% confluence were transfected with MATra-A reagent (IBA, Germany) according to the manufacturer's recommendation (15 minutes on the magnet plate, 2 μg/mL of shRNA plasmid). Four different plasmids of TGFBRI shRNA were transfected separately or combined, as well as a control shRNA. Protocols used were as described.[18] For siRNA sequences and further experimental details, see the Supporting Materials and Methods.

Migration Assays. Cell motility was examined by two different methods: (1) a wound-healing assay[16] and (2) real-time migration assay through the xCELLigence system (Roche Applied Science). For the wound-healing assay, cells were grown at basal conditions to 95% confluence and monolayers were scratched with a pipette tip (0 hours). Cell migration was recorded by phase contrast microscopy (Olympus IX-70) at 48 hours after wound scratch. For real-time monitoring of cell migration, the xCELLigence system was used; 4×10^4 cells/well were seeded onto the top chamber of a CIM plate, which features microelectronic sensors integrated on the underside of the microporous membrane of a Boyden-like chamber. CIM plates were placed onto the Real-Time Cell Analyzer (RTCA) station (xCELLigence System, Roche, Mannheim, Germany). Cell migration was continuously monitored by measuring changes in the electrical impedance at the electrode/cell interface, as a population of cells migrated from the top to the bottom chamber. Continuous values are represented as cell index (CI), a dimensionless parameter that reflects a relative change in measured electrical impedance, and quantified as a slope (h^{-1}) of the first 5 hours.

Diethylnitrosamine (DEN)-Induced Hepatocarcinogenesis in Mice. Male mice at day 15 of age received intraperitoneal injections of DEN (5 mg/kg) diluted in saline buffer, control animals were injected with saline buffer intraperitoneally. At 6, 9, and 12 months of age, mice were sacrificed and their livers removed. For histological studies, liver lobes were fixed in 4% paraformaldehyde overnight and paraffin-embedded for immunohistochemistry staining. Total RNA was isolated from frozen tissues to analyze gene expression by real-time quantitative PCR. Three to four animals/condition and two different tissue pieces/animal were processed for RNA extraction.

Statistics. All data represent at least three experiments and are expressed as the mean ± SEM. Differences between groups were compared using either Student t test or one-way analysis of variance (ANOVA) associated with Dunnett's test. Statistical significance was assumed when $P < 0.05$. The analysis was performed using GraphPad Prism software (Graph-Pad for Science, San Diego, CA). For data from human samples, statistical significance between means was determined by the nonparametric Mann-Whitney U test. Correlation between TGF-β and CXCR4 mRNA levels was determined by the Pearson correlation coefficient.

Results

Mesenchymal-Like Phenotype in HCC Cells Correlates With SMADs Activation and Resistance to TGF-β-Induced Suppressor Effects. In order to evaluate the relevance of the autocrine stimulation of TGF-β pathway in the acquisition of mesenchymal-like features, we analyzed the phenotype of six different human liver tumor cell lines whose characteristics are detailed in Supporting Table 1. A correlation between the decrease in E-cadherin and cytokeratin-18 (CK-18) expression, characteristics of an epithelial phenotype, and the appearance of cells expressing vimentin (a mesenchymal intermediate filament) was observed (Fig. 1A). The acquisition of a mesenchymal-like phenotype occurred concomitantly with an increase in the expression of *TGFB1* (Fig. 1B) and with nuclear localization of both SMAD2 and SMAD3 (Supporting Fig. 1). Analysis of TGF-β in the culture medium revealed increased amounts of this cytokine in mesenchymal-like versus epithelial cell lines. Furthermore, conditioned medium from mesenchymal-like HCC cells induced higher Smad2 phosphorylation in immortalized mice hepatocytes (Supporting Fig. 1). With the exception of the HepG2 cells that show mutations in *NRAS* and are

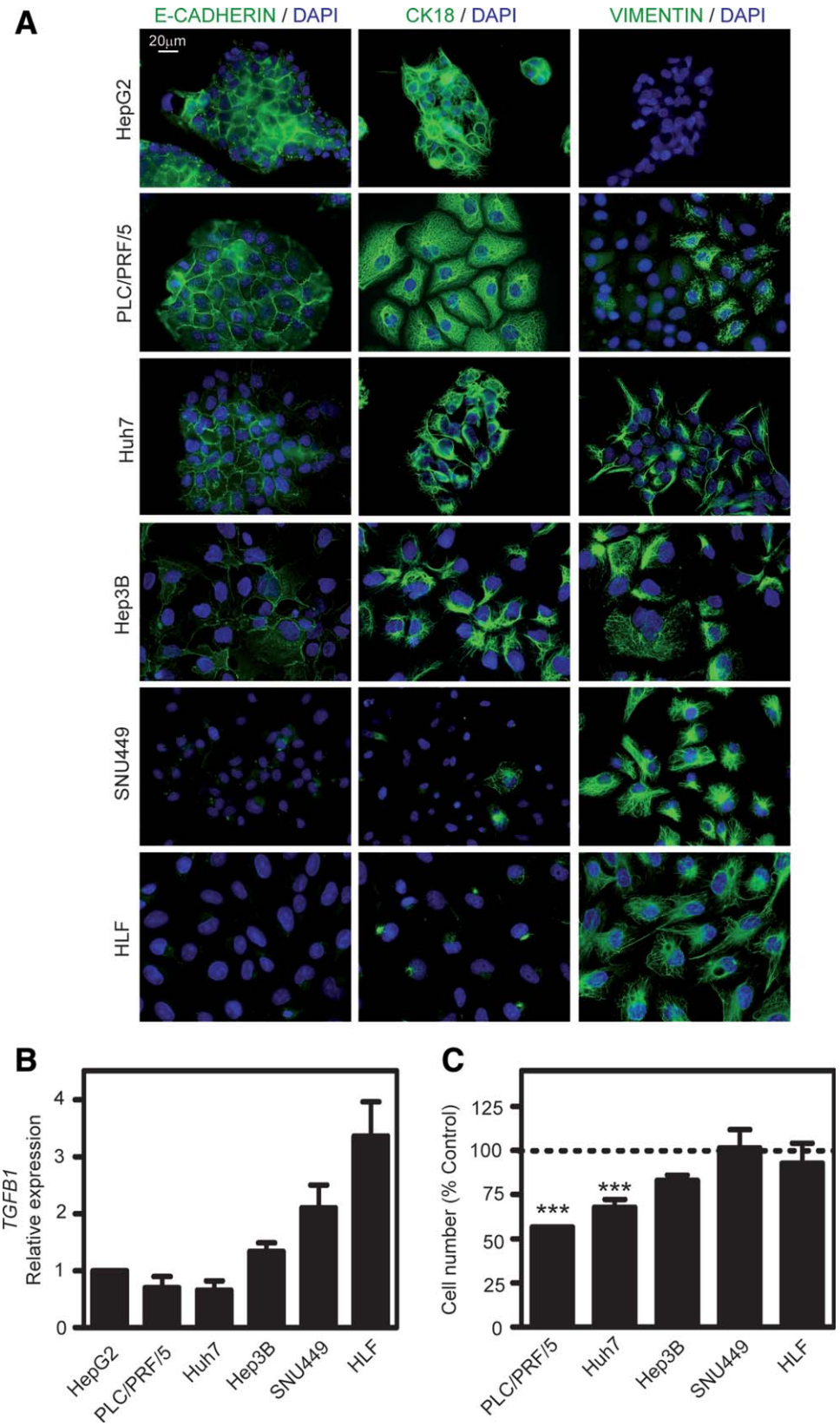

Fig. 1. Autocrine stimulation of the TGF-β pathway in HCC cells correlate with a mesenchymal-like phenotype and resistance to TGF-β-induced suppressor effects. HepG2, PLC/PRF/5, Huh7, Hep3B, SNU449, HLF were cultured under standard conditions in 10% FBS. (A) Immunofluorescence of E-cadherin (green), CK-18 (green), vimentin (green), and DAPI (blue). (B) *TGFB* expression levels determined by real-time PCR. Mean $\pm$ SEM (n = 5). (C) Effect of 48 hours of treatment with 2 ng/mL TGF-β on cell viability, analyzed by Crystal violet staining: data were calculated relative to zero time and represent the mean $\pm$ SEM of at least six independent experiments. Student *t* test was calculated versus zero time for each cell type: $***P < 0.001$.

resistant to TGF-β-induced suppressor effects,[19] the epithelial phenotype correlated with response to TGF-β as a cytostatic factor, whereas cells with a mesenchymal-like phenotype did not arrest proliferation in the presence of TGF-β (Fig. 1C). This behavior confirms a previous classification of these cell lines according to the TGF-β signature[9] (early for PLC/PRF/5 and Huh7; late for SNU449, HLF). Results in Hep3B indicate that these cells represent a transition from an epithelial to a mesenchymal-like phenotype, since they showed decreased expression of E-cadherin and simultaneous expression of epithelial (CK-18) and mesenchymal (vimentin) intermediate filaments (Fig. 1A). Interestingly, this mixed phenotype correlated with a high activation of the TGF-β pathway (Supporting Fig. 1) and lower suppressor response to this cytokine (Fig. 1C). In summary, mesenchymal-like phenotype in HCC cell lines correlates with autocrine stimulation of the TGF-β pathway and resistance to TGF-β-induced suppressor effects.

Mesenchymal-Like Phenotype in HCC Cells Correlates With CXCR4 Up-regulation and Asymmetric Distribution, Which Is Required for Cell Migration. The analysis of the cytoskeleton organization reflected that cells with more mesenchymal phenotype presented F-actin located in stress fibers, whereas the more epithelial ones showed more pericellular distribution (Fig. 2A, left panels). Cells with mesenchymal characteristics showed CXCR4 in an asymmetric distribution in a great percentage of them (Fig. 2A, right panels). HepG2 cells showed homogeneous distribution of CXCR4 with no apparent polarization, whereas in the epithelial Huh7 and PLC/PRF/5 localization of CXCR4 was variable, with some cells showing polarized areas, but a great percentage containing homogeneous intracellular localization (Fig. 2A, right panels, quantification of the protrusions in Fig. 2B). Furthermore, analysis of *CXCR4* expression at the messenger RNA (mRNA) levels revealed that cells with mesenchymal-like characteristics presented a higher expression of *CXCR4*, when compared with the more epithelial ones (such as HepG2) (Fig. 2C). Levels of *TGFB1* mRNA showed correlation not only with the mesenchymal-like phenotype, but also with *CXCR4* levels (Fig. 2D). In agreement with their mesenchymal characteristics and F-actin distribution, the migratory capacity of Hep3B and SNU449 was much higher than that observed in HepG2, analyzed through the xCELLigence technology or in a wound-healing assay (Fig. 2E,F). Interestingly, in mesenchymal-like cells, such as Hep3B (Fig. 2G) or SNU449 (results not shown), the cells in the migration front showed a strong polarization of CXCR4. The presence of AMD3100, a well-known inhibitor of the CXCR4 receptor, inhibited migration of both Hep3B and SNU449 (Fig. 2F). Furthermore, only cells that showed *CXCR4* elevated expression and asymmetrical distribution, such as SNU449, responded to CXCL12 inducing migration, whereas HepG2 cells did not (Supporting Fig. 2). All these results together indicate that autocrine stimulation of the TGF-β pathway in HCC cell lines correlates with activation of the CXCR4/CXCL12 axis, which mediates cell migration.

Targeting TGF-β Receptor I Attenuates the Mesenchymal Phenotype, Decreases CXCR4 Expression, and Impairs Cell Migration in HCC Cells. To analyze whether the autocrine stimulation of the TGF-β pathway induces CXCR4 expression and/or its asymmetric distribution, we stably silenced *TGFBR1* expression with specific shRNA in Hep3B (Fig. 3A) and PLC-PRF5 cells (Supporting Fig. 3). Increase in E-cadherin, which presented a pericellular distribution, and decrease in vimentin expression were observed in *TGFBR1*-silenced Hep3B cells (Fig. 3B,C, left). Cytoskeleton organization changed in the absence of *TGFBR1* expression, showing a more pericellular distribution and fewer stress fibers (Fig. 3C,D). *CXCR4* expression was inhibited in these cells (Fig. 3B,C, right, and D), which correlated with a significantly lower capacity to migrate (Fig. 3E). Silencing of *TGFBR1* also correlated with reorganization of cytoskeleton and attenuation of *CXCR4* expression and asymmetric distribution in PLC/PRF/5 cells (Supporting Fig. 3). A pharmacological inhibitor of the kinase activity of TGFBR1, LY36497, which attenuated SMAD2 phosphorylation in HCC cells both in the absence or presence of TGF-β (Supporting Fig. 4), decreased *CXCR4* levels (Fig. 4A), increased E-cadherin (*CDH1*) mRNA levels (although changes were more moderate and less significant than the *TGFBR1* silencing: Supporting Fig. 4), reorganized the cytoskeleton and decreased the percentage of cells with an asymmetric distribution of CXCR4 (Fig. 4B). Interestingly, treatment with LY36497 inhibited the capacity of cells to close the wound in migration experiments (Fig. 4C). In summary, TGF-β signaling is responsible for up-regulation and asymmetric distribution of CXCR4 in HCC cells.

Mice Tumors From DEN-Induced Liver Carcinogenesis Show High Expression of Both TGF-β1 and CXCR4. In order to know whether the TGF-β/CXCR4 crosstalk shows significance during *in vivo* hepatocarcinogenesis, we started with the analysis of tumors in a model of DEN-induced experimental liver tumorigenesis in mice. At different times after a single

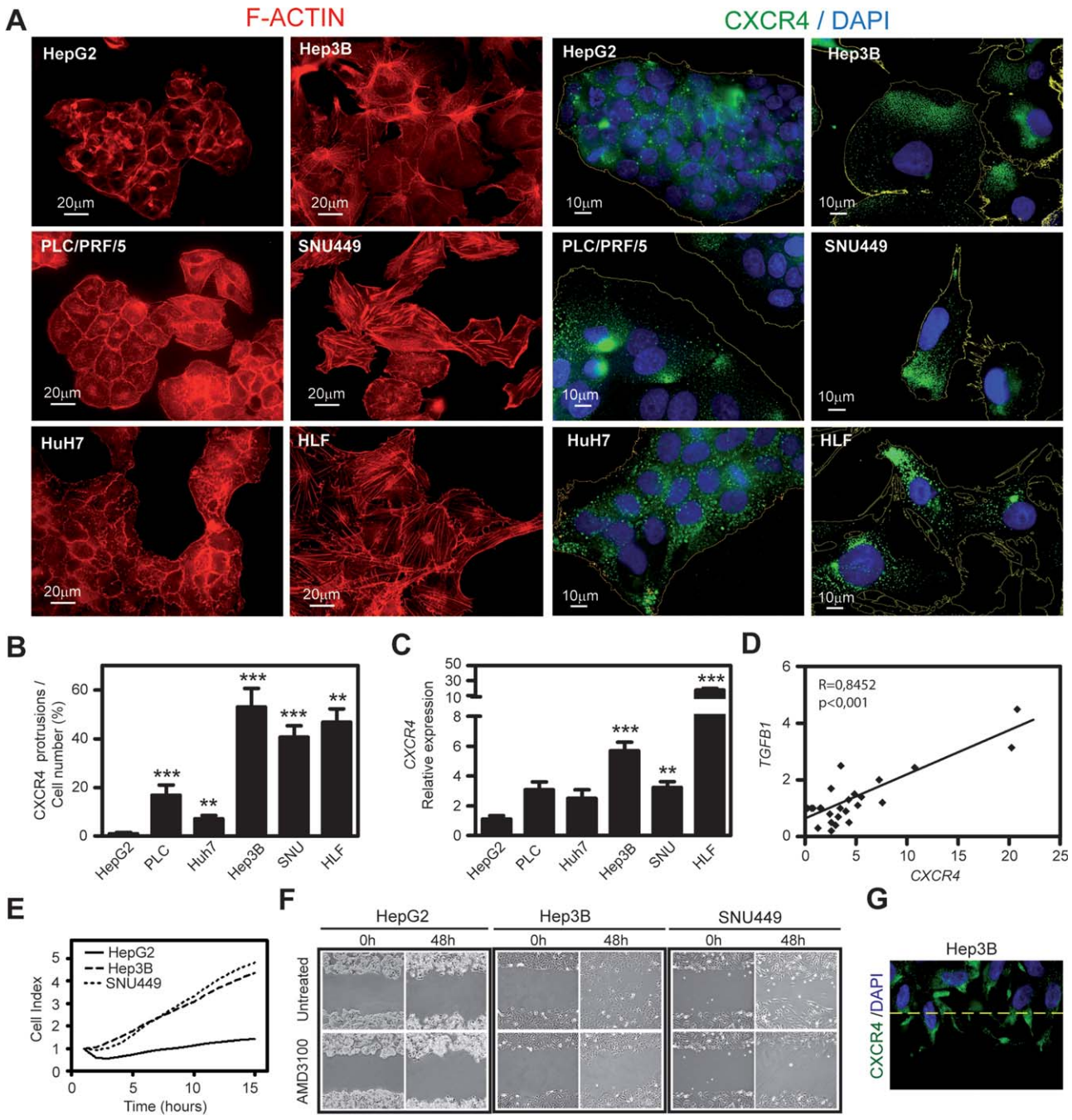

Fig. 2. Overactivation of the TGF-β pathway correlates with high expression and asymmetric distribution of CXCR4, which is required for cell migration. (A) Immunofluorescence of F-ACTIN (red), CXCR4 (green), and DAPI (blue). (B) Percentage of CXCR4 protrusions/cell number. (C) *CXCR4* mRNA levels by real-time PCR relative to HepG2 levels. (B,C) Mean ± SEM (n = 3). Student *t* test versus HepG2 cells: $^{**}P < 0.01$, $^{***}P < 0.001$. (D) Correlation among *TGFB* and *CXCR4* mRNA levels in the individual analyses performed in the different cell lines. (E) Real-time migration assay (xCELLigence system, Roche). (F) Cells were untreated or treated with 1 μg/mL AMD3100. Wound-healing assay (48 hours after wound scratch). (G) Immunofluorescence of CXCR4 (green) and DAPI (blue) of Hep3B, 10 minutes after wound scratch. (E-G) Representative experiments (n = 3).

dose of DEN in 15-day-old animals, liver was collected and analyzed. The appearance of tumors was observed microscopically in all male mice at 9 months of age, but clear macroscopic observation of relevant tumor masses was not observed until 12 months (Supporting Fig. 5). Real-time PCR analysis revealed a progressive increase in the expression of *TGFB1, TGFBR1,* and *CXCR4* in livers from mice of 9 to 12 months of age (Fig. 5A). Increased expression of *TGFB1* correlated with a higher percentage of cells

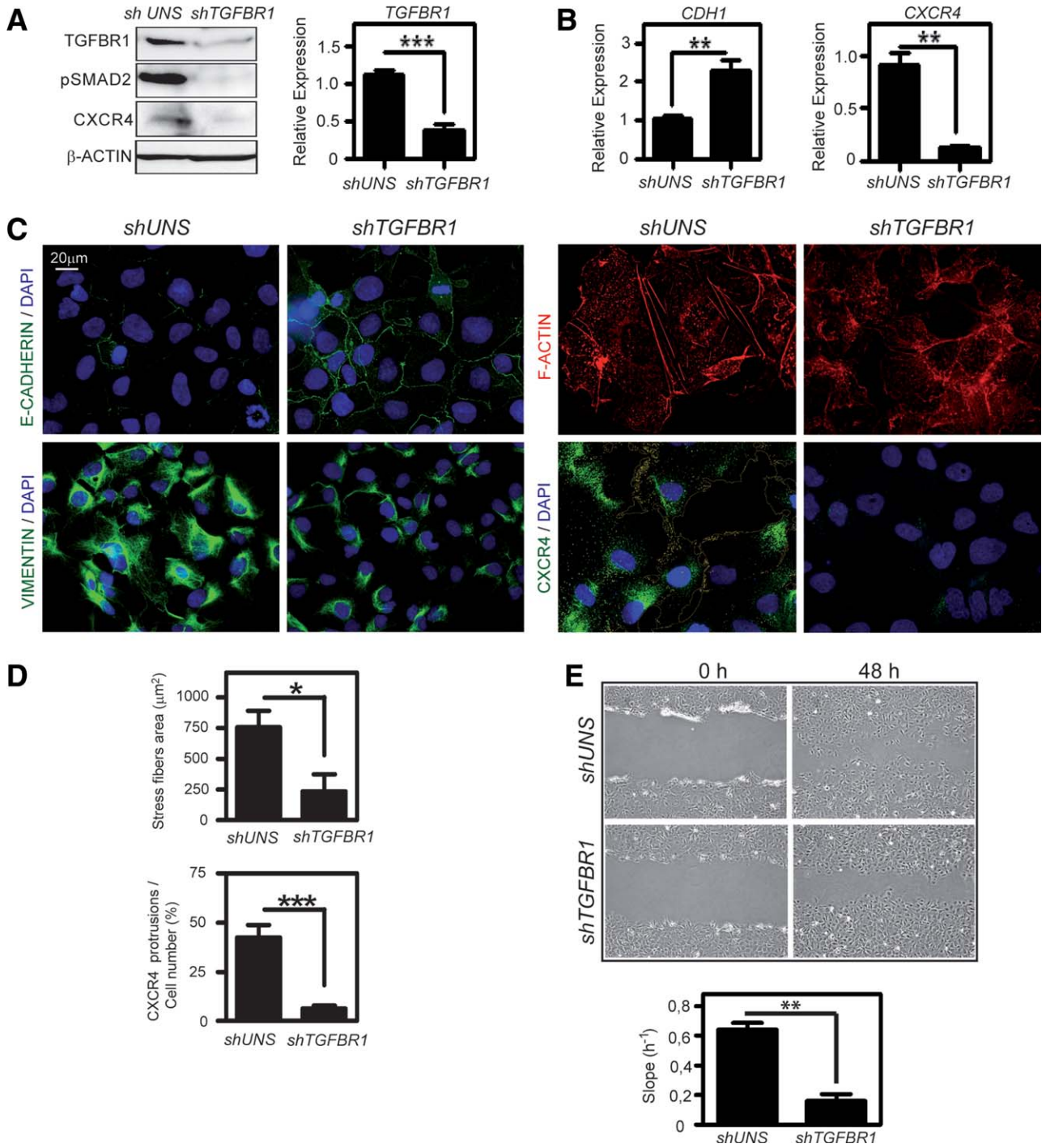

Fig. 3. Stable silencing of TGFBR1 recovers the epithelial phenotype and attenuates CXCR4 expression, inhibiting cell migratory capacity. Hep3B cells were stably transfected with an unspecific shRNA (Hep3B-shUns) or a pool of four different shRNAs against TGFBRI, as detailed in the Supporting Materials and Methods, (Hep3B-shTGFBR1) and were comparatively studied: (A) western blot (left) and real-time PCR of *TGFBRI* (right). (B) E-cadherin (*CDH1*) and *CXCR4* expression levels by real-time PCR. (C) Immunofluorescence of: left: E-cadherin (green), vimentin (green), and DAPI (blue); right: F-ACTIN (red), CXCR4 (green), and DAPI (blue). (D) Quantitative analysis of the F-ACTIN stress fibers area (top) and the number of CXCR4 protrusions relative to the number of cells (bottom). (E) Analysis of cell migration. Top: wound-healing experiment (48 hours after wound scratch). Bottom: real-time migration assay (xCELLigence system). (A, left, C, E, top) Representative experiments (n = 3). (A, right, B, D, E, bottom) Mean ± SEM (n = 3). Student *t* test $*P < 0.05$, $**P < 0.01$, $***P < 0.001$.

showing nuclear localization of phospho-SMAD2 and phospho-SMAD3 in immunohistochemical studies (Fig. 5B). Cells in the border of the tumor presented the maximal level of CXCR4 expression (Fig. 5C). Importantly, it was possible to observe some CXCR4-positive cells invading the stroma. The expression of

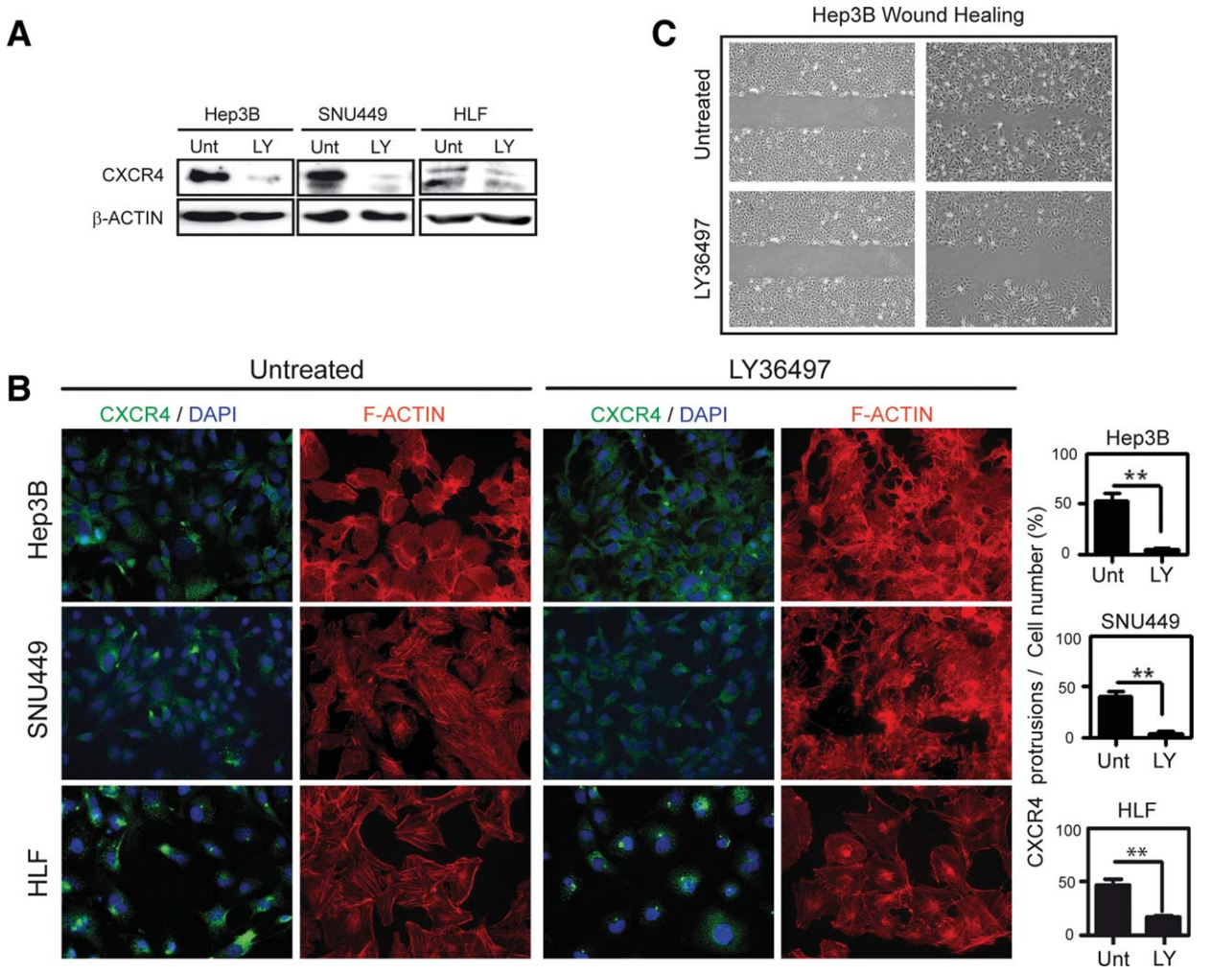

Fig. 4. Pharmacological inhibition of TGFBR1 kinase activity prevents CXCR4 expression and polarization in the mesenchymal HCC cell lines. Hep3B, SNU449, and HLF cells were incubated in the presence or absence of 3 μM LY36497 for 48 hours. (A) Western blot analysis of CXCR4. A representative experiment of three is shown. (B) Immunofluorescence of F-ACTIN (red), CXCR4 (green), and DAPI (blue). Percentage of CXCR4 protrusions/cell number is represented on the right of each picture as the mean $\pm$ SEM of three independent experiments. Student *t* test versus untreated cells: $^{**}P < 0.01$. (C) Wound-healing experiment in Hep3B cells with or without 3 μM LY36497 at 48 hours after wound scratch.

CXCL12/SDF-1α was concentrated in perivascular or ductal cells, which could induce the stimulus for cells to migrate toward these areas. Furthermore, we found that immortalized mice hepatocytes in culture were able to respond to TGF-β by inducing *CXCR4* expression, a process that was SMAD2/3-dependent (Fig. 5D). In summary, tumor cells in the DEN-induced mice model of liver tumorigenesis show increased activation of the TGF-β pathway, which correlates with enhanced CXCR4 levels that concentrates particularly in the cells of the tumor border line.

Expression of CXCR4 in Human HCC Tissues Correlates With an Active TGF-β Pathway and Is Concentrated in Areas of Cell Spreading. Finally, we wanted to know whether TGF-β1 signaling and CXCR4 expression correlated in human HCC tissues. We analyzed tissues from 17 patients with HCC from different etiologies (Table 1). Heterogeneity among HCC tumors, with variable expression of *TGFB1* and its receptor *TGFBR1*, was observed. Nevertheless, when calculated as the mean among the patients, the expression was significantly increased in tumor tissues versus their surrounding nontumoral tissues. Analysis of *CXCR4* was also variable, but again the tendency was to an increased expression in the tumor tissues (Fig. 6A). However, the most interesting way to dissect the results was individually (Fig. 6B), considering each patient independently. In all the patients showing increased expression of *CXCR4, TGFB1* expression was also enhanced, with the exception of patient 8, who presented *CXCR4* expression mainly in areas of infiltration (results not shown). This patient suffered from an autoimmune disease. This direct correlation was not necessarily true the other way around, since some

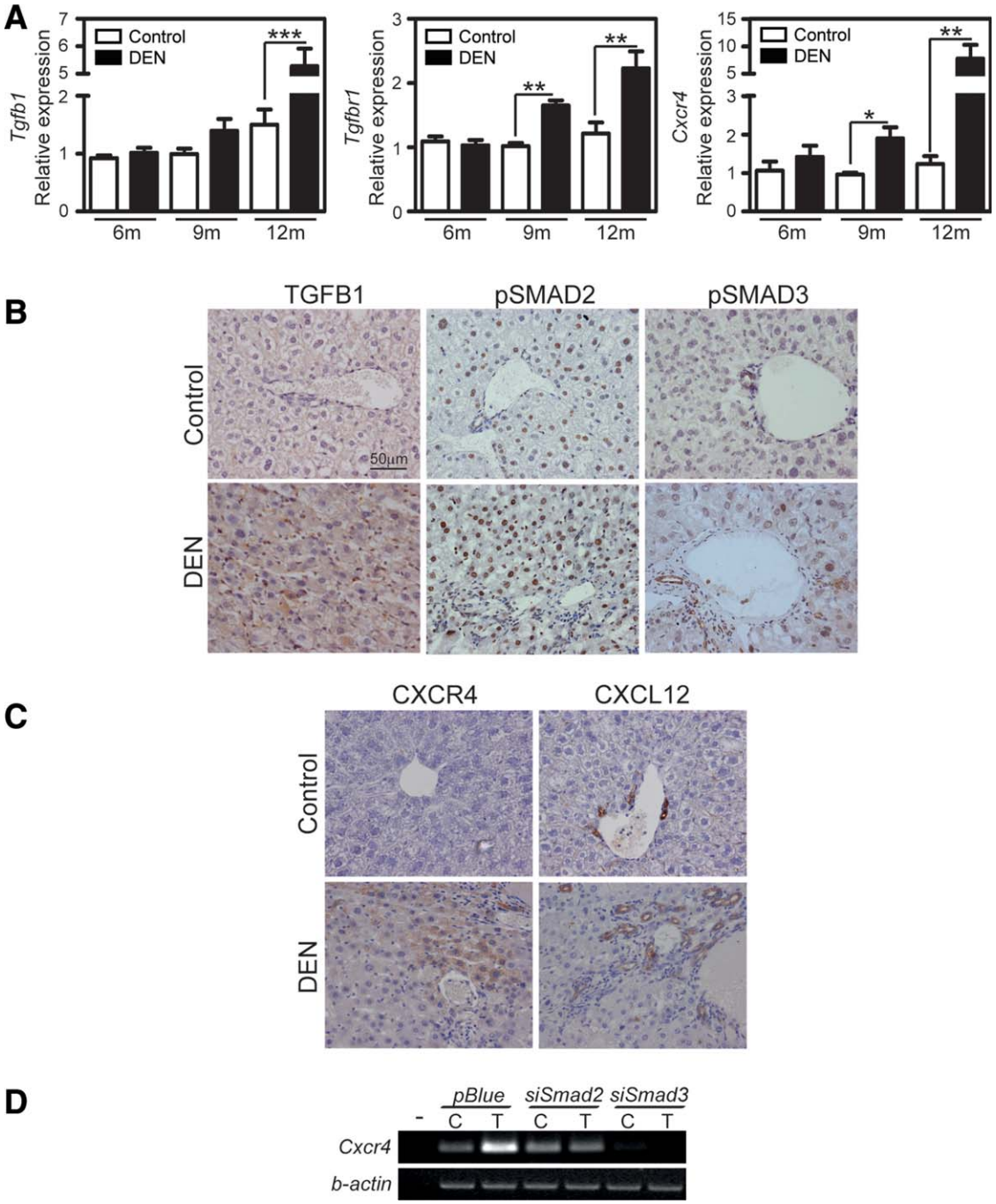

Fig. 5. Tumorigenesis in mice following DEN treatment is associated with increased TGF-β and CXCR4 signaling. (A) *Tgfb, Tgfbrl,* and *Cxcr4* transcript levels analyzed by real-time PCR in control liver (PBS treatment) versus tumoral tissues in animals at 6, 9, and 12 months of age. Data represent mean ± SEM (n = 4 in control animals; 3 in DEN-treated animals; analysis in two different pieces of tissue/animal). Student *t* test $*P < 0.05$, $**P < 0.01$, $***P < 0.001$. (B,C) Immunohistochemistry analysis of serial sections of liver from mice after DEN or PBS treatment (12 months). (D) Effect of transient knockdown of SMAD2 or SMAD3 on *Cxcr4* mRNA levels analyzed by RT-PCR in immortalized neonatal hepatocytes treated during 24 hours with or without 2 ng/mL TGF-β. A representative experiment (n = 3).

patients with increased expression of *TGFB1* did not show higher expression of *CXCR4* (patients 9, 10, 13, 17). Of note, the increased expression of *TGFB1* at the mRNA level correlated with higher levels of TGFB1 protein in the tissues from these patients, not only in the tumoral cells but also in the surrounding stroma and perivascular areas (Fig. 6B,C). Nuclear location of phospho-SMAD2 confirmed the activation of the TGF-β signaling. In a similar way to that observed in the mice model, CXCR4-positive cells were mainly located in the border of the tumor or in the perivascular area (Fig. 6B,C) and CXCL12

Table 1. Patient and Tumor Characteristics

Case	Age/Sex	Etiology	Background	Size (cm)	Tumoral Focus/ Satellite Nodules	Histological Grade	Microscopic Vascular Invasion	Macroscopic Vascular Invasion	pT / Stage
1	46/M	Alc	LC	3	1/0	3	No	No	1 / I
2	50/M	Alc, HCV	LC	2,5	2/0	2-3	No	No	2 / II
3	75/M	Alc	LC	3	1/0	3	No	No	1 / I
4	49/F	U	NL	27	1/0	3	No	No	1 / I
5	78/F	U	NL	7,5	1/1	3	Yes	No	2 / II
6	50/M	Alc	LC	2	9/0	2	Yes	No	2 / II
7	69/M	HCV	LC	3	-	3	No	Yes	1 / I
8	65/F	Aut	LC	6	5/0	2	Yes	No	3 / IIIa
9	61/M	HCV	LC	2,5	-	2	No	No	2 / II
10	62/M	HCV	LC	4,5	1/0	3	No	No	1 / I
11	74/M	U	NL	6	1/0	2	No	No	1 / I
12	52/M	HCV	LC	3,8	1/0	2	No	No	1 / I
13	82/M	U	NL	7	1/0	1-2	No	No	1 / I
14	46/M	HCV	LC	8,5	1/multi	3	Yes	No	2a / II
15	71/M	U	NL	20	1/multi	2	Yes	No	2 / II
16	64/M	HCV	LC	3,3	1/0	3	No	No	1 / I
17	71/M	HCV	LC	4,5	1/1	2-3	No	No	1 / I

Gender: F (female); M (male). Histological grade according to the criteria of Edmondson and Steiner: 1, well differentiated; 2, moderately differentiated; 3, poorly differentiated; 4, undifferentiated. Etiology: HBV (hepatitis B virus); HCV (hepatitis C virus); NBNC (HBV(-), HCV(-)); alcohol (heavy alcohol use); U (unknown etiology); Aut (autoimmune); background: NL (normal liver); LC (liver cirrhosis).

expression was found in the stroma, infiltration areas, and in ductal and perivascular cells. It is worth noting that it was possible to observe CXCR4-positive cells trying to invade the vasculature and infiltrating the peritumoral capsule (Fig. 6D). Interestingly, CXCR4-positive tumor cells surrounding vascular areas showed disorganization of E-cadherin, which reflects a less differentiated, more mesenchymal, and migratory phenotype (Fig. 6C). In fact, the highest expression of both TGF-β and CXCR4 significantly correlated with the lowest stages of differentiation in the HCC patients analyzed (Supporting Fig. 6A). Furthermore, patients with a cirrhotic background showed the highest levels of CXCR4 and, interestingly, the tumor surrounding (cirrhotic) tissue from these patients contained significantly higher levels of both TGF-β and CXCR4 when compared with the surrounding tissue from noncirrhosis patients (Supporting Fig. 6B). Immunohistochemical analysis of CXCR4 in tissues from patients with different grades of fibrosis (no tumors yet) revealed progressive increase in the expression of this protein, which correlated with higher activation of the TGF-β pathway, analyzed as SMAD2 phosphorylation (Supporting Fig. 6C).

In summary, a great percentage of HCC tumors express high levels of CXCR4 that is always coincident with activation of the TGF-β pathway and correlates with a dedifferentiation stage and a cirrhotic background. CXCR4 concentrates particularly in the cells of the tumor border and in the perivascular areas, a fact that may suggest its potential involvement in tumor cell migration.

Discussion

In addition to the clear evidence for TGF-β signaling as a liver tumor suppressor, different studies have identified overexpression of TGF-β1 in HCC, which correlates with tumor progression and a bad prognosis.[9,10] The ability of TGF-β to contribute to tumor progression depends on the capacity of the cells to overcome its growth inhibitory and proapoptotic effects. Different mechanisms could account for this resistance, among others: (1) alteration of oncogenic pathways, such as Ras/Erks or p53[19,20]; (2) alterations in the TGF-β suppressor arm, such as dysregulation of embryonic liver fodrin (ELF, a crucial SMAD3/4 adaptor)[21] or up-regulation of SMAD7[22,23]; or (3) interaction with hepatitis B virus X (HBx) protein.[24] Tumor cells that overcome TGF-β suppressor effects become susceptible to respond to these cytokine-inducing other effects, such as EMT processes that contribute to either fibrosis and/or tumor dissemination.[25] Furthermore, TGF-β may exert multiple effects on the microenvironment, as well as on vasculogenesis.[26] For all these reasons, the TGF-β signaling pathway is starting to be considered as a pharmaceutical target in HCC.[8] However, whereas interference with TGF-β signaling in various short-term animal models has provided promising results, liver disease progression in humans is a process of decades with different phases where targeting of TGF-β might have both beneficial and/or adverse effects.[27] Indeed, dissecting the downstream signals that govern the protumorigenic effects of the

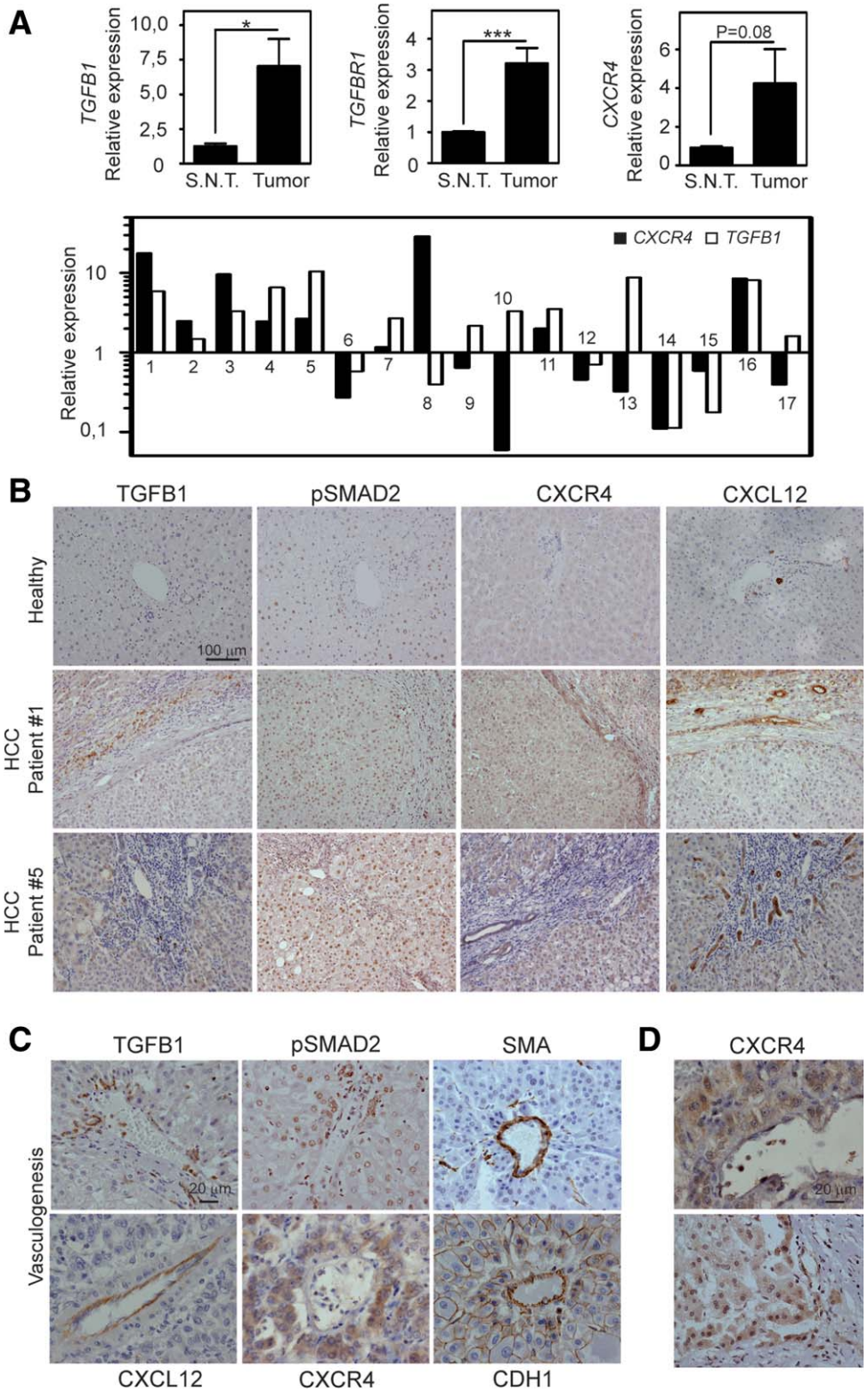

Fig. 6. High expression of CXCR4 correlates with activation of the TGF-β pathway and a less differentiated phenotype in HCC tumor tissues. (A) *TGFB, TGFBRI,* and *CXCR4* transcript levels analyzed by real-time PCR, comparing tumor versus surrounding tissue in 17 HCC patients (up). Relative expression of *TGFB and CXCR4* of each individual tumor versus its respective surrounding tissue, represented in a logarithmic scale for a better understanding of changes observed (down). (B) Immunohistochemistry analysis of serial sections in two representative HCC patients (1 and 5), compared with healthy tissue. (C) Immunohistochemistry analysis of tumor arteries. (D) Magnification of different CXCR4 localizations within the tumor.

TGF-β pathway in liver tumor cells may help in the design of more specific targeted therapies for downstream TGF-β receptors and/or to select patients in whom a potential positive response to TGF-β inhibitors is predicted.

In this work, we show that some human HCC cells display a mesenchymal-like phenotype and migratory capacity under basal conditions, which is coincident with overactivation of the TGF-β pathway. An inverse correlation between the mesenchymal-like phenotype and the response to TGF-β as a tumor suppressor is observed. In liver cancer cells EMT, through Snail1 up-regulation, overcomes TGF-β-induced tumor-suppressor effects, switching its response to tumor progression, making cells resistant to cell death and prone to acquire invasive properties.[28] Furthermore, correlating with the autocrine stimulation of TGF-β, HCC cells express high levels of CXCR4, which is asymmetrically distributed and concentrated at the presumptive cell migratory front and mediates cell migration. Interestingly, both mesenchymal-like features and expression/polarization of CXCR4 are attenuated in cells where TGFBR1 expression is decreased with a specific shRNA, which correlates with the impairment of their migratory capacity. Although previous reports had reported the overexpression of TGF-β in HCC[9,10] and the correlation of CXCR4 expression with invasive potential of HCC cells,[13,15,29,30] this is the first study demonstrating that the tumor-promoting function of TGF-β signaling involves CXCR4/CXCL12, which results in enhanced migration in human liver tumor cells. Furthermore, activation of CXCR4 would affect several major signaling pathways related not only to cell migration, but also to proliferation and survival,[16] which may have relevant consequences in tumor progression.[31]

The results presented here also indicate that in the animal model of DEN-induced liver carcinogenesis, expression of TGF-β1 and CXCR4 is progressively increased, reaching maximum levels at late stages where tumors are macroscopically observed. We have also proven that in cultures of immortalized hepatocytes, TGF-β induces CXCR4 expression, a process that requires activation of both SMAD2 and SMAD3. In fact, an integrative genomic analysis of CXCR4 transcriptional regulation had previously suggested that TGF-β, Nodal, and Activin signals may induce CXCR4 upregulation based on SMAD2/3 and FOX family members.[32] The study in humans also indicates that a relevant percentage of liver tissues from HCC patients show a higher expression of CXCR4, which is always coincident with overactivation of the TGF-β pathway and correlates with a less differentiated phenotype and cirrhotic background. Cells that present a higher amount and polarized localization of CXCR4 are located in the borders of the tumor, in the migratory fronts, or in the perivascular zone, coincident with high expression of TGF-β in these areas. Interestingly, expression of CXCL12 is higher in the peritumoral cells, which suggest a paracrine regulation of the CXCR4 pathway. Indeed, overactivation of the TGF-β pathway sensitizes tumor cells to respond to CXCL12 produced by tumoral surrounding tissue. All these results together support the existence of crosstalk among TGF-β and CXCR4 pathways in HCC human tumors, which may contribute to tumor progression and dissemination.

The inhibition of the TGF-β pathway is emerging as a new therapeutic tool in cancer.[33] Since it regulates several steps in tumor progression, blocking this mediator should have multiple beneficial effects.[8] However, based on the results presented here, from both *in vitro* and *in vivo* experiments, the heterogeneity of the tumors might condition the response to these inhibitors. Indeed, overactivation of the TGF-β pathway differs among the different cell lines tested, as well as among the different tissues from patients. Interestingly, a strong correlation between TGF-β overactivation and mesenchymal-like and migratory phenotypes is observed, locating CXCR4 as a target of TGF-β both in cell lines and in HCC patients. From these results, CXCR4 localization in the migratory fronts of tumor tissues, coincident with high expression of TGF-β and/or high nuclear localization of p-SMAD2, may be used as biomarkers to predict the beneficial response to therapeutic agents that act on the TGF-β pathway. Increasing evidence demonstrates that activation of the CXCR4/CXCL12 pathway is a potential mechanism of tumor resistance to both conventional therapies and biological agents by way of complementary actions.[34] The use of TGF-β inhibitors, or inhibitors of the CXCR4/CXCL12 pathway, might increase the response to other therapeutic drugs when used in combination.

In conclusion, overactivation of the TGF-β pathway in HCC cells confers on them a mesenchymal-like phenotype and migratory properties through activation of the CXCR4/CXCL12 axis, a mechanism that would contribute to tumor progression in HCC patients. CXCR4 localization in the migratory fronts of tumor tissues, coincident with overactivation of the TGF-β signaling, may be considered in the future as a prognostic factor to predict patient response to drugs that target the TGF-β pathway.

Acknowledgment: The authors thank Greta Ripoll for technical support and participation in the analysis of the DEN model of hepatocarcinogenesis by Dr. Joana Visa (and the IDIBELL animal core facility) and graduate student Miguel Reina. We thank Drs. Perales and Giannelli for providing cells.

References

1. Massague J. TGFbeta in cancer. Cell 2008;134:215-230.
2. Valdes F, Murillo MM, Valverde AM, Herrera B, Sanchez A, Benito M, et al. Transforming growth factor-beta activates both pro-apoptotic and survival signals in fetal rat hepatocytes. Exp Cell Res 2004;292:209-218.
3. Caja L, Ortiz C, Bertran E, Murillo MM, Miro-Obradors MJ, Palacios E, et al. Differential intracellular signalling induced by TGF-beta in rat adult hepatocytes and hepatoma cells: implications in liver carcinogenesis. Cell Signal 2007;19:683-694.
4. Murillo MM, del Castillo G, Sanchez A, Fernandez M, Fabregat I. Involvement of EGF receptor and c-Src in the survival signals induced by TGF-beta1 in hepatocytes. Oncogene 2005;24:4580-4587.
5. Gotzmann J, Huber H, Thallinger C, Wolschek M, Jansen B, Schulte-Hermann R, et al. Hepatocytes convert to a fibroblastoid phenotype through the cooperation of TGF-beta1 and Ha-Ras: steps towards invasiveness. J Cell Sci 2002;115:1189-1202.
6. Valdes F, Alvarez AM, Locascio A, Vega S, Herrera B, Fernandez M, et al. The epithelial mesenchymal transition confers resistance to the apoptotic effects of transforming growth factor beta in fetal rat hepatocytes. Mol Cancer Res 2002;1:68-78.
7. Reichl P, Haider C, Grubinger M, Mikulits W. TGF-beta in epithelial to mesenchymal transition and metastasis of hepatocellular carcinoma. Curr Pharm Des 2012;18:4135-4147.
8. Giannelli G, Mazzocca A, Fransvea E, Lahn M, Antonaci S. Inhibiting TGF-beta signaling in hepatocellular carcinoma. Biochim Biophys Acta 2011;1815:214-223.
9. Coulouarn C, Factor VM, Thorgeirsson SS. Transforming growth factor-beta gene expression signature in mouse hepatocytes predicts clinical outcome in human cancer. Hepatology 2008;47:2059-2067.
10. Fransvea E, Angelotti U, Antonaci S, Giannelli G. Blocking transforming growth factor-beta up-regulates E-cadherin and reduces migration and invasion of hepatocellular carcinoma cells. Hepatology 2008;47: 1557-1566.
11. Sheu BC, Chang WC, Cheng CY, Lin HH, Chang DY, Huang SC. Cytokine regulation networks in the cancer microenvironment. Front Biosci 2008;13:6255-6268.
12. Zlotnik A. New insights on the role of CXCR4 in cancer metastasis. J Pathol 2008;215:211-213.
13. Li W, Gomez E, Zhang Z. Immunohistochemical expression of stromal cell-derived factor-1 (SDF-1) and CXCR4 ligand receptor system in hepatocellular carcinoma. J Exp Clin Cancer Res 2007;26:527-533.
14. Sutton A, Friand V, Brule-Donneger S, Chaigneau T, Ziol M, Sainte-Catherine O, et al. Stromal cell-derived factor-1/chemokine (C-X-C motif) ligand 12 stimulates human hepatoma cell growth, migration, and invasion. Mol Cancer Res 2007;5:21-33.
15. Schimanski CC, Bahre R, Gockel I, Muller A, Frerichs K, Horner V, et al. Dissemination of hepatocellular carcinoma is mediated via chemokine receptor CXCR4. Br J Cancer 2006;95:210-217.
16. Bertran E, Caja L, Navarro E, Sancho P, Mainez J, Murillo MM, et al. Role of CXCR4/SDF-1alpha in the migratory phenotype of hepatoma cells that have undergone epithelial-mesenchymal transition in response to the transforming growth factor-beta. Cell Signal 2009;21:1595-1606.
17. Gonzalez-Rodriguez A, Clampit JE, Escribano O, Benito M, Rondinone CM, Valverde AM. Developmental switch from prolonged insulin action to increased insulin sensitivity in protein tyrosine phosphatase 1B-deficient hepatocytes. Endocrinology 2007;148:594-608.
18. Caja L, Sancho P, Bertran E, Ortiz C, Campbell JS, Fausto N, et al. The tyrphostin AG1478 inhibits proliferation and induces death of liver tumor cells through EGF receptor-dependent and independent mechanisms. Biochem Pharmacol 2011;82:1583-1592.
19. Caja L, Sancho P, Bertran E, Iglesias-Serret D, Gil J, Fabregat I. Overactivation of the MEK/ERK pathway in liver tumor cells confers resistance to TGF-{beta}-induced cell death through impairing up-regulation of the NADPH oxidase NOX4. Cancer Res 2009;69:7595-7602.
20. Morris SM, Baek JY, Koszarek A, Kanngurn S, Knoblaugh SE, Grady WM. Transforming growth factor-beta signaling promotes hepatocarcinogenesis induced by p53 loss. Hepatology 2012;55:121-131.
21. Baek HJ, Lim SC, Kitisin K, Jogunoori W, Tang Y, Marshall MB, et al. Hepatocellular cancer arises from loss of transforming growth factor beta signaling adaptor protein embryonic liver fodrin through abnormal angiogenesis. Hepatology 2008;48:1128-1137.
22. Matsuzaki K, Date M, Furukawa F, Tahashi Y, Matsushita M, Sugano Y, et al. Regulatory mechanisms for transforming growth factor beta as an autocrine inhibitor in human hepatocellular carcinoma: implications for roles of SMADs in its growth. Hepatology 2000;32:218-227.
23. Dooley S, Weng H, Mertens PR. Hypotheses on the role of transforming growth factor-beta in the onset and progression of hepatocellular carcinoma. Dig Dis 2009;27:93-101.
24. Murata M, Matsuzaki K, Yoshida K, Sekimoto G, Tahashi Y, Mori S, et al. Hepatitis B virus X protein shifts human hepatic transforming growth factor (TGF)-beta signaling from tumor suppression to oncogenesis in early chronic hepatitis B. Hepatology 2009;49:1203-1217.
25. Moustakas A, Heldin CH. Induction of epithelial-mesenchymal transition by transforming growth factor beta. Semin Cancer Biol 2012;22: 446-454.
26. Fransvea E, Mazzocca A, Antonaci S, Giannelli G. Targeting transforming growth factor (TGF)-betaRI inhibits activation of beta1 integrin and blocks vascular invasion in hepatocellular carcinoma. Hepatology 2009;49:839-850.
27. Dooley S, ten Dijke P. TGF-beta in progression of liver disease. Cell Tissue Res 2012;347:245-256.
28. Franco DL, Mainez J, Vega S, Sancho P, Murillo MM, de Frutos CA, et al. Snail1 suppresses TGF-beta-induced apoptosis and is sufficient to trigger EMT in hepatocytes. J Cell Sci 2010;123:3467-3477.
29. Liu H, Pan Z, Li A, Fu S, Lei Y, Sun H, et al. Roles of chemokine receptor 4 (CXCR4) and chemokine ligand 12 (CXCL12) in metastasis of hepatocellular carcinoma cells. Cell Mol Immunol 2008;5:373-378.
30. Li N, Guo W, Shi J, Xue J, Hu H, Xie D, et al. Expression of the chemokine receptor CXCR4 in human hepatocellular carcinoma and its role in portal vein tumor thrombus. J Exp Clin Cancer Res 2010; 29:156.
31. Zhang XH, Wang Q, Gerald W, Hudis CA, Norton L, Smid M, et al. Latent bone metastasis in breast cancer tied to Src-dependent survival signals. Cancer Cell 2009;16:67-78.
32. Katoh M, Katoh M. Integrative genomic analyses of CXCR4: transcriptional regulation of CXCR4 based on TGFbeta, Nodal, Activin signaling and POU5F1, FOXA2, FOXC2, FOXH1, SOX17, and GFI1 transcription factors. Int J Oncol 2010;36:415-420.
33. Seoane J. The TGFBeta pathway as a therapeutic target in cancer. Clin Transl Oncol 2008;10:14-19.
34. Duda DG, Kozin SV, Kirkpatrick ND, Xu L, Fukumura D, Jain RK. CXCL12 (SDF1alpha)-CXCR4/CXCR7 pathway inhibition: an emerging sensitizer for anticancer therapies? Clin Cancer Res 2011;17:2074-2080.

Free Radical Biology and Medicine 69 (2014) 338–347

Contents lists available at ScienceDirect

Free Radical Biology and Medicine

journal homepage: www.elsevier.com/locate/freeradbiomed

Original Contribution

The NADPH oxidase NOX4 inhibits hepatocyte proliferation and liver cancer progression

Eva Crosas-Molist [a], Esther Bertran [a], Patricia Sancho [a,1], Judit López-Luque [a], Joan Fernando [a], Aránzazu Sánchez [b], Margarita Fernández [b], Estanis Navarro [a], Isabel Fabregat [a,c,*]

[a] Bellvitge Biomedical Research Institute, L'Hospitalet de Llobregat, 08908 Barcelona, Spain
[b] Departamento de Bioquímica y Biología Molecular II, Facultad de Farmacia, Universidad Complutense, Instituto de Investigación Sanitaria del Hospital Clínico San Carlos, 28080 Madrid, Spain
[c] Departament de Ciències Fisiològiques II, Universitat de Barcelona, Campus de Bellvitge, Barcelona, Spain

ARTICLE INFO

Article history:
Received 24 October 2013
Received in revised form
23 January 2014
Accepted 28 January 2014
Available online 6 February 2014

Keywords:
NOX4
NADPH oxidase
Reactive oxygen species
Hepatocyte proliferation
Hepatocellular carcinoma
Liver cancer
Liver regeneration
Hepatocarcinogenesis
Free radicals

ABSTRACT

The NADPH oxidase NOX4 has emerged as an important source of reactive oxygen species in signal transduction, playing roles in physiological and pathological processes. NOX4 mediates transforming growth factor-β-induced intracellular signals that provoke liver fibrosis, and preclinical assays have suggested NOX4 inhibitors as useful tools to ameliorate this process. However, the potential consequences of sustained treatment of liver cells with NOX4 inhibitors are yet unknown. The aim of this work was to analyze whether NOX4 plays a role in regulating liver cell growth either under physiological conditions or during tumorigenesis. In vitro assays proved that stable knockdown of NOX4 expression in human liver tumor cells increased cell proliferation, which correlated with a higher percentage of cells in S/G2/M phases of the cell cycle, downregulation of p21(CIP1/WAF1), increase in cyclin D1 protein levels, and nuclear localization of β-catenin. Silencing of NOX4 in untransformed human and mouse hepatocytes also increased their in vitro proliferative capacity. In vivo analysis in mice revealed that NOX4 expression was downregulated under physiological proliferative situations of the liver, such as regeneration after partial hepatectomy, as well as during pathological proliferative conditions, such as diethylnitrosamine-induced hepatocarcinogenesis. Xenograft experiments in athymic mice indicated that NOX4 silencing conferred an advantage to human hepatocarcinoma cells, resulting in earlier onset of tumor formation and increase in tumor size. Interestingly, immunochemical analyses of NOX4 expression in human liver tumor cell lines and tissues revealed decreased NOX4 protein levels in liver tumorigenesis. Overall, results described here strongly suggest that NOX4 would play a growth-inhibitory role in liver cells.

Reactive oxygen species (ROS) are intracellular physiological signals, but also disease triggers. Their relative excess or shortage is potentially deleterious [1]. The NADPH oxidase (NOX) family has emerged in the past years as important sources of ROS in signal transduction [2]. NOX-derived ROS may modulate gene expression, cytoskeleton remodeling, migration, and differentiation, as well as cell proliferation and death [1,2]. The first NOX described was the respiratory burst NADPH oxidase complex, whose catalytic subunit is now known as NOX2. The other family members have been cloned and studied in the past 15 years. The NOX family consists of seven members, NOX1–5 and two dual oxidases (DUOX1 and 2), which share analogies in structure and catalytic function, because all of them mediate the reduction of oxygen using NADPH as an electron donor. However, important differences in regulation and cellular functions are observed among them. The functional analysis of the isoenzyme NOX4 revealed unique characteristics compared to other NADPH oxidases [3]. NOX4 associates with their regulators (p22phox or Poldip2) in intracellular membranes, where the superoxide anion is rapidly converted to H_2O_2 [3,4]. It is believed that H_2O_2 is responsible for the majority of NOX4 downstream effects. None of the known cytosolic oxidase proteins nor

Abbreviations: DEN, diethylnitrosamine; HCC, hepatocellular carcinoma; NOX, NADPH oxidase; ROS, reactive oxygen species; TGF-β, transforming growth factor β

* Corresponding author at: Bellvitge Biomedical Research Institute, L'Hospitalet de Llobregat, 08908 Barcelona, Spain. Fax: +34 932 607426.
E-mail address: ifabregat@idibell.cat (I. Fabregat).
[1] Present address: Spanish National Cancer Research Center, Madrid, Spain.

http://dx.doi.org/10.1016/j.freeradbiomed.2014.01.040
0891-5849

the GTPase Rac is required for its activity, which seems to be regulated mainly at the transcriptional level [3,5,6]. Strong pieces of evidence support the role of NOX4 in various pathologies. In particular, NOX4 has been proposed to be a relevant mediator of fibrotic processes in lung [7] or liver [8]. For these reasons there is an increasing interest in the development and test of new NOX inhibitors that could be clinically useful to ameliorate fibrosis [9–11]. However, what could be the consequences of sustained treatment with NOX4 inhibitors? This is an unanswered question yet.

In the liver, NOXs play relevant roles mediating transforming growth factor-β (TGF-β) actions. In stellate cells, NOX4 signals for their activation to myofibroblasts, but in hepatocytes, it mediates cell death [8]. A similar situation occurs in the lung [12]. ROS generated by NOX4 are required for the mitochondrial-mediated apoptosis induced by TGF-β in hepatocytes [13], through modulation of the expression of the proapoptotic genes BIM and BMF [14]. TGF-β is a well-known tumor suppressor factor in epithelial cells through its capacity to inhibit growth as well as to induce apoptosis. Indeed, inhibition of NOX4 in epithelial cells might lead to a situation in which protumorigenic processes would be favored because of the lack of a suppressor gene. However, this is a hypothesis that remains to be proved.

The aim of this work was to analyze whether NOX4 plays a role in regulating liver cell growth either under physiological conditions or during liver tumorigenesis. Overall, results described here strongly suggest that NOX4 would play a growth-inhibitory role in liver cells.

Material and methods

Reagents

Human recombinant TGF-β1 was from Calbiochem (La Jolla, CA, USA). Fetal bovine serum (FBS) was from Sera Laboratories International (Cinder Hill, UK). Anti-NOX4 rabbit polyclonal antiserum was raised by Sigma–Genosys (Suffolk, UK) against a peptide corresponding to the C-terminal loop region (amino acids 499–511). Specificity was tested by ELISA with the purified peptide [14]. This NOX4 antibody is currently available from Merck Millipore (Billerica, MA, USA; Cat. No. ABC459).

Cell culture

Hep3B and PLC/PRF/5 cell lines were obtained from the European Collection of Cell Cultures. HLF cells were from the Japanese Collection of Research Bioresources (JCRB Cell Bank) and were kindly provided by Dr. Giannelli (University of Bari, Bari, Italy). The human liver cell line CCL-13 (Chang liver, CHL) was from the American Type Culture Collection. Neonatal mouse hepatocytes were immortalized as described previously [15]. Hep3B cells were maintained in minimal essential medium, HLF in RPMI medium, and PLC/PRF/5, CHL, and neonatal mouse hepatocytes in Dulbecco's modified Eagle's medium, supplemented with 10% fetal bovine serum, in a humidified atmosphere at 37 °C, 5% CO_2.

Knockdown assays

For stable transfection of short hairpin (sh) RNA, cells at 50–60% confluence were transfected with MAtra-A reagent (IBA GmbH, Goettingen, Germany) at a dilution of 1:600 in complete medium, according to the manufacturer's recommendation (15 min on the magnet plate), using 2 μg/ml shRNA plasmid. Four different plasmids of NOX4 shRNA were transfected, as well as a control nonspecific shRNA. After 24 h, the medium was changed to complete medium, and selection of transfected cells was done with puromycin (for 50 days before experiments). ShRNA plasmids were selected from Mission SH, Sigma (Madrid, Spain) and the sequences were the following: No. 1, CCGGGAGCCTCAGCATCTGTTCTTACTCGAGTAAGAACAGATGCTGAGGCTCTTTTTG; No. 2, CCGGCCCTCAACTTCTCAGTGAATTCTCGAGAATTCACTGAGAAGTTGAGGGTTTTTG; No. 3, CCGGCAGAGTTTACCCAGCACAAATCTCGAGATTTGTGCTGGGTAAACTCTGTTTTTG; and No. 4, CCGGGCTGTATATTGATGGTCCTTTCTCGAGAAAGGACCATCAATATACAGCTTTTTG. The protocols used were previously described [16,17].

For transient small interfering (si) RNA transfection, cells at 70% confluence were transfected using TransIT-siQuest (Mirus, Madison, WI, USA) at 1:300 dilution in complete medium, as described previously [18]. Oligos were obtained from Sigma–Genosys. Oligo sequences were the following: unsilencing, 5′-GUAAGACACGACUUAUCGC-3′; human NOX4, 5′-GCCUCUACAUAUGCAAUAA-3′, and mouse Nox4, 5′-CAAGAAGAUUGUUGGAUAA-3′. The unsilencing siRNA used was selected from previous works [19].

Partial hepatectomy in mice

Animals used in this study were male C57/BL6 mice, ages 10 to 14 weeks. Partial hepatectomies were performed by removal of two-thirds of the adult mouse liver, according to the method described by Higgins and Anderson [20]. Mice were euthanized at 2, 8, 24, 48, and 72 h and 7days after the surgery and tissue samples were frozen immediately in liquid nitrogen for RNA extraction or fixed in 4% paraformaldehyde for immunohistochemistry analysis.

Diethylnitrosamine (DEN)-induced hepatocarcinogenesis in mice

Male mice at day 15 of age received intraperitoneal injections of DEN (5 mg/kg) diluted in saline buffer, control animals were injected with saline buffer intraperitoneally. After 6, 9, or 12 months, the mice were sacrificed and their livers removed. For histological studies, liver lobes were fixed in 4% paraformaldehyde overnight and paraffin-embedded for immunohistochemistry staining. Total RNA was isolated from these tissues to analyze gene expression by real-time quantitative PCR.

Xenograft model of subcutaneous tumor growth in vivo

Athymic nude mice were purchased from Harlan Laboratories. A total of 16 male mice, 7 weeks of age, were used. Hep3B cells transfected with either a control shRNA or a NOX4 silencing shRNA (shNOX4(No. 3)) were grown in the presence of 10% FBS. Then, the cells were trypsinized and counted, being diluted at a final concentration of 5×10^7 cells/ml in HBSS. A total of 16 nude mice were randomly divided into two groups (shControl and shNOX4 (No. 3), 8 mice per group) and the cell suspension (0.1 ml/mouse) was subcutaneously injected into the left flank of the mouse. Tumor growth was measured every 2 days.

Crystal violet staining

Cells were washed twice with phosphate-buffered saline and the remaining viable adherent cells were stained with crystal violet (0.2% in 2% ethanol) and analyzed spectrophotometrically, as described previously [21].

Analysis of caspase-3 activity

Fluorimetric analysis of caspase-3 activity was determined as described previously [22], with 20 μg protein extract. Fluorescence was measured in a Fluostar Optima microplate fluorescence reader. A unit of caspase-3 activity is the amount of active enzyme

necessary to produce an increase in 1 fluorescence unit and results are presented as units of caspase-3 activity/h/μg protein.

DNA synthesis assay

After incubation of cells for 48 h, DNA synthesis was evaluated by [*methyl*-^{3}H]thymidine (GE Healthcare, Barcelona, Spain) incorporation into trichloroacetic acid (TCA)-precipitable material during the last 40 h, as described previously [23].

Analysis of DNA content by flow cytometry

Cell ploidy was estimated by flow cytometry DNA analysis [24]. Cell cycle analysis was carried out using the software ModFit LTTM (Verity Software House, USA).

Measurement of redox state

The oxidation-sensitive fluorescent probe 2′,7′-dichlorodihydrofluorescein diacetate (H_2DCFDA; from Invitrogen, UK) was used to analyze the intracellular oxidant levels [19]. Extracellular H_2O_2 was measured in intact cells using horseradish peroxidase-linked Amplex Ultra Red (Invitrogen). Briefly, Amplex Ultra Red (50 μM) and horseradish peroxidase (0.1 U/ml) were added to the cellular samples for 2 h. Fluorescence readings were made in duplicate in a 96-well plate at ex/em 530/590 nm using 100 μl samples of medium. Fluorescence was measured in a Fluostar Optima microplate fluorescence reader and expressed as percentage of control after correction for protein content with H_2DCFDA and for cell number (crystal violet assay) with Amplex Ultra Red.

Analysis of gene expression

RNeasy Mini Kit (Qiagen, Valencia, CA, USA) was used for total RNA isolation. Reverse transcription was carried out using the High Capacity reverse transcriptase kit (Applied Biosystems, Foster City, CA, USA) and 1 μg of total RNA from each sample for complementary DNA synthesis. For real-time quantitative PCR, expression levels were determined in duplicate in an ABI Prism7700 system, using the Sybr Green PCR master mix (Applied Biosystems) for mouse primers and in a LightCycler 480 real-time PCR system, using the LightCycler 480 SYBR Green I Master (Roche Applied Science) for human primers. Reactions were performed with the specific primers listed in Table 1.

Western blot analysis

Total protein extracts and Western blotting procedures were carried out as described previously [19,25]. The antibodies used were mouse anti-β-actin (clone AC-15) from Sigma–Aldrich (St. Louis, MO, USA), rabbit anti-NOX4 raised by Sigma–Genosys [14], and rabbit anti-cyclin D1 (M-20) from Santa Cruz Biotechnology (Santa Cruz, CA, USA). Antibodies were used at 1:1000 dilutions, except β-actin (1:3000). Protein concentration was measured with a BCA protein assay kit (Pierce).

Immunofluorescence staining

Fluorescence microscopy studies were performed as described previously [25]. For rabbit anti-NOX4 (Sigma–Genosys) staining, cells were fixed with 4% paraformaldehyde in phosphate-buffered saline. For rabbit anti-Ki67 (Abcam, Cambridge, UK) and mouse anti-β-catenin (BD Transduction Laboratories, Erembodegem, Belgium) staining, cells were fixed with 4% paraformaldehyde in phosphate-buffered saline and permeabilized with 0.2% Triton X-100. The secondary antibodies Alexa Fluor 488-conjugated anti-rabbit and anti-mouse immunoglobulin were from Molecular Probes (Eugene, OR, USA). Blue signal represents the nuclear DNA staining with DAPI from Sigma–Aldrich. Cells were visualized in a Nikon Eclipse 80i microscope with the appropriate filters. Representative images were taken with a Nikon DS-Ri1 digital camera. NOX4 staining was visualized on a Leica TCS SP5 spectral confocal microscope with a HCX PL APO λ blue 63 × 1.4 oil objective lens and excited with the 488-nm laser line of an argon laser. Acquisition software was Leica Application Suite Advanced Fluorescence (LAS AF). The projections of Z stacks are shown. Fluorescence intensity was quantified using Fiji open source software.

Table 1
Specific primers used in this study.

Primer	Sequence
Human CDKN1A forward	5′-TGTCACTGTCTTGTACCCTTG-3′
Human CDKN1A reverse	5′-GGCGTTTGGAGTGGTAGAA-3′
Human NOX4 forward	5′-GCAGGAGAACCAGGAGATTG-3′
Human NOX4 reverse	5′-CACTGAGAAGTTGAGGGCATT-3′
Human L32 forward	5′-AACGTCAAGGAGCTGGAAG-3′
Human L32 reverse	5′-GGGTTGGTGACTCTGATGG-3′
Mouse Nox4 forward	5′-TCCAAGCTCATTTCCCACAG-3′
Mouse Nox4 reverse	5′-CGGAGTTCCATTACATCAGAGG-3′
Mouse p22phox forward	5′-ACACAGTGGTATTTCGGCG-3′
Mouse p22phox reverse	5′-CAGGTACTTCTGTCCACATCG-3′
Mouse 18S forward	5′-CGAGACTCTGGCATGCTAA-3′
Mouse 18S reverse	5′-CGCCACTTGTCCCTCTAAG-3′

Immunohistochemistry

Paraffin-embedded samples, both from xenografts and from partial hepatectomy experiments, were cut into 4-μm-thick sections and stained with hematoxylin and eosin (H&E) or the following primary antibodies (diluted from 1:50 to 1:100): rabbit anti-Ki67 (Abcam), rabbit anti-cleaved caspase-3 (Asp-175) (Cell Signaling Technology, Danvers, MA, USA), and rabbit anti-NOX4 (Sigma–Genosys). The primary antibodies were incubated overnight at 4 °C and binding developed with the Vectastain ABC kit (Vector Laboratories, Burlingame, CA, USA). Tissues were visualized in a Nikon Eclipse 80i microscope with the appropriate filters. Representative images were taken with a Nikon DS-Ri1 digital camera.

Tissue array

A human liver tissue array (Cat. No. Z7020056; BioChain Institute, San Francisco, CA, USA) containing duplicates of 70 cases covering (1) HCC and a few samples of other types of liver cancer, (2) 3 cases of other nonmalignant liver tissues, and (3) 2 normal liver tissues was used. Rabbit anti-NOX4 (Sigma–Genosys) was used as a primary antibody. The same procedure as for immunohistochemistry was used. Staining was quantified by densitometry using the software Quantity One (Bio-Rad Laboratories, Hercules, CA, USA) and the ratio between each case and the mean of normal tissues was represented.

Statistical analyses

All data represent at least three experiments and are express as the mean ± SEM. Differences between groups were compared using Student's *t* test. Statistical significance was assumed when $p < 0.05$.

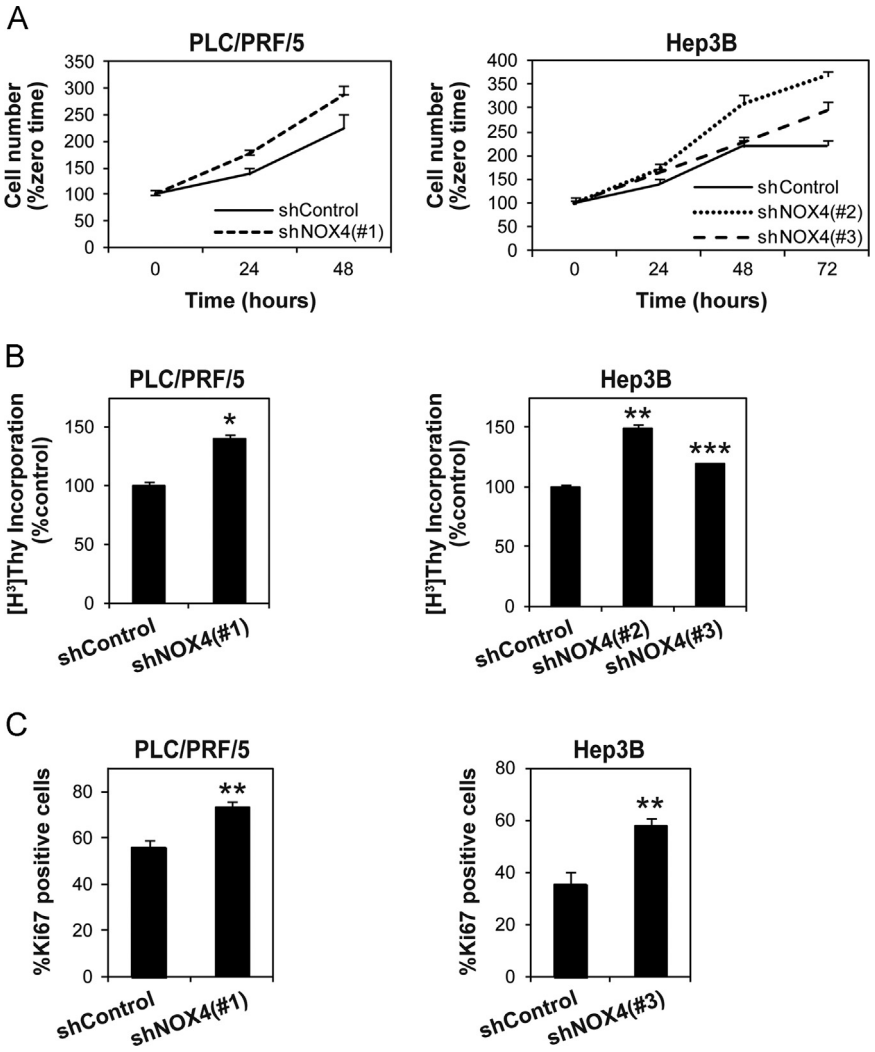

Fig. 1. Stable silencing of NOX4 confers a proliferative advantage to human HCC cells. Comparison of the proliferative capacity of NOX4-silenced cells (shNOX4) versus cells transfected with a nonspecific shRNA (shControl). The cell line and the shNOX4 used are indicated. (A) Number of viable cells analyzed by crystal violet at the times indicated. Results are expressed as a percentage of increase relative to time 0. (B) DNA synthesis, analyzed as [^{3}H]thymidine incorporation (48 h) and expressed as a percentage of the control (nonspecific-shRNA-transfected) cells. (C) Detection of proliferative cells through immunocytochemistry with an anti-Ki67 antibody; quantification of the positive nuclei expressed as a percentage of total nuclei number. Data are means ± SEM of three independent experiments. Student's *t* test versus control (nonspecific-shRNA-transfected) cells was used in (B) and (C): $^*p < 0.05$, $^{**}p < 0.01$, $^{***}p < 0.001$.

Results

In vitro analysis of the effect of silencing NOX4 on the proliferation of liver tumor and untransformed cells

To know the role of NOX4 on liver tumor cell growth, we targeted NOX4 for knockdown with specific shRNA in the HCC cell lines PLC/PRF/5 and Hep3B and selected stable clones (Supplementary Fig. 1). Western blot revealed specific reduction of a 60-kDa band, the expected size for NOX4, as well as of two additional bands of slightly smaller size (Supplementary Fig. 1A). NOX4-targeting knockdown correlated with a decrease in intracellular oxidant levels, through H_2DCFDA fluorescence analysis, as well as in extracellular hydrogen peroxide levels, through Amplex red assay (Supplementary Fig. 1B). To analyze the loss of NOX4 function we evaluated the cell response to TGF-β in terms of apoptosis, a process that requires NOX4 [13]. As expected, TGF-β-induced activation of caspase-3 was significantly diminished when NOX4 was knocked down (Supplementary Fig. 1C).

We first decided to analyze the effect of canceling NOX4 on in vitro growth of HCC cells. For this, we performed experiments to compare the proliferative capacity of NOX4-silenced cells versus their respective controls. Two different cell lines were analyzed (PLC/PRF/5 and Hep3B), with similar results. Cell number, as well as DNA synthesis analyzed as [^{3}H]thymidine incorporation into TCA-precipitable material or Ki67-positive cells, was significantly increased in NOX4-knockdown cells (Fig. 1). Enhancement of cell proliferation correlated with significant lower percentage of cells in G1 phase of the cell cycle and significant increase in the percentage of cells in S phase (Fig. 2A). Previous reports had proposed a role for NOX4 in TGF-β-induced senescence through upregulation of p21(CIP1/WAF1) and p15INK4b [26]. For this, we decided to analyze the expression of these cyclin-dependent kinase inhibitors. We found that attenuation of NOX4 expression provoked a decrease in the transcript levels of *CDKN1A* (p21) (Fig. 2B). No significant changes in *p15INK4b* were observed (results not shown). Correlating with this, analysis of cyclin D1 protein by Western blot revealed higher levels in NOX4-silenced versus control cells (Fig. 2C). Interestingly, HCC cells in which NOX4 expression was knocked down showed higher nuclear localization of β-catenin (Fig. 2D). To know whether the role of NOX4 in controlling proliferation was a specific characteristic of tumor cells or whether it also occurs in untransformed cells, we performed experiments of transient targeting knockdown of NOX4

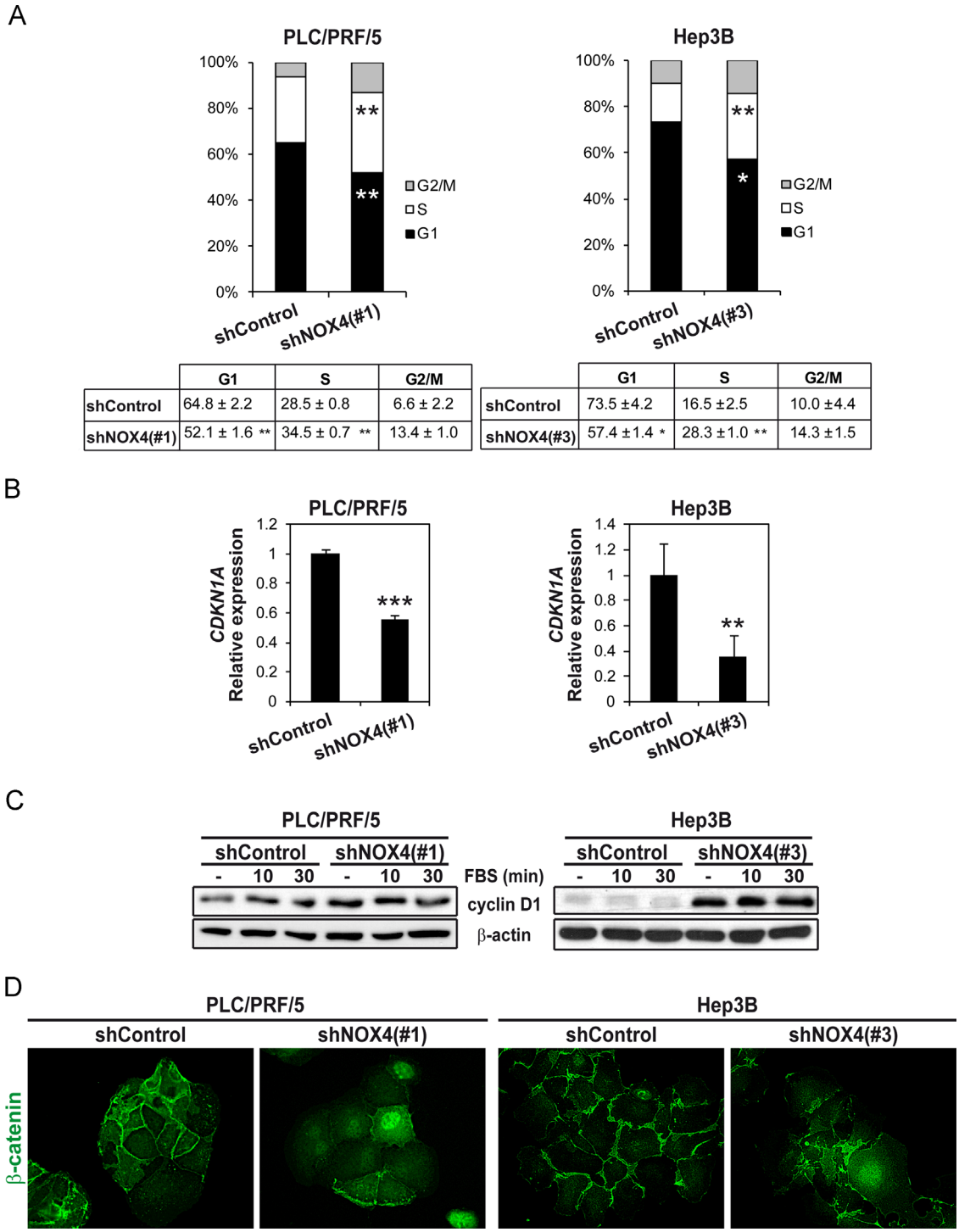

	G1	S	G2/M
shControl	64.8 ± 2.2	28.5 ± 0.8	6.6 ± 2.2
shNOX4(#1)	52.1 ± 1.6 **	34.5 ± 0.7 **	13.4 ± 1.0

	G1	S	G2/M
shControl	73.5 ±4.2	16.5 ±2.5	10.0 ±4.4
shNOX4(#3)	57.4 ±1.4 *	28.3 ±1.0 **	14.3 ±1.5

Fig. 2. Stable silencing of NOX4 increases the proportion of HCC cells in proliferating phases of the cell cycle. The cell line and the shNOX4 used are indicated. (A) Analysis of the percentage of cells in the various phases of the cell cycle in control and NOX4-silenced (shNOX4) cells. (B) Analysis of *CDKN1A* expression by real-time PCR. (C) Analysis of cyclin D1 by Western blot at 10 and 30 min after 10% FBS stimulation. (D) Immunofluorescence analysis of β-catenin (green). Data in (A) and (B) are means ± SEM of at least three independent experiments. Student's *t* test versus control (nonspecific-shRNA-transfected) cells was used: $^{*}p < 0.05$, $^{**}p < 0.01$, $^{***}p < 0.001$. (C) and (D) show a representative experiment.

in the untransformed human hepatocyte cell line CHL and in an immortalized mouse hepatocyte cell line. As shown in Fig. 3, silencing of NOX4 (Fig. 3A), which correlated with a significant decrease in the intracellular oxidant levels (Fig. 3B), significantly increased the growth of both cell lines (Fig. 3C). All these results indicated that NOX4 negatively controls the proliferation of liver tumor and untransformed cells.

NOX4 expression is downregulated during liver regeneration after partial hepatectomy in mice

Because results described above indicated an inverse correlation between NOX4 expression and liver cell growth in in vitro experiments, we hypothesized that NOX4 expression may inversely correlate with hepatocyte proliferation under physiological

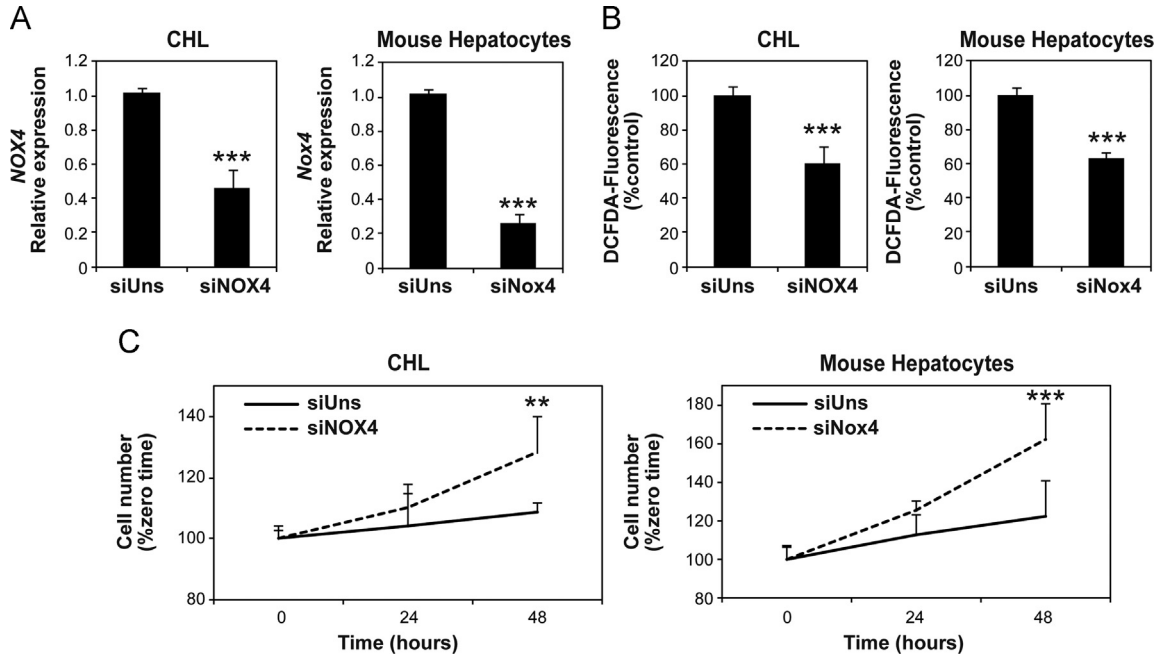

Fig. 3. NOX4-targeted knockdown increases proliferation in both human and mouse hepatocytes. CHL cells and mouse hepatocytes were transfected with an unsilencing siRNA (siUns) or a specific NOX4 siRNA (siNOX4). (A) Analysis of NOX4 mRNA expression by real-time PCR. (B) Analysis of intracellular oxidant levels. (C) Number of viable cells analyzed by crystal violet at the indicated times. Results are expressed as a percentage of increase relative to time 0. Student's *t* test versus control (nonspecific-siRNA-transfected) cells was used: $^{**}p < 0.01$, $^{***}p < 0.001$.

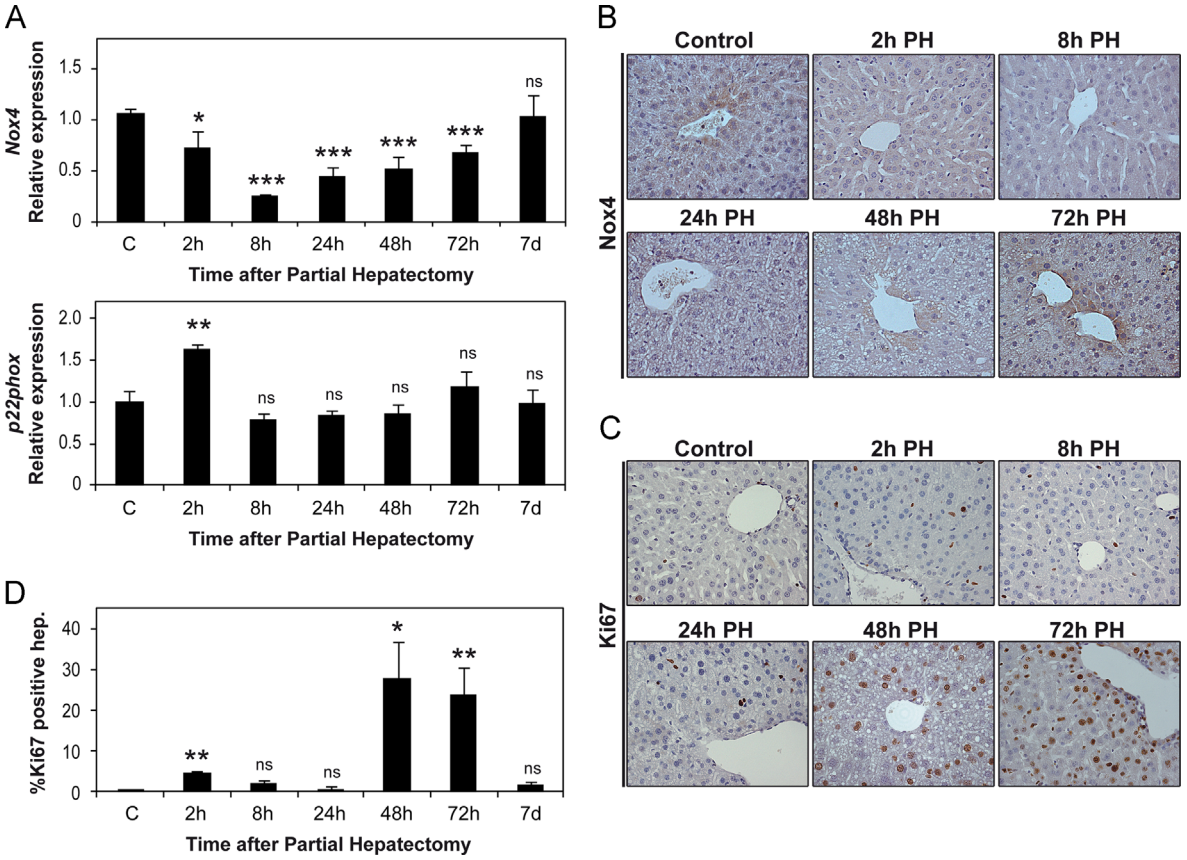

Fig. 4. Downregulation of NOX4 during liver regeneration after partial hepatectomy in mice. (A) Analysis of NOX4 and p22phox mRNA expression by real-time PCR at the indicated times after partial hepatectomy. Immunohistochemistry of (B) NOX4 and (C) Ki67 at the indicated times after partial-hepatectomy. (D) Quantification of the percentage of Ki67-labeled nuclei. Data in (A) and (D) are means ± SEM of at least three mice per group. Student's *t* test versus control was used: $^{*}p < 0.05$, $^{**}p < 0.01$, $^{***}p < 0.001$.

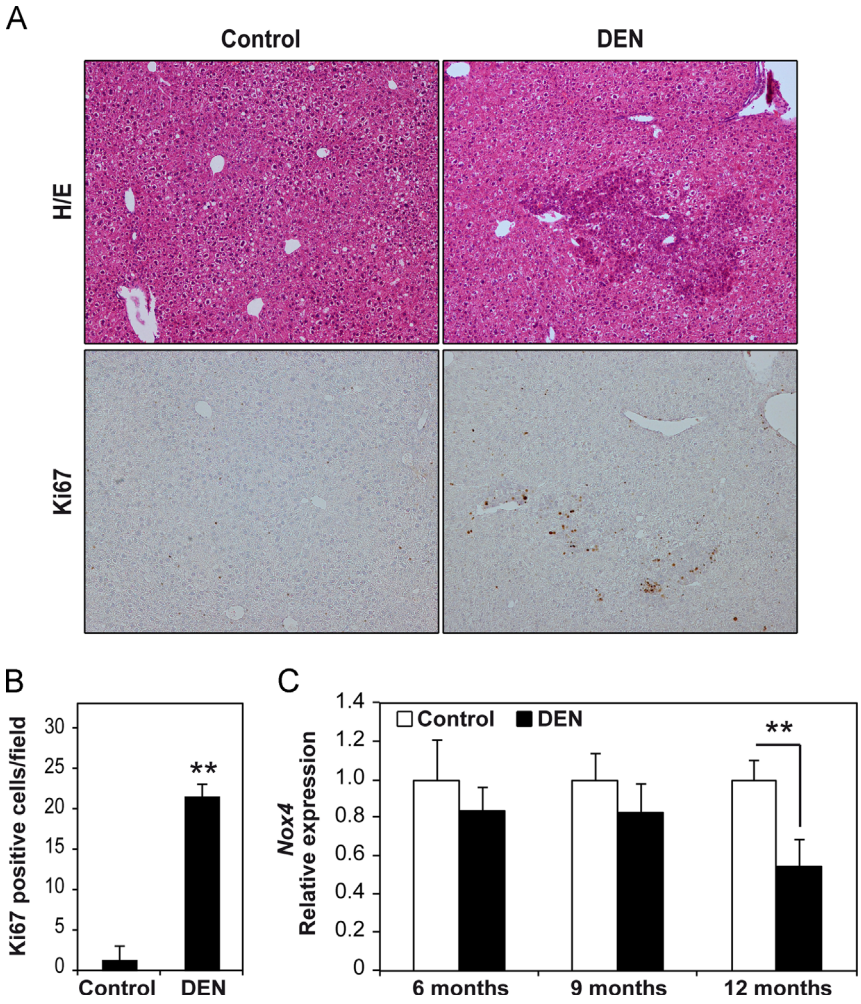

Fig. 5. Tumorigenesis in mice after DEN treatment is associated with decreased NOX4 expression. (A) Immunohistochemistry of 12-month-old mouse livers. Top: H&E stain. Bottom: immunohistochemistry of Ki67. (B) Quantification of the number of Ki67-labeled nuclei per field. (C) *NOX4* transcript levels analyzed by real-time PCR in control liver (PBS treatment) versus tumoral tissues in animals at 6, 9, and 12 months of age. Data represent means ± SEM (number of animals: 4 control animals; 3 DEN-treated animals; analysis in two different pieces of tissue/animal). Student's *t* test was used: $^{**}p < 0.01$.

and/or pathological situations where proliferation of liver cells takes place. To confirm this hypothesis, we studied changes in the expression of NOX4 after two-thirds partial hepatectomy in mice, a situation that pushes hepatocytes to leave the G0 phase of the cell cycle to proliferate and regenerate the liver. As shown in Fig. 4A, partial hepatectomy provoked a downregulation of NOX4 expression between 2 and 72 h, which completely recovered after 7 days, without changes in *p22phox* expression, correlating with lower NOX4 protein levels in hepatocytes analyzed by immunohistochemistry (Fig. 4B). This effect preceded the peak of maximal DNA synthesis in hepatocytes (Fig. 4C and D). Thus, in vivo liver cell proliferation correlates with a decrease in NOX4 expression.

Inverse correlation between NOX4 expression and liver tumor progression in experimental animal models

The treatment of mice with DEN at day 15 of age provokes a situation of liver injury that develops in the appearance of liver tumors between 9 and 12 months of age in mice. We had previously reported the use of this model for analyzing molecular mechanisms of liver tumorigenesis [27]. At 12 months of age all the male mice presented multifocal liver tumors, well recognized as neoplastic areas where proliferating cells were localized (Fig. 5A and B). We decided to analyze NOX4 mRNA levels in the livers of DEN-treated mice at 6, 9, and 12 months of age. Interestingly, a significant decrease in NOX4 expression was observed in 12-month-old animals, coincident with the appearance of liver tumors. These results indicated that in vivo liver tumor cell proliferation also correlates with a decrease in NOX4 expression in an experimental model in mice.

Considering all the results described above we hypothesized that silencing of NOX4 expression may increase the tumorigenic capacity of HCC cells. To confirm this hypothesis, we studied the tumor formation and progression capacities of control and NOX4-knockdown Hep3B cells in xenograft experiments into athymic nude mice (Fig. 6A and B). Results indicated that attenuation of NOX4 significantly increased the cell tumorigenic capacity, as tumors appeared earlier and reached a much higher volume than those induced by shControl Hep3B cells. Maintenance of the decrease in NOX4 expression in tumors from NOX4-knockdown HCC cells was corroborated by immunohistochemical analysis of the tumor tissues (Supplementary Fig. 2). Interestingly, increased rate in tumor progression correlated with significant enhancement in tumor cell proliferation (Fig. 6C). Number of apoptotic cells was low in both cohorts of tumors (Fig. 6D) and when caspase-3 activity was analyzed in tissues, although a tendency to decrease was observed in the tumors originating from NOX4-knockdown cells, the effect was not statistically significant (Fig. 6E).

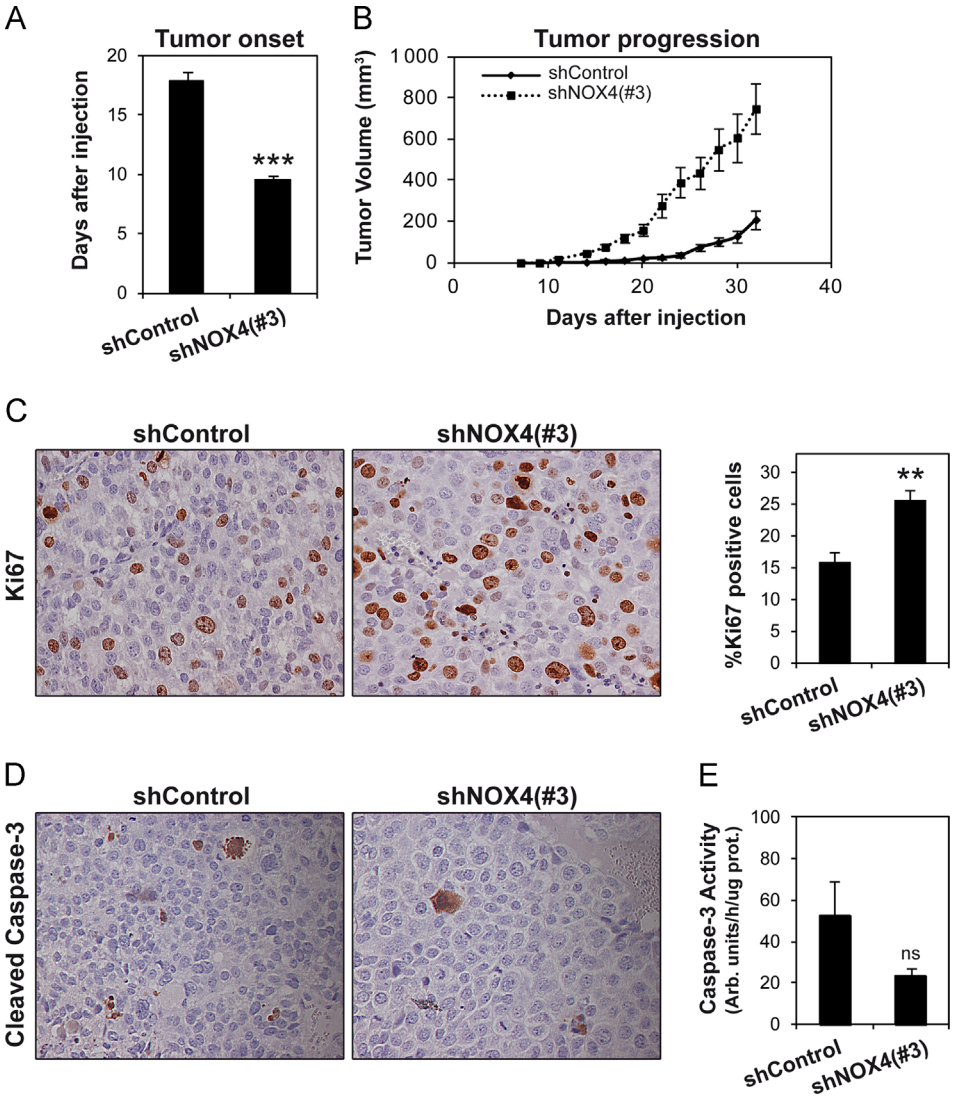

Fig. 6. Stable silencing of NOX4 in human HCC cells increases their tumorigenic capacity when injected subcutaneously into athymic nude mice. Hep3B cells stably transfected with a plasmid containing either an shRNA against NOX4 (shNOX4(No. 3)) or an unsilencing sequence (shControl) were injected subcutaneously into athymic nude mice. (A) Number of days after injection when tumors appeared. (B) Tumor volumes over time. (C) Left: immunohistochemistry of Ki67. Right: quantification of the percentage of labeled nuclei. (D) Immunohistochemistry of cleaved caspase-3. (E) Analysis of caspase-3 activity. Data are means ± SEM of at least six mice per group. Student's *t* test versus control (nonspecific-shRNA-transfected cells) was used: $^{**}p < 0.01$, $^{***}p < 0.001$.

Human liver tumors show decreased levels of NOX4 protein

Owing to the observed effect of targeting NOX4 knockdown on liver tumor progression in animal models, we decided to evaluate NOX4 protein levels in human HCC cell lines as well as in tissues from human liver tumors (Fig. 7). Immunofluorescence analysis in normal hepatocytes (CHL) and different HCC cell lines (PLC/PRF/5, Hep3B, and HLF) revealed that NOX4 is downregulated in transformed cell lines compared to normal cells (Fig. 7A). A tissue array that contained 65 samples (in duplicate) of liver tumors, of which 62 were HCC, as well as 2 samples (in duplicate) of healthy tissue (as control) and 3 samples (in duplicate) of nonmalignant lesions, was used for immunohistochemical analysis of NOX4. It was evidenced that most of the HCC tissues showed lower NOX4 expression compared to the control samples or even compared to the nonmalignant lesions (Fig. 7B). Interestingly, although few samples were included to get significant results, spots from cholangiocarcinoma and hepatoblastoma also showed lower NOX4 levels. Quantitative analysis corroborated decreased levels of NOX4 in most of the tumor samples (Fig. 7B, right). In 47% of the cases the ratio of NOX4 expression in tumor versus healthy tissues was lower than 0.8, and in 13% of the cases it was lower than 0.5.

Discussion

The recent discovery of new members of the NADPH oxidase family opened up perspectives about the roles of these ROS-producing enzymes in human physiology and pathology. However, we are only at the beginning of understanding the players and their interactions. The recent implication of these enzymes in pathological processes, such as cardiovascular diseases or fibrosis, prompted the discovery of drugs that target their function and ameliorate the diseases. However, it is necessary to dissect all the functions of these enzymes to predict what would be the consequences of their targeting. NOX4 has been proved to mediate fibrosis in the liver [8] and NOX inhibitors are being tested in preclinical assays as a new therapy in liver fibrosis [9,10]. However, results presented in this article indicate that NOX4 may also play a tumor suppressor function in the liver. A variety of evidence supports this hypothesis: (1) targeting NOX4 confers selective

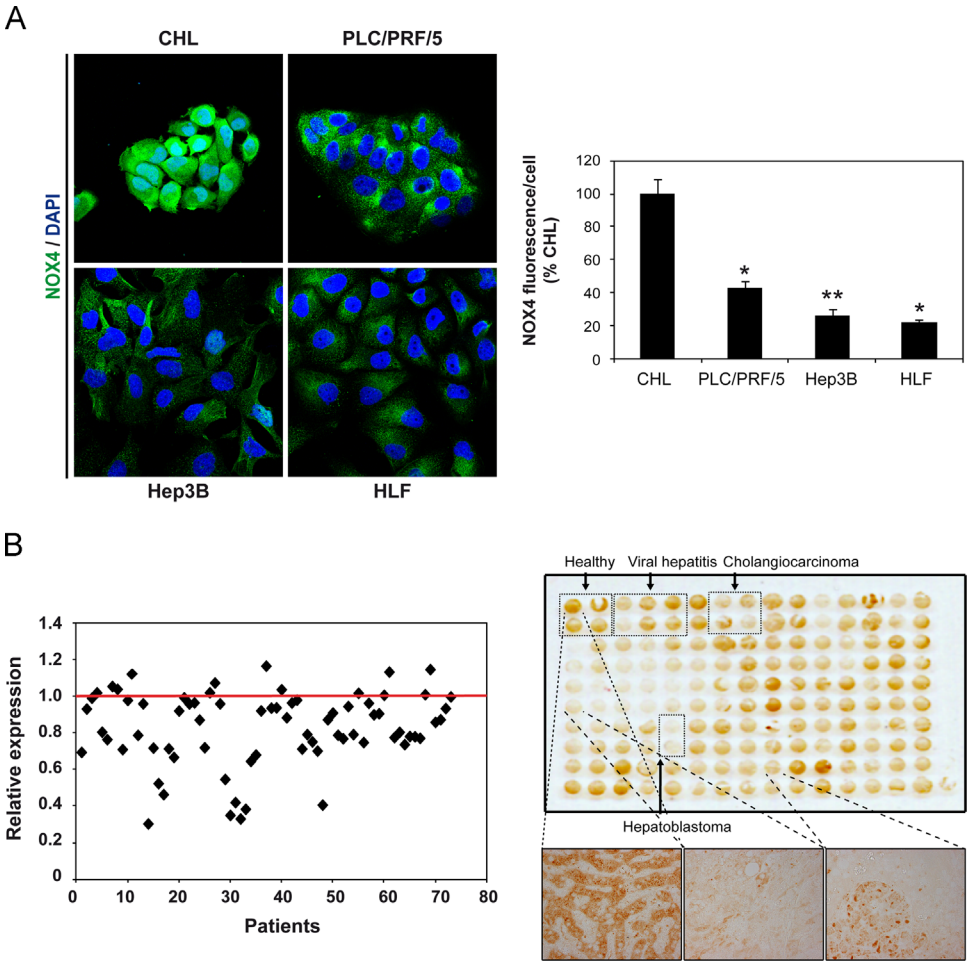

Fig. 7. NOX4 is downregulated in both human HCC cell lines and tissues. (A) Left: NOX4 (green) and DAPI (blue) staining in human hepatocytes (CHL) and human HCC cell lines (PLC/PRF/5, Hep3B, and HLF). Right: quantification of NOX4 fluorescence per cell represented as percentage versus CHL. Data are means ± SEM and Student's *t* test versus normal hepatocytes (CHL) was used: $^{*}p < 0.05$, $^{**}p < 0.01$. (B) Right top: macro overview of the NOX4 immunohistochemistry staining of the human liver tumor tissue array. Spots corresponding to healthy donors, viral hepatitis patients, cholangiocarcinoma, or hepatoblastoma are indicated. All the other spots correspond to hepatocellular carcinoma. Right bottom: representative microscopy images of one of the healthy liver spots and two of the HCC patients' spots. Left: densitometric quantification of each HCC tissue spot versus healthy tissue. Red line represents healthy tissue values.

advantage to liver cells to proliferate in vitro; (2) during liver regeneration after two-thirds partial hepatectomy in mice, a process that requires hepatocytes to leave quiescence and enter the cell cycle, *NOX4* expression is transiently downregulated; 3) liver tumorigenesis in an experimental model in mice correlates with downregulation of *NOX4;* (4) targeting NOX4 in HCC cells confers an advantage for tumor progression in a xenograft model of in vivo tumorigenesis; and (5) lower levels of NOX4 are found in human HCC cell lines and in a great percentage of human liver tumor tissues.

Correct progression through the cell cycle and its precise regulation is essential to an organism for proliferation and survival. The production of ROS in early growth factor-induced signaling pathways has led to the proposal that ROS regulate the G0 to G1 transition of the cell cycle through the regulation of cyclin D1 expression [28]. Furthermore, recent results indicate that NOX4 in human normal fibroblasts is required to suppress the p53-dependent checkpoint of proliferation [29]. However, various pieces of evidence locate ROS and, in particular, oxidative stress induced by NOX4 in a completely opposite role, i.e., inducing cell cycle arrest and cell death through either senescence or apoptosis. A possible explanation for these pleiotropic and sometimes contradictory actions of ROS may be related to the intracellular compartment where ROS are produced. NOX4 is associated with intracellular compartments, including the endoplasmic reticulum (ER), mitochondria, and nucleus. Nuclear NOX4 has been proposed to mediate ROS-induced DNA damage that leads to a loss of replicative potential and subsequent senescence [30,31]. In this same line of evidence, NOX4 mediates TGF-β-induced senescence in HCC cells through upregulation of p21(CIP1/WAF1) and p15INK4b [26].

Intracellular NOX4-derived ROS may also mediate signal transduction in normal cells by regulating redox-sensitive cysteine residues in specific effector proteins including tyrosine phosphatases [32]. Indeed, ER localization of NOX4 is critical for the regulation of protein tyrosine phosphatase (PTP1B), also an ER resident, through redox-mediated signaling. NOX4-mediated oxidation and inactivation of PTP1B in the ER serves as a regulatory switch for epidermal growth factor (EGF) receptor trafficking and specifically acts to terminate EGF (and maybe other growth factors) signaling [33].

Here we show that physiological proliferative situations in the liver, such as liver regeneration after partial hepatectomy in mice, or neoplastic liver pathologies, such as that found in the mouse model of DEN-induced hepatocarcinogenesis, concur with significant decreases in NOX4 expression. These results, together with the higher tumorigenic capacity of NOX4-silenced HCC cells in xenograft experiments in mice, point to the in vivo relevance of the in vitro results, in that the attenuation of NOX4 expression is coincident with a higher proportion of cells in the S phase of the

cell cycle, downregulation of *CDKN1A* (p21), and upregulation of cyclin D1. Interestingly, NOX4-knockdown cells show nuclear translocation of β-catenin and it has been reported that HCCs with β-catenin activation display significantly higher proliferation rate and larger tumor size compared with β-catenin-negative tumors [34]. All these results together indicate that NOX4 in liver tumor cells acts as a growth inhibitor, compatible with its potential role in counteracting growth factor signals and/or inducing senescence. In support of this, it is worth noting that NOX4 levels appear to be decreased in a cohort of tissues from human liver tumors, most of them HCC.

In conclusion, our results suggest a role for NOX4 as a redox enzyme involved in controlling proliferation of liver cells. Overall, NOX4 would play an essential tumor suppressor role in the liver. Considering that fibrotic processes frequently develop in cirrhosis, which is a preneoplastic situation, it is necessary to be cautious in the use of NOX4 inhibitors in these pathologies.

Acknowledgments

This work was supported by grants to I.F. from the Ministry of Economy and Competitiveness, Spain (BFU2009-07219, BFU2012-35538, ISCIII-RTICC RD06/0020, and RD12-0036-0029) and AGAUR-Generalitat de Catalunya (2009SGR-312). E.C.-M. was the recipient of a predoctoral fellowship from the FPU program, Ministry of Education, Culture, and Sport, Spain. J.L.-L. and J.F. were recipients of predoctoral fellowships from the Bellvitge Biomedical Research Institute (IDIBELL) program. We thank Dr. Esther Castaño (Serveis Cientificotècnics, Institut d'Investigació Biomèdica de Bellvitge, Universitat de Barcelona) for her technical assistance with the flow cytometry, Dr. Carmen Casal for her technical assistance with the confocal microscope, and the team of the Animal Core Facility of IDIBELL for their help in tumorigenesis experiments in mice.

Appendix A. Supplementary material

Supplementary data associated with this article can be found in the online version at http://dx.doi.org/10.1016/j.freeradbiomed.2014.01.040.

References

[1] Altenhofer, S.; Kleikers, P. W.; Radermacher, K. A.; Scheurer, P.; Hermans, J. J. R.; Schiffers, P.; et al. The NOX toolbox: validating the role of NADPH oxidases in physiology and disease. *Cell. Mol. Life Sci.* **69:**2327–2343; 2012.

[2] Brown, D. I.; Griendling, K. K. Nox proteins in signal transduction. *Free Radic. Biol. Med.* **47:**1239–1253; 2009.

[3] Martyn, K. D.; Frederick, L. M.; von Loehneysen, K.; Dinauer, M. C.; Knaus, U. G. Functional analysis of Nox4 reveals unique characteristics compared to other NADPH oxidases. *Cell. Signalling* **18:**69–82; 2006.

[4] Lyle, A. N.; Deshpande, N. N.; Taniyama, Y.; Seidel-Rogol, B.; Pounkova, L.; Du, P.; et al. Poldip2, a novel regulator of Nox4 and cytoskeletal integrity in vascular smooth muscle cells. *Circ. Res.* **105:**249–259; 2009.

[5] Lambeth, J. D.; Kawahara, T.; Diebold, B. Regulation of Nox and Duox enzymatic activity and expression. *Free Radic. Biol. Med.* **43:**319–331; 2007.

[6] Serrander, L.; Cartier, L.; Bedard, K.; Banfi, B.; Lardy, B.; Plastre, O.; et al. NOX4 activity is determined by mRNA levels and reveals a unique pattern of ROS generation. *Biochem. J.* **406:**105–114; 2007.

[7] Hecker, L.; Vittal, R.; Jones, T.; Jagirdar, R.; Luckhardt, T. R.; Horowitz, J. C.; et al. NADPH oxidase-4 mediates myofibroblast activation and fibrogenic responses to lung injury. *Nat. Med.* **15:**1077–1081; 2009.

[8] Sancho, P.; Mainez, J.; Crosas-Molist, E.; Roncero, C.; Fernandez-Rodriguez, C. M.; Pinedo, F.; et al. NADPH oxidase NOX4 mediates stellate cell activation and hepatocyte cell death during liver fibrosis development. *PLoS One* **7:**e45285; 2012.

[9] Aoyama, T.; Paik, Y. H.; Watanabe, S.; Laleu, B.; Gaggini, F.; Fioraso-Cartier, L.; et al. Nicotinamide adenine dinucleotide phosphate oxidase in experimental liver fibrosis: GKT137831 as a novel potential therapeutic agent. *Hepatology* **56:**2316–2327; 2012.

[10] Jiang, J. X.; Chen, X.; Serizawa, N.; Szyndralewiez, C.; Page, P.; Schroder, K.; et al. Liver fibrosis and hepatocyte apoptosis are attenuated by GKT137831, a novel NOX4/NOX1 inhibitor in vivo. *Free Radic. Biol. Med.* **53:**289–296; 2012.

[11] Laleu, B.; Gaggini, F.; Orchard, M.; Fioraso-Cartier, L.; Cagnon, L.; Houngninou-Molango, S.; et al. First in class, potent, and orally bioavailable NADPH oxidase isoform 4 (Nox4) inhibitors for the treatment of idiopathic pulmonary fibrosis. *J. Med. Chem.* **53:**7715–7730; 2010.

[12] Carnesecchi, S.; Deffert, C.; Donati, Y.; Basset, O.; Hinz, B.; Preynat-Seauve, O.; et al. A key role for NOX4 in epithelial cell death during development of lung fibrosis. *Antioxid. Redox Signaling* **15:**607–619; 2011.

[13] Carmona-Cuenca, I.; Roncero, C.; Sancho, P.; Caja, L.; Fausto, N.; Fernandez, M.; et al. Upregulation of the NADPH oxidase NOX4 by TGF-beta in hepatocytes is required for its pro-apoptotic activity. *J. Hepatol.* **49:**965–976; 2008.

[14] Caja, L.; Sancho, P.; Bertran, E.; Iglesias-Serret, D.; Gil, J.; Fabregat, I. Overactivation of the MEK/ERK pathway in liver tumor cells confers resistance to TGF-{beta}-induced cell death through impairing up-regulation of the NADPH oxidase NOX4. *Cancer Res.* **69:**7595–7602; 2009.

[15] Gonzalez-Rodriguez, A.; Clampit, J. E.; Escribano, O.; Benito, M.; Rondinone, C. M.; Valverde, A. M. Developmental switch from prolonged insulin action to increased insulin sensitivity in protein tyrosine phosphatase 1B-deficient hepatocytes. *Endocrinology* **148:**594–608; 2007.

[16] Caja, L.; Sancho, P.; Bertran, E.; Fabregat, I. Dissecting the effect of targeting the epidermal growth factor receptor on TGF-beta-induced-apoptosis in human hepatocellular carcinoma cells. *J. Hepatol.* **55:**351–358; 2011.

[17] Caja, L.; Sancho, P.; Bertran, E.; Ortiz, C.; Campbell, J. S.; Fausto, N.; et al. The tyrphostin AG1478 inhibits proliferation and induces death of liver tumor cells through EGF receptor-dependent and independent mechanisms. *Biochem. Pharmacol.* **82:**1583–1592; 2011.

[18] Sancho, P.; Martin-Sanz, P.; Fabregat, I. Reciprocal regulation of NADPH oxidases and the cyclooxygenase-2 pathway. *Free Radic. Biol. Med.* **51:**1789–1798; 2011.

[19] Sancho, P.; Bertran, E.; Caja, L.; Carmona-Cuenca, I.; Murillo, M. M.; Fabregat, I. The inhibition of the epidermal growth factor (EGF) pathway enhances TGF-beta-induced apoptosis in rat hepatoma cells through inducing oxidative stress coincident with a change in the expression pattern of the NADPH oxidases (NOX) isoforms. *Biochim. Biophys. Acta* **1793:**253–263; 2009.

[20] Higgins, G.; Anderson, G. M. Experimental pathology of the liver: restoration of the liver of the white rat following partial surgical removal. *Arch. Pathol.* **12:**186–202; 1931.

[21] Sanchez, A.; Alvarez, A. M.; Benito, M.; Fabregat, I. Apoptosis induced by transforming growth factor-beta in fetal hepatocyte primary cultures: involvement of reactive oxygen intermediates. *J. Biol. Chem.* **271:**7416–7422; 1996.

[22] Murillo, M. M.; del Castillo, G.; Sanchez, A.; Fernandez, M.; Fabregat, I. Involvement of EGF receptor and c-Src in the survival signals induced by TGF-beta1 in hepatocytes. *Oncogene* **24:**4580–4587; 2005.

[23] de Juan, C.; Benito, M.; Alvarez, A.; Fabregat, I. Differential proliferative response of cultured fetal and regenerating hepatocytes to growth factors and hormones. *Exp. Cell Res.* **202:**495–500; 1992.

[24] Valdes, F.; Alvarez, A. M.; Locascio, A.; Vega, S.; Herrera, B.; Fernandez, M.; et al. The epithelial mesenchymal transition confers resistance to the apoptotic effects of transforming growth factor beta in fetal rat hepatocytes. *Mol. Cancer Res.* **1:**68–78; 2002.

[25] Caja, L.; Ortiz, C.; Bertran, E.; Murillo, M. M.; Miro-Obradors, M. J.; Palacios, E.; et al. Differential intracellular signalling induced by TGF-beta in rat adult hepatocytes and hepatoma cells: implications in liver carcinogenesis. *Cell. Signalling* **19:**683–694; 2007.

[26] Senturk, S.; Mumcuoglu, M.; Gursoy-Yuzugullu, O.; Cingoz, B.; Akcali, K. C.; Ozturk, M. Transforming growth factor-beta induces senescence in hepatocellular carcinoma cells and inhibits tumor growth. *Hepatology* **52:**966–974; 2010.

[27] Bertran, E.; Crosas-Molist, E.; Sancho, P.; Caja, L.; Lopez-Luque, J.; Navarro, E.; et al. Overactivation of the TGF-β pathway confers a mesenchymal-like phenotype and CXCR4-dependent migratory properties to liver tumor cells. *Hepatology* **58:**2032–2044; 2013.

[28] Burch, P. M.; Heintz, N. H. Redox regulation of cell-cycle re-entry: cyclin D1 as a primary target for the mitogenic effects of reactive oxygen and nitrogen species. *Antioxid. Redox Signaling* **7:**741–751; 2005.

[29] Salmeen, A.; Park, B. O.; Meyer, T. The NADPH oxidases NOX4 and DUOX2 regulate cell cycle entry via a p53-dependent pathway. *Oncogene* **29:**4473–4484; 2010.

[30] Weyemi, U.; Dupuy, C. The emerging role of ROS-generating NADPH oxidase NOX4 in DNA-damage responses. *Mutat. Res.* **751:**77–81; 2012.

[31] Weyemi, U.; Lagente-Chevallier, O.; Boufraqech, M.; Prenois, F.; Courtin, F.; Caillou, B.; et al. ROS-generating NADPH oxidase NOX4 is a critical mediator in oncogenic H-Ras-induced DNA damage and subsequent senescence. *Oncogene* **31:**1117–1129; 2012.

[32] Finkel, T. Signal transduction by reactive oxygen species. *J. Cell Biol.* **194:**7–15; 2011.

[33] Chen, K.; Kirber, M. T.; Xiao, H.; Yang, Y.; Keaney Jr J. F. Regulation of ROS signal transduction by NADPH oxidase 4 localization. *J. Cell Biol.* **181:**1129–1139; 2008.

[34] Calvisi, D. F.; Conner, E. A.; Ladu, S.; Lemmer, E. R.; Factor, V. M.; Thorgeirsson, S. S. Activation of the canonical Wnt/beta-catenin pathway confers growth advantages in c-Myc/E2F1 transgenic mouse model of liver cancer. *J. Hepatol.* **42:**842–849; 2005.

HEPATOLOGY
Official Journal of the American Association for the Study of Liver Diseases

Dissecting the Role of Epidermal Growth Factor Receptor Catalytic Activity During Liver Regeneration and Hepatocarcinogenesis

Judit López-Luque,[1]* Daniel Caballero-Díaz,[1]* Adoración Martinez-Palacián,[2]* César Roncero,[2]** Joaquim Moreno-Càceres,[1]** María García-Bravo,[3,4,5]** Esther Grueso,[3,4] Almudena Fernández,[4,6] Eva Crosas-Molist,[1] María García-Álvaro,[2] Annalisa Addante,[2] Esther Bertran,[1] Angela M. Valverde,[7,8] Águeda González-Rodríguez,[7,8] Blanca Herrera,[2] Lluis Montoliu,[4,6] Teresa Serrano,[9] Jose-Carlos Segovia,[3,4,5] Margarita Fernández,[2] Emilio Ramos,[10] Aránzazu Sánchez,[2]*** and Isabel Fabregat[1,11]***

Different data support a role for the epidermal growth factor receptor (EGFR) pathway during liver regeneration and hepatocarcinogenesis. However, important issues, such as the precise mechanisms mediating its actions and the unique versus redundant functions, have not been fully defined. Here, we present a novel transgenic mouse model expressing a hepatocyte-specific truncated form of human EGFR, which acts as negative dominant mutant (ΔEGFR) and allows definition of its tyrosine kinase–dependent functions. Results indicate a critical role for EGFR catalytic activity during the early stages of liver regeneration. Thus, after two-thirds partial hepatectomy, ΔEGFR livers displayed lower and delayed proliferation and lower activation of proliferative signals, which correlated with overactivation of the transforming growth factor-*β* pathway. Altered regenerative response was associated with amplification of cytostatic effects of transforming growth factor-*β* through induction of cell cycle negative regulators. Interestingly, lipid synthesis was severely inhibited in ΔEGFR livers after partial hepatectomy, revealing a new function for EGFR kinase activity as a lipid metabolism regulator in regenerating hepatocytes. In spite of these profound alterations, ΔEGFR livers were able to recover liver mass by overactivating compensatory signals, such as c-Met. Our results also indicate that EGFR catalytic activity is critical in the early preneoplastic stages of the liver because ΔEGFR mice showed a delay in the appearance of diethyl-nitrosamine-induced tumors, which correlated with decreased proliferation and delay in the diethyl-nitrosamine-induced inflammatory process. *Conclusion*: These studies demonstrate that EGFR catalytic activity is critical during the initial phases of both liver regeneration and carcinogenesis and provide key mechanistic insights into how this kinase acts to regulate liver pathophysiology. (HEPATOLOGY 2016;63:604-619)

See Editorial on Page 371

The liver is a unique organ in displaying reparative response and regenerative capacity. However, prolonged liver regeneration as a consequence of

Abbreviations: DEN, diethyl-nitrosamine; EGFR, epidermal growth factor receptor; ERK, extracellular signal–regulated kinase; HCC, hepatocellular carcinoma; HGF, hepatocyte growth factor; mRNA, messenger RNA; NADPH, reduced nicotinamide adenine dinucleotide phosphate; PH, partial hepatectomy; qRT-PCR, quantitative reverse-transcriptase polymerase chain reaction; TGF-α/-β, transforming growth factor (α/β); TNF-α, tumor necrosis factor-α; uPA, urokinase-type plasminogen activator; WT, wild type.

From the [1]Bellvitge Biomedical Research Institute (IDIBELL), L'Hospitalet de Llobregat, Barcelona, Spain; [2]Department of Biochemistry and Molecular Biology II, School of Pharmacy, Complutense University of Madrid, and Instituto de Investigación Sanitaria del Hospital Clínico San Carlos, IdISSC, Madrid, Spain; [3]Cell Differentiation and Cytometry Unit, Hematopoietic Innovative Therapies Division, Centro de Investigaciones Energéticas, Medioambientales y Tecnológicas (CIEMAT), Madrid, Spain; [4]Centro de Investigación Biomédica en Red de Enfermedades Raras (CIBERER), Madrid, Spain; [5]Advanced Therapies Mixed Unit, CIEMAT/IIS Fundación Jiménez Díaz, Madrid, Spain; [6]Department of Molecular and Cellular Biology, National Centre for Biotechnology (CNB-CSIC), Madrid, Spain; [7]Instituto de Investigaciones Biomédicas "Alberto Sols" (CSIC/UAM), Madrid, Spain; [8]Centro de Investigación Biomédica en Red de Diabetes y Enfermedades Metabólicas Asociadas (CIBERDEM), ISCIII, Spain; [9]Pathological Anatomy Service, University Hospital of Bellvitge, Barcelona, Spain; [10]Department of Surgery, Liver Transplant Unit, University Hospital of Bellvitge, Barcelona, Spain; [11]Department of Physiological Sciences II, School of Medicine, University of Barcelona, Spain.

chronic liver diseases produces the appearance of genetic/epigenetic alterations that finally concur in the development of hepatocarcinogenesis. The epidermal growth factor receptor (EGFR/ErbB1) pathway plays an essential role in virtually all steps of these processes.[1] However, many questions remain unanswered. It is not well understood which of its two main functions (cell proliferation and survival) plays more essential roles during liver regeneration or hepatocarcinogenesis. Additionally, EGF/EGFR and hepatocyte growth factor (HGF)/Met signaling play both redundant and specific roles in these phenomena.[2-4] Nevertheless, their specific mechanisms are not completely known. We previously reported that the EGFR pathway impairs the suppressor arm of the transforming growth factor-β (TGF-β) pathway in hepatocytes and liver tumor cells *in vitro*[5,6]; however, there is no evidence that this effect may be relevant *in vivo*. Furthermore, there is a lack of knowledge about how necessary the catalytic domain of the EGFR pathway is in its *in vivo* actions, which is very important for the design of therapeutic strategies targeting this pathway. It would be expected that the enzymatic phosphorylation capacity of the EGFR is essential. In this sense, targeting EGFR by small interfering RNA technology or inhibiting its enzymatic capacity with gefitinib produced similar effects in liver tumor cells.[7] However, it has been also proposed that hepatocyte priming during liver regeneration involves modulation of the EGFR-mediated growth responses without an increase in its receptor tyrosine kinase activity.[8]

Taking all this into consideration, we decided to generate a new experimental animal model to explore the role of hepatocyte EGFR tyrosine kinase activity in liver regeneration and hepatocarcinogenesis. A transgenic animal was generated which expresses specifically in hepatocytes a truncated form of the human EGFR that lacks the intracellular catalytic domain (previously generated by Schlessinger's group[9]). This truncated form is able to undergo EGF-induced dimerization with wild-type (WT) receptors, allowing the binding of EGFR ligands but acting as a negative dominant mutant.[10,11] This model has the advantage, compared with the knockout mouse model, that the EGFR ligands bind to the receptors in the hepatocyte membrane and no excess of EGFR ligand is available to the nonparenchymal cells. Furthermore, only the intracellular domain of the EGFR is missed, which means that the specific role of the phosphorylation-dependent EGFR activity will be analyzed. Partial hepatectomy (PH) and diethylnitrosamine (DEN) treatment were performed to analyze the specific roles of the EGFR catalytic activity during liver regeneration and hepatocarcinogenesis.

Materials and Methods

Generation of Transgenic EGFR Mice and Hepatocyte Cell Lines. A complementary DNA coding for a truncated form of the human EGFR, lacking the kinase domain in its intracytosolic region (amino acids 654-1186), was cloned in transference bacterial artificial chromosome clone RP23-279P6 (kindly provided by Prof. Dr. Günther Schütz, Molekularbiologie der Zelle I, Deutsches Krebsforschungszentrum (DKFZ) Heidelberg, Germany) carrying *Albumin* locus and *Chloramphenicol* resistance gene. The truncated EGFR was introduced just in the ATG starting codon of the albumin gene, surrounded by 160 kb of the albumin chromosomal genomic sequence, as described (Fig. 1A).[12]

E. Grueso's present address is: Division of Medical Biotechnology, Paul Ehrlich Institute, Langen, Germany

Received April 14, 2015; accepted August 21, 2015.

Additional Supporting Information may be found at http://onlinelibrary.wiley.com/doi/10.1002/hep.28134/suppinfo.

Cofunded by the Ministry of Economy and Competitiveness-MINECO and the European Regional Development Fund-FEDER, Spain (Contract grant numbers: BFU2012-35538 and ISCIII-RTICC RD12-0036-0029 to I.F.-IDIBELL; SAF2009-12477 to A.S.-UCM/IdISSC; RETICS-RD12/0019/0023 and SAF2011-30526-C02-01 to J.-C.S.-CIEMAT/CIBERER/IIS-FJD; SAF2012-33283 to A.M.V.-CSIC/CIBERDEM). People Programme (Marie Curie Actions) of the FP7-2012, under REA grant agreement #PITN-GA-2012-316549 (IT-LIVER) to I.F.-IDIBELL and to A.S.-UCM/IdISSC. AGAUR-Generalitat de Catalunya to I.F-IDIBELL (Contract grant number: 2009SGR-312). Dirección General de Investigación de la Comunidad de Madrid, Spain (Contract grant number S2010/BMD-2402 to A.S.-UCM/IdISSC). Fundación Eugenio Rodríguez Pascual to M.G.-B.-CIEMAT/CIBERER/IIS-FJD. J.L.-L. was recipient of a predoctoral fellowship from IDIBELL; D.C.-D. and A.M.-P. were recipients of predoctoral fellowships from MINECO, Spain (Contract grant number: FPI - BES-2013-064609 and BES-2007-16187, respectively). [Correction added October 21, 2015, after first online publication: funding information was added.]

**These authors contributed equally to this work as first authors.*

***These authors contributed equally to this work as second authors.*

****These authors contributed equally to this work as senior authors.*

Address reprint requests to: Isabel Fabregat, Bellvitge Biomedical Research Institute (IDIBELL), Gran via de l'Hospitalet, 199, L'Hospitalet, 08908 Barcelona, Spain. E-mail: ifabregat@idibell.cat; tel: +34 932607828; fax: +34 932607426.

View this article online at wileyonlinelibrary.com.

DOI 10.1002/hep.28134

Potential conflict of interest: Nothing to report.

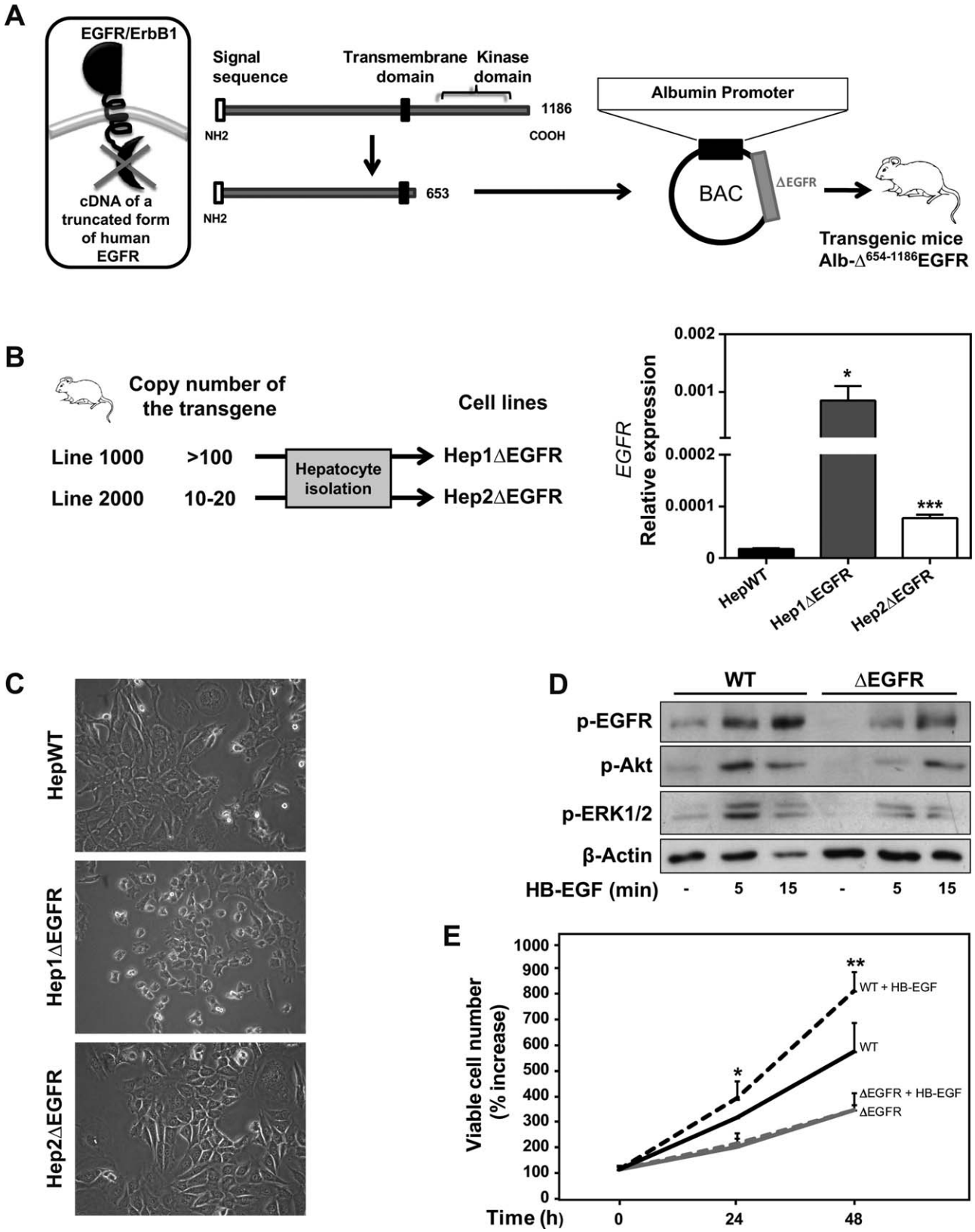

Fig. 1. Characterization of the transgenic model of Alb-$\Delta^{654\text{-}1186}$EGFR (abbreviated as ΔEGFR) mice. (A) A complementary DNA coding for a truncated form of the EGFR that had a deletion in its intracytosolic region (amino acids 654-1186) was cloned in a transference plasmid under the control of a specific hepatocyte promoter formed by the albumin locus just before ATG of the albumin mouse gene. Three different lines of transgenic mice were established and named as 1000, 2000, and 4000, which presented different copy number of the transgene. (B) Left: Primary hepatocytes were isolated from WT and ΔEGFR of the two mouse lines that presented a higher transgene copy number and immortalized as described in Materials and Methods. Right: Levels of human EGFR transcripts in mice analyzed by qRT-PCR. Mean ± standard error of the mean of three independent experiments. (C) Morphology of the isolated hepatocytes. (D) Response to heparin binding EGF-like growth factor in terms of EGFR phosphorylation (fetal bovine serum depleted medium) was attenuated in the Hep1ΔEGFR hepatocytes. Western blot analysis, a representative experiment of five is shown. (E) Differences in the response to heparin binding EGF-like growth factor (fetal bovine serum depleted medium) in terms of cell proliferation between WT and Hep1ΔEGFR hepatocytes. Cell number was analyzed by trypan blue staining. Mean ± standard error of the mean of two independent experiments performed in triplicate. (B,E) Student *t* test was used: $*P < 0.05$, $**P < 0.01$, $***P < 0.001$. Abbreviations: BAC, bacterial artificial chromosome; cDNA, complementary DNA; HB-EGF, heparin binding EGF-like growth factor.

Linearized bacterial artificial chromosome DNA was microinjected into the pronuclei of mouse B6CBAF2 zygotes according to reported protocols,[13] which were later transferred to pseudopregnant recipient females, finally obtaining transgenic mice Alb-$\Delta^{654\text{-}1186}$EGFR (from now abbreviated as ΔEGFR). Six different founder mice were bred with C57BL/6 WT mice. Three of them gave littermates and showed germline transmission of the transgene. The ΔEGFR F1 mice obtained were interbred to generate stable transgenic mouse lines, which were kept heterozygous. Transgenic lines are archived in the European Mouse Mutant Archive as B6CBA-Tg(Alb-deltaEGFR). Genotyping was assessed by polymerase chain reaction as specified in the European Mouse Mutant Archive. Using specific primers that exclusively detect expression of the human EGFR gene, we demonstrated the transgene expression in ΔEGFR mice by quantitative reverse-transcriptase polymerase chain reaction (qRT-PCR) analysis, which was confirmed at the protein level by western blot (Supporting Fig. S1).

For generation of immortalized hepatocytes, pools of four to six livers from WT and ΔEGFR neonates (5-7 days old) were used. Isolation of the cells (by collagenase dispersion) and immortalization were achieved as described.[14] For further details, culture conditions, cell viability, and apoptosis analyses, see the Supporting Information.

PH in Mice. PH was performed in animals at 8-12 weeks of age by removal of two-thirds of the liver, as described by Higgins and Anderson.[15] Mice were killed at 6, 12, 24, 48, and 72 hours and 7 days after surgery; and tissue samples were immediately frozen in liquid nitrogen for RNA and protein extraction, cryopreserved in optimal cutting temperature compound for oil red O staining, or fixed in 4% paraformaldehyde for immunohistochemical analysis. Sham-operated mice were used as control.

DEN-Induced Hepatocarcinogenesis in Mice. Male mice at day 15 of age received intraperitoneal injections of DEN (10 mg/kg) diluted in saline buffer. At 9 and 12 months of age, mice were sacrificed and their livers removed. For histological studies, liver lobes were fixed in 4% paraformaldehyde overnight and paraffin-embedded for immunohistochemical staining. Total RNA and protein were isolated from frozen tissues for qRT-PCR and western blotting analyses. Three to four animals/condition and at least two different tissue pieces/animal were processed for RNA extraction.

Western Blot Analysis. Total protein extracts and western blotting procedures were carried out as described.[16,17]

For more details and other methods, ethics statement, and statistical analysis, see the Supporting Information.

Results

Generation of Transgenic Mice Expressing a Truncated Form of the EGFR, Which Lacks the Catalytic Intracellular Domain in Hepatocytes. Three different lines of transgenic mice were established from founder mice expressing different copy numbers of the transgene (Fig. 1A). Primary hepatocytes were isolated and immortalized, as described above. EGFR messenger RNA (mRNA) expression levels were proportional to the copy number of the transgene (Fig. 1B). Analysis of cell morphology revealed that hepatocytes from line 1000 (highest expression of the transgene) presented lower viability (Fig. 1C) and decreased basal proliferative capacity compared with the WT ones. Response to heparin binding EGF-like growth factor was significantly attenuated in terms of EGFR phosphorylation/signaling, at either short (Fig. 1D) or long (results not shown) time points, as well as in terms of cell proliferation (Fig. 1E). TGF-β transactivates the EGFR in hepatocytes, which inhibits its proapoptotic activity.[7,18] Hepatocytes isolated from ΔEGFR mice did not phosphorylate the EGFR under TGF-β treatment, which correlated with impairment in the activation of survival signals, such as extracellular signal–regulated kinase (ERK) mitogen-activated protein kinases (Supporting Fig. S2A), higher growth inhibition, and apoptosis (Supporting Fig. S2B-D). Interestingly, ΔEGFR hepatocytes showed higher basal apoptosis compared with WT ones. These results indicate the suitability of the animal and cell model to study the specific implication of the hepatocyte EGFR catalytic domain in liver physiology and pathology.

ΔEGFR Mice Show Delayed Hepatocyte Proliferation After Two-Thirds PH Coincident With a Higher Activation of the TGF-β Pathway. To explore the specific role of hepatocyte EGFR activity during liver regeneration, we performed two-thirds PH in WT and ΔEGFR mice, selecting the two mouse lines with a higher expression of the transgene. WT animals activated the EGFR pathway in the remaining liver after PH, analyzed as EGFR phosphorylation in hepatocytes by immunohistochemical analysis of paraffined tissues (Fig. 2A). ΔEGFR animals, in contrast, did not show phosphorylation of the EGFR. This was not due to differences in expression of the endogenous EGFR or its ligand TGF-α, the EGFR ligand highly expressed in hepatocytes during liver regeneration[19] (Supporting Fig. S3A), which proves that the human ΔEGFR transgene indeed acts as a negative dominant, inhibiting the hepatocyte response to EGFR ligands. No compensatory increases in the expression of other members of the EGFR family

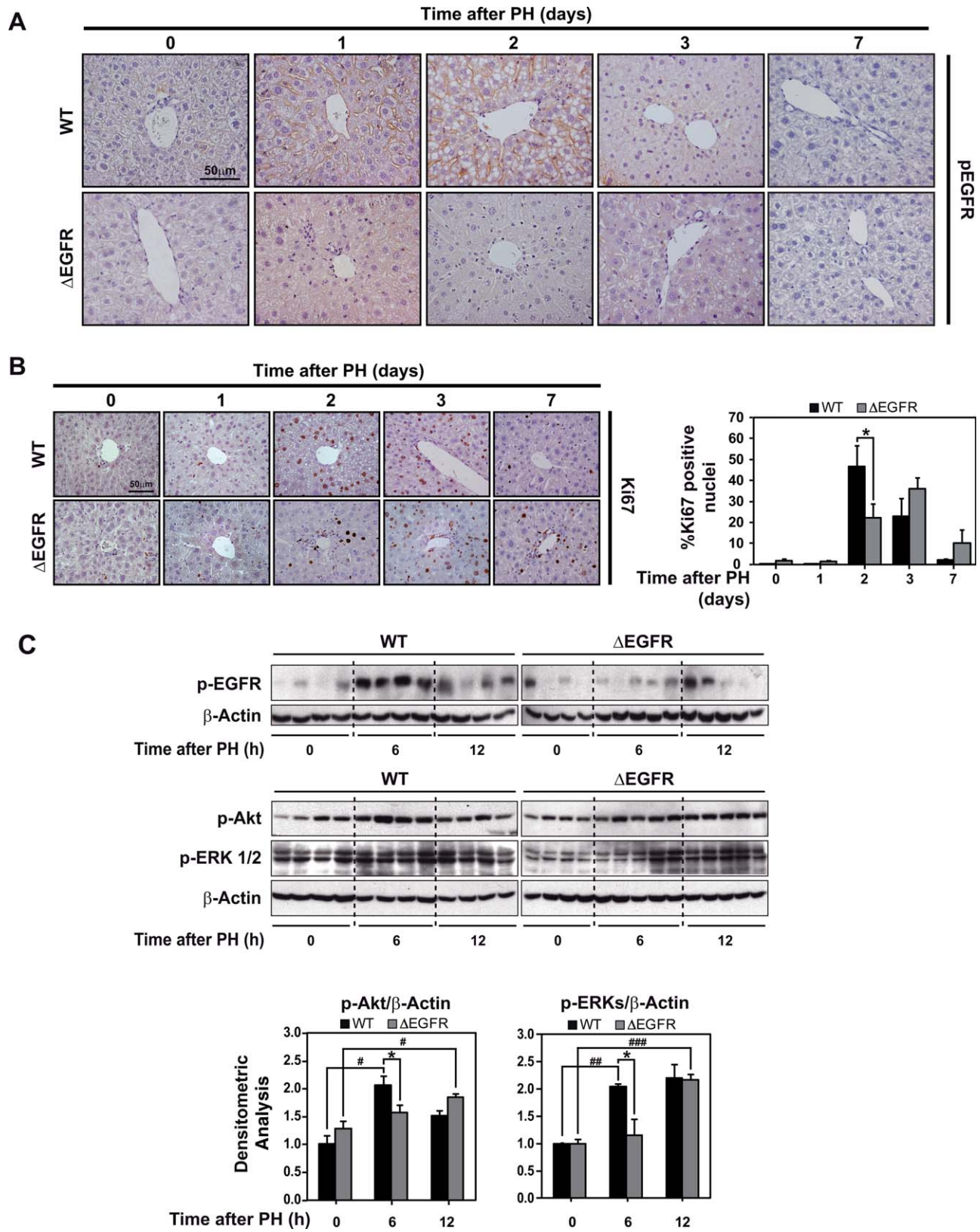

Fig. 2. Hepatocyte proliferation induced after two-thirds partial PH is delayed in ΔEGFR transgenic mice. Immunohistochemical analysis of phospho-EGFR (A) and Ki67 (B, left) in paraffined liver tissues from WT and ΔEGFR mice at the indicated times after PH. (B) Right: Quantification of the percentage of Ki67-labeled nuclei. (C) Upper: Western blot analysis of the protein levels of phospho-EGFR, phospho-Akt, and phospho-ERKs as early proliferative signals. Lower: Quantification of the densitometric analysis. (B, right; C, lower) Data are mean ± standard error of the mean of at least four animals per group. Student *t* test was used: $*P < 0.05$ compared to WT; $\#P < 0.05$, $\#\#P < 0.01$, and $\#\#\#P < 0.001$ compared to time 0.

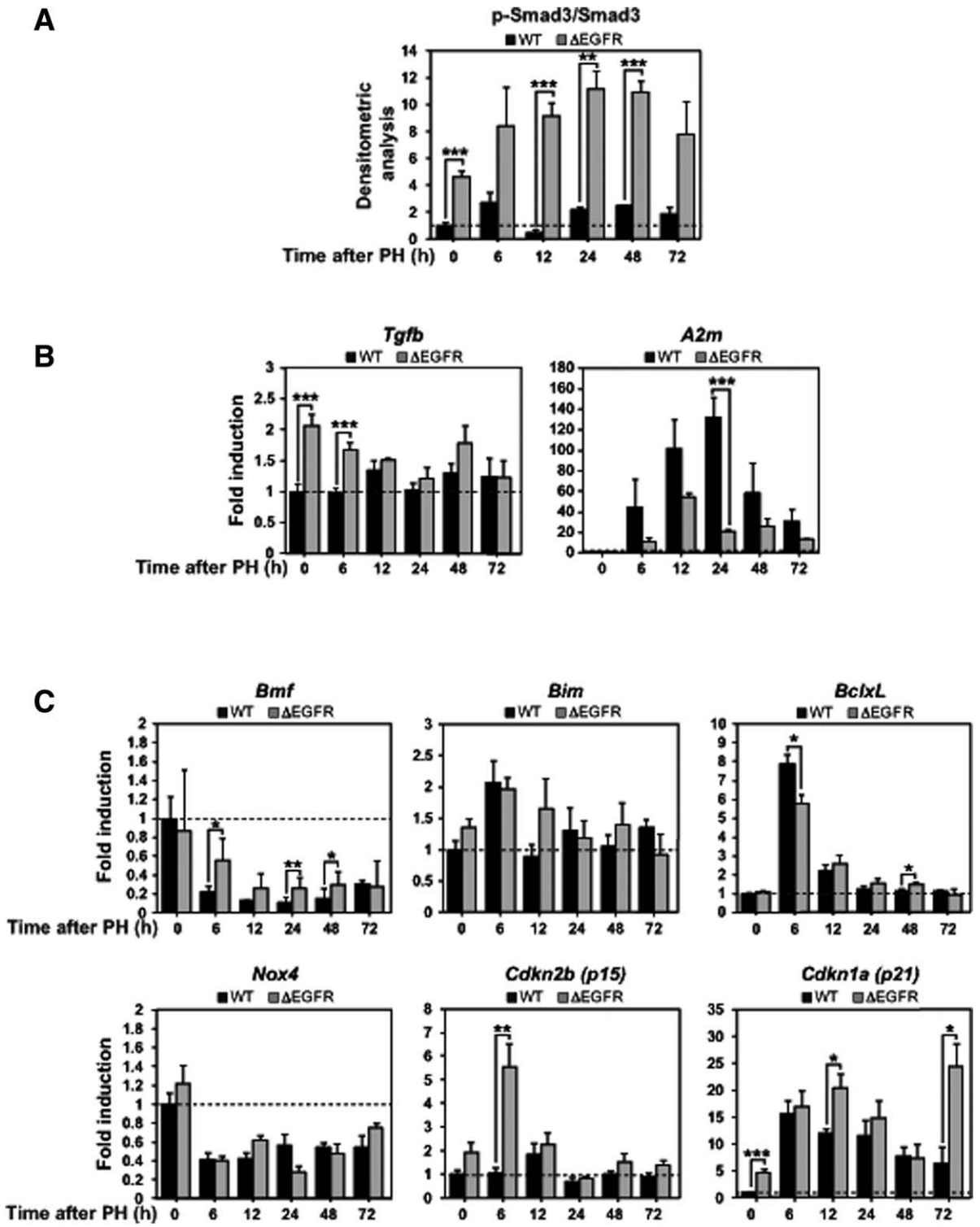

Fig. 3. Overactivation of the TGF-β pathway in ΔEGFR mice under basal conditions and during liver regeneration after PH. (A) Ratio of phospho-Smad3 versus Smad3 protein levels (densitometric analyses of western blots shown in Supporting Fig. S4) at basal conditions and at the indicated times after PH. (B) qRT-PCR analysis of *TGF-β1* and *A2m* mRNA levels. (C) Analysis of the mRNA levels of the indicated genes by qRT-PCR at different times after PH. (A-C) Data are mean ± standard error of the mean of at least four animals per group. Student *t* test was used: $*P < 0.05$, $**P < 0.01$, and $***P < 0.001$. Abbreviation: A2m, α_2-macroglobulin.

(*Erbb2*, *Erbb3*, and *Erbb4*), due to inactivation of the EGFR function, were found (Supporting Fig. S3B). Immunohistochemical analysis of Ki67 revealed lower and delayed hepatocyte proliferation in ΔEGFR mice (Fig. 2B). WT animals showed an early increase in the levels of intracellular signals that mediate hepatocyte

proliferation, such as p-AKT and p-ERK mitogen-activated protein kinases (Fig. 2C). However, ΔEGFR livers presented a significantly lower response. Cytokines such as interleukin-6 and tumor necrosis factor-α (TNF-α) are considered relevant for priming hepatocytes to proliferate[2-4]; however, both WT and ΔEGFR livers showed similar changes in the expression of these cytokines at 12-24 hours after PH, which correlated with a similar inflammatory response (results not shown).

Considering the relevant role played by EGF in counteracting the TGF-β suppressor effects,[6] we wondered whether ΔEGFR animals may show higher Smads phosphorylation and/or higher activation of TGF-β downstream pathways. Results indicated that Smad3 phosphorylation, a hallmark of TGF-β activation, is higher in ΔEGFR animals at basal levels and at all the times analyzed after PH (Fig. 3A; Supporting Fig. S4). Interestingly, the decrease in Smad3 phosphorylation observed in WT animals at 12 hours after PH was not observed in ΔEGFR mice, which maintained a high activation of the pathway. Levels of TGF-β1 transcripts were significantly higher in ΔEGFR livers before PH as well as at short times after PH compared with WT ones (Fig. 3B, left). Furthermore, α_2-macroglobulin, a plasma protein previously proposed as a binding protein for TGF-β that attenuates its effects,[20] was up-regulated in WT, but not in ΔEGFR, animals after PH (Fig. 3B right). Indeed, the EGFR pathway may up-regulate α_2-macroglobulin, which could in turn counteract TGF-β activity. All these data suggest a stronger activation of the TGF-β pathway in ΔEGFR livers compared with WT ones.

As *in vitro* experiments had indicated that EGF counteracts TGF-β-induced apoptosis by inhibiting its effects on *Bim* and *Bmf* up-regulation,[7] we tested for potential differences in the expression of these genes between WT and ΔEGFR mice. *Bmf*, but not *Bim*, expression was down-regulated after PH in both animals; but, interestingly, levels remained higher in ΔEGFR compared with WT mice (Fig. 3C). Expression of *Bcl-x$_L$*, an antiapoptotic Bcl-2 member known to be a TGF-β target gene in hepatocytes,[6] increased early after PH in both animal models, although the increase in ΔEGFR mice was slightly lower. However, in spite of these differences, analysis of the active form of caspase-3 by immunohistochemistry or caspase-3 activity in tissues revealed no differences between WT and ΔEGFR livers at any of the different times analyzed (Supporting Fig. S5). Because *Bim* and *Bcl-x$_L$* expression undergoes also posttranscriptional regulation, we analyzed their protein levels; but we could not find significant differences between WT and ΔEGFR mice (results not shown). Additionally, we searched for changes in the expression of *Nox4*, a reduced nicotinamide adenine dinucleotide phosphate (NADPH) oxidase whose expression is up-regulated by TGF-β and mediates its apoptotic actions,[21] an effect that is impaired by EGF.[5] *Nox4* expression significantly decreased after PH, as we have recently described.[22] However, no significant differences were observed between WT and ΔEGFR animals (Fig. 3C).

As apoptosis failed to explain the observed delay in the hepatocyte proliferative response, we next focused on the expression of cell cycle regulators modulated by TGF-β. We found a significant increase in the expression of *Cdkn2b* (the gene encoding p15INK4b) at 6 hours after PH in ΔEGFR mice that was not observed in WT animals (Fig. 3C). Levels of *Cdkn1a* transcripts (the gene encoding p21/WAF1/CIP1) increased at short times after PH in both animals, but whereas in WT animals levels slowly returned to basal ones, in ΔEGFR mice levels remained high, the differences being particularly relevant at 72 hours after PH. These results suggest that high levels of p15 could be responsible for the delay in the early proliferative response of ΔEGFR hepatocytes to PH and that high levels of p21 at later times could slow the proliferation during the entire regenerative process. Interestingly, both p15 and p21 levels were increased in nonhepatectomized ΔEGFR livers compared with WT ones. Indeed, a functional EGFR pathway may be necessary to counteract the cytostatic effects of TGF-β in hepatocytes, a process that is particularly crucial after two-thirds PH of the liver.

Regulation of Lipid Metabolism After Two-Thirds PH Is Altered in ΔEGFR Mice. When histological analysis by hematoxylin and eosin was performed, we observed that WT livers 48 hours after PH showed vacuolated cells, with the appearance of multifocal drops (Fig. 4A), whereas ΔEGFR livers did not show this appearance. Suspecting that they could be deposits of lipids, we performed oil red O staining, confirming the accumulation of lipid drops, which correlated with an increase in triglyceride levels in WT, but not in ΔEGFR, livers (Fig. 4B,C). Among different regulatory genes analyzed, the increase in lipid accumulation in WT livers was coincident with up-regulation of the mRNA levels of fatty acid synthase, a key enzyme involved in *de novo* fatty acid synthesis, and glucose-6-phosphate dehydrogenase, the regulatory enzyme of the pentose-phosphate cycle, responsible for NADPH production. However, up-regulation of these enzymes was altered in ΔEGFR animals (Fig. 4D). These results suggest that the EGFR pathway regulates lipid metabolism in hepatocytes after PH.

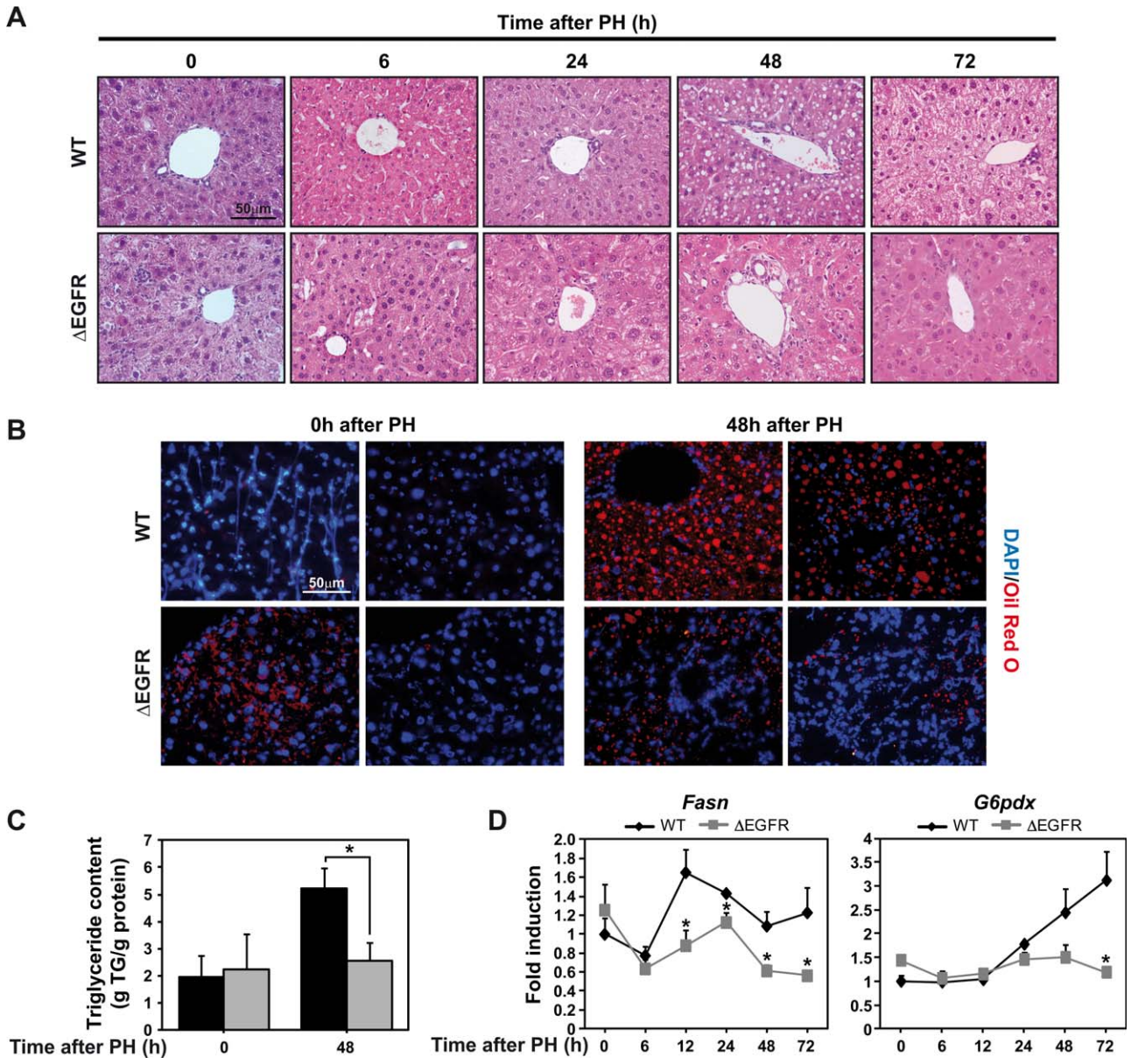

Fig. 4. ΔEGFR mice show differences in lipid metabolic changes during liver regeneration. (A) Histological analysis of the livers from WT and ΔEGFR mice by hematoxylin and eosin staining. (B) Immunohistochemical analysis of the lipid content by oil red O staining performed in frozen liver sections. (C) Analysis of triglyceride content in WT and ΔEGFR livers at basal conditions and 48 hours after PH. (D) qRT-PCR analysis of the levels of expression of *Fasn* and *G6pdx* at the indicated times after PH. (C) Data are mean ± standard error of the mean of three animals per group. Student *t* test was used: $*P < 0.05$. Abbreviations: DAPI, 4′,6-diamidino-2-phenylindole; TG, triglyceride.

ΔEGFR Mice Are Able to Regenerate the Liver: Potential Role of HGF/Met in This Process. Regardless of the described alterations, ΔEGFR mice showed only a slight, but not significant, increase in the mortality after two-thirds PH (Fig. 5A). Remaining animals overcame liver injury (analyzed by serum parameters; Supporting Table S2) and were able to fully regenerate the liver with a similar kinetic to WT animals (Fig. 5B). These results led us to state that in spite of the delay in hepatocyte proliferation, the capacity of the liver to recover its mass was not affected by the inhibition of EGFR signaling. Hence, we focused on identifying other potential mitogenic signals that could be overactivated in ΔEGFR livers. We observed that ΔEGFR mice expressed higher levels of *Hgf* mRNA than WT mice, both under basal conditions and shortly after PH (Fig. 5C, left). Interestingly, we also found differences in the expression of urokinase-type plasminogen activator (uPA), which mediates the release of HGF from extracellular matrix during liver regeneration.[23] uPA mRNA levels were elevated in ΔEGFR livers, compared with WT mice, this difference being particularly significant at

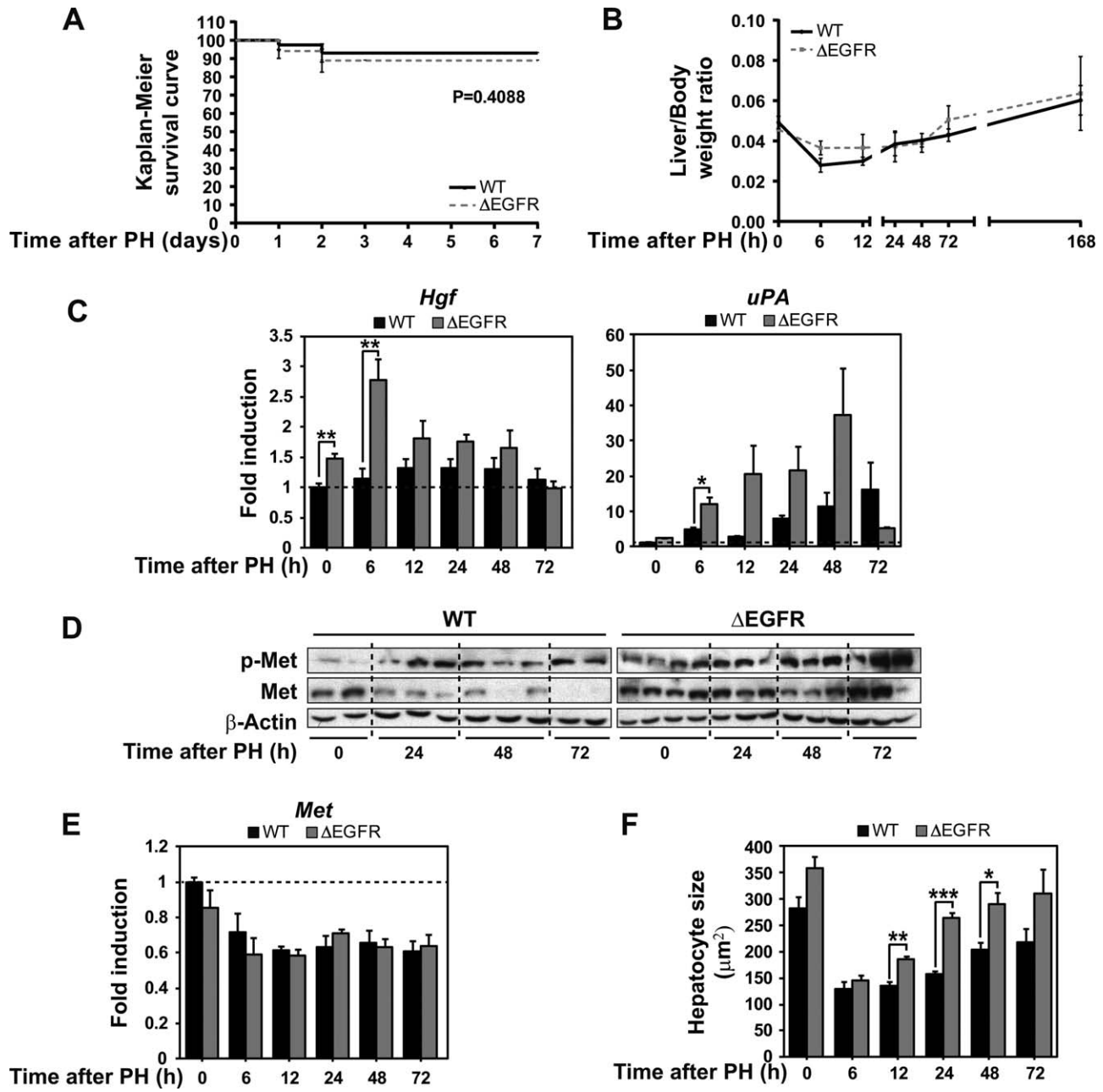

Fig. 5. ΔEGFR livers that are able to regenerate after PH show overactivation of the HGF/Met pathway and a significantly greater cell size compared with WT mice. (A) Kaplan-Meier survival curve. ΔEGFR mice showed a slight increase in mortality after two-thirds PH, although differences were not statistically significant. (B) Remaining animals fully regenerate the liver. Liver/body weight ratio. (C) qRT-PCR analysis of the mRNA levels of *Hgf* (left) and *uPA* (right). (D) Analysis of phospho-Met and total Met by western blot at the indicated times after PH in WT and ΔEGFR livers. (E) qRT-PCR analysis of the mRNA levels of *Met*. (F) Quantification of hepatocyte size at the indicated times (after immunostaining of E-cadherin to label the cell membrane; Supporting Fig. S6) using ImageJ software. (B,C,E,F) Data are mean ± standard error of the mean of at least three animals per group. Student *t* test was used: $*P < 0.05$, $**P < 0.01$, and $***P < 0.001$.

6 hours after PH (Fig. 5C, right). The increase in *Hgf* expression correlated with higher levels of c-Met phosphorylation in ΔEGFR livers. Notably, levels of phosphorylated c-Met remained high at 3 days after PH in ΔEGFR livers (Fig. 5D). It is worth noting that, although c-Met mRNA levels decreased after PH in both WT and ΔEGFR livers (Fig. 5E), the decrease in protein levels was only observed in WT animals, whereas ΔEGFR mice maintained, or even increased, c-Met levels at all time points analyzed (Fig. 5D). This suggests that a posttranscriptional regulation of c-Met may allow the maintenance of high protein levels after PH in ΔEGFR mice, resulting in a sustained activation of this pathway. All these results indicate that the HGF

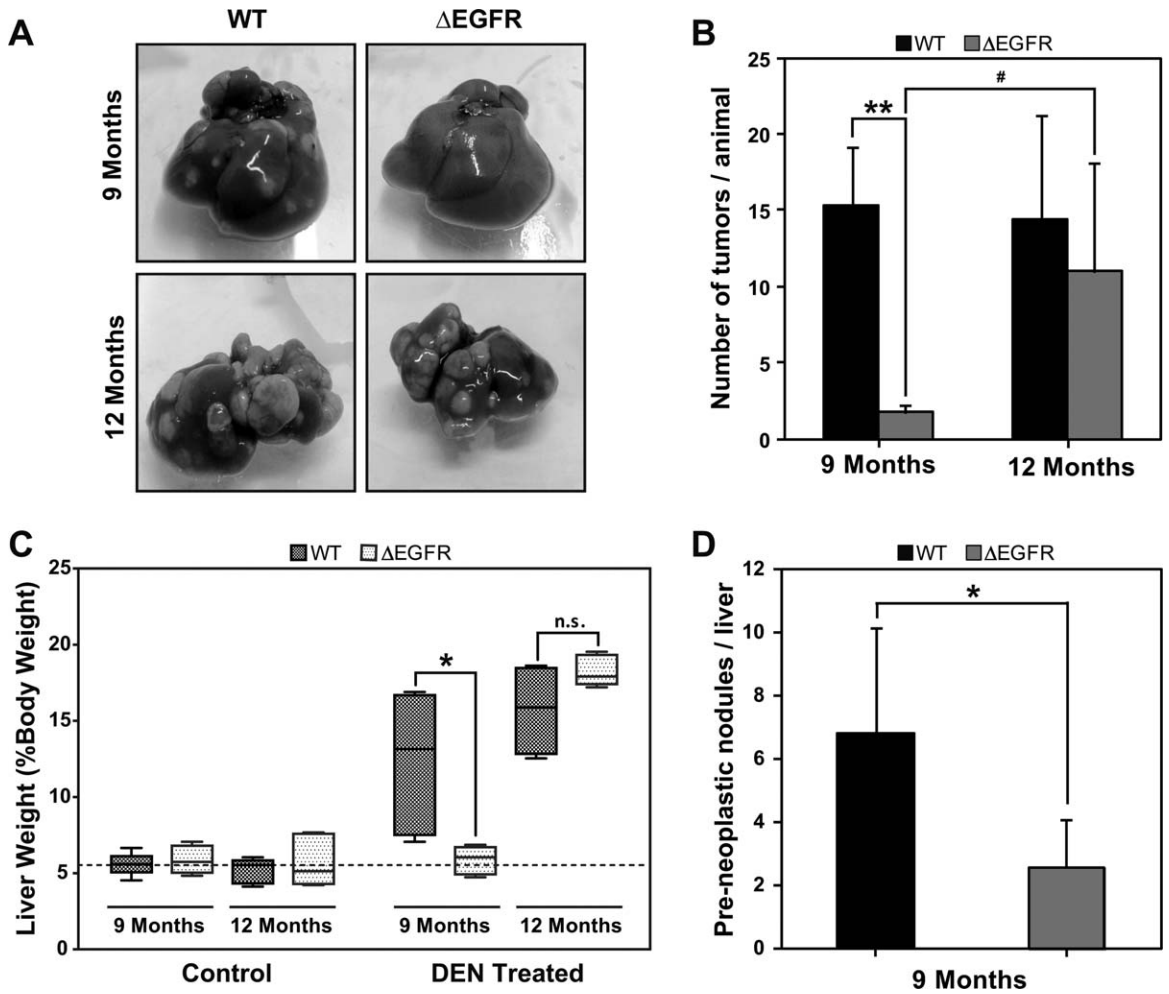

Fig. 6. ΔEGFR mice show a delay in the appearance of DEN-induced tumors. WT and ΔEGFR male mice were treated at day 15 of age with phosphate-buffered saline or DEN, and livers were collected at 9 and 12 months of age. (A) Representative images of livers from DEN-treated mice at the time of sacrifice. (B) Quantification of macroscopic tumors per animal. (C) Analysis of the liver/body weight ratio of WT and ΔEGFR mice. (D) Appearance of microscopic preneoplastic lesions at 9 months of age. (B-D) Data are mean ± standard error of the mean of at least four animals per group. Student *t* test was used: $*P < 0.05$ and $**P < 0.01$ compared to WT mice; $\#P < 0.05$ compared to 9 months. Abbreviation: n.s., no significance.

pathway is overactivated in ΔEGFR livers after PH and could justify that, although delayed, an efficient regeneration is observed in these animals.

It is worth mentioning that hepatocyte size significantly decreased at short times after PH in both WT and ΔEGFR animals; however, ΔEGFR mice showed a quick recovery of size such that after 24 hours hepatocyte size in ΔEGFR livers was significantly higher than that observed in WT livers (see Supporting Fig. S6 for images of the cells and Fig. 5F for quantification of the size). This hypertrophy could also contribute to the maintenance of liver functions and the low percentage of failure observed in ΔEGFR mice.

ΔEGFR Mice Show Delayed Appearance of Liver Tumors Induced by DEN Treatment. When we submitted 15-day-old WT and ΔEGFR mice to an acute treatment with DEN, liver injury (analyzed by serum parameters; Supporting Table S2) was higher in ΔEGFR animals, indicating a role for EGFR as a survival pathway in hepatocytes when submitted to a toxic insult. However, at 9 months of age, WT animals developed macroscopically visible tumors, which were barely observed in ΔEGFR mice (Fig. 6A,B). Consistently, the liver to body weight ratio significantly increased in WT, but not in ΔEGFR, mice (Fig. 6C). However, 12 months after DEN injection, ΔEGFR animals presented macroscopic tumors (Fig. 6A,B), and the liver to body weight ratio increase was quite similar in mice of both phenotypes (Fig. 6C). Expression of the truncated form of the *hEGFR* was maintained at this age in the ΔEGFR animals, which did not show changes in the mRNA levels of any of the EGFR family members (Supporting Fig. S7).

Immunohistological and proliferative (Ki67 staining) analysis of tissues at 9 months after DEN treatment

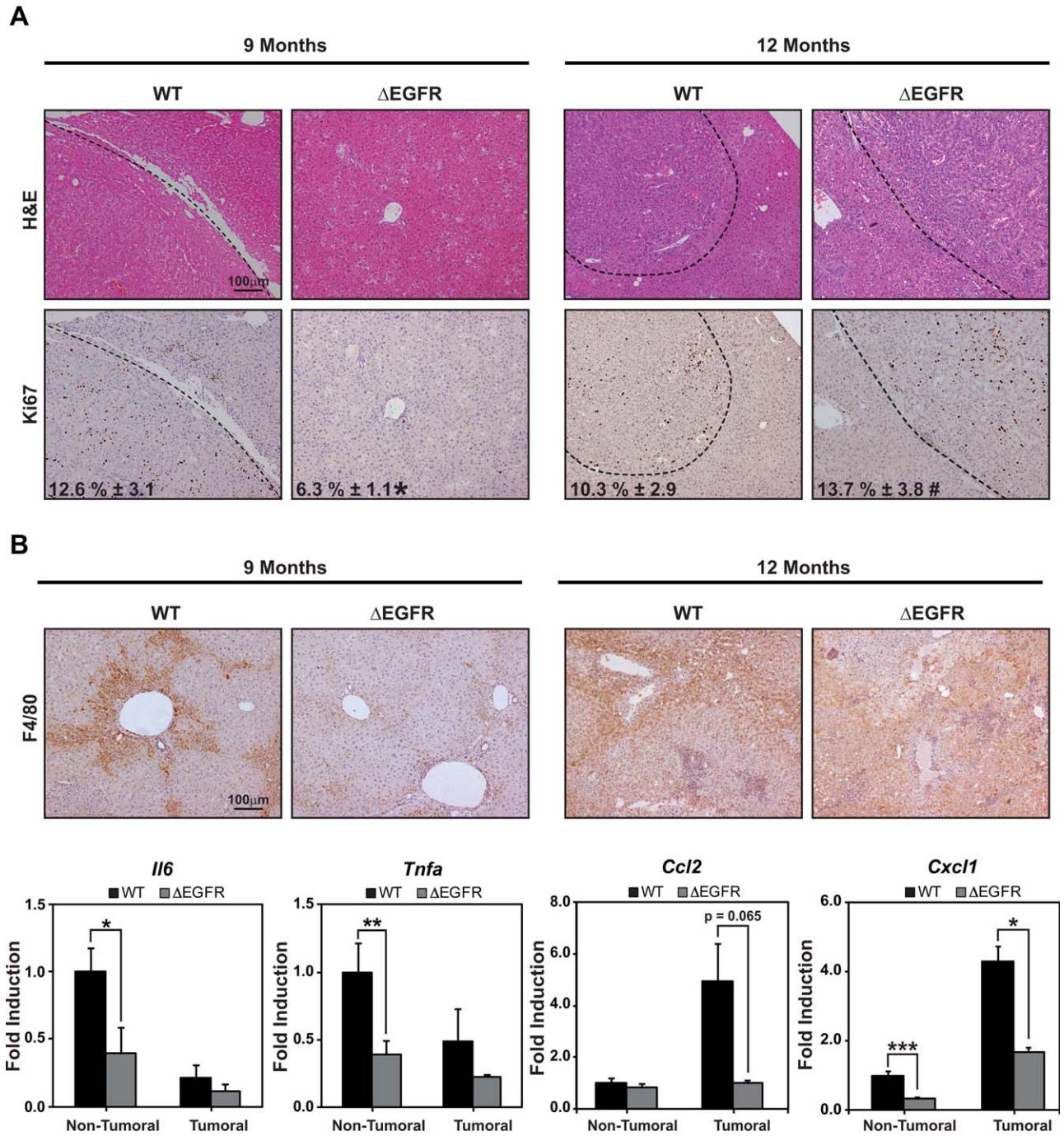

Fig. 7. Immunohistochemical analysis of proliferative and inflammatory areas in livers from DEN-treated WT and ΔEGFR mice. (A) Representative hematoxylin and eosin and immunohistochemical analyses of proliferation (Ki67 staining) in preneoplastic areas in livers from WT and ΔEGFR mice. Quantification of Ki67-positive cells (percentage) is in the bottom of each image. (B) Upper: Inflammatory lesions analyzed by F4/80 staining (macrophage marker). Lower: qRT-PCR analysis of mRNA levels of the proinflammatory cytokines interleukin-6 (*Il6*) and TNF-α (*Tnfa*) and chemokines CCL2 (*Ccl2*) and CXCL1 (*Cxcl1*) in macroscopically selected tumoral areas as well as in the surrounding tissue at 9 months of age in WT and ΔEGFR animals. (A,B) Data are mean ± standard error of the mean of at least four animals per group (three sections/animal). Student *t* test was used: $*P < 0.05$ and $**P < 0.01$ compared to WT mice; $\#P < 0.05$ compared to 9 months. Abbreviation: H&E, hematoxylin and eosin.

revealed the appearance of early preneoplastic lesions detectable only under the microscope. The number of lesions at 9 months of age in WT mice was much higher than that in ΔEGFR ones (Fig. 6D). Analysis of cell proliferation rate by Ki67 immunohistochemistry in the neoplastic areas revealed a lower proliferative rate in ΔEGFR tumors at 9 months compared with WT tumors but a similar proliferative rate at 12 months of

age (Fig. 7A). These results suggest that lack of the catalytic activity of the EGFR delays the appearance of tumors but cannot fully prevent the hepatocarcinogenic process.

DEN-Induced Hepatic Inflammatory Process Is Delayed in ΔEGFR Mice. Considering that hepatocellular carcinoma (HCC) is a clear example of inflammation-related cancer, we evaluated inflammatory markers in histological sections of nontumoral areas of WT and ΔEGFR livers. As shown in Fig. 7B, WT livers showed strong positive areas for F4/80 staining, a macrophage marker, 9 months after DEN treatment, while ΔEGFR mice did not. At 12 months of age the situation in WT and ΔEGFR livers was comparable as both animals showed similar extent of inflammation. Furthermore, some fibrotic areas could be observed at 9 months of age in WT mice, whereas in ΔEGFR mice collagen deposits were only seen around the portal triads and perivascular regions (Supporting Fig. S8), as occurs in healthy liver. Larger collagen deposits were found in ΔEGFR livers at 12 months of age, similar to the situation in WT animals. These results indicate that lack of EGFR catalytic activity in the hepatocytes provokes a delay in the DEN-induced inflammatory process in the liver. Analysis of the expression of classical cytokines involved in liver inflammation revealed lower *Il6* and *TNFa* mRNA levels (Fig. 7B) but no changes in *Il1b* or *Il17a* (results not shown) in the tumor-surrounding tissues of ΔEGFR livers compared with WT ones. Furthermore, among different inflammatory chemokines for which some evidence exists that may be controlled by the EGFR pathway in HCC,[24] we found decreased expression of *Ccl2* in the tumoral tissues and of *Cxcl1* in both tumoral and nontumoral areas in ΔEGFR livers (Fig. 7B). No differences were found in other analyzed chemokines (*Ccl20*, *Cxcl2*, *Cxcl3*, or *Cxcl5*; results not shown).

Following the previous hypothesis about crosstalk between TGF-β and the EGFR, we next analyzed the expression of *TGF-β1* mRNA and the levels of phosphorylation of Smads in livers from WT and ΔEGFR mice at 9 months of DEN treatment. We could not find significant differences in either *TGF-β1* levels (Fig. 8A) or phospho-Smad3 levels (results not shown). Of relevance, none of the apoptosis or cell cycle regulatory genes analyzed showed differences in ΔEGFR livers (in either tumor or surrounding areas) that could correlate with their lower tumor progression (Fig. 8A). Nonetheless, it was really interesting to find a significant difference in the levels of *Nox4*, the NADPH oxidase that mediates some of the suppressor actions of TGF-β and for which we have recently found a relevant liver tumor suppressor role.[22] Finally, analysis of *Hgf* mRNA levels revealed a significant increase in the livers of ΔEGFR mice (nontumoral tissue). No evidence was observed for increases in *uPA* or *Met* at the mRNA level (Fig. 8B).

These results together indicate that delay in the inflammation process is the most evident alteration observed in ΔEGFR mice that justifies the retarding of the appearance of DEN-induced tumors. The increased levels of Nox4, a liver growth suppressor protein, could also contribute. The increase in HGF levels might replace the EGF-induced growth once the tumor is formed.

Discussion

The purpose of this study was to elucidate the specific role of the EGFR catalytic activity in a physiological (liver regeneration) and a pathological (hepatocarcinogenesis) situation of the liver where proliferation of adult hepatocytes takes place. Our results demonstrate that although EGFR signaling plays crucial roles in these processes, its absence only results in an overall delay in both regeneration and carcinogenesis, suggesting the existence of at least partial functional compensation by alternative routes.

First of all, we propose an essential role for EGFR in the early phases of the regenerative response after PH in mice, mediating a fast and efficient process. In a previous study, Natarajan et al.[25] generated a mouse model carrying a floxed EGFR allele to inactivate the EGFR in the adult liver. They proposed that EGFR is a critical regulator of hepatocyte proliferation in the initial phases of liver regeneration. Here, we confirm these results using a novel and unique animal model, but we also associate these effects with the catalytic activity of the EGFR and provide new insights about the molecular mechanisms by which this occurs, particularly overactivation of the TGF-β pathway and alterations in lipid metabolism.

Inactivation of TGF-β signaling in hepatocytes results in an increased proliferative response after PH.[26,27] One of the main effects of TGF-β in liver cells is the induction of apoptosis through up-regulation of *Bim* and *Bmf*, proapoptotic members of the Bcl-2 family. The EGF pathway counteracts TGF-β proapoptotic effects by impairing up-regulation of both genes and up-regulating $Bclx_L$ and *Mcl-1*, two antiapoptotic members of the Bcl-2 family,[6,7] an effect mediated by survival signals such as the phosphoinositide 3-kinase/Akt and ERK pathways. However, our study demonstrates that the major role of EGF during liver regeneration after PH is not cell survival, probably because apoptosis is not relevant in a model where there is no hepatocyte damage. In contrast, the decrease and delay in activation

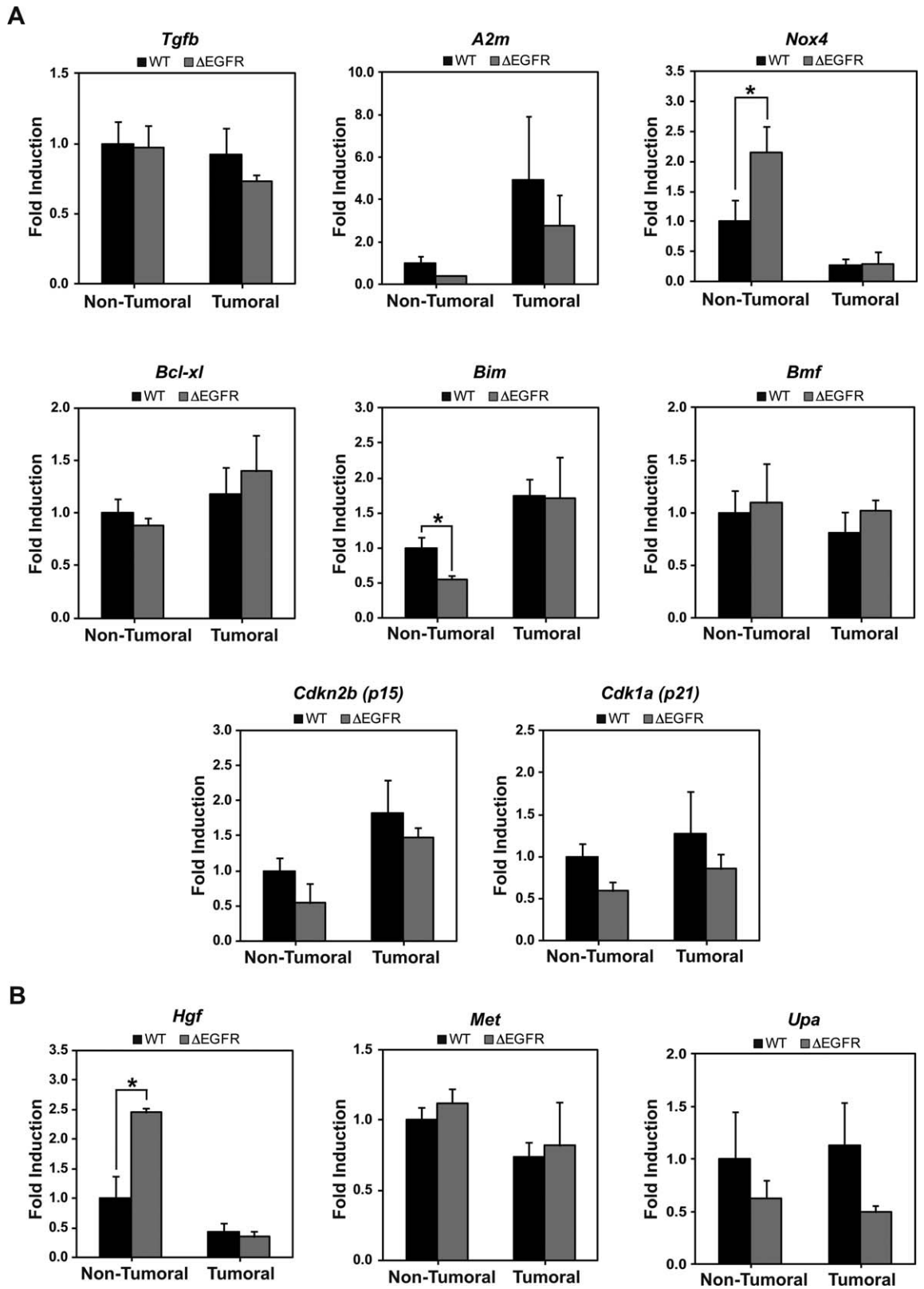

Fig. 8. Transcriptomic (qRT-PCR) analysis in tumoral and nontumoral areas in liver tissues from 9-month DEN-treated WT and ΔEGFR mice. (A) *Tgfb*, apoptosis, and cell cycle regulatory genes. (B) HGF signaling pathway. (A,B) Data are mean ± standard error of the mean of at least four animals per group (three sections/animal). Student *t* test was used: $*P < 0.05$.

of the phosphoinositide 3-kinase/Akt and ERK pathways at early times after PH in ΔEGFR animals, concomitant with high expression of the cyclin-dependent kinase inhibitor p15INK4, suggest a relevant role for the EGFR pathway in priming hepatocytes to enter into the cell cycle. We suggest that this delay could be related, at least partially, to the overexpression of TGF-β1 and overactivation of the TGF-β pathway observed in animals with attenuated EGFR signaling. Although initially it was supposed that TGF-β could play a relevant role in mediating termination of liver regeneration, the latest results indicate that it is not necessary during this stage.[26] In contrast, a higher and accelerated DNA synthesis peak after PH was found in a *Tgfbr2* knockout (R2LivKO) animal model.[26] Indeed, in contrast to previous predictions, TGF-β could play an essential role in the first stages of liver regeneration; and here we show that the EGFR pathway may be essential in regulating its expression and signaling.

It is well known that after PH hepatocellular fat accumulation occurs, concomitant with up-regulation of genes related to the adipogenic program,[28] which has been suggested to be a mammalian target of rapamycin–dependent process.[29] Disruption of hepatic adipogenesis is associated with impaired hepatocellular proliferation following PH[28] (for review, see Rudnick and Davidson[30]). Here we show for the first time that the EGFR pathway is required for fat accumulation and up-regulation of two key enzymes related to the *de novo* lipid synthesis. Further studies will be required to determine the precise molecular mechanisms mediating these effects.

In spite of these alterations, most of the ΔEGFR mice survived to the PH and no significant differences could be observed in the serum parameters related to liver injury or in the liver to body mass ratio. It is true that a higher mortality was observed in the first 48 hours after PH, as also suggested by Natarajan et al. in the mice carrying a floxed EGFR[25]; but differences were not statistically significant. Our results are in agreement with the work of Michalopoulos's group where the consequences of *in vivo* silencing of the EGFR on rat liver regeneration using EGFR-specific short hairpin RNAs were analyzed.[31] Despite suppression of hepatocyte proliferation lasting into day 3 after PH, liver restoration occurred. Interestingly, hepatocytes in short hairpin EGFR–treated rats were considerably larger compared with short hairpin RNA–treated controls, an effect that we also observed in the ΔEGFR animals. Furthermore, we show that ΔEGFR mice presented higher phosphorylation levels of c-Met that could compensate for the lack of EGFR-mediated proliferative signals, a possibility that was also suggested in Michalopoulos et al.'s work.[31] Interestingly, we demonstrate up-regulation not only of the expression of *Hgf* in ΔEGFR livers after PH but also of its activator uPA, whose deficiency was shown to retard liver regeneration by impairing the HGF pathway.[23] However, even though the HGF/Met pathway is clearly overactivated in ΔEGFR animals, the contributions made by EGFR are unique in some aspects and not compensated by c-Met. In particular, early activation of phosphoinositide 3-kinase/Akt and ERK signaling would require EGFR signaling. Interestingly, Factor et al. elegantly demonstrated that c-Met signaling in hepatocytes is essential for sustaining long-term ERK1/2 activation throughout liver regeneration, and alternative pathways may account for the early ERK1/2 activation.[32] Furthermore, here we show that compensation of the cytostatic effects of the TGF-β pathway and regulation of lipid metabolism after PH appear to be fully dependent on EGFR and may be necessary for more efficient liver regeneration but dispensable for restoring liver mass in those animals that survive the first hours after PH. In agreement with these results, lack of Nogo-B (reticulon 4B) produces overactivation of the TGF-β pathway after PH in mice, coincident with a delay in hepatocyte proliferation, but did not affect the liver to body mass ratio in the regenerative process.[33]

We also show here that attenuation of EGFR catalytic activity induces a significant delay in the appearance of tumorigenic lesions in DEN-treated animals. However, once tumors appear, the proliferative rate is similar in ΔEGFR and WT animals. Surprisingly, no significant differences were observed in the TGF-β pathway or in the expression of apoptosis or cell cycle regulatory genes, which could justify the delay in tumorigenesis. The only significant change was the mRNA levels of *Nox4*, a member of the NADPH oxidase family that is down-regulated in HCC patients and negatively modulates hepatocyte proliferation.[22] Interestingly, EGF inhibits *Nox4* expression, acting at the transcriptional level on the *Nox4* promoter.[21] Indeed, the more significant difference lies in the appearance of preneoplastic lesions. In agreement with this result, a previous study using gefitinib (an EGFR inhibitor) in DEN-induced hepatocarcinogenesis in mice revealed that the gefitinib-treated animals showed significantly lower numbers of HCC nodules but that the mean tumor size was not different between untreated and gefitinib-treated mice.[34] Similar to what was found during liver regeneration, levels of HGF were much higher in ΔEGFR animals, which suggests that this cytokine might replace the mitogenic function of the EGFR ligands.

Our study indicates that the delay in the appearance of tumoral lesions might be associated with attenuation of the inflammatory process. In support of these results, pharmacological inhibition of EGFR signaling effectively prevented the progression of cirrhosis and regressed fibrosis in animal models.[35] EGFR signaling has been proposed as a critical junction between inflammation-related signals and potent cell regulating machineries.[36] Recent evidence indicates that the EGFR pathway regulates the expression of inflammatory factors and chemokine ligands produced by liver tumor cells.[24] Our results indicate differences in the expression of interleukin-6 and TNF-α in the tumor surrounding tissue, which suggests that the transgene expression in hepatocytes affects the production of inflammatory cytokines by themselves or other surrounding cells. Interestingly, the EGFR pathway plays an essential role in liver macrophages to mediate the inflammatory process in DEN-induced HCC.[37] Indeed, we cannot exclude that the overexpression of a truncated form of the EGFR that binds its ligands, but does not transduce the signal, may decrease the number of free EGFR ligands able to act on the nonparenchymal cells. Furthermore, it is worth pointing out that CCL2, a chemokine considered to be a central coordinator of hepatocyte-mediated inflammation,[38] showed decreased expression in ΔEGFR tumors. Finally, CXCL1, considered a critical player in both inflammation and tumor growth in HCC,[39] presented significantly decreased mRNA levels in ΔEGFR tumoral and nontumoral areas. Regardless of the mechanism and considering together our results and others in the literature, there is no doubt that one of the most essential functions of the EGFR pathway during hepatocarcinogesis should be regulation of inflammation addressed by parenchymal and/or nonparenchymal cells.

In conclusion, here we provide a novel research tool, a ΔEGFR transgenic mouse model, which has proved to be very useful in deciphering the molecular mechanisms underlying the functions of EGFR signaling in the adult liver, in particular uncovering its tyrosine kinase–dependent functions in liver regeneration and carcinogenesis. We believe this model will open new possibilities for exploring the EGFR pathway as a targeted therapeutic strategy in chronic liver diseases and carcinogenesis.

Acknowledgment: We thank Aurora de la Cal and Sergio Losada for their collaboration in the administrative work at the CIEMAT/CIBERER/ISS-FJD and Filip Radom and Alba Marin (graduate students at the IDIBELL) for their technical support and help.

References

1. **Berasain C**, **Avila MA**. The EGFR signalling system in the liver: from hepatoprotection to hepatocarcinogenesis. J Gastroenterol 2014;49:9-23.
2. Michalopoulos GK. Liver regeneration after partial hepatectomy: critical analysis of mechanistic dilemmas. Am J Pathol 2010;176:2-13.
3. Riehle KJ, Dan YY, Campbell JS, Fausto N. New concepts in liver regeneration. J Gastroenterol Hepatol 2011;26(Suppl. 1):203-212.
4. Fausto N, Campbell JS, Riehle KJ. Liver regeneration. J Hepatol 2012; 57:692-694.
5. Carmona-Cuenca I, Herrera B, Ventura J-J, Roncero C, Fernández M, Fabregat I. EGF blocks NADPH oxidase activation by TGF-beta in fetal rat hepatocytes, impairing oxidative stress, and cell death. J Cell Physiol 2006;207:322-330.
6. Fabregat I, Herrera B, Fernández M, Alvarez AM, Sánchez A, Roncero C, et al. Epidermal growth factor impairs the cytochrome C/caspase-3 apoptotic pathway induced by transforming growth factor beta in rat fetal hepatocytes via a phosphoinositide 3-kinase-dependent pathway. Hepatology 2000;32:528-535.
7. Caja L, Sancho P, Bertran E, Fabregat I. Dissecting the effect of targeting the epidermal growth factor receptor on TGF-*β*-induced-apoptosis in human hepatocellular carcinoma cells. J Hepatol 2011;55:351-358.
8. Skarpen E, Oksvold MP, Grøsvik H, Widnes C, Huitfeldt HS. Altered regulation of EGF receptor signaling following a partial hepatectomy. J Cell Physiol 2005;202:707-716.
9. Livneh E, Prywes R, Kashles O, Reiss N, Sasson I, Mory Y, et al. Reconstitution of human epidermal growth factor receptors and its deletion mutants in cultured hamster cells. J Biol Chem 1986;261: 12490-12497.
10. Kashles O, Yarden Y, Fischer R, Ullrich A, Schlessinger J. A dominant negative mutation suppresses the function of normal epidermal growth factor receptors by heterodimerization. Mol Cell Biol 1991;11:1454-1463.
11. Murillas R, Larcher F, Conti CJ, Santos M, Ullrich A, Jorcano JL. Expression of a dominant negative mutant of epidermal growth factor receptor in the epidermis of transgenic mice elicits striking alterations in hair follicle development and skin structure. EMBO J 1995;14:5216-5223.
12. Warming S, Costantino N, Court DL, Jenkins NA, Copeland NG. Simple and highly efficient BAC recombineering using galK selection. Nucleic Acids Res 2005;33:e36.
13. Giraldo P, Montoliu L. Size matters: use of YACs, BACs and PACs in transgenic animals. Transgenic Res 2001;10:83-103.
14. Valverde AM, Burks DJ, Fabregat I, Fisher TL, Carretero J, White MF, et al. Molecular mechanisms of insulin resistance in IRS-2-deficient hepatocytes. Diabetes 2003;52:2239-2248.
15. Higgins GM, Anderson R. Experimental pathology of the liver. I. Restoration of the liver of the white rat following partial surgical removal. Arch Pathol 1931;12:186-202.
16. Sancho P, Bertran E, Caja L, Carmona-Cuenca I, Murillo MM, Fabregat I. The inhibition of the epidermal growth factor (EGF) pathway enhances TGF-beta-induced apoptosis in rat hepatoma cells through inducing oxidative stress coincident with a change in the expression pattern of the NADPH oxidases (NOX) isoforms. Biochim Biophys Acta 2009;1793:253-263.
17. Caja L, Ortiz C, Bertran E, Murillo MM, Miró-Obradors MJ, Palacios E, et al. Differential intracellular signalling induced by TGF-beta in rat adult hepatocytes and hepatoma cells: implications in liver carcinogenesis. Cell Signal 2007;19:683-694.
18. Murillo MM, del Castillo G, Sánchez A, Fernández M, Fabregat I. Involvement of EGF receptor and c-Src in the survival signals induced by TGF-beta1 in hepatocytes. Oncogene 2005;24:4580-4587.
19. Mitchell C, Nivison M, Jackson LF, Fox R, Lee DC, Campbell JS, et al. Heparin-binding epidermal growth factor-like growth factor links hepatocyte priming with cell cycle progression during liver regeneration. J Biol Chem 2005;280:2562-2568.

20. Arandjelovic S, Freed TA, Gonias SL. Growth factor-binding sequence in human alpha2-macroglobulin targets the receptor-binding site in transforming growth factor-beta. Biochemistry (Mosc) 2003;42:6121-6127.
21. Carmona-Cuenca I, Roncero C, Sancho P, Caja L, Fausto N, Fernández M, et al. Upregulation of the NADPH oxidase NOX4 by TGF-beta in hepatocytes is required for its pro-apoptotic activity. J Hepatol 2008;49:965-976.
22. Crosas-Molist E, Bertran E, Sancho P, López-Luque J, Fernando J, Sánchez A, et al. The NADPH oxidase NOX4 inhibits hepatocyte proliferation and liver cancer progression. Free Radic Biol Med 2014;69:338-347.
23. Shimizu M, Hara A, Okuno M, Matsuno H, Okada K, Ueshima S, et al. Mechanism of retarded liver regeneration in plasminogen activator-deficient mice: impaired activation of hepatocyte growth factor after Fas-mediated massive hepatic apoptosis. Hepatology 2001;33:569-576.
24. **Huang P**, **Xu X**, Wang L, Zhu B, Wang X, Xia J. The role of EGF-EGFR signalling pathway in hepatocellular carcinoma inflammatory microenvironment. J Cell Mol Med 2014;18:218-230.
25. Natarajan A, Wagner B, Sibilia M. The EGF receptor is required for efficient liver regeneration. Proc Natl Acad Sci USA 2007;104:17081-17086.
26. **Oe S**, **Lemmer ER**, Conner EA, Factor VM, Levéen P, Larsson J, et al. Intact signaling by transforming growth factor beta is not required for termination of liver regeneration in mice. Hepatology 2004;40:1098-1105.
27. **Romero-Gallo J**, **Sozmen EG**, Chytil A, Russell WE, Whitehead R, Parks WT, et al. Inactivation of TGF-beta signaling in hepatocytes results in an increased proliferative response after partial hepatectomy. Oncogene 2005;24:3028-3041.
28. **Shteyer E**, **Liao Y**, Muglia LJ, Hruz PW, Rudnick DA. Disruption of hepatic adipogenesis is associated with impaired liver regeneration in mice. Hepatology 2004;40:1322-1332.
29. Obayashi Y, Campbell JS, Fausto N, Yeung RS. Impaired lipid accumulation in the liver of Tsc2-heterozygous mice during liver regeneration. Biochem Biophys Res Commun 2013;437:146-150.
30. **Rudnick DA**, **Davidson NO.** Functional relationships between lipid metabolism and liver regeneration. Int J Hepatol 2012;2012:549241.
31. Paranjpe S, Bowen WC, Tseng GC, Luo J-H, Orr A, Michalopoulos GK. RNA interference against hepatic epidermal growth factor receptor has suppressive effects on liver regeneration in rats. Am J Pathol 2010;176:2669-2681.
32. Factor VM, Seo D, Ishikawa T, Kaposi-Novak P, Marquardt JU, Andersen JB, et al. Loss of c-Met disrupts gene expression program required for G_2/M progression during liver regeneration in mice. PloS One 2010;5(9).
33. **Gao L**, **Utsumi T**, **Tashiro K**, Liu B, Zhang D, Swenson ES, et al. Reticulon 4B (Nogo-B) facilitates hepatocyte proliferation and liver regeneration in mice. Hepatology 2013;57:1992-2003.
34. Schiffer E, Housset C, Cacheux W, Wendum D, Desbois-Mouthon C, Rey C, et al. Gefitinib, an EGFR inhibitor, prevents hepatocellular carcinoma development in the rat liver with cirrhosis. Hepatology 2005;41:307-314.
35. Fuchs BC, Hoshida Y, Fujii T, Wei L, Yamada S, Lauwers GY, et al. Epidermal growth factor receptor inhibition attenuates liver fibrosis and development of hepatocellular carcinoma. Hepatology 2014;59:1577-1590.
36. Berasain C, Perugorria MJ, Latasa MU, Castillo J, Goñi S, Santamaría M, et al. The epidermal growth factor receptor: a link between inflammation and liver cancer. Exp Biol Med (Maywood) 2009;234:713-725.
37. **Lanaya H**, **Natarajan A**, **Komposch K**, Li L, Amberg N, Chen L, et al. EGFR has a tumour-promoting role in liver macrophages during hepatocellular carcinoma formation. Nat Cell Biol 2014;16:972-981.
38. **Ziraldo C**, **Vodovotz Y**, Namas RA, Almahmoud K, Tapias V, Mi Q, et al. Central role for MCP-1/CCL2 in injury-induced inflammation revealed by in vitro, in silico, and clinical studies. PloS One 2013;8:e79804.
39. Han K-Q, He X-Q, Ma M-Y, Guo X-D, Zhang X-M, Chen J, et al. Inflammatory microenvironment and expression of chemokines in hepatocellular carcinoma. World J Gastroenterol 2015;21:4864-4874.

Author names in bold denote shared co-first authorship.

Supporting Information

Additional Supporting Information may be found at http://onlinelibrary.wiley.com/doi/10.1002/hep.28134/suppinfo.